



UNIVERSIDAD DE LA RIOJA

TESIS DOCTORAL

Título
Design of smart linkers and their applications in controlled-release drug delivery systems
Autor/es
Xhenti Ferhati
Director/es
Francisco Corzana López y Gonçalo Bernardes
Facultad
Facultad de Ciencia y Tecnología
Titulación
Departamento
Química
Curso Académico



Design of smart linkers and their applications in controlled-release drug delivery systems, tesis doctoral de Xhenti Ferhati, dirigida por Francisco Corzana López y Gonçalo Bernardes (publicada por la Universidad de La Rioja), se difunde bajo una Licencia Creative Commons Reconocimiento-NoComercial-SinObraDerivada 3.0 Unported. Permisos que vayan más allá de lo cubierto por esta licencia pueden solicitarse a los titulares del copyright.

© El autor
© Universidad de La Rioja, Servicio de Publicaciones, 2020
publicaciones.unirioja.es
E-mail: publicaciones@unirioja.es

FACULTAD DE CIENCIA Y TECNOLOGÍA



**UNIVERSIDAD
DE LA RIOJA**

Departamento de Química

Centro de Investigación en Síntesis Química

Área de Química Orgánica

TESIS DOCTORAL

Design of smart linkers and their applications in controlled-release drug delivery systems

Memoria presentada en la Universidad de la Rioja para optar al grado de
Doctor en Química por

Xhenti Ferhati

Septiembre 2019

Dr. FRANCISCO CORZANA LÓPEZ, Profesor Titular de Química Orgánica del Departamento de Química de la Universidad de La Rioja y

Dr. GONÇALO BERNARDES, University Lecturer del Departamento de Química de La Universidad de Cambridge

HACEN CONSTAR:

*Que la memoria " Design of smart linkers and their applications in controlled-release drug delivery systems" realizada por **Xhenti Ferhati** en el Departamento de Química de la Universidad de La Rioja y bajo su inmediata dirección, reúne las condiciones exigidas para optar al grado de Doctor en Química.*

Logroño, Septiembre de 2019

Los directores

Francisco Corzana López

Gonçalo J. L. Bernardes

Abstract

Antibody drug conjugates (ADC) represents an interesting strategy in tumour targeted therapy . The approach is based on the combination of the high affinity of an antibody towards its antigen and the high cytotoxicity of a drug, leading to a selective therapeutic agent with improved efficacy and safety.

When considering the development of an ADC, several factors are of great importance. On the one hand, conjugation chemistry defines the properties of the ADC, such as antibody to drug ratio (DAR) and is fundamental to yield stable and homogeneous conjugates. On the other hand, the linker used to connect the drug with the antibody plays an important role in the stability of the final conjugate and its efficiency in terms of cell killing.

Considering the importance of these two factors in ADC development, this Thesis has been focused on conjugation reactions and linker chemistry. First, new conjugation strategies have been proposed for the design of homogeneous, stable and efficacious ADCs. The use of carbonyl acrylamide derivatives has allowed the irreversible cysteine-selective protein modification. Thus, when combined with Thiomab technology, an ADC with DAR 2 was obtained in high yield, using stoichiometric amount of the reagent and under mild conditions. Similarly, a new, ultrafast reagent, based on quaternised vinyl pyridinium scaffold, has been described. After proving that the compound is also cysteine selective in proteins and antibodies, the synthesis of a vinyl pyridinium bearing an alkyne tag for further functionalization was optimized. This approach allowed the introduction of a drug, and the resulting derivative was efficiently used for ADC synthesis.

Concerning the linker, we have demonstrated that acetals represent an interesting cleavable moiety for the preparation of ADCs as well as small molecules drug conjugates (SMDC). We have prepared acetal linkers featuring coumarin as fluorophore and a duocarmycin analogue as an example of cytotoxic drug. Markedly, it represents the first example a duocarmycin analogue is protected with an acid cleavable moiety. Kinetic studies were performed on these linkers and showed that they are stable in plasma,

while being rapidly cleaved under acidic conditions. This methodology was applied then to the design of a small molecule drug conjugate (SMDC), as well as an antibody drug conjugate (ADC). Of note, interesting outcomes emerged from the stability studies performed on the ADC. In fact, our results showed that the stability of the ADC depends not only on the conjugation site, but also different payloads can affect the stability of the acetal linker, depending on the 3D disposition they adopt in the antibody pocket.

Finally, we have exploited the use of the Grob fragmentation to design 'self-immolative' linkers for controlled drug release. Although the reaction mechanism is well known and presents several synthetic applications, no biological application has been described to date. The screening of different substrates allowed the identification of 3-aminocyclohexanol scaffold as a suitable moiety for fragmentation reaction under biological mimicking conditions. The novel methodology has been applied to the controlled release of Crizotinib, a drug used for the treatment of metastatic lung cancer. Thus, blocking the Grob fragmentation pathway, the pro-drug is stable and intact; at the same time, activation of the pathway by removing the amine protecting group of 3-aminocyclohexanol derivative, results in drug release.

Resumen

Los derivados fármaco- anticuerpo representan una interesante estrategia en la terapia antitumoral dirigida. Dicha estrategia combina la gran afinidad que los anticuerpos presentan por sus correspondientes antígenos con la presencia de fármacos altamente citotóxicos. Como resultado se obtiene un agente terapéutico selectivo, a la vez que altamente eficaz y seguro.

En el diseño de estos derivados fármaco-anticuerpo existen muchos factores para tener en cuenta. Así, por ejemplo, la reacción química utilizada en la conjugación define las propiedades del compuesto final (conjugado), así como el número de fármacos presentes por anticuerpo, y es decisiva para obtener un anticuerpo estable y homogéneo. Además, el *linker* que conecta el fármaco con el anticuerpo juega un papel importante en la estabilidad del conjugado final y en su eficacia respecto a la toxicidad en células tumorales.

Teniendo en cuenta la importancia de estos dos factores, esta tesis doctoral se ha centrado en el desarrollo de nuevas estrategias de conjugación y en el diseño de nuevos *linkers*. En primer lugar, se han propuesto metodologías de conjugación alternativas para el diseño de nuevos conjugados. Para ello, se ha descrito la síntesis de derivados de fármacos que llevan una carbonil acrilamida, la cual reacciona selectivamente con los residuos cisteína presentes en las proteínas o anticuerpos. Así, combinado esta estrategia con un Thiomab se han preparado conjugados estables y que presentan dos unidades de fármaco por anticuerpo. De forma similar, se ha descrito el uso de vinil piridinas cuaternizadas, las cuales pueden reaccionar también de forma selectiva con las cisteínas presentes en la proteína.

Con respecto al *linker*, en esta Tesis se ha demostrado que los acetales pueden ser un grupo funcional interesante para la preparación de ADCs y de pequeñas moléculas (SMDC), donde el fluoróforo o el fármaco al que están unidos estas entidades se liberan en medio ácido gracias a la hidrólisis del acetal. En este sentido, se han preparado acetales unidos a cumarina y a un análogo de duocarmicina. Este último compuesto representa el primer ejemplo de un análogo de duocarmicina que está protegido con un *linker* sensible al medio ácido. En paralelo, se han realizado estudios cinéticos con estos

linkers y se ha demostrado que, aunque son estables en el plasma, se hidrolizan rápidamente en condiciones ácidas. Es de destacar que la estabilidad del ADC con un *linker* tipo acetal depende no sólo del sitio de la conjugación, sino que también de la naturaleza del fármaco o fluoróforo unido a este conector.

Finalmente, hemos explotado el uso de la fragmentación de Grob para diseñar *linkers* "auto-inmolativos" para con el objetivo de liberar fármacos de forma controlada. Aunque el mecanismo de esta reacción es bien conocido y presenta varias aplicaciones sintéticas, hasta la fecha no se ha descrito ninguna aplicación en el ámbito de la biológica. El cribado de diferentes sustratos permitió identificar al 3-aminociclohexanol como una molécula adecuada para llevar a cabo la reacción de fragmentación en condiciones que imitan a un medio biológico. La nueva metodología se ha aplicado a la liberación controlada de crizotinib, un fármaco utilizado para el tratamiento del cáncer de pulmón metastásico. Así, bloqueando la fragmentación de Grob, el profármaco es estable y no tóxico. Sin embargo, la activación de la reacción mediante la eliminación del grupo protector de amina del derivado 3-aminociclohexanol, resulta en la liberación del fármaco.

Index

1. Introduction	1
1.1 Ligand targeted drug delivery	5
1.2 References	8
2. Background	11
2.1 Antibody drug conjugates	13
2.1.1 Site selective ADC chemistry	18
2.1.1.1 <i>Non-natural amino-acid introduction</i>	20
2.1.1.2 <i>Disulfide stapling</i>	21
2.1.1.3 <i>Thiomab antibodies</i>	24
2.2 Linker chemistry in ADC Synthesis	25
2.2.1 Chemical cleavable linkers	26
2.2.2 Enzyme cleavable linkers	30
2.3 Small molecule drug conjugates	32
2.4 References	35
3. Objectives	41
4. New Cysteine selective reagents for ADC synthesis	45
4.1 Introduction	47
4.1.1 Modifications at natural amino acids	48
4.1.2 Conjugation strategies based on cysteine modification	50
4.1.3 Background and objectives	53
4.2 Carbonylacrylic reagents for protein modifications	55
4.2.1 Synthesis	55
4.2.2 Antibody conjugation and stability	58
4.3 Vinyl Pyridinium reagents for protein modification	62
4.3.1 Synthesis of MMAE-vinyl pyridinium derivative	67

4.3.2	ADC synthesis and biological assays	69
4.4	Conclusions	71
4.5	Experimental section	73
4.5.1	Synthesis	73
4.5.2	Kinetic studies	77
4.5.3	Antibody conjugation	78
4.5.4	Cell assays	81
4.5.5	Quantum Mechanical calculations	82
4.6	References	84

5. Acetals as new acid cleavable linker for ADC and SMDC synthesis **89**

5.1	Introduction	91
5.1.1	Acid cleavable linkers for drug release application	93
5.1.2	Use of acetals as acid cleavable linkers	96
5.2	Background and main goals	98
5.3	Coumarin based acetals	101
5.3.1	Synthesis	101
5.3.2	Coumarin derivatives stability	105
5.3.2.1	<i>NMR kinetic study</i>	106
5.3.2.2	<i>Fluorescence release study</i>	110
5.4	Duocarmycin derivatives synthesis	111
5.4.1	Stability assays	113
5.5	Small Molecule Drug Conjugate	115
5.5.1	SMDC synthesis and stability studies	116
5.5.2	<i>In vitro</i> assays of SMDC 33	118
5.6	Antibody Drug Conjugate	119
5.6.1	Synthesis of carbonyl acrylamide derivatives	119
5.6.2	ADC synthesis and stability	120
5.6.3	<i>In vitro</i> assays	123
5.6.4	Molecular Dynamics simulations	125
5.7	Conclusions	127

5.8	Experimental section	129
5.8.1	Synthesis	129
5.8.2	Stability studies	142
5.8.3	Antibody Drug Conjugates synthesis and stability	143
5.8.4	<i>In vitro</i> assays	145
5.8.5	Molecular Dynamics simulations	146
5.9	References	148

6. Grob fragmentation for the controlled release of drugs **153**

6.1	Introduction	155
6.1.1	Fragmentations reactions: the Grob fragmentation	158
6.1.2	Background and main goals	160
6.2	Substrate screening for Grob fragmentation	161
6.2.1	Synthesis of Grob fragmentation substrates	162
6.2.2	Study of the reactions under biological conditions	168
6.3	Application to the controlled release of Crizotinib	178
6.3.1	Synthesis of Grob fragmentation scaffold with cathepsin B triggered release for conjugation with antibodies	182
6.4	Conclusions	185
6.5	Experimental section	187
6.5.1	Synthesis	187
6.5.2	NMR study of the Grob fragmentation	205
6.5.3	UPLC release of Crizotinib derivative from 68 and 69	206
6.6	References	207

7. Conclusions **211**

7.1	Conclusions	213
7.2	Conclusiones	214
7.3	Scientific publications derived from this dissertation	216
7.4	Other scientific publications	217
7.5	Contribution to congresses	218

8. Supplementary Informations	221
8.1 Reagents and general synthetic procedures	223
8.2 General protein conjugation methods	223
8.3 Supplementary information of <i>Chapter 4</i>	224
8.4 Supplementary information of <i>Chapter 5</i>	228
8.5 Supplementary information of <i>Chapter 6</i>	236

Abbreviations

^{13}C NMR	carbon nuclear magnetic resonance
^{19}F NMR	fluorine nuclear magnetic resonance
^1H NMR	proton nuclear magnetic resonance
Ac ₂ O	acetic anhydride
AcOEt	ethyl acetate
AcOH	acetic acid
ADC	antibody drug conjugate
Arom.	aromatic
Bn	benzyl
Boc	<i>tert</i> -butoxycarbonyl
brs	broad singlet
CAIX	carbonic anhydrase 9
calcd.	calculated
Cit	Citrulline
COSY	^1H - ^1H Correlation spectroscopy
Cq	quaternary carbon
CSA	camphor sulfonic acid
d	doublet
dHAA	dehydroascorbic acid
DAR	drug to antibody ratio
DCC	<i>N,N</i> -dicyclohexylcarbodiimide
DIPEA	<i>N,N</i> -diisopropylethylamine
DMAP	4-dimethylaminopyridine
DME	dimethoxyethane
DMEM	Dulbecco's modified Eagle medium
DMF	<i>N,N</i> -dimethylformamide
DMSO	dimethylsulfoxide
DNS	dansyl or 5-(Dimethylamino)naphthalene-1-sulfonyl
DUPA	2-(3-((S)-5-amino-1-carboxypentyl)ureido)pentanedioic acid
EEDQ	2-Ethoxy-1-ethoxycarbonyl-1,2-dihydroquinoline
EPR	enhanced permeability and retention effect
equiv.	equivalents
ESI-MS	electrospray ionization-mass spectrometry
Et ₂ O	diethyl ether

FBS	fetal bovine serum
Fmoc	9-fluorenylmethyloxycarbonyl
GSH	glutathione
HAMA	human anti mouse antibody
HBTU	<i>N,N,N',N'</i> -Tetramethyl- <i>O</i> -(1H-benzotriazol-1-yl)uronium hexafluorophosphate
HC	heavy chain
HEPES	<i>N</i> -2-Hydroxyethylpiperazine- <i>N'</i> -2-Ethanesulfonic Acid
HOBt	1-hydroxybenzotriazole
HOAt	7-aza-1-hydroxybenzotriazole
HPLC	high performance liquid chromatography
HRMS	high resolution mass spectrometry
HSQC	heteronuclear single quantum correlation spectroscopy
IBCF	isobutyl chloroformate
IC ₅₀	half maximal inhibitory concentration
IEDDA	inverse electron demand Diels-Alder
iPrOH	isopropanol
<i>J</i>	coupling constant
<i>k</i>	kinetic constant
<i>k_a</i>	acid dissociation constant
<i>K_d</i>	dissociation constant
LC	light chain
LC-MS	liquid chromatography-mass spectrometry
<i>m</i>	multiplet
mAb	monoclonal antibody
MALDI	matrix-assisted laser desorption/ionization
MD	molecular dynamics
MED	minimum effective dose
MeOH	methanol
MMAE	Monomethyl Auristatin E
MMAF	Monomethyl Auristatin F
MS	mass spectrometry
MTD	maximum tolerated dose
NaPi	phosphate buffer
NEAA	non essential amino acids
NHS	<i>N</i> -hydroxy succinimide
NMM	<i>N</i> -methyl morpholine
NMR	nuclear magnetic resonance

NOESY	Nuclear Overhauser effect spectroscopy
PABA	<i>para</i> -amino benzylalcohol
PBD	pyrrolobenzodiazepines
PBS	phosphate buffered saline
PDB	protein data bank
PEG	polyethylene glycol
PFB	2,3,4,5,6-pentafluorobenzyl
PG	protecting group
ppm	parts per million
pyr	pyridine
q	quartet
R	substituent
RP-HPLC	reversed phase high performance liquid chromatography
rt	room temperature
s	singlet
ScFv	single chain variable fragment
SMDC	small molecule drug conjugate
SPAAC	strain promoted azido alkyne cycloaddition
Su	succinimide
sx	sextuplet
t	triplet
t _R	retention time
TCO	trans cyclooctene
TDC	Thiomab drug conjugate
Tf ₂ O	trifluoromethanesulfonic anhydride
TFA	trifluoroacetic acid
THF	tetrahydrofuran
TLC	thin layer chromatography
TMS	tetramethylsilane
UV	ultraviolet
Val	valine
z	charge

Introduction

- 1.1 Ligand targeted drug delivery
- 1.2 References

Cancer is the main health problem worldwide and the second cause of death in developed countries.^[1] Nowadays, mainly used therapeutic strategies to treat cancer include surgery, radiotherapy, immunotherapy and chemotherapy.^[2] Mechlorethamine was the first chemotherapeutic agent introduced in 1949 and it acts by irreversibly alkylating the DNA. Since then, several cytotoxic molecules were introduced in the market and are still used in current therapies. Most famous examples include methotrexate (1953), vincristine (1963), doxorubicin (1974), paclitaxel (1992), among other alkaloids, alkylating drugs and antibiotics.^[3] This class of compounds, belonging to conventional chemotherapeutics, exert their effects on fast proliferating cells, such as cancer cells. However, this property is not enough to achieve selectivity, and therefore healthy tissues are also affected by the chemotherapeutic agent. Most affected tissues include bone marrow, skin, gastrointestinal tract, kidneys, but also heart and lungs experience the negative effect of the drug. For instance, in **Figure 1.1** it is reported the bio-distribution of ^{11}C radiolabelled paclitaxel in a patient with lung tumour. One hour after the injection, the highest percentage of the drug is up-taken by the liver.^[4]

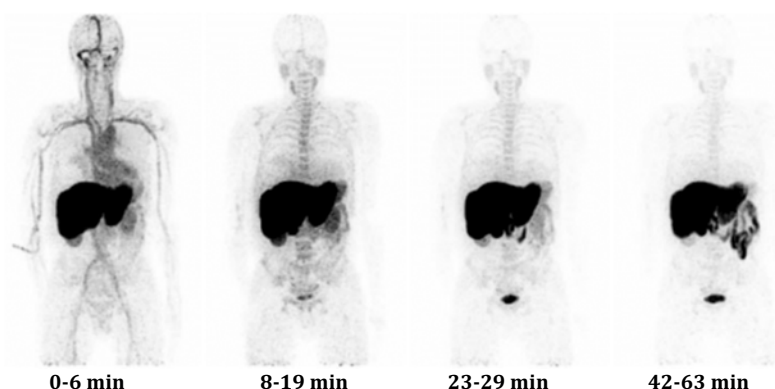


Figure 1.1: tissue up-take of radiolabelled ^{11}C paclitaxel. The highest amount of the drug is found in liver and spleen.^[4]

As a main consequence, patients receiving chemotherapy experience severe collateral effects, both immediate (acute toxicity) and after the treatment (chronic toxicity).^[5] Moreover, drug absorption from healthy tissues limits the amount of the drug able to reach the tumour site, therefore the therapy efficiency is notably reduced. A study

reported in 2004 showed that among 5-year survival cases in the USA, only 2.1 % was achieved by using chemotherapeutics alone.^[6]

To overcome these problems, targeted tumour therapy has emerged as one of the most promising strategies. Paul Ehrlich first introduced this concept in 1900: his 'magic bullet' consists in an agent that can kill microbes or, more generally, malignant cells, while not affecting healthy organs.^[7] This concept represents the basis of modern selective tumour chemotherapy, which consists in an emerging class of therapeutics able to target and exert their toxic effect uniquely in tumour cells, overcoming problems arising from conventional chemotherapy. The increasing interest in tumour selective therapy has produced a high number of tumour specific drugs introduced in the market in the last 20 years. According to a study performed in 2014, 65 of the 89 drugs approved by the FDA since the 2000s are selective drugs.^[3] This has been achieved owing to the progresses in cancer metabolism, function and signalling pathways knowledge. For example, new drugs acting on specific pathways of cancer cells have been developed.^[8-10] Great advances have been made in tumour immunology and eliciting an immunological response against cancer cells is a rising trend in tumour therapy.^[11-13]

Moreover, the design of selective delivery methods, able to increase the local concentration of toxic molecules and control drug bio-distribution, have improved the efficiency of pre-existing drugs and allowed the use of highly toxic ones. This is the case of compounds with high cytotoxicity (toxicity of nanomolar or picomolar range) that could not be used at the optimal dose due to critical side effects, such as dolostatin analogues, duocarmycins or pyrrolbenzodiazepines (PBD).^[14]

For the selective delivery of toxic cargos to the disease site, it is possible to take advantage of the different properties between tumour and healthy tissues. As an example, tumour tissues present leaky vasculature due to abnormal angiogenesis. This produces the so called enhanced permeability and retention effect (EPR), which allows preferential accumulation of nanoparticles at tumour site.^[15-18] This is known as the passive targeting approach. Furthermore, it is well known that the alteration of tumour cell pathways produces modifications on the cell membrane. This leads to the exposure on cell surface of antigens and receptors mainly or uniquely expressed in diseased

tissues. The use of ligands with high affinity towards these receptors allows active targeting of cancer cells. Such approach is a promising strategy to alter the bio-distribution of the drug in favour of cancer tissues, avoiding problems arising from conventional chemotherapy.

1.1 Ligand targeted drug delivery

Ligand mediated drug delivery is one of the best strategies to target pathologic cells. The high affinity of a ligand to its receptor allows the accumulation of the toxic compound at the disease site and, consequently, an efficient cell killing after ligand-drug system metabolization. The general structure of a ligand targeted drug delivery system is represented in **Figure 1.2**.^[19] It consists of the targeting moiety, connected through a linker and eventually a spacer to the therapeutic payload.

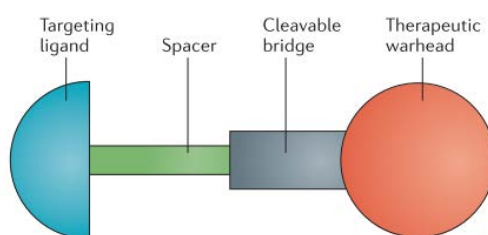


Figure 1.2: schematic representation of a ligand targeted drug delivery system.^[19]

Compared to conventional chemotherapy, this approach presents many advantages: toxic payloads are delivered to cancer cells selectively, without affecting healthy ones and considerably reducing side effects. The drug reaches high concentration at disease site, therefore lower amount of drug can be administered. This permits the use of highly toxic compound since the maximum tolerated dose (MTD) is notably increased through the use of a targeted delivery system. In fact, ligand-drug conjugates, compared to chemotherapeutics alone, present a better therapeutic window, a factor that is defined as the ratio between the maximum tolerated dose and the minimum effective dose (MED, **Figure 1.3**).^[19-21]

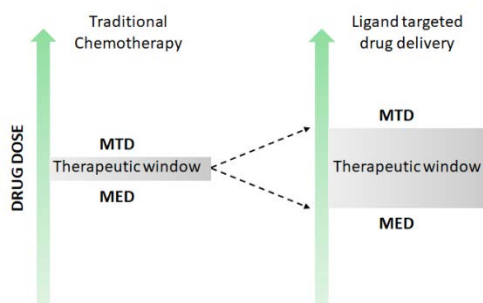


Figure 1.3: Schematic representation of the therapeutic index. Ligand targeted drug delivery expands the therapeutic window of traditionally used chemotherapeutic agents.

The presence of specific tumour markers and selection of the appropriate target is the first step in designing a targeted delivery system directed against tumour tissues. In principle, the target receptor must be exposed exclusively in pathologic cells. However, also different levels of expression between healthy and cancer cells or different receptor isoforms are enough to accomplish selectivity. Receptor expression must be at least 3-times greater in tumour tissues than in healthy ones to avoid off-target toxicity.^[22-24] For instance, Her2 receptor has been efficiently targeted with several ligands to develop new breast cancer treatments, despite it presents only a 2-fold increased expression in tumour tissues compared to healthy ones.^[25-28] Targeted receptors should have a high internalization rate and recycling rate. This would allow the best efficiency in terms of drug internalization, which is fundamental to reach the minimum intracellular drug concentration needed to produce the desired toxic effect.^[21] Most receptors used for targeting are expressed on cell surface.^[21] This is the case of the aforementioned Her2, a membrane protein belonging to the protein kinase families, which is involved in tumour signalling pathways for cell growth and survival. Its overexpression is directly correlated with malignant transformations and its presence is directly associated with poor prognosis in breast, ovarian and gastric cancers.^[29,30] The overexpression of CD30 receptor on lymphoma cells allows its targeting with antibodies for treatment of hematopoietic malignancies, such as large cell lymphoma and Hodgkin lymphoma.^[31] CD33 receptor up-regulation is useful for targeting acute myeloid leukaemia cells.^[32] Aberrant glycosylation pathways cause the expression of abnormal MUC1 bearing truncated carbohydrate forms. Tumour associated MUC1 can be targeted by specific antibodies for drug delivery.^[33] All these

proteins are membrane receptors, but also intracellular targets have been used for selective therapy.^[34] In lack of a specific cell receptor overexpression, tumour environment with its specific markers can be targeted using appropriate ligands.^[35,36] On the other hand, different ligands may be used to address tumour targets. They include both small molecule ligands and inhibitors,^[37] peptides,^[38,39] aptamers,^[40-42] vitamins^[43,44] and antibodies.^[45-47]

As we have commented, the choice of the suitable target is the first step in designing a targeted delivery system directed against tumour cells. However, the efficacy of the entire complex depends on many other factors. The drug, for example, needs to be released inside the target cell, and this can be achieved by using an appropriate linker. Chemical linkage between the targeting ligand and the drug needs to be controlled and carefully designed to obtain stable and functional delivery systems.

In this PhD dissertation, the linker for controlled drug release from ligand-targeted delivery system will be studied and applied to the design of small molecule drug conjugates (SMDC) and antibody drug conjugates (ADC). In the case of ADCs, new compounds bearing a reactive tag for controlled conjugation with the antibody will be investigated.

1.2 References

- [1] R. L. Siegel, K. D. Miller, A. Jemal, *CA. Cancer J. Clin.* **2018**, *68*, 7–30.
- [2] N. Dan, S. Setua, V. K. Kashyap, S. Khan, M. Jaggi, M. M. Yallapu, S. C. Chauhan, *pharmaceuticals* **2018**, *11*, 32.
- [3] J. Sun, Q. Wei, Y. Zhou, J. Wang, Q. Liu, H. Xu, *BMC Syst. Biol.* **2017**, *11*, 87.
- [4] A. A. M. Van der Veldt, N. H. Hendrikse, E. F. Smit, M. P. J. Mooijer, A. Y. Rijnders, W. R. Gerritsen, J. J. M. van der Hoeven, A. D. Windhorst, A. A. Lammertsma, M. Lubberink, *Eur. J. Nucl. Med. Mol. Imaging* **2010**, *37*, 1950–1958.
- [5] V. Schirmacher, *Int. J. Oncol.* **2019**, *54*, 407–419.
- [6] G. Morgan, R. Ward, M. Barton, *Clin. Oncol.* **2004**, *16*, 549–560.
- [7] R. S. Schwartz, *N. Engl. J. Med.* **2004**, *350*, 1079–1080.
- [8] R. Nahta, F. J. Esteva, *Cancer Lett.* **2006**, *232*, 123–138.
- [9] T. Vu, F. X. Claret, *Front. Oncol.* **2012**, *2*, 1–6.
- [10] G. Marcucci, D. Perrotti, M. A. Caligiuri, *Clin. Cancer Res.* **2003**, *9*, 1248–1252.
- [11] I. Melero, S. Hervas-Stubbs, M. Glennie, D. M. Pardoll, L. Chen, *Nat. Rev. Cancer* **2007**, *7*, 95.
- [12] C. N. Baxevanis, S. A. Perez, M. Papamichail, *Crit. Rev. Clin. Lab. Sci.* **2009**, *46*, 167–189.
- [13] D. M. Pardoll, *Nat. Med.* **1998**, *4*, 525–531.
- [14] Y. Wang, Y. Li, X. Liu, X. Lu, X. Cao, B. Jiao, *Mar. Drugs* **2017**, *15*, 18.
- [15] T. M. Allen, P. R. Cullis, *Science (80-.)*. **2004**, *303*, 1818–1822.
- [16] H. Maeda, Y. Matsumura, *Cancer Res.* **1986**, *46*, 6387–6392.
- [17] S. Tran, P.-J. DeGiovanni, B. Piel, P. Rai, *Clin. Transl. Med.* **2017**, *6*, 44.
- [18] D. Rosenblum, N. Joshi, W. Tao, J. M. Karp, D. Peer, *Nat. Commun.* **2018**, *9*, 1410.
- [19] M. Srinivasarao, C. V Galliford, P. S. Low, *Nat. Rev. Drug Discov.* **2015**, *14*, 203–219.
- [20] T. M. Allen, *Nat. Rev. Cancer* **2002**, *2*, 750–763.
- [21] M. Srinivasarao, P. S. Low, *Chem. Rev.* **2017**, *117*, 12133–12164.
- [22] N. Parker, M. J. Turk, E. Westrick, J. D. Lewis, P. S. Low, C. P. Leamon, *Anal. Biochem.* **2005**, *338*, 284–293.
- [23] N. Nomura, S. Pastorino, P. Jiang, G. Lambert, J. R. Crawford, M. Gymnopoulos, D.

- Piccioni, T. Juarez, S. C. Pingle, M. Makale, et al., *Cancer Cell Int.* **2014**, *14*, 26.
- [24] S. Eckerle, V. Brune, C. Döring, E. Tiacci, V. Bohle, C. Sundström, R. Kodet, M. Paulli, B. Falini, W. Klapper, et al., *Leukemia* **2009**, *23*, 2129–2138.
- [25] N. Ponde, P. Aftimos, M. Piccart, *Curr. Treat. Options Oncol.* **2019**, *20*, 37.
- [26] S. Loibl, L. Gianni, *Lancet* **2017**, *389*, 2415–2429.
- [27] I. Kümler, M. K. Tuxen, D. L. Nielsen, *Cancer Treat. Rev.* **2014**, *40*, 259–270.
- [28] R. Seshadri, F. A. Firgaira, D. J. Horsfall, K. McCaul, V. Setlur, P. Kitchen, *J. Clin. Oncol.* **1993**, *11*, 1936–1942.
- [29] A. Ruiz-Saenz, M. M. Moasser, *J. Clin. Oncol.* **2016**, *118*, 6072–6078.
- [30] W. Tai, R. Mahato, K. Cheng, *J. Control. Release* **2010**, *146*, 264–275.
- [31] C. A. Van Der Weyden, S. A. Pileri, A. L. Feldman, J. Whisstock, H. M. Prince, *Blood Cancer J.* **2017**, *7*, 603.
- [32] A. A. Laing, C. J. Harrison, B. E. S. Gibson, K. Keeshan, *Exp. Hematol.* **2017**, *54*, 40–50.
- [33] P. R. Hamann, L. M. Hinman, C. F. Beyer, L. M. Greenberger, C. Lin, D. Lindh, A. T. Menendez, R. Wallace, F. E. Durr, J. Upešlacis, *Bioconjug. Chem.* **2005**, *16*, 346–353.
- [34] L. Rajendran, H. J. Knölker, K. Simons, *Nat. Rev. Drug Discov.* **2010**, *9*, 29–42.
- [35] F. Danhier, O. Feron, V. Prétat, *J. Control. Release* **2010**, *148*, 135–146.
- [36] R. Raavé, T. H. van Kuppevelt, W. F. Daamen, *J. Control. Release* **2018**, *274*, 1–8.
- [37] C. S. Kue, A. Kamkaew, K. Burgess, L. V. Kiew, L. Y. Chung, H. B. Lee, *Med. Res. Rev.* **2016**, *36*, 494–575.
- [38] Y. Wang, A. G. Cheetham, G. Angacian, H. Su, L. Xie, H. Cui, *Adv. Drug Deliv. Rev.* **2017**, *110*, 112–126.
- [39] E. I. Vrettos, G. Mező, A. G. Tzakos, *Beilstein J. Org. Chem.* **2018**, *14*, 930–954.
- [40] W. Xuan, Y. Peng, Z. Deng, T. Peng, H. Kuai, Y. Li, J. He, C. Jin, Y. Liu, R. Wang, et al., *Biomaterials* **2018**, *182*, 216–226.
- [41] B. Powell Gray, L. Kelly, D. P. Ahrens, A. P. Barry, C. Kratschmer, M. Levy, B. A. Sullenger, *Proc. Natl. Acad. Sci.* **2018**, *115*, 4761–4766.
- [42] G. Zhu, G. Niu, X. Chen, *Bioconjug. Chem.* **2015**, *26*, 2186–2197.
- [43] G. Russell-Jones, K. McTavish, J. McEwan, J. Rice, D. Nowotnik, *J. Inorg. Biochem.* **2004**, *98*, 1625–1633.

- [44] A. Pettenuzzo, R. Pigot, L. Ronconi, *Eur. J. Inorg. Chem.* **2017**, 2017, 1625–1638.
- [45] P. Polakis, *Pharmacol. Rev.* **2016**, 68, 3–19.
- [46] H. Yao, F. Jiang, A. Lu, G. Zhang, *Int. J. Mol. Sci.* **2016**, 17, 194.
- [47] R. V. J. Chari, M. L. Miller, W. C. Widdison, *Angew. Chemie - Int. Ed.* **2014**, 53, 3796–3827.

Background

2.1 Antibody Drug Conjugates

2.1.1 Site-selective ADC chemistry

2.1.1.1 Non-natural amino acid introduction

2.1.1.2 Disulfide stapling

2.1.1.3 Thiomab antibodies

2.2 Linker chemistry in ADC synthesis

2.2.1 Chemical cleavable linkers

2.2.2 Enzyme cleavable linkers

2.3 Small Molecules Drug conjugates

2.4 References

To date, several targeted delivery systems have been developed for tumour therapy. They may differ in target and ligand choice, linker chemistry and drug conjugated.^[1] Each of these delivery systems may have advantages and disadvantages, and the selection depends on the tumour to be treated and its accessibility. In this chapter, critical features of antibody-drug conjugates and the main progresses made in the field during the last years will be described. Moreover, some successful application of small molecule drug conjugates for drug delivery will be commented.

2.1 Antibody Drug Conjugates

Antibody drug conjugates (ADC) are targeted systems that take advantage of the high affinity that monoclonal antibodies (mAb) present towards their antigens, normally located in cancer cells, to deliver a toxic payload to cancer tissues. The general structure of an ADC consists of an antibody connected through a linker, either cleavable or non-cleavable one, to a highly cytotoxic drug (**Figure 2.1**).



Figure 2.1: schematization of an ADC structure.

After target recognition and binding, ADC is, in general, internalized through receptor-mediated endocytosis. In this process, it is trafficked to the endosome and lysosome, where it is metabolized. Herein, the drug is released through different mechanisms, depending on the linker structure. Lysosomal proteolytic enzymes digest the ADC, in the case of non-cleavable linker, and an active metabolite of the drug is released.^[2] In presence of a cleavable linker, endosomal and lysosomal conditions themselves can trigger the release of the drug (**Figure 2.2**).^[3] A recent work demonstrates the importance of these processes and the influence of its regulators on ADC final toxicity.^[4] After internalization, receptor is recycled and re-exposed to cell-surface.^[5] This is the

mechanism accepted for most ADCs developed so far; however, in the last years the use of non-internalizing antibody conjugates has emerged as a new strategy to deliver the drug. In this case, a cleavable linker is fundamental to allow extracellular release of the drug and its subsequent diffusion inside the target cell. [6,7]

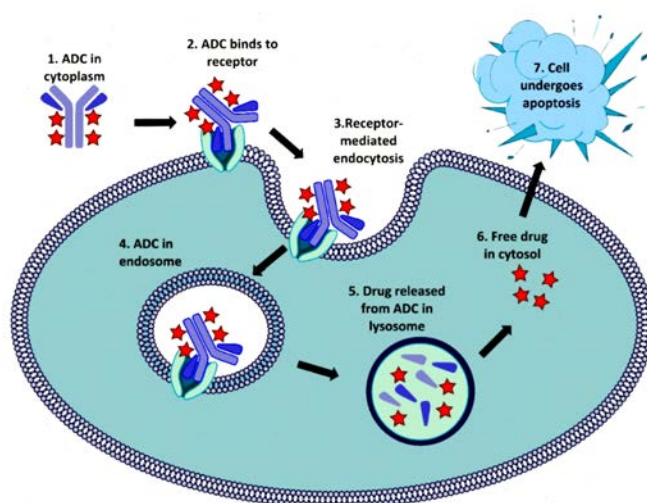


Figure 2.2: schematization of ADC binding and internalization in cancer cells.[8]

Optimization of each component of an ADC is essential to achieve efficiency *in vivo*. For instance, conjugation chemistry is important to define the pharmacokinetic properties and affinity of the ADC. Depending on antibody and receptor properties, adequate linker chemistry needs to be developed. On the other hand, drug properties, in combination with the linker chosen, have a direct effect on ADC toxic effect in tumours.[9-11]

From an historical point of view, examples of ADC injected in mice have emerged in the literature in late 1980s,[12] and in the late 90s the first ADC reached the clinical trials. This was the case of BR96-doxorubicin conjugate; this ADC consists of the murine antibody BR96, targeting Lewis Y antigen, conjugated to doxorubicin through an acid cleavable hydrazone linker (**Figure 2.3 a**).

However, this first ADC failed in the clinical trials due to no net clinical benefit when compared to the free drug administration. Indeed, while localization studies displayed

the ability of the antibody to accumulate in breast cancer cells, Phase I and Phase II clinical trials showed that this was not sufficient to enhance the toxicity compared to the parental drug.^[13] The same happened to other ADCs, containing methotrexate and desacetylvinblastine as drugs. The failure of these first-generation ADCs was due to several issues. Firstly, the drug was not toxic enough. In fact, targeted drug delivery with ADC causes a lower concentration of the drug inside the cell; this depends on the rate of receptor binding and internalization processes. Therefore, more potent payloads are required for the development of powerful conjugates.^[14] Secondly, original ADCs made use of murine antibodies for targeting, which elicited an immune response in patients after treatment. Human Anti Mouse Antibodies (HAMA) were found in the serum of patients treated with these ADCs.^[15] This was detrimental for the therapeutic activity, since the ADC presented a faster clearance rate.^[14]

To improve these initial results, a second-generation ADC was developed, addressing the problems of first immunoconjugates. Conventional drugs were substituted with more toxic payloads, such as auristatines, maytansinoids, duocarmycins and pyrrolobenzodiazepines (PBD). Moreover, the immunogenicity of murine antibodies was avoided using chimeric or humanized variants. These improvements led to the commercialization of three ADCs:

1. Gemtuzumab-ozogamicine (Mylotarg, **Figure 2.3 b**), which was approved for the treatment of acute myeloid leukaemia,^[16-18]
2. Trastuzumab-emtansine (Kadcyla, **Figure 2.3 c**), which was approved for the treatment of metastatic breast cancer,^[19] and
3. Brentuximab vedotin (Adcetris, **Figure 2.3 d**) for the treatment of Hodgkin's Lymphoma and T-cell lymphoma.^[20]

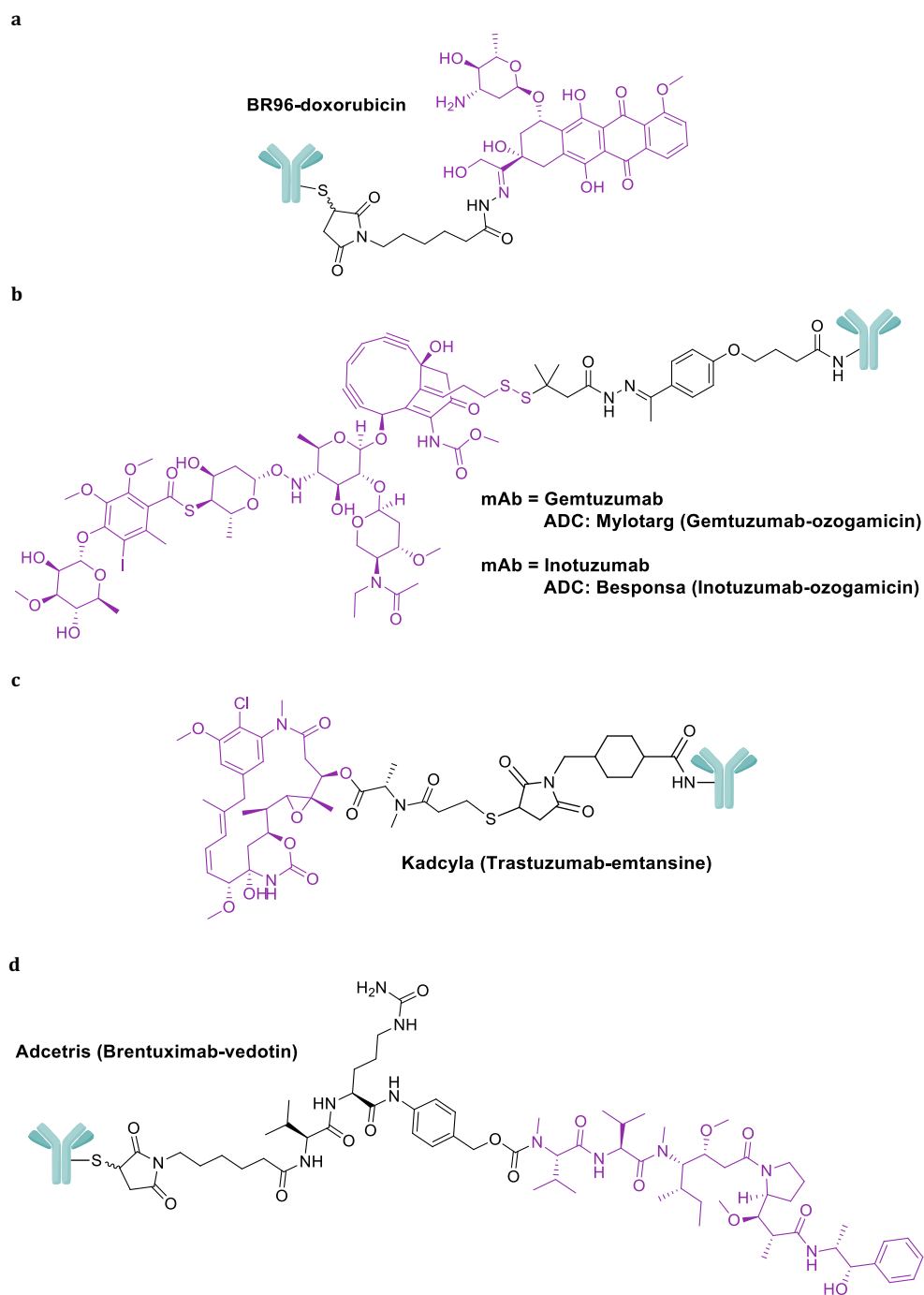


Figure 2.3: structures of the second-generation of ADCs approved by FDA.

Mylotarg targets CD33 expressing cells. Its acid sensitive hydrazone linker is hydrolysed in the endosomes, releasing calicheamicin. On the other hand, Trastuzumab-DM1 conjugate is obtained by reacting lysines with a DM1 drug derivative. The antibody targets Her2 expressing cells, and after internalization and cell metabolization, DM1 acts by inhibiting tubulin polymerization. Kadcyla is based on the chimeric brentuximab antibody that targets leukemic cells with high expression of CD30 receptor. This conjugate features a valine-citrulline linker, which after internalization is cleaved by protease action and self-immolation of *para*-aminobenzyl alcohol (PABA) spacer allows the release of free MMAE, which exerts a toxic function by inhibiting tubulin polymerization.

Inotuzumab ozogamicin is the last ADC approved by the FDA in 2017. It presents the same drug-linker system of Mylotarg, but it targets CD22 antigen, which is an objective for the treatment of refractory and relapsed acute lymphocytic leukaemia.^[21]

Considering these examples, it is clear that humanized or fully human antibodies need to be used to improve the efficacy of the ADCs. Although all ADCs approved to date present the IgG (immunoglobulin) presentation, new antibody formats are emerging as an interesting alternative for drug delivery.^[22,23] For instance, the antigen binding fragment (Fab),^[24] avoiding the use of the whole antibody, has been successfully used for the delivery of highly toxic pyrrolobenzodiazepine drug. Equally, single chain variable fragments (ScFv) have been used for the modification with cytotoxic drugs and fluorophores for internalization studies.^[25] Such fragments are more easily manufactured and their smaller structure favours tumour penetration, especially in solid tumours. Also, they exhibit faster clearance rate, which may reduce off-target toxicity.^[26]

Many other features may be improved to enhance ADC potency *in vivo*. First, all ADCs approved so far are heterogeneous mixtures of conjugates. Each conjugate has a different Drug to Antibody Ratio (DAR), a value that has significant influence in its properties and thus need to be carefully controlled through site-specific conjugation methods.

Linker properties are also pivotal to achieve efficacy *in vivo*. To date, most of clinically used ADC relies on a cleavable linker for the intracellular release of the drug. These two aspects will be described in detail in the following sections.

2.1.1 Site-selective ADC chemistry

Conjugation strategy considerably affects the properties of the final ADC, since it can lead to homogenous or heterogeneous ADC mixtures. Heterogeneous ADCs present several issues. First, reaction conditions need to be carefully controlled when using non-selective conjugation methods to avoid batch to batch differences.^[27]

Moreover, heterogeneous conjugates present poor pharmacokinetic properties.^[28] As a consequence of the heterogeneous product distribution, part of the therapeutic agent is constituted by unconjugated antibody, which competes with drug-loaded antibody for receptor binding. Depending on its relative amount, efficiency of the treatment can be reduced. For instance, in the case of Kadcyla and Adcetris, free antibody amount is less than 5% and it does not represent an issue, but in Mylotarg more than 50% is unconjugated antibody.^[29]

Moreover, in a specific batch, species with different DARs are present. In such conjugates, the number of drugs attached is reported as an average value, and the heterogeneity renders the characterization of the ADC a challenging task in terms of pharmacokinetic properties and toxic dose. Indeed, conjugates with different DAR present different antitumor activity,^[30] being products with DAR of 2 and 4 the most efficient ones. In general, lower DAR would mean poor toxicity and higher DARs, such as 8, give unstable ADCs, with aggregation issues and faster clearance.^[31,32] These heterogeneous mixtures of ADCs are obtained by using 'conventional' conjugation strategies based on the particular reactivity of the side chains of lysine and cysteine with appropriate chemical reagents. As an example, previously described Trastuzumab-emtansine is obtained by reacting the solvent-exposed lysine residues of the antibody with NHS esters to give amides. Lysine chemistry yields a complex heterogeneous mixture, in terms of number of drugs attached to the antibody and the site of attachment. In trastuzumab-emtansine, an average of 3.5 molecules of DM1 are attached to the antibody, and in general, with this conjugation method, DAR is

statistically distributed from 0 to 8. However, since an antibody contains in average 40 lysine residues, more than one million different conjugates can be generated.^[33]

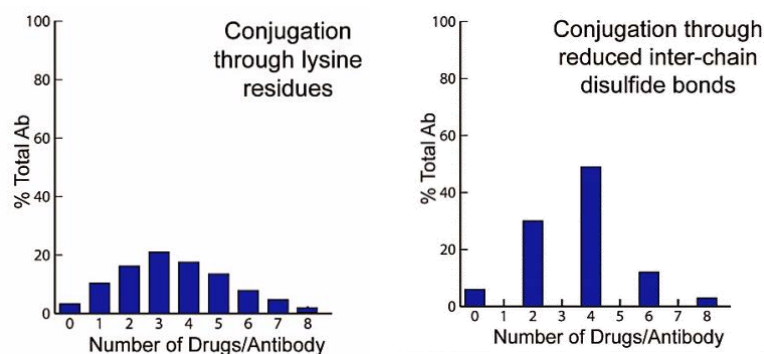


Figure 2.4: DAR distribution in heterogeneous conjugates obtained by reacting lysine (left) or cysteine (right)^[33] residues.

Cysteine is the natural amino acid of choice for conjugation reaction. When dealing with proteins, cysteine is very low abundant, and several proteins bear just one exposed cysteine residue able to react. In antibodies, the situation is more complicated: cysteines in antibodies are normally engaged in disulfide bonds, even intrachain or interchain. While intrachain disulfide bonds are normally buried into the antibody structure, interchain disulfides are more solvent exposed and labile.^[34] Importantly, interchain disulfide bonds are not fundamental to maintain ADC overall structure, which is kept by other non-covalent interactions.^[35]

Conjugation chemistry through interchain thiols improves the results obtained through lysine chemistry, however some degree of heterogeneity is still present (**Figure 2.4**).

Problems deriving from heterogeneous ADC mixtures can be overcome by site-specific antibody drug conjugates, which present a controlled DAR, better pharmacokinetic properties and improved therapeutic index.^[36]

Therefore, conjugation methods to generate site-specific antibody drug conjugates are required. Most efficient site-specific conjugation strategies include the introduction through genetic engineering techniques of unnatural amino acids into the antibody sequence.^[37-39]

Moreover, cysteine engineered antibodies (named Thiomabs) can be produced: these modified antibodies present a unique, highly reactive, solvent exposed cysteine that can be selectively modified.

Also, the use of disulfide-stapling reagents, that react with intrachain reduced thiols, have found wide application for homogeneous ADCs synthesis.^[40-42]

2.1.1.1 Non-natural amino acid introduction

The introduction of non-canonical amino acids into proteins and antibodies has made significant progress in the last years due to the improvement in genetic engineering techniques. Unnatural amino acids, containing aldehyde, azido, alkyne or ketone group have been successfully obtained and purified from *E.Coli*, yeast and mammalian cells.^[43,44]

The protein or the antibody bearing the non-canonical residue can react in a bio-orthogonal fashion with the desired organic compound to obtain homogenous conjugates (**Figure 2.5**).

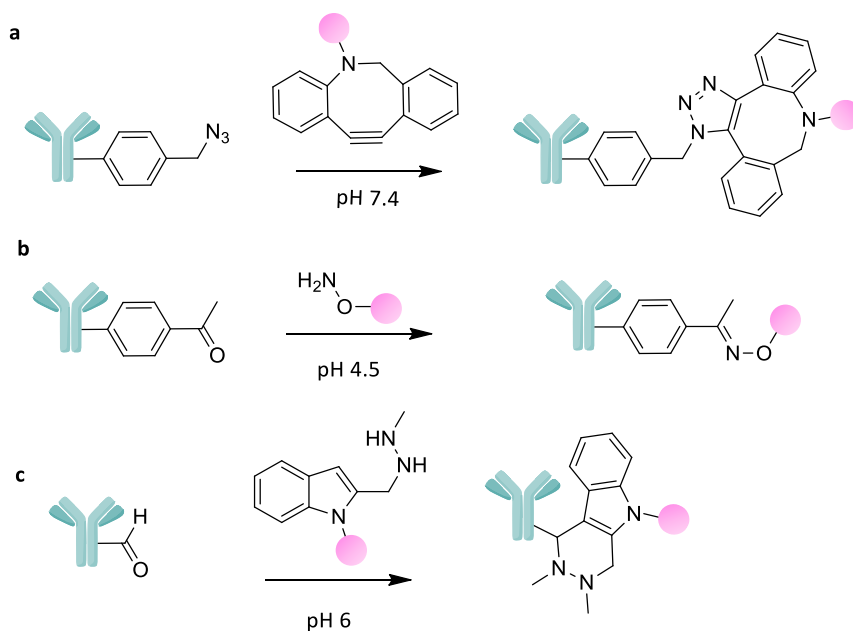


Figure 2.5: examples of non-canonical amino acids present in mAb and their biorthogonal reactivity for site-selective conjugation.

As an example, *p*-azidomethyl-L-phenylalanine has been incorporated into the IgG Trastuzumab, allowing its conjugation via strain-promoted azide-alkyne cycloaddition (SPAAC) with a dibenzocyclooctyl-MMAF derivative. The resulting ADC retained the ability of Trastuzumab to select Her2 positive cells and showed interesting cytotoxicity profile in cell assays (**Figure 2.5 a**).^[45]

In other studies, mAb sequence was modified with the introduction of the unnatural *p*-acetyl-L-phenylalanine residue. The unique ketone underwent oxime ligation with substituted hydroxylamine derivatives, obtaining, under acidic condition, a stable antibody with increased *in vivo* safety (**Figure 2.5 b**).^[46,47]

As above commented, the amino acid substitution can be introduced into the antibody sequence through enzyme assisted modification. Cysteines, when inserted in the **CxPxR** sequence, can be recognised by formylglycine generating enzyme (FGE). These enzymes are able to introduce a formylglycine unit per cysteine, and the aldehyde handle can be in turn modified via Hydrazino-Pictet-Spengler conjugation method with suitable derivatives (**Figure 2.5 c**).^[48,49]

These are some examples of how the introduction of unnatural functional groups in the antibody sequence allows the use of biorthogonal chemistry for the production of chemically-defined ADCs.

2.1.1.2 Disulfide stapling

Site-selective disulfide re-bridging is a modification technique that relies on the use of specific, bifunctional reagents to link covalently reduced intra-chain thiols of an antibody. In this case, natural cysteine reactivity is exploited and the use of an appropriate linker for re-bridging allows the installation of a third functionality for conjugation with a drug. A homogenous ADC with a DAR up to 4 can be obtained through this technology. Moreover, since the modification is inserted far from Fab region, antibody functionalities are not compromised.^[37,50]

Several reagents have been proposed for such purpose.^[41] Mostly used are bifunctional sulfones,^[42,51] bis-substituted maleimides,^[40,52] and pyridazinediones (**Figure 2.6 a**).^[53]

More recently, new reagents have been developed. For example, the use of dibromoxetanes allowed the re-bridging of disulfide bonds in peptides and therapeutic proteins, without altering their activity. Also, application of this technique to the Fab of an anti Her2 antibody improved its stability in plasma and under physiological conditions, compared to the unstable native antibody bearing a disulfide bond.^[54]

Divinyl pyrimidines allowed the functional stapling of the antiHer2 Trastuzumab. Incorporation of MMAE in the structure, produced a homogenous ADC with DAR 4, able to selectively kill Her2 expressing cells (**Figure 2.6 b**).^[55]

Although, in general, ADCs with DAR 4 are easily obtained by employing these techniques, the careful study of the structure of the linker can afford an ADC with a DAR 2. In a recent work, a linker having two dibromopyridazinedione units for molecule, separated by a PEG spacer with appropriate length was used for this purpose. This linker is able to re-bridge 2 disulfide bonds at the same time and can be conjugated with a drug molecule. As a result, an homogeneous and functional ADC with DAR 2 is obtained (**Figure 2.6 c**).^[56]

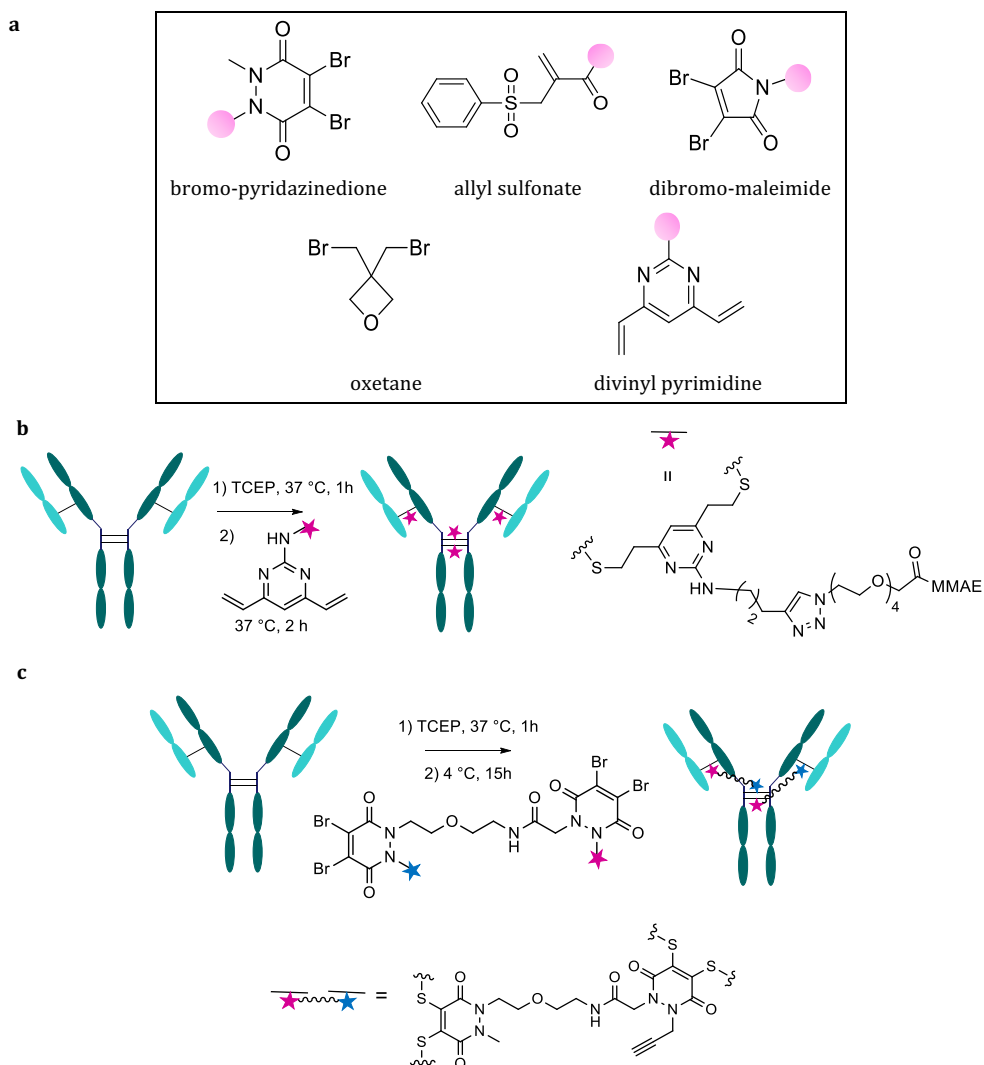


Figure 2.6: a) structure of reagents used for disulfide re-bridging in proteins and antibodies. Pink dots indicate the payload or a functional group that allows further modification; b) reaction between divinyl pyrimidine based reagent and Trastuzumab antibody. Using MMAE as toxic payload, an homogeneous ADC with DAR 4 is obtained; c) specific bis-dibromopyridazinedione linker allows functional rebridging and addition of only 2 functional modules. Reaction of alkyne with adequate azides allows the synthesis of an homogeneous ADC with DAR 2.

2.1.1.3 Thiomab antibodies

Thiomab antibodies are engineered mAb in which a natural amino acid has been replaced by a cysteine. This residue, which is solvent exposed and thus highly reactive, allows site-selective modification. Indeed, after the selected conjugation reaction, it gives a homogeneous antibody with DAR 2. The introduced cysteine is inserted in the constant region of antibody's Fab to not affect antibody's binding ability.^[36]

First Thiomab generated with this technique was an anti MUC16 antibody, bearing a HC-A114C substitution.^[36] The cysteine was introduced easily by site-directed mutagenesis. However, after expression, it was 'blocked' as a mixed disulfide with glutathione or cysteine, as a consequence of the production process. The liberation of the engineered cysteine is not trivial, since it is quite difficult to selectively reduce this disulfide while not affecting intra-chain disulfide bonds. After some optimization of the process, a protocol for selective engineered cysteine liberation was developed: by using TCEP as reducing agent, followed by mild re-oxidation with CuSO_4 or dehydro ascorbic acid (dhAA) free thiol was restored (**Figure 2.7**).

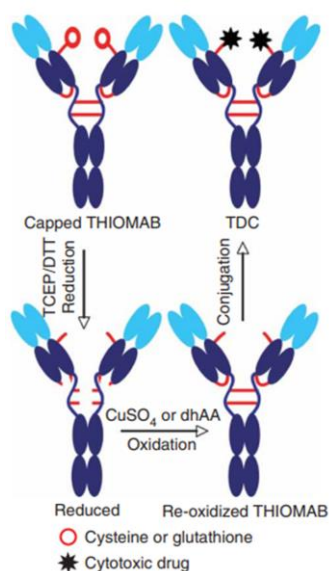


Figure 2.7: Thiomab preparation and cysteine 'decapping' protocol.^[36]

In this way, the engineered Thio-MUC16 was obtained and conjugated to MMAE using maleimide as cysteine selective reagent. The direct comparison between Thiomab conjugate and the ADC obtained by conventional disulfide reduction/alkylation strategy showed that Thiomab drug conjugate (TDC) cytotoxicity is similar to the analogue ADC, but TDC is better tolerated than the conventional ADC. Through this first Thiomab-conjugate it was demonstrated the higher therapeutic index of a site-selective, homogenous conjugate compared to the heterogeneous one.^[36]

Application of Thiomab technology for site-selective conjugates synthesis has been applied to other antibodies, as Trastuzumab. A Trastuzumab bearing an engineered cysteine at position 114 of the heavy chain has been prepared and conjugated with DM1, affording a homogenous ADC with DAR 2. Compared to the commercially available Trastuzumab-emtansine, obtained through non-selective lysine amidation, Thiomab-conjugate showed again improved therapeutic window, having higher efficiency and reduced toxicity *in vivo*.^[57]

When developing a Thiomab antibody particular attention need to be paid to the modification site. Within this context, several studies have shown that the position of modification clearly affects antibody stability.^[58-60] In this respect, since Thiomab conjugates obtained by Michael addition with maleimides can undergo fast retro-Michael in serum, it has been proposed that the choice of a less solvent accessible site for the conjugation could improve this significant issue.^[59]

Moreover, conjugation site and accessibility influences drug-linker metabolism in cell and thus TDC activity.^[61]

Once chosen the conjugation site, most conjugation strategies reported so far for the generation of a homogenous TDC rely on the use of maleimides as Michael acceptors,^[36] disulfide bond formation,^[62] although other conjugation strategies that improve stability of TDC have been proposed.^[63]

2.2 Linker chemistry in ADC synthesis

The linker used to connect the mAb with the drug have a great influence on the final properties of the ADC. As a main aspect, linker has to be highly stable during systemic circulation, in order to avoid uncontrolled release and consequent off-target toxicity.

However, once the target has been reached, the linker must be cleaved and allow the release of the drug to have the desired toxic effect. Depending on their release mechanism, linkers can be divided into two main categories: cleavable and non-cleavable linkers.

Non-cleavable linkers were the first used and they rely on cell metabolism for the release of the drug. Cleavable linkers, on the contrary, depend on a specific trigger to allow drug release. If the trigger is present only inside the cell or limited to the tumour microenvironment, linker integrity during circulation should be ensured. Non-cleavable linkers may be preferred to cleavable ones for their higher stability during systemic circulation. However, several examples have shown that ADCs bearing a non-cleavable linker have a lower *in vivo* efficiency compared to those ADCs bearing a cleavable one.^[64] This might be attributable to a lower toxicity of the drug metabolite that is released and to the impossibility to exert a by-stander effect *in vivo*.^[65] By-stander effect consists in the toxicity induced in nearby cells by a drug released in the extracellular environment. After intracellular ADC metabolization and drug release, if the drug is membrane permeable, it can diffuse to nearby cells and induce toxicity. Due to this effect, tumours that presents an heterogeneous antigen expression could be efficiently treated with the ADC.^[64,66,67]

Moreover, the use of a cleavable linker is fundamental in non-internalizing ADCs, where the drug need to be released in the extracellular environment to enter in the target cell.^[68]

Currently, around 75% of clinically used ADCs present a cleavable linker in their structure, pointing out their fundamental importance.

Depending on the stimulus that triggers the release of the drug, the linkers can be divided in chemically and enzymatically cleavable linkers.

2.2.1 Chemical cleavable linkers

Chemically cleavable linkers are sensitive to a chemical variation, such as pH, reductive potential, or to the presence of a specific compound that triggers the cleavage.

Acid cleavable linkers rely on different stability in acid or neutral media to allow drug release. The cleavage occurs under acidic conditions, while in neutral or basic media the linker is stable. *Chapter 5* is focused on the synthesis of new acid-cleavable linkers for ADC design; thus, this type of linker will be described there in detail.

Reducible linkers are disulfide bonds susceptible to the variation of reduction potential between intracellular compartments and circulation. Such difference is due to a higher concentration of glutathione inside the cell (1-10 mM), compared to its plasma concentration (2-20 μ M). Furthermore, intracellular glutathione levels are even higher in tumour cells.^[69] These variations allows conditional drug release from reducible disulfide linkers.

Regarding their application, reductively cleavable linkers have been used for the controlled intracellular release of maytansine derivatives, a class of compounds that act by inhibiting tubulin polymerization (**Figure 2.8 a**). Conjugates bearing a labile disulfide present a higher efficacy *in vivo*, when compared to analogues bearing a non-cleavable linker.^[70,71]

Since most drugs do not present a thiol in their structure, a carbamate self-immolative spacer is added, to allow the traceless release of the toxic compound. In this way, MMAE and PBD were conjugated to antibodies and, after disulfide cleavage, native drug was efficiently released inside the target cell (**Figure 2.8 b**).^[72]

Moreover, cysteine in antibodies can be directly paired into a disulfide bond to obtain a reducible linker inside the structure. These types of disulfide linker have shown promising activity due to their higher stability caused by the less accessible disulfide bond, which is close to the antibody (**Figure 2.8 c**).^[73]

Notably, tumour microenvironment features, in general, a high glutathione concentration, which besides is increased due to glutathione release by dying cells. As a consequence, the use of reducible disulfide has been used for the efficient drug release in non-internalizing ADC.^[6]

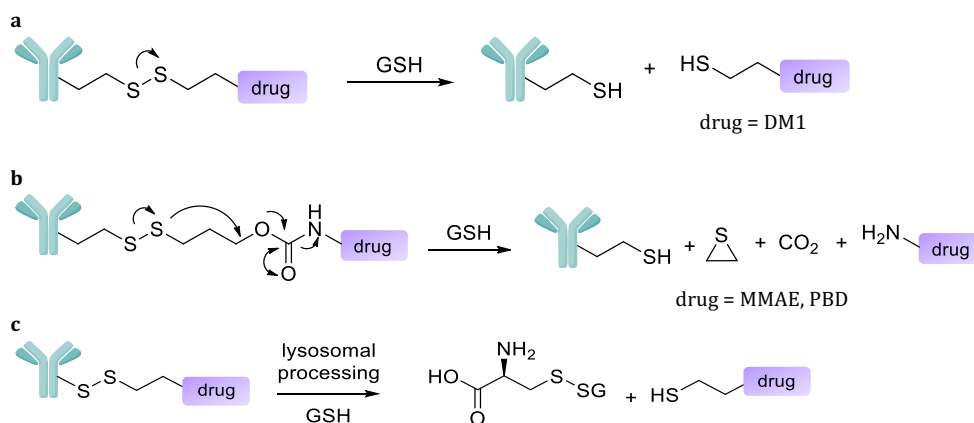


Figure 2.8: schematization of drug release from ADCs bearing disulfide cleavable linkers.

To date, both acid labile and disulfide cleavable linkers represent the most widespread chemically labile linkers employed in ADC design. However, new release strategies are being developed. For example, it is possible to take advantage of high Fe (II) concentration inside tumour cell and its microenvironment. A trioxolane based linker, susceptible to the occurrence of Fe (II) has been designed for MMAE conjugation and smart release from a Her2 targeting antibody (**Figure 2.9**). The conjugate presents excellent stability and selectivity towards Her2 positive cells, with IC_{50} values comparable to free MMAE.^[74]

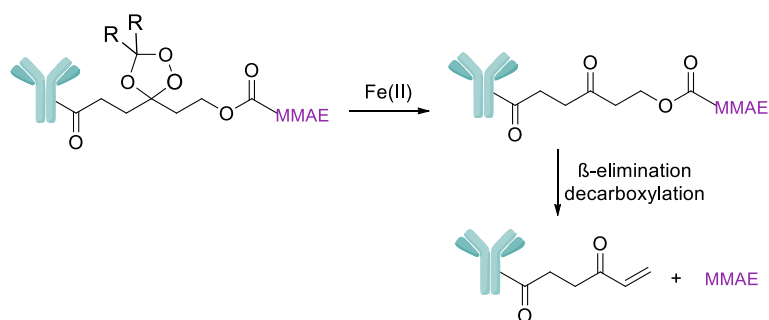


Figure 2.9: Fe(II)-mediated release from an antiHer2 antibody.

Moreover, external chemicals can be used for the intracellular release of a drug. Within this context, the advances in biorthogonal chemistry has led to the development of new

reagents able to react in a selective way with specific functional groups. Importantly, such compounds do not react with the great variety of organic moieties present in biological systems.^[75,76] Following this trend, several linkers, susceptible to the presence of an external reagent, have been applied to the design of ADCs. In general, bio-orthogonally cleavable linkers present increased stability compared to 'conventional' cleavable linkers due to their resistance to endogenous stimulus.

As an example, Pd complexes can be used to trigger the cleavage of a thioether propargyl carbamate linker (**Figure 2.10 a**). Thioether function directs palladium triggered cleavage, which induces carbamate elimination and release of the active drug. Such strategy was efficiently applied to the development of a doxorubicin prodrug. An anti-Her2 nanobody delivers the prodrug in cancer cells; once there, palladium activates the drug, which in turn is able to induce its toxic effect.^[77]

Also, tetrazines have been used for the decaging of drugs from an ADC containing *trans*-cyclooctene (TCO) linker. This Inverse Electron Demand Diels-Alder (IEDDA) is one of the fastest bio-orthogonal reactions developed, having a kinetic constant up to $1 \cdot 10^6 \text{ M}^{-1} \text{ s}^{-1}$, that renders it suitable for chemistry in living systems.^[78]

In this context, Robillard has reported the use of a bifunctional linker for ADC synthesis, bearing a TCO-MMAE pro-drug (**Figure 2.10 b**). ADC is stable as the native antibody and able to release MMAE. This work represents the first time a biorthogonal linker was tested *in vivo*, producing a tumour regression in mice. ^[79]

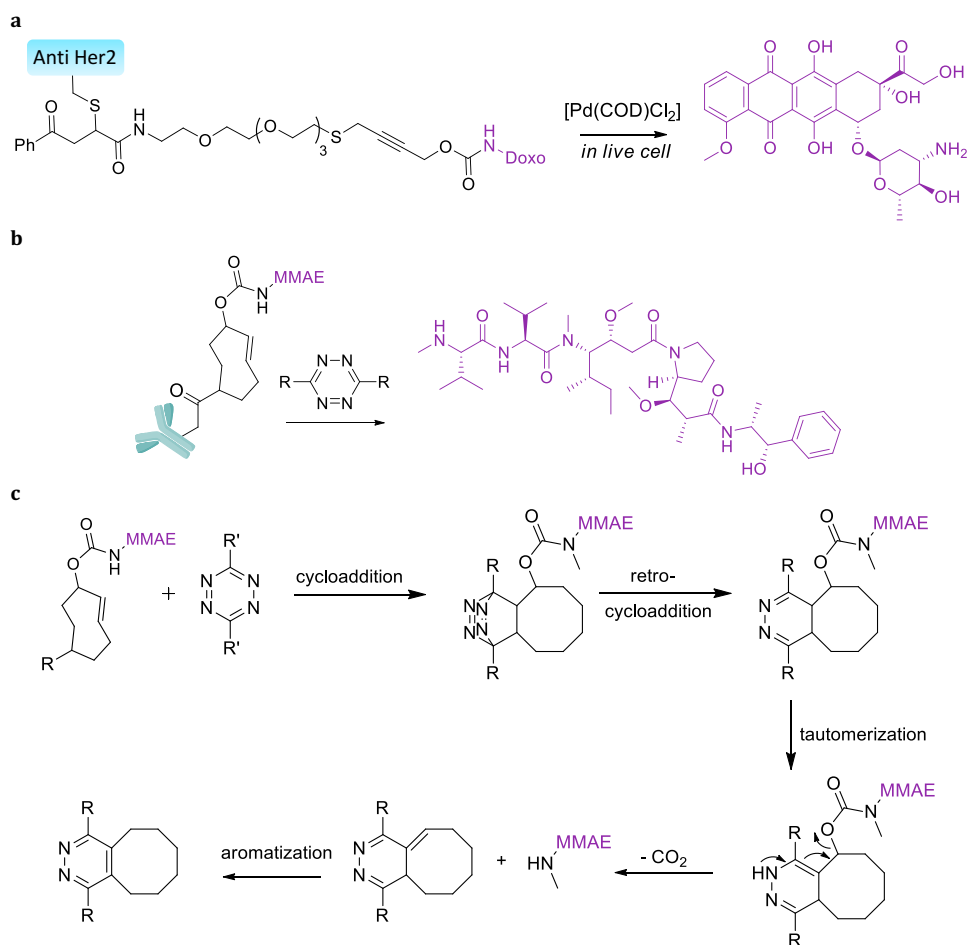


Figure 2.10: a) a thioether propargyl carbamate linker for *in vitro* decaging with Pd complexes; b) TCO-tetrazine mediated release of MMAE and c) IEDDA release mechanism.

However, the decaging yield *in vivo* is often low due to the fast clearance rate of the small organic compound. As an example, tetrazines are cleared from circulation within 1 minute, therefore quantitative release is prevented.^[80] This is further worsened considering the slow reaction rate *in vivo*, that limits the application of this biorthogonal linkers in drug controlled release.^[81]

2.2.2 Enzyme cleavable linkers

Intracellular enzymes can be used for the liberation of a toxic compound from a pro-drug.^[82] Lysosomes are rich of hydrolytic enzymes, which can be employed to trigger

the release of a drug from an ADC. Mostly used enzymes for this purpose are proteases, namely cathepsin B,^[83] and glycosidases, such as β -glucuronidase.^[84]

Cathepsin B is a lysosomal cysteine protease that is highly up-regulated in malignant cells,^[85] making it attractive for pro-drug activation. Notably, the concentration of this enzyme in plasma is lower compared to its lysosome concentration; moreover, its activity is maximum at acidic pH values, while the slightly basic pH of circulation inactivates the enzyme, avoiding premature release of the drug. Cathepsin B is able to recognize and cleave specific dipeptide sequences. A preliminary screening showed that doxorubicin can be efficiently released from specific dipeptides upon cathepsin B incubation. Among more than 10 dipeptides screened, Valine-Citrulline (Val-Cit) linker was the most promising one, being recognized by the protease and being stable in human and mouse serum. Consequently, the use of Val-Cit linker (**Figure 2.11**) has been widespread among enzymatically cleavable linkers in ADC design.^[86] This is the linker exhibited, for instance, in Brentuximab Vedotin (**Figure 2.3**).^[87] Moreover, about 20% of ADCs that reached clinical trials are equipped with a Val-Cit linker to control drug release.^[88] This popularity is due to the increased stability of this linker, when compared with analogues bearing an hydrazone, another popular cleavable linker in ADC chemistry.^[89]

Importantly, Val-Cit linker is always paired to a self-immolative spacer, which ensures linker recognition by the enzyme, and in turn, avoids possible steric hindrance. To date, amide hydrolysis has been attributed only to Cathepsin B. However, a recent study has demonstrated that also other proteases are involved in the cleavage process. As an evidence, MMAE and PBD bearing ADCs were toxic even in cells with no expression of this enzyme.^[90]

Apart from Val-Cit, other dipeptides have been used for protease triggered release. As an example, the simple Val-Ala linker has been used to conjugate MMAE to an anti Her2 targeting antibody. The final ADC has similar performance compared to the one bearing a Val-Cit linker, but it is more easily produced and presents less aggregation problems.^[91]

The introduction of a glycosidase cleavable linker, featuring a hydrophilic sugar moiety, helps also to overcome the aggregation issues. Owing to the increased hydrophilicity of

the carbohydrate, up to 8 molecules of hydrophobic MMAE can be conjugated to the antibody. The resulting ADC does not present the common problems arising from high DARs, such as aggregation issues and faster clearance.^[92] Within this context, β -glucuronidase labile linkers (**Figure 2.11**) have been used also for controlled release of duocarmycin derivatives from an anti CD30 ADC.^[93]

Combination of β -glucuronic acid glycoside and a Val-Cit dipeptide allowed efficient release of a PBD dimer from an ADC in Her2 positive cell lines. Again, the increased hydrophilicity of the linker increases the stability of the ADC.^[94] As for dipeptide linkers, a PABA spacer is required to allow recognition and to have a second functional group for antibody attachment. However, drugs bearing an alcohol group (such as duocarmycin and its analogues) can be directly attached to the sugar moiety, without compromising the enzymatic recognition.^[95]

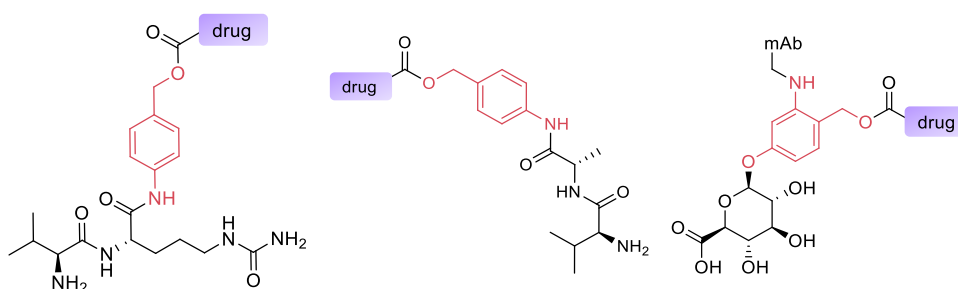


Figure 2.11: enzymatic cleavable linkers for ADC; Val-Cit-PABA linker (left); Val-Ala-PABA linker (middle); β -glucuronic acid linker. In red it is highlighted the self-immolative spacer.

2.3 Small Molecules Drug conjugates

Small molecules drug conjugates (SMDC) are ligand targeted drug delivery system that make use of a small ligand to deliver the drug at tumour site. In a similar way to ADCs, the structure of a SMDC consists of a ligand, connected through a linker and eventually a spacer to a cytotoxic compound (**Figure 2.12**). Regarding the linker and the drug, the same considerations made for ADCs are valid for SMDCs; linker may be either cleavable or non-cleavable and the drug needs to be highly cytotoxic.



Figure 2.12: schematization of a SMDC.

In the case of SMDC, the choice of the ligand is essential: its K_d must be > 10 nM to have accumulation of the SMDC at tumour site. In some cases, to compensate low affinity values, multivalent presentation of the ligand can increase the affinity and thus tumour accumulation.^[1,96]

On the one hand, SMDCs are more efficiently produced and characterized than ADCs. On the other hand, these small molecules are preferred to ADCs when dealing with solid tumours. In this case, poor penetration and extravasation ability of ADCs can be tackled by the use of these smaller conjugates.

The main difficulty arising from SMDC design is the ligand choice. In principle, antibodies can be produced against every antigen, while an efficient ligand for a given receptor overexpressed in a cancer cell is not always available. However, some membrane receptors have been successfully targeted with small molecule ligands.^[97]

This is the case of Carbonic anhydrase IX (CAIX), an enzyme overexpressed in solid tumours, which has been targeted with acetazolamide (**Figure 2.13**), a small sulphonamide-based inhibitor that is able to deliver toxic payloads at tumour site. Linker choice is fundamental in acetazolamide conjugate. In this respect, it has been shown that the stability of different cathepsin B labile dipeptides directly influences therapeutic effect of the SMDC.^[7]

Prostate-specific membrane receptor (PSMA), tumour marker of prostate cancer, presents high affinity towards (*S,S*)-2-[3-(1,3-dicarboxypropyl)ureido]pentanedioic acid (DUPA, **Figure 2.13**), with a K_d constant of 47 nM. Conjugation of DUPA with specific drugs through a disulfide labile linker has led to the development of efficient delivery system able to reduce tumour growth in mice.^[98]

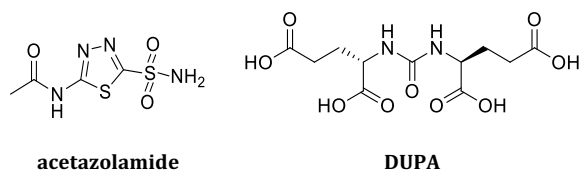


Figure 2.13: small molecule ligands used for targeted drug delivery.

2.4 References

- [1] M. Srinivasarao, P. S. Low, *Chem. Rev.* **2017**, *117*, 12133–12164.
- [2] J. Lu, F. Jiang, A. Lu, G. Zhang, *Int. J. Mol. Sci.* **2016**, *17*, 561.
- [3] C. Chalouni, S. Doll, *J. Exp. Clin. Cancer Res.* **2018**, *37*, 20.
- [4] C. K. Tsui, R. M. Barfield, C. R. Fischer, D. W. Morgens, A. Li, B. A. H. Smith, M. A. Gray, C. R. Bertozzi, D. Rabuka, M. C. Bassik, *Nat. Chem. Biol.* **2019**, DOI 10.1038/s41589-019-0342-2.
- [5] F. R. Maxfield, T. E. McGraw, *Nat. Rev. Mol. Cell Biol.* **2004**, *5*, 121–132.
- [6] G. J. L. Bernardes, G. Casi, S. Trüssel, I. Hartmann, K. Schwager, J. Scheuermann, D. Neri, *Angew. Chemie - Int. Ed.* **2012**, *51*, 941–944.
- [7] A. D. Corso, S. Cazzamalli, M. Mattarella, D. Neri, *Bioconjug. Chem.* **2017**, *28*, 1826–1833.
- [8] H. Chen, Z. Lin, K. E. Arnst, D. D. Miller, W. Li, *Molecules* **2017**, *22*, 1281.
- [9] A. M. Wu, P. D. Senter, *Nat. Biotechnol.* **2005**, *23*, 1137–1146.
- [10] J. R. McCombs, S. C. Owen, *Am. Assoc. Pharm. Sci.* **2015**, *17*, 339–351.
- [11] J. M. Lambert, A. Berkenblit, *Annu. Rev. Med.* **2018**, *69*, 191–207.
- [12] H. L. Perez, P. M. Cardarelli, S. Deshpande, S. Gangwar, G. M. Schroeder, G. D. Vite, R. M. Borzilleri, *Drug Discov. Today* **2014**, *19*, 869–881.
- [13] A. W. Tolcher, S. Sugarman, K. A. Gelmon, R. Cohen, M. Saleh, C. Isaacs, L. Young, D. Healey, N. Onetto, W. Slichenmyer, *J. Clin. Oncol.* **1999**, *17*, 478.
- [14] R. V. J. Chari, M. L. Miller, W. C. Widdison, *Angew. Chemie - Int. Ed.* **2014**, *53*, 3796–3827.
- [15] B. H. Petersen, S. V DeHerdt, D. W. Schneck, T. F. Bumol, *Cancer Res.* **1991**, *51*, 2286 LP-2290.
- [16] E. Y. Jen, C.-W. Ko, J. E. Lee, P. L. Del Valle, A. Aydanian, C. Jewell, K. J. Norsworthy, D. Przepioraka, L. Nie, J. Liu, et al., *Clin. Cancer Res.* **2018**, *24*, 3242–3246.
- [17] P. F. Bross, J. Beitz, G. Chen, X. H. Chen, E. Duffy, L. Kieffer, S. Roy, R. Sridhara, A. Rahman, G. Williams, et al., *Clin. cancer Res.* **2001**, *7*, 1490–1496.
- [18] P. R. Hamann, L. M. Hinman, I. Hollander, C. F. Beyer, D. Lindh, R. Holcomb, W. Hallett, H. Tsou, J. Upeslakis, D. Shochat, et al., *Bioconjug. Chem.* **2002**, *13*, 47–

- 58.
- [19] I. Krop, E. P. Winer, *Clin. Cancer Res.* **2014**, *20*, 15–20.
- [20] P. D. Senter, E. L. Sievers, *Nat. Biotechnol.* **2012**, *30*, 631–637.
- [21] Y. N. Lamb, *Drugs* **2017**, *77*, 1603–1610.
- [22] D. A. Richards, *Drug Discov. Today Technol.* **2018**, *30*, 35–46.
- [23] A. Alibakhshi, F. Abarghooi Kahaki, S. Ahangarzadeh, H. Yaghoobi, F. Yarian, R. Arezumand, J. Ranjbari, A. Mokhtarzadeh, M. de la Guardia, *J. Control. Release* **2017**, *268*, 323–334.
- [24] B. T. Ruddle, R. Fleming, H. Wu, C. Gao, N. Dimasi, *ChemMedChem* **2019**, *14*, 1185–1195.
- [25] H. Xu, L. Gan, Y. Han, Y. Da, J. Xiong, S. Hong, Q. Zhao, N. Song, X. Cai, X. Jiang, *RSC Adv.* **2019**, *9*, 1909–1917.
- [26] M. P. Deonarain, *Drug Discov. Today Technol.* **2018**, *30*, 47–53.
- [27] J. Ou, Y. Si, K. Goh, N. Yasui, Y. Guo, J. Song, L. Wang, R. Jaskula-Sztul, J. Fan, L. Zhou, et al., *PLoS One* **2018**, *13*, e0206246.
- [28] K. Lin, J. Tibbitts, *Pharm. Res.* **2012**, *29*, 2354–2366.
- [29] A. Beck, L. Goetsch, C. Dumontet, N. Corvaia, *Nat. Rev. Drug Discov.* **2017**, *16*, 315–337.
- [30] K. J. Hamblett, P. D. Senter, D. F. Chace, M. M. C. Sun, J. Lenox, C. G. Cerveny, K. M. Kissler, S. X. Bernhardt, A. K. Kopcha, R. F. Zabinski, et al., *Clin. Cancer Res.* **2004**, *15*, 7063–7070.
- [31] E. M. Moussa, J. P. Panchal, B. S. Moorthy, J. S. Blum, M. K. Joubert, L. O. Narhi, E. M. Topp, *J. Pharm. Sci.* **2016**, *105*, 417–430.
- [32] Y. T. Adem, K. A. Schwarz, E. Duenas, T. W. Patapoff, W. J. Galush, O. Esue, *Bioconjug. Chem.* **2014**, *25*, 656–664.
- [33] S. Panowski, S. Bhakta, H. Raab, P. Polakis, J. R. Junutula, *MAbs* **2014**, *6*, 34–45.
- [34] H. Liu, K. May, *MAbs* **2012**, *4*, 17–23.
- [35] M. M. C. Sun, K. S. Beam, C. G. Cerveny, K. J. Hamblett, R. S. Blackmore, M. Y. Torgov, F. G. M. Handley, N. C. Ihle, P. D. Senter, S. C. Alley, *Bioconjug. Chem.* **2005**, *16*, 1282–1290.
- [36] J. R. Junutula, H. Raab, S. Clark, S. Bhakta, D. D. Leipold, S. Weir, Y. Chen, M. Simpson, S. P. Tsai, M. S. Dennis, et al., *Nat. Biotechnol.* **2008**, *26*, 925–932.

- [37] V. Chudasama, A. Maruani, S. Caddick, *Nat. Chem.* **2016**, *8*, 114–119.
- [38] P. Akkapeddi, S.-A. Azizi, A. M. Freedy, P. M. S. D. Cal, P. M. P. Gois, G. J. L. Bernardes, *Chem. Sci.* **2016**, *7*, 2954–2963.
- [39] N. Krall, F. P. da Cruz, O. Boutureira, G. J. L. Bernardes, *Nat. Chem.* **2015**, *8*, 103–113.
- [40] J. P. M. Nunes, M. Morais, V. Vassileva, E. Robinson, V. S. Rajkumar, M. E. B. Smith, R. B. Pedley, S. Caddick, J. R. Baker, V. Chudasama, *Chem. Commun.* **2015**, *51*, 10624–10627.
- [41] S. L. Kuan, T. Wang, T. Weil, *Chem. - A Eur. J.* **2016**, *22*, 17112–17129.
- [42] T. Wang, A. Riegger, M. Lamla, S. Wiese, P. Oeckl, M. Otto, Y. Wu, S. Fischer, H. Barth, S. L. Kuan, et al., *Chem. Sci.* **2016**, *7*, 3234–3239.
- [43] K. Lang, J. W. Chin, *Chem. Rev.* **2014**, *114*, 4764–4806.
- [44] L. Davis, J. W. Chin, *Nat. Rev. Mol. Cell Biol.* **2012**, *13*, 168.
- [45] E. S. Zimmerman, T. H. Heibeck, A. Gill, X. Li, C. J. Murray, M. R. Madlansacay, C. Tran, N. T. Uter, G. Yin, P. J. Rivers, et al., *Bioconjug. Chem.* **2014**, *25*, 351–361.
- [46] S. A. Kularatne, V. Deshmukh, J. Ma, V. Tardif, R. K. V Lim, H. M. Pugh, Y. Sun, A. Manibusan, A. J. Sellers, R. S. Barnett, et al., *Angew. Chemie - Int. Ed.* **2014**, *53*, 11863–11867.
- [47] J. Y. Axup, K. M. Bajjuri, M. Ritland, B. M. Hutchins, C. H. Kim, S. A. Kazane, R. Halder, J. S. Forsyth, A. F. Santidrian, K. Stafin, et al., *Proc. Natl. Acad. Sci.* **2012**, *109*, 16101 LP-16106.
- [48] P. M. Drake, A. E. Albers, J. Baker, S. Banas, R. M. Bar, A. S. Bhat, G. W. DeHart, A. W. Garofalo, P. Holder, L. C. Jones, et al., *Bioconjug. Chem.* **2014**, *25*, 1331–1341.
- [49] D. Rabuka, J. S. Rush, W. DeHart, P. Wu, C. R. Bertozzi, *Nat. Protoc.* **2012**, *7*, 1052–1067.
- [50] N. Forte, V. Chudasama, J. R. Baker, *Drug Discov. Today Technol.* **2018**, *30*, 11–20.
- [51] Z. Li, R. Huang, H. Xu, J. Chen, Y. Zhan, X. Zhou, H. Chen, B. Jiang, *Org. Lett.* **2017**, *19*, 4972–4975.
- [52] M. Morais, J. P. M. Nunes, K. Karu, N. Forte, I. Benni, M. E. B. Smith, S. Caddick, V. Chudasama, J. R. Baker, *Org. Biomol. Chem.* **2017**, *15*, 2947–2952.
- [53] E. Robinson, J. P. M. Nunes, V. Vassileva, A. Maruani, J. C. F. Nogueira, M. E. B.

- Smith, R. B. Pedley, S. Caddick, J. R. Baker, V. Chudasama, *RSC Adv.* **2017**, *7*, 9073–9077.
- [54] N. Martínez-Sáez, S. Sun, D. Oldrini, P. Sormanni, O. Boutureira, F. Carboni, I. Compañón, M. J. Deery, M. Vendruscolo, F. Corzana, et al., *Angew. Chemie - Int. Ed.* **2017**, *56*, 14963–14967.
- [55] S. J. Walsh, S. Omarjee, W. R. J. D. Galloway, T. T. L. Kwan, H. F. Sore, J. S. Parker, M. Hyvönen, J. S. Carroll, D. R. Spring, *Chem. Sci.* **2019**, *10*, 694–700.
- [56] M. T. W. Lee, A. Maruani, D. A. Richards, J. R. Baker, S. Caddick, V. Chudasama, *Chem. Sci.* **2017**, *8*, 2056–2060.
- [57] J. R. Junutula, K. M. Flagella, R. A. Graham, K. L. Parsons, E. Ha, H. Raab, S. Bhakta, T. Nguyen, D. L. Dugger, G. Li, et al., *Clin. Cancer Res. Cancer Res* **2010**, *16*, 4769–4778.
- [58] P. Strop, S. Liu, M. Dorywalska, K. Delaria, R. G. Dushin, T. Tran, W. Ho, S. Farias, M. G. Casas, Y. Abdiche, et al., *Chem. Biol.* **2013**, *20*, 161–167.
- [59] B. Shen, K. Xu, L. Liu, H. Raab, S. Bhakta, M. Kenrick, K. L. Parsons-reponte, J. Tien, S. Yu, E. Mai, et al., *Nat. Biotechnol.* **2012**, *30*, 184–189.
- [60] R. Ohri, S. Bhakta, A. Fourie-O'Donohue, J. Dela Cruz-Chuh, S. P. Tsai, R. Cook, B. Wei, C. Ng, A. W. Wong, A. B. Bos, et al., *Bioconjug. Chem.* **2018**, *29*, 473–485.
- [61] D. Su, K. R. Kozak, J. Sadowsky, S. F. Yu, A. Fourie-O'Donohue, C. Nelson, R. Vandlen, R. Ohri, L. Liu, C. Ng, et al., *Bioconjug. Chem.* **2018**, *29*, 1155–1167.
- [62] J. D. Sadowsky, T. H. Pillow, J. Chen, F. Fan, C. He, Y. Wang, G. Yan, H. Yao, Z. Xu, S. Martin, et al., *Bioconjug. Chem.* **2017**, *28*, 2086–2098.
- [63] J. T. Patterson, S. Asano, X. Li, C. Rader, C. F. Barbas, *Bioconjug. Chem.* **2014**, *25*, 1402–1407.
- [64] Y. V. Kovtun, C. A. Audette, Y. Ye, H. Xie, M. F. Ruberti, S. J. Phinney, B. A. Leece, T. Chittenden, W. A. Blättler, V. S. Goldmacher, *Cancer Res.* **2006**, *66*, 3214–3221.
- [65] Y. V. Kovtun, V. S. Goldmacher, *Cancer Lett.* **2007**, *255*, 232–240.
- [66] F. Li, K. K. Emmerton, M. Jonas, X. Zhang, J. B. Miyamoto, J. R. Setter, N. D. Nicholas, N. M. Okeley, R. P. Lyon, D. R. Benjamin, et al., *Cancer Res.* **2016**, *26*, 2710–2719.
- [67] S. Gol, C. Kopitz, A. Kahnert, I. Heisler, C. A. Schatz, B. Stelte-ludwig, A. Mayer-

- bartschmid, K. Unterschemmann, S. Bruder, L. Linden, et al., *Mol. Cancer Ther.* **2014**, *13*, 1537–1549.
- [68] A. H. Staudacher, M. P. Brown, *Br. J. Cancer* **2017**, *117*, 1736–1742.
- [69] V. I. Lushchak, *J. Amino Acids* **2012**, *2012*, 736837.
- [70] B. A. Kellogg, L. Garrett, Y. Kovtun, K. C. Lai, B. Leece, M. Miller, G. Payne, R. Steeves, K. R. Whiteman, W. Widdison, et al., *Bioconjug. Chem.* **2011**, *22*, 717–727.
- [71] H. Erickson, S. Wilhelm, W. Widdison, B. Leece, X. Sun, Y. Kovtun, R. Singh, R. Chari, *Cancer Res.* **2008**, *68*, 2150–2150.
- [72] T. H. Pillow, M. Schutten, S.-F. Yu, R. Ohri, J. Sadowsky, K. A. Poon, W. Solis, F. Zhong, G. Del Rosario, M. A. T. Go, et al., *Mol. Cancer Ther.* **2017**, *16*, 871–878.
- [73] T. H. Pillow, J. D. Sadowsky, D. Zhang, S.-F. Yu, G. Del Rosario, K. Xu, J. He, S. Bhakta, R. Ohri, K. R. Kozak, et al., *Chem. Sci.* **2017**, *8*, 366–370.
- [74] B. Spangler, T. Kline, J. Hanson, X. Li, S. Zhou, J. A. Wells, A. K. Sato, A. R. Renslo, *Mol. Pharm.* **2018**, *15*, 2054–2059.
- [75] E. M. Sletten, C. R. Bertozzi, *Angew. Chemie - Int. Ed.* **2009**, *48*, 6974–6998.
- [76] J. Li, P. R. Chen, *Nat. Chem. Biol.* **2016**, *12*, 129–37.
- [77] B. J. Stenton, B. L. Oliveira, M. J. Matos, L. Sinatra, G. J. L. Bernardes, *Chem. Sci.* **2018**, *9*, 4185–4189.
- [78] B. L. Oliveira, Z. Guo, G. J. L. Bernardes, *Chem. Soc. Rev.* **2017**, *46*, 4811–5174.
- [79] R. M. Versteegen, W. Hoeve, R. Rossin, M. A. R. De Geus, H. M. Janssen, M. S. Robillard, *Angew. Chemie - Int. Ed.* **2018**, *57*, 10494–10499.
- [80] R. Rossin, S. M. J. Van Duijnhoven, W. Ten Hoeve, H. M. Janssen, L. H. J. Kleijn, F. J. M. Hoeben, R. M. Versteegen, M. S. Robillard, *Bioconjug. Chem.* **2016**, *27*, 1697–1706.
- [81] S. Davies, B. J. Stenton, G. J. L. Bernardes, *Chimia (Aarau).* **2018**, *72*, 771–776.
- [82] R. Walther, J. Rautio, A. N. Zelikin, *Adv. Drug Deliv. Rev.* **2017**, *118*, 65–77.
- [83] Y. Zhong, L. Shao, Y. A. N. Li, *Int. J. Oncol.* **2013**, *42*, 373–383.
- [84] S. C. Jeffrey, J. De Brabander, J. Miyamoto, P. D. Senter, *ACS Med. Chem.* **2010**, *1*, 277–280.
- [85] V. Turk, V. Stoka, O. Vasiljeva, M. Renko, T. Sun, B. Turk, D. Turk, *Biochim. Biophys. Acta* **2012**, *1824*, 68–88.

- [86] G. M. Dubowchik, R. A. Firestone, *Bioorg. Med. Chem. Lett.* **1998**, *8*, 3341–3346.
- [87] A. Younes, U. Yasothan, P. Kirkpatrick, *Nat. Rev. Drug Discov.* **2012**, *11*, 19–20.
- [88] N. Jain, S. W. Smith, S. Ghone, B. Tomczuk, *Pharm. Res.* **2015**, *32*, 3526–3540.
- [89] S. O. Doronina, B. E. Toki, M. Y. Torgov, B. A. Mendelsohn, C. G. Cerveny, D. F. Chace, R. L. DeBlanc, R. P. Gearing, T. D. Bovee, C. B. Siegall, et al., *Nat. Biotechnol.* **2003**, *21*, 778–784.
- [90] N. G. Caculitan, J. dela Cruz Chuh, Y. Ma, D. Zhang, K. R. Kozak, Y. Liu, T. H. Pillow, J. Sadowsky, T. K. Cheung, Q. Phung, et al., *Cancer Res.* **2017**, *77*, 7027 LP-7037.
- [91] Y. Wang, S. Fan, W. Zhong, X. Zhou, S. Li, *Int. J. Mol. Sci.* **2017**, *18*, 1860.
- [92] P. J. Burke, J. Z. Hamilton, S. C. Jeffrey, J. H. Hunter, S. O. Doronina, N. M. Okeley, J. B. Miyamoto, M. E. Anderson, I. J. Stone, M. L. Ulrich, et al., *Mol. Cancer Ther.* **2017**, *16*, 116–123.
- [93] S. C. Jeffrey, M. T. Nguyen, R. F. Moser, D. L. Meyer, J. B. Miyamoto, P. D. Senter, *Bioorganic Med. Chem. Lett.* **2007**, *17*, 2278–2280.
- [94] S. J. Gregson, A. M. Barrett, N. V. Patel, G.-D. Kang, D. Schiavone, E. Sult, C. S. Barry, B. Vijayakrishnan, L. R. Adams, L. A. Masterson, et al., *Eur. J. Med. Chem.* **2019**, *179*, 591–607.
- [95] L. F. Tietze, F. Major, I. Schuberth, *Angew. Chemie Int. Ed.* **2006**, *45*, 6574–6577.
- [96] N. Krall, F. Pretto, D. Neri, *Chem. Sci.* **2014**, *5*, 3640–3644.
- [97] G. Casi, D. Neri, *J. Med. Chem.* **2015**, *58*, 8751–8761.
- [98] J. Roy, T. X. Nguyen, A. K. Kanduluru, C. Venkatesh, W. Lv, P. V. N. Reddy, P. S. Low, M. Cushman, *J. Med. Chem.* **2015**, *58*, 3094–3103.

Objectives

3

Considering the increasing importance of targeted delivery system in cancer therapy and the use of antibody-drug-conjugates (ADCs) as an exciting via to attain this purpose, the main goal of this thesis is the design of cleavable linkers that features, on the one hand, a functional group not explored so far that allows the controlled release of the drug once the tumor cell has been reached and, on the other side, that present a novel scaffold that allows an efficient and irreversible antibody-cysteine bioconjugation. To expand the scope of this technology, it will also implement in the context of small molecules drug conjugates (SMDC).

More specifically, the following aims have been proposed:

- 1) Synthesis of new drug derivatives that feature novel Michael acceptors for an efficient and irreversible cysteine-selective modification of proteins and antibodies. Both carbonyl acrylic and vinyl pyridine reagents will be used for this purpose.
- 2) Design, synthesis and characterization of new linkers, based on acetals for the controlled release of drugs. This group will be equipped with a pre-drug or a fluorophore, whose fluorescence properties will be attenuated upon the attachment to the acetal. The behaviour of the resulting compounds will be evaluated then in acid and neutral media. The structure presenting the best properties in terms of acid lability and plasma stability will be applied to the design of different targeted delivery systems, such as an ADC and a SMDC.
- 3) Study and optimization of the Grob fragmentation reaction under physiological conditions for its application in controlled drug release. Thus, several Grob fragmentation substrates will be synthesized and their reactivity under biological mimicking conditions will be monitored. Equally, a strategy to control and 'switch-off' the Grob fragmentation pathway will be developed. The substrate with the best performance will be selected to develop a linker featuring a pro-drug. The stability and ability of the linker to release the drug under controlled condition will be assessed.

New cysteine selective reagents for ADC synthesis

4.1 Introduction

- 4.1.1 Modifications at natural amino acids
- 4.1.2 Conjugation strategies based on cysteine modification
- 4.1.3 Background and objectives

4.2 Carbonylacrylic reagents for protein modifications

- 4.2.1 Synthesis
- 4.2.2 Antibody conjugation and stability

4.3 Vinyl Pyridinium reagents for protein modification

- 4.3.1 Synthesis of MMAE-vinyl pyridinium derivative
- 4.3.2 ADC synthesis and biological assays

4.4 Conclusions

4.5 Experimental section

- 4.5.1 Synthesis
- 4.5.2 Kinetic studies
- 4.5.3 Antibody conjugation
- 4.5.4 Cell assays
- 4.5.5 Quantum Mechanical calculations

4.6 References

4.1 Introduction

Protein bio-conjugation represents an invaluable tool to obtain modified proteins for application in biology and medicine.^[1,2] Main protein modifications include acylation, methylation, phosphorylation and glycosylation. Those modifications enable the study of complex protein functions through the controlled introduction of a post-translational modification.^[3] Also, introduction of fluorophores or radionuclides to study protein biodistribution *in vivo*,^[4-10] or drug attachment to obtain therapeutic protein conjugates could be achieved via bio-conjugation chemistry.^[11,12]

To obtain such complex structures, it is essential relying on selective modification techniques, which would allow the preparation of stable, homogeneous and well-characterized protein conjugates.

Therefore, new methodologies that permit site-selective modification of peptides and proteins represents a field of high relevance, especially when dealing with the construction of antibody-drug-conjugates (ADCs).

As described in *Section 2.1.1*, in this area, conjugation techniques aim at the development of a homogeneous, regio- and chemo-selective product, which could improve the biological behaviour of the therapeutic agent, together with its pharmacokinetic and stability properties.

Indeed, this was the problem of the first generation of antibody drug conjugates, which, relying on non-selective methods, yielded a heterogeneous mixture of products, with various drug-to-antibody ratios (DARs) and, probably different biological behaviours.^[13-15] Logically, the use of site selective chemistry may allow overcoming all those problems.

The reactions on protein present several complications. Indeed, these transformations need to be performed under mild conditions, such as aqueous buffer (pH between 6 and 8) and 37 °C to avoid alteration of protein structure and functionality. Moreover, bio-conjugation reactions are carried out at low reagent concentration, causing kinetic problems. Another main issue is to get selectivity in such transformation, because several functional groups naturally occurring in the protein may compete under the same reaction conditions.

Trying to solve these issues, several methods for protein efficient modifications have been developed in the last years, including both genetic engineering techniques, and chemical reactions on proteins. In the first case, unnatural amino acids with unique bio-orthogonal reactivity are introduced as mutations in the protein structure to achieve selectivity, while in the second case natural amino acid reactivity would allow the conjugation reaction.^[16-19]

Examples of unnatural amino acids used for protein site-selective modification have been described in the general introduction (*Section, 2.1.1.1*). Therefore, herein reactivity of natural amino acids will be described,

4.1.1 Modifications at natural amino acids

In the case of non-canonical amino acids, chemo-selectivity is achieved owing to the introduction of an organic moiety with a special reactivity inside the protein. On the contrary, when exploiting the natural reactivity of the amino acid side chains, cross-reactivity and side reactions must be considered. As an example, lysine and cysteine may be competing nucleophiles with electrophile reagents, depending on the working conditions. Despite those issues, several methods based on selective reactions of lysines,^[20,21] cysteines,^[16] methionine,^[22,23] tryptophan,^[24,25] tyrosine,^[26] histidine,^[27] the N-^[28] and C-terminus^[29] have been developed.

As an example, tyrosine has been modified via a three component Mannich reaction with anilines and aldehydes (**Figure 4.1 a**).^[30] The special structure of the N-terminus allows its selective reaction with 2-pyridinecarboxaldehyde (**Figure 4.1 b**).^[31] A metal-free modification, based on the use of N-O radicals, has been reported on tryptophan residues recently (**Figure 4.1 c**).^[24] This interesting methodology, which is very selective in terms of amino acid reactivity, suffers from the need to use acid conditions, that may not be compatible with every protein structure.

Methionine modification methods result interesting for the low abundance of this amino acid, which normally is buried into the protein structure. For those reason, when exposed methionines are available, they can be reacted to give homogenous conjugates. In a recently developed strategy, methionine in proteins and peptides has been labelled

using iodonium reagents. The diazo-sulfonium group can be further functionalized to introduce a second modification. (**Figure 4.1 d**).^[22]

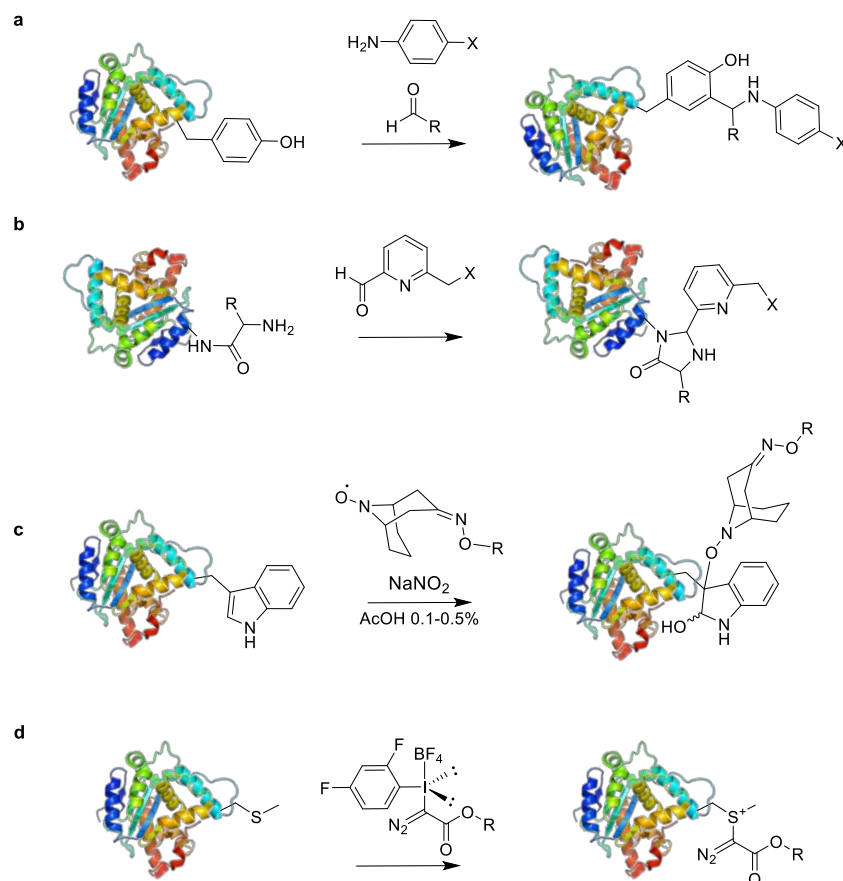


Figure 4.1: bio-conjugation reaction on natural amino acid side chains.

However, even though all these compelling strategies have been successfully applied to protein modification, in the context of clinically useful protein and antibody-drug conjugates, cysteine is still the residue with the best reactivity profile. Because of this, the conjugation approaches based on this residue will be described in the following section.

4.1.2 Conjugation strategies based on cysteine modification

Among natural amino acids, cysteine is probably the residue with the most convenient chemical reactivity for application in protein conjugates synthesis. Its sulfhydryl side chain has the highest nucleophilicity and its pKa is lower in comparison to other groups (pKa cysteine-SH ~ 8; pKa lysines-NH₂, ~ 10.5), which in general makes this residue the most reactive under physiological conditions towards electrophiles. Moreover, the low abundance of free, solvent exposed cysteines (around 1.9 %),^[28] facilitates the formation of conjugates with high homogeneity and controlled DAR (in the field of ADCs).

Classical cysteine reactivity includes mixed disulphide formation, alkylation with α -carbonyl compounds (e.g. iodoacetamides), and conjugated addition to Michael acceptors, such as vinylsulfones, allenamides, maleimides, and acrylates.^[17,19] Modifications have also been introduced into mAb with Julia-Kocienski-like reagents^[32] or with 3-arylpropionitriles,^[33] leading to homogenous ADC with excellent stability in human plasma. Some of the cited examples are resumed in **Figure 4.2**.

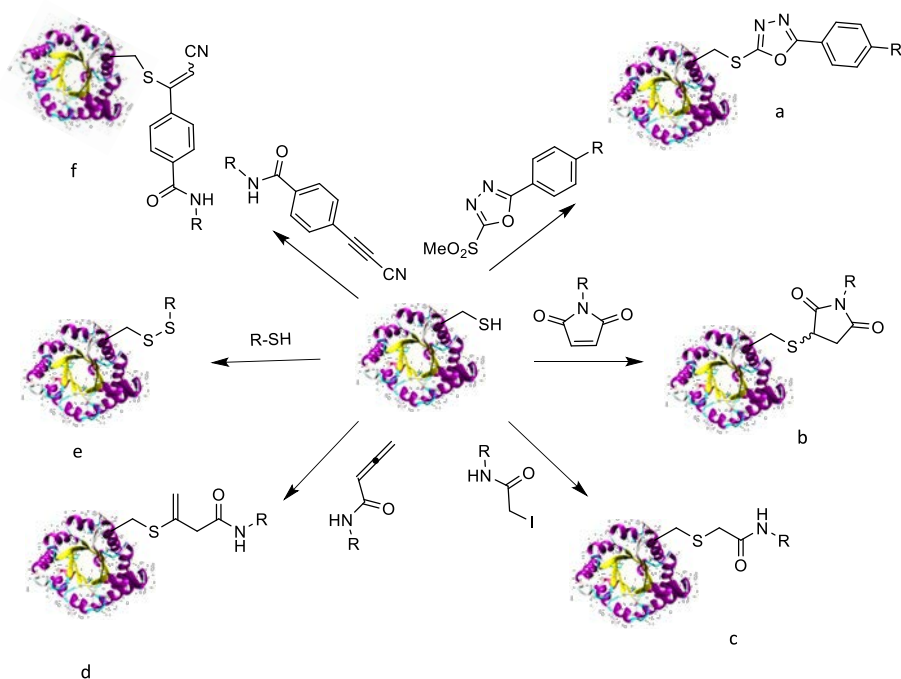


Figure 4.2: thiol-selective conjugation strategy for protein modification. a) use of Julia-Kocienski like reagents; b) modification with maleimides; c) use of α -iodoacetamide derivatives; d) allenamide derivative based method; e) disulfide bond formation; f) modification with 3-arylpropionitriles.

In a strategy developed by Davis, cysteine has also been successfully converted to dehydroalanine (DHA) in proteins and antibodies.^[34,35] This could be achieved in several ways,^[36] but the most efficient strategy involves double nucleophilic substitution and elimination mediated by dibromoalkane derivatives on cysteines. Thus, a Michael acceptor is introduced in the protein, which in turn can react in a bio-orthogonal way with thiols, amines, and radicals to form stable C-S,^[37] C-N^[38] and C-C bonds (**Figure 4.3**).^[39] Interestingly, this methodology has been successfully applied to the generation of a homogenous Thiomab conjugate with excellent plasma stability and maintained selectivity towards Her2 expressing cell lines.^[38]

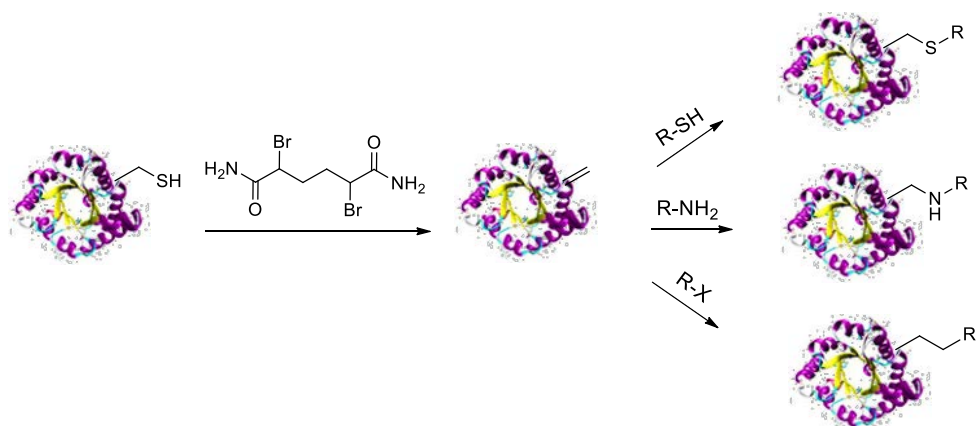


Figure 4.3: protein chemical modification via DHA installation into proteins.

Transition metal based reagents were also used to modify cysteine residues in proteins and antibodies.^[40] As an example, Pentelute and Buchwald described the arylation of thiols mediated by organometallic palladium reagents: the reaction is fast, having a kinetic similar to thiol-maleimide addition and the product is stable in a variety of biological conditions. Application of this methodology to antibodies lead to an ADC with near homogenous DAR, without need for antibody engineering (**Figure 4.4**).^[41]

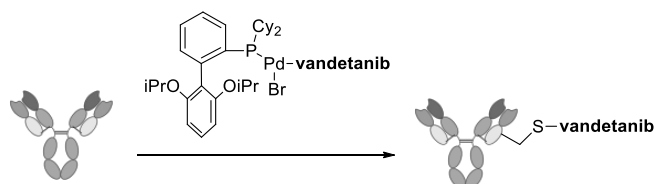


Figure 4.4: methodology developed by Pentelute's group for a selective conjugation based on cysteine arylation with organopalladium reagents.

Despite the high number of methods reported, we can still claim that maleimide chemistry is the method of choice when dealing with the development of ADCs; as a matter of fact, the therapeutic ADC Brentuximab Vedotin, is obtained with maleimide conjugation chemistry.^[42]

However, this technique presents some drawbacks that need to be solved: for example, conjugation has to be performed in slightly acidic pH to prevent cross-reactivity with histidine and lysine side chains,^[43] and maleimide reagents need to be used in excess to

achieve complete conversion. More importantly, the main limitation of this technique is the instability of maleimide conjugates in human plasma, due to exchange with biological thiols.^[44-46]

Several strategies have been proposed to overcome this problem, mainly acting on the kinetic of the retro-Michael reaction. To this purpose, exocyclic olefins have been suggested as maleimide analogues,^[47] or N-Aryl maleimides have proved to have a greater plasma stability.^[48] Based on the idea that the hydrolysis of the succinimide ring is able to block the retro-Michael, self-hydrolysing maleimides have been designed.^[49] Furthermore, a careful design of the conjugation site influences the stability of the thioether, by promoting the spontaneous hydrolysis of the succinimide ring.^[50] These methodologies improves *in vivo* stability, but still have some problems, such as the need of high excess reagents, sometimes ring hydrolysis is incomplete and the dependence of the site of conjugation on the spontaneous hydrolysis limits the scope of the methodology.

4.1.3 Background and objectives

Despite the high number of techniques currently available for the selective modification of proteins, there are still several challenges to overcome when trying to synthesize protein conjugates, and in particular, therapeutic ADCs.

Indeed, even if significant improvements have been achieved in protein chemistry, there is still the need to find efficient reagent that allow easy and fast functionalization and that lead to stable products, overcoming the main problem linked to thiol-maleimide chemistry. This one is still the election of choice in protein bio-conjugation, but instability of the thioether linker needs to be faced.

Taking all this into account, we have recently described the properties of new, highly reactive benzoyl acrylic acid derivatives, able to target thiols in proteins irreversibly and in a chemo-selective fashion.^[51]

Small-peptide studies showed that benzoyl acrylic acid esters and amides were highly reactive towards cysteines, while leaving unaltered lysine residues, even when reactions are performed at slightly basic pH (**Figure 4.5 a and b**). The selectivity is

maintained in proteins, as corroborated by chemical controls using Ellmann's reagent. Importantly, addition of cysteine to carbonyl acrylates presents a high reaction rate (of the $10 \text{ M}^{-1} \text{ s}^{-1}$ order) and comparable with the addition to maleimides, as demonstrated by NMR competition experiments. Moreover, when compared to thio-maleimide conjugates, products obtained with this technology present increased resistance to plasma degradation (**Figure 4.5 c**).

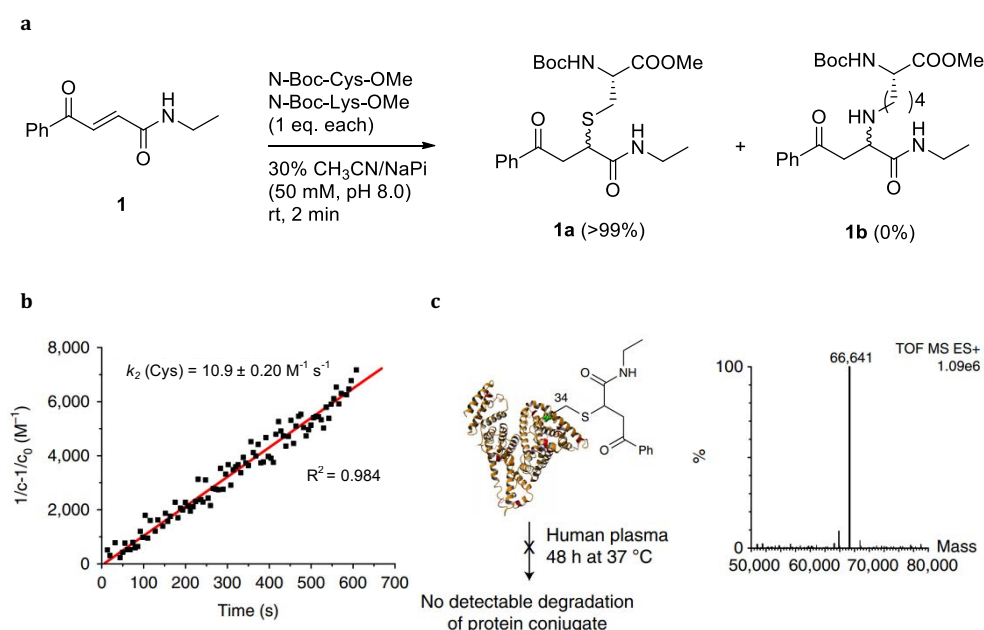


Figure 4.5: a) competitive reactivity study of cysteine and lysine addition on carbonyl acrylate yielded 99% of cysteine adduct **1a**, while no Lysine adduct **1b** was detected; b) second order kinetic constant of the reaction ; c) albumin modification with carbonyl acrylamide is resistant to plasma degradation.

To expand the applicability of this methodology, we designed and synthesized complex drug-acrylamide derivatives, which were successfully conjugated to cysteine-bearing antibodies, yielding a stable and homogenous product. This part of the work will be described in the following section.

In this chapter, we also describe a new class of quaternised vinyl pyridine reagents that allows cysteine modification by ultrafast Michael type addition (**Figure 4.6**). Nitrogen quaternisation increases the reaction rate and allows protein modification using

stoichiometric amount of reagents. To demonstrate selectivity towards thiols, both computational and NMR studies on small molecules were performed, and the kinetic of such transformations has been determined. Finally, to apply vinyl pyridine chemistry to the synthesis of functional ADCs, we designed the synthesis of a monomethylauristatin E (MMAE) derivative to obtain an antibody drug conjugate, as will be described in *Section 4.3*.

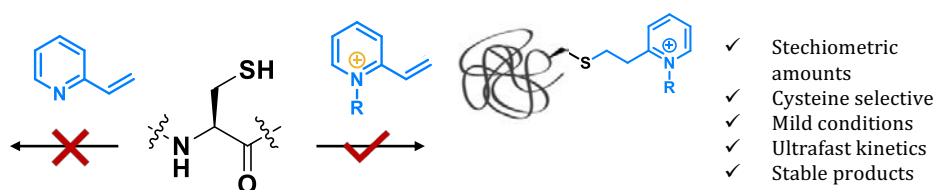


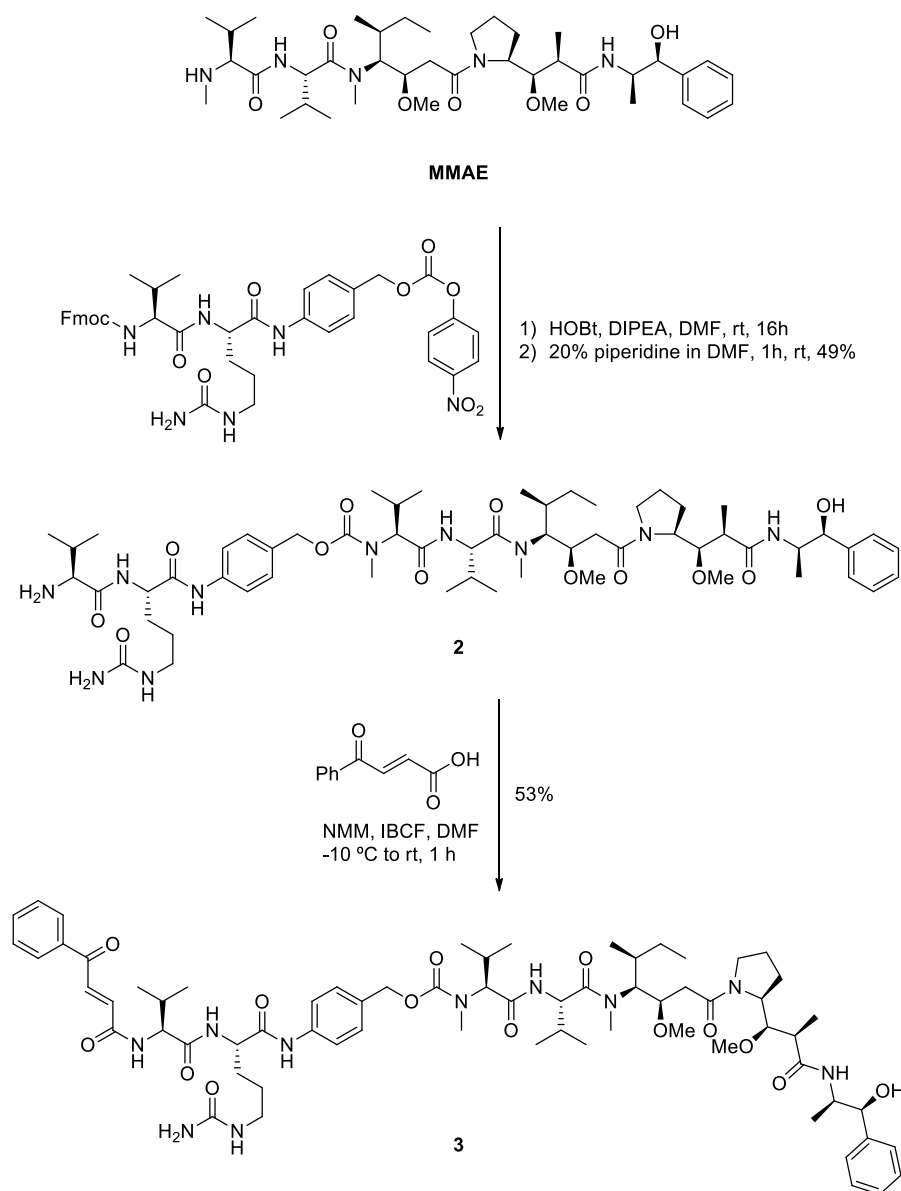
Figure 4.6: schematic representation of the use of vinyl pyridinium reagent for protein modification.

4.2 Carbonylacrylic reagents for protein modifications

4.2.1 Synthesis

To demonstrate the potential of carbonylacrylic reagents as good candidates for selective chemical protein modifications, MMAE bearing a benzoyl acrylamide moiety was prepared. This drug, toxic at sub-nanomolar concentration in several cell lines, acts by inhibiting tubulin polymerization.^[52] It has found wide application for ADC development and it represents the warhead of the clinically used ADC brentuximab vedotin.^[53] Between acrylamide tag and MMAE, the enzymatically cleavable valine-citrulline linker, paired with the self-immolative p-aminobenzylalcohol (PABA) spacer, has been inserted. Its role is to ensure cathepsin B mediated release inside the target cells.^[54]

Starting from commercially available MMAE, acrylamide derivative **3** was obtained in two steps (Scheme 4.1).

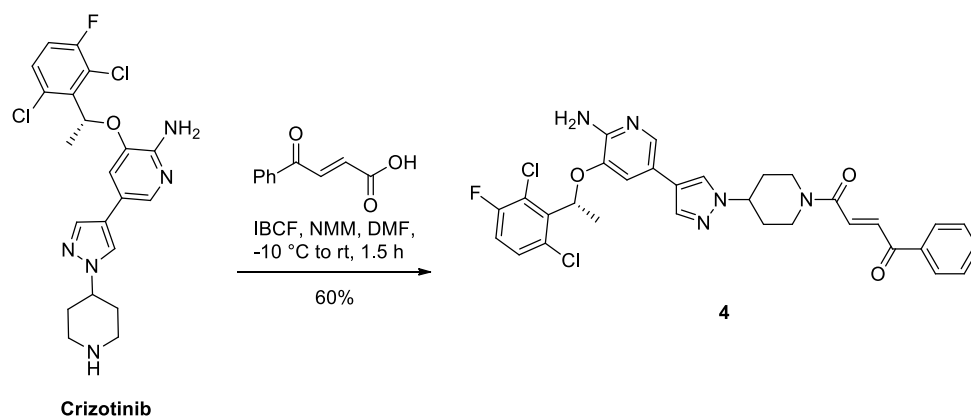


Scheme 4.1: synthesis of MMAE with carbonyl acrylate tag for protein modification.

In the first step, coupling of MMAE with the cleavable linker was achieved through reaction of 4-nitrophenyl activated carbonate, conveniently protected at the primary amino group as Fmoc. The carbamate formation was favoured by adding HOBt in presence of DIPEA in DMF. Indeed, much lower conversion to the desired carbamate

was obtained when no HOBt is added to the reaction mixture. Then, the crude reaction was treated with 20 % piperidine in DMF to remove the Fmoc protecting group. Next, the crude was directly purified by preparative HPLC to afford pure compound **2** with 57% yield over two steps. To obtain acrylamide **3**, amine **2** was treated with *trans*-3-benzoylacrylic acid, pre-activated at -10° C with IBCF and NMM in DMF. After 1 h at rt, the reaction was complete as determined by MALDI-TOF analysis. The crude reaction mixture was diluted with CH₃CN and H₂O and directly purified by reversed phase HPLC. Carbonyl acrylamide derivative **3** was obtained in 53% yield after purification.

To extend the scope of this methodology and show the synthetic accessibility of carbonyl acrylic reagents, we decided to use Crizotinib as a second example of drug. This drug is an inhibitor of tyrosine kinase receptor ALK and has been indicated for the treatment of locally advanced or metastatic non-small-cell lung cancer.^[55] Also, its structure contains a piperidine ring that can be efficiently coupled with *trans*-3-benzoylacrylic acid in one synthetic step (**Scheme 4.2**). Under the same coupling conditions reported before (i.e. using NMM and IBCF in DMF), a non-cleavable drug-carbonyl acrylamide derivative was prepared from commercially available Crizotinib. After purification by column chromatography, compound **4** was obtained with 60% yield and ready-to-use in conjugation reaction.



Scheme 4.2: synthesis of Crizotinib-carbonyl acrylamide derivative.

4.2.2 Antibody conjugation and stability

With these compounds in hands, the synthesis of stable, homogenous and well-characterized antibody drug conjugates was achieved.

To synthesize a potentially therapeutic ADC, we chose as starting material a modified Trastuzumab antibody, which features an engineered cysteine at position 205 of the light chain (LC-V205C). The introduced modification does not affect its structure and its binding properties, and at the same time the solvent exposed cysteine is highly reactive.^[56] From now on, we will refer to the engineered Trastuzumab antibody LC-V205C as Thiomab.

Optimised conjugation conditions for proteins with benzoyl acrylates consist of neutral or slightly basic buffer, at room temperature or 37 °C. Full conversion is achieved at low antibody concentration (10-20 µM), using low excess of reagent and after few hours incubation.^[51] However, when using an antibody as the protein starting material, some further optimization is needed to achieve full conversion.

Indeed, in the case of our Thiomab, when the reaction is performed in phosphate buffer at pH 8.0 or 9.0 (50 mM), low yields of the desired conjugated were achieved. However, lowering the ionic strength and the pH of the buffer enabled us to obtain Thiomab-3 conjugate with >95% conversion after 6 h of reaction, using a limited amount of carbonyl acrylate **3** (only 5 equivalents per cysteine).

The conditions tested are summarized in Table 4.1.

Buffer	Conditions	Conversion
NaPi 50 mM, pH 8.0	10 equiv. compound 3 , 37 °C, 24 h	0 %
NaPi 50 mM, pH 9.0	10 equiv. compound 3 , 37 °C, 24 h	0 %
NaPi 20 mM, pH 7.0,	10 equiv. compound 3 , 37 °C, 6 h	>95 %

Table 4.1: optimization of reaction conditions for the preparation of Thiomab-3 conjugate.

Finally, the conjugate was obtained with a single modification per light-chain and no modifications were detected in the heavy chain, as expected according to what

previously reported for the modification of Thiomab LC-V205C using a maleimide analogue of compound **3**.^[56] After 6 h of incubation at 37°C, the reaction was complete, as confirmed by mass analysis of the mixture (**Figure 4.7**). The conjugate was purified before cell assays by size-exclusions membranes.

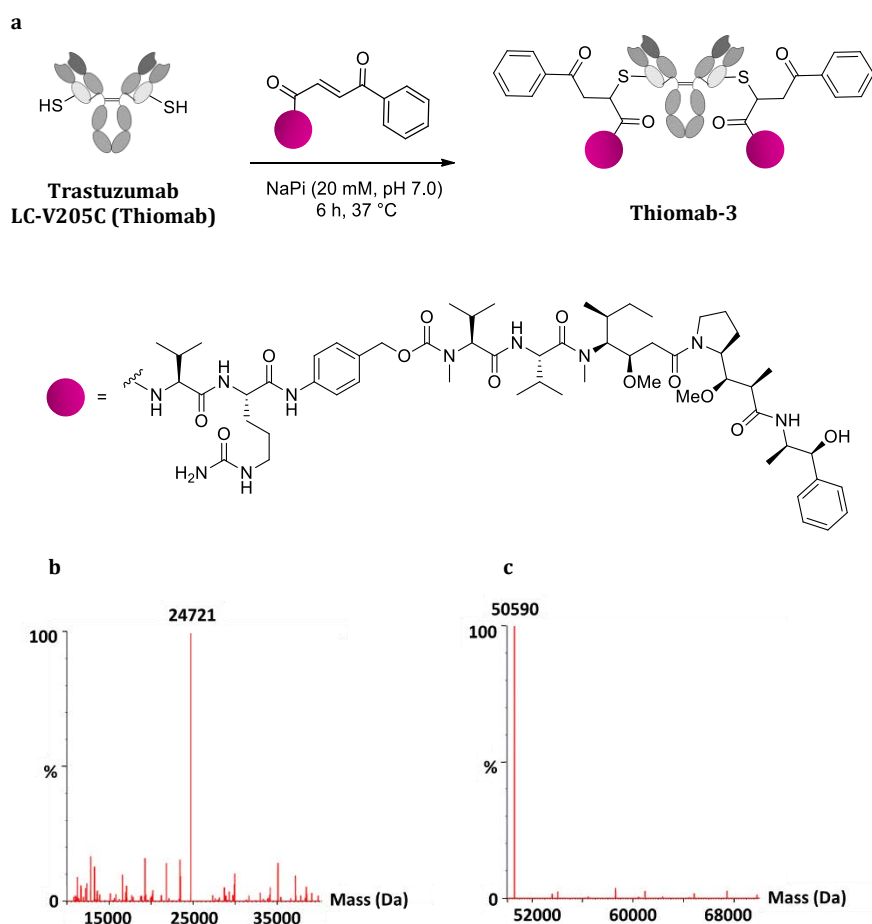


Figure 4.7: a) schematic representation of the conjugation reaction; b) deconvoluted ESI-MS of the light chain of Thiomab-3 (calcd. 24721 Da; observed 24721); c) deconvoluted ESI-MS spectra of unmodified light chain of Thiomab-3 (calcd. 50594 Da; observed 50590).

To demonstrate that these results can be extended also to other antibodies, both carbonyl acrylamide derivatives synthesized (compounds **3** and **4**) were used to modify F16 antibody, a fully human antibody that targets tenascin C and is able to accumulate at tumour microenvironment in mouse models.^[57,58] The free cysteine residue reacted

efficiently at 37 °C in NaPi buffer (20 mM, pH 7.0) with carbonyl acrylates **3** and **4**, yielding with high conversion (>95 %) a doubly modified F16 antibody with one modification per light chain, as confirmed by LC-MS analysis (**Figure 4.8**).

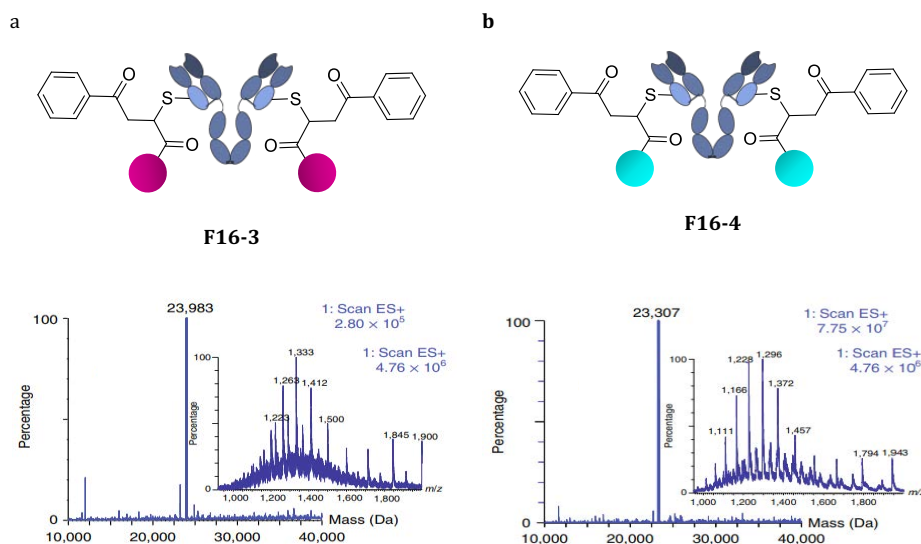


Figure 4.8: MS-ESI analysis of F16 conjugates with acrylamide compounds; a) ion series and deconvoluted mass spectra for F16-3 conjugate (calcd: 23985, obs 23983); b) ion series and deconvoluted mass spectra for F16-4 conjugate (calcd: 23312, obs.23307). The fuchsia and green balls represent compounds **3** and **4**, respectively.

To evaluate if the new thioether compound is resistant to degradation in human plasma, stability studies were performed on a simpler carbonyl acrylamide derivative. Conjugate Thiomab-1, obtained by reacting compound **1** with Thiomab under standard condition was used as a model for the stability assay. In this case, a doubly modified antibody is observed, with DAR = 4. This abnormal reactivity is probably due to the small structure of this simple carbonyl acrylamide, which can react with an additional cysteine deriving from a spontaneously cleaved disulphide bond.

However, when incubated in human serum at 37 °C, no significant degradation was observed after 48 h, making these reagents suitable for ADC synthesis (**Figure 4.9**).

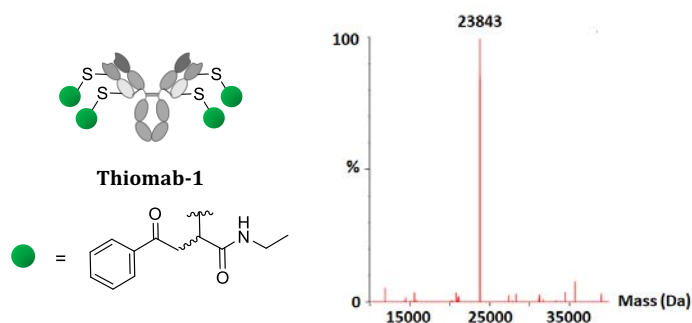


Figure 4.9: Structure of Thiomab-1 and deconvoluted mass spectrum after 48 h incubation with human serum: no significant degradation peak is observed. Mass peak corresponds to the doubly modified antibody (calcd. mass for two modifications: 23846 Da; found 23843 Da).

Moreover, in order to prove that the reaction condition and the modification does not alter the protein structure, the affinity of the antibody towards its antigen was evaluated. To this purpose, cell assays on SKBR3 cell line, which have a high level of Her2 antigen expression, were performed and the binding of modified Thiomab-3 antibody to cell membrane was assessed by flow cytometry.

As we can see in Figure 4.10, Thiomab-3 retains the affinity for Her2 antigen.

Therefore, this feature, together with the increased stability of the thioether linker, confers this conjugate good properties for *in vivo* application of these compounds.

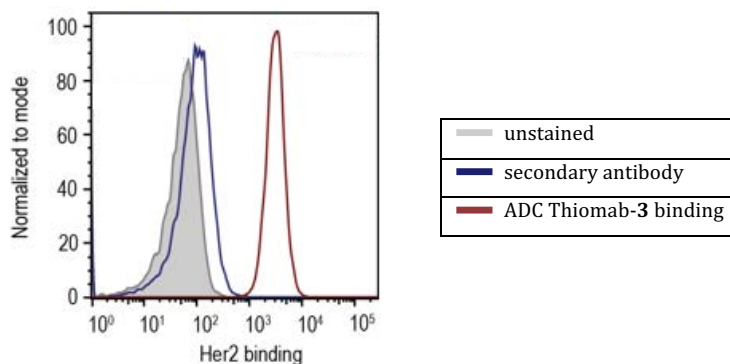


Figure 4.10: flow cytometry graph to analyse ADC Thiomab-3 binding.

4.3 Vinyl Pyridinium reagents for protein modification

In order to find new selective reagents for cysteine modification, a computational directed study has been performed on new electrophiles for protein conjugation. With the help of computational predictions, we envisaged in vinyl pyridinium and alkynyl pyridinium new suitable reagents for chemo-selective cysteine modification. In fact, modelling the reactivity between reagents **5**, **6**, **7** and **8** and different nucleophiles, suggested that the quaternisation of nitrogen atom on pyridine dramatically increases the reaction rate. Moreover, according to the calculations, both reagents reacts around a thousand time faster with thiolates than with amines (methyl thiol and methyl amine were used as the simplest model in these calculations), suggesting a preferential reactivity towards cysteines in proteins (**Figure 4.11**).

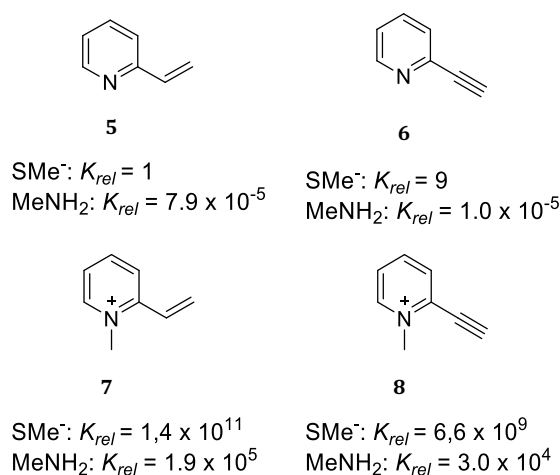


Figure 4.11: Relative kinetic constants of vinyl pyridine based reagents with SMe⁻ and MeNH₂ calculated with PCM(H₂O)/M06-2X/6-31+G(d,p).

The computational predictions were corroborated by small molecule studies of the reaction. Propane thiol, propyl amine and adequately protected cysteine and lysines were used for the reaction kinetic study by NMR, and the results are reported in the following table (**Table 4.2**).

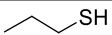
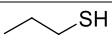


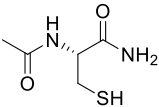
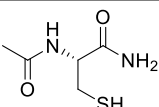
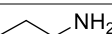
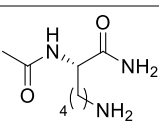
Entry	Electrophile	Nucleophile	Conversion (%)			k_2 (M ⁻¹ s ⁻¹)
			4 min	1 h	24 h	
1	5		0	10	62	6.81
2	7		83	99	-	6.21 x 10 ³
3	6		0	0	6	0.22
4	8		84	99	-	8.71 x 10 ³
5	5		2	36	89	0.62
6	7		93	93	-	2 x 10 ²
7	7		0	1	3	0.1
8	7		0	1	6	0.23

Table 4.2: experimental results for pyridine derivatives with different nucleophiles. All data reported refer to a typical reaction performed in deuterated NaPi buffer (100 mM, pH 7.6) at 37 °C, as described in the experimental part (Section 4.5.2).

The kinetic constants of these reactions were determined by ¹H-NMR studies in deuterated phosphate buffer at pH 7.6. Under these conditions, the fastest reactions occurs between thiols and quaternised reagents **7** and **8** (entries 2, 4 and 6, **Table 4.2**), with a kinetic constant >10² in all cases. Lysine and propyl amine, as predicted by the computational study, were much slower nucleophiles (kinetic constant up to 10³ times lower) with less than 6 % conversion after 24 h reactions in both cases (entry 7 and 8, **Table 4.2**).

2-alkynyl pyridinium derivative **8** was as much reactive as its analogue **7**, but it undergoes double addition when treated even with low thiol excess, yielding a stable dithioacetal. This might be interesting for other applications, such as disulfide stapling reagent or for tagging with biomolecules after conjugation, but in our case the resulting double bond may lead to undesired side reactions. So, in order to avoid potential

formation of reactive alkene isomers on proteins, electrophile **7** was chosen as the most convenient compound for protein modification.

Four proteins were selected to test the selectivity and the efficiency of the modification strategy with electrophile **7**.

C2Am domain of Synaptotagmin-I, Annexin-V, Ubiquitin and Albumin were used as model proteins. They have one cysteine residue, both engineered or naturally present and several lysines (and histidines eventually) that can act as nucleophiles. Moreover, all of these proteins have a relevant biological function that makes interesting the design of their conjugates. As an example, Annexin-V conjugates can be used for the early detection of apoptosis. ^[59]

Interestingly, in all the investigated proteins, the conjugation reaction was complete after 1 h incubation at 37 °C in NaPi buffer (50 mM, pH 8.0), as determined by mass analysis of the reaction mixtures using low excess of vinyl pyridinium **7** (from 1-10 equivalents, **Figure 4.12**).

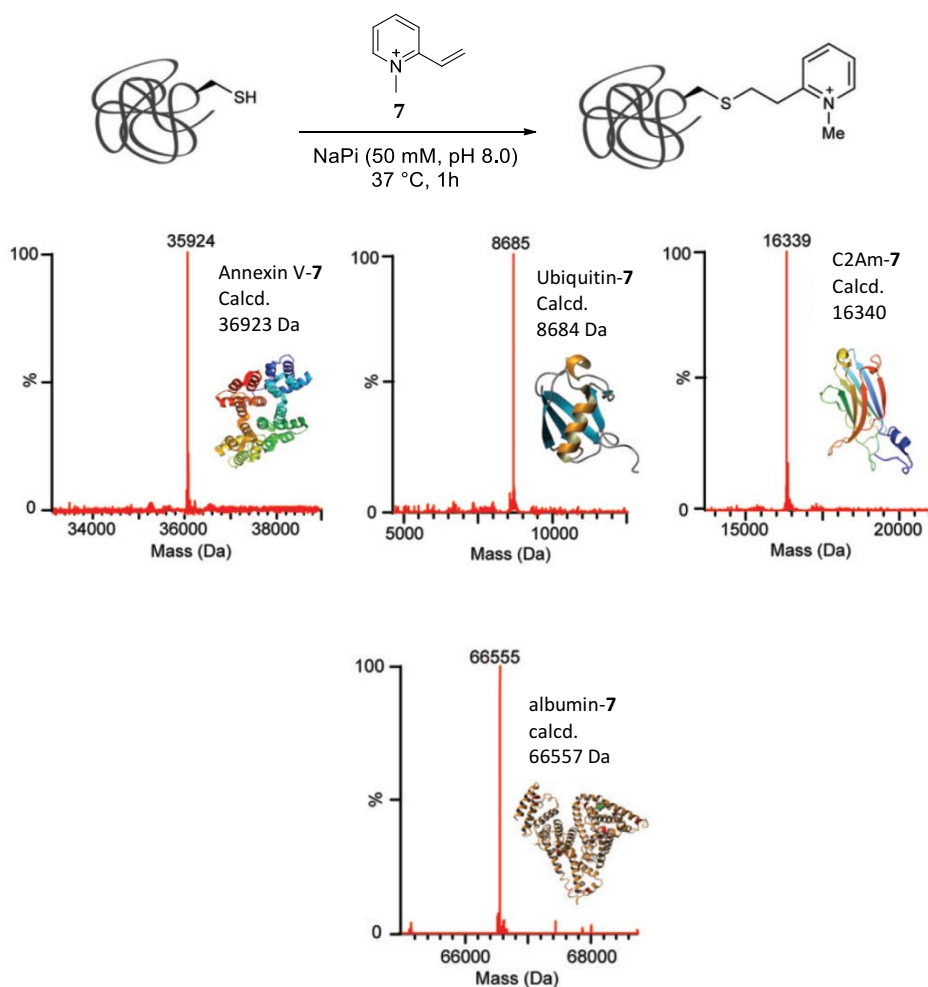


Figure 4.12: cysteine selective targeting with 1-methyl-2-vinylpyridinium 7; ES-MS spectra for the reaction of Annexin V, Ubiquitin, C2Am and albumin.

Under these conditions, the proteins were modified exclusively at the cysteine residue. This fact was corroborated by using Ellmann's reagent (**Figure 4.13**) as a control. This compound reacts only with thiols and it is used for the determination of free cysteine in proteins.^[60] Thus, blocking the cysteine residue in a protein with Ellmann's reagent before the conjugation reaction in the conditions described above, yielded no modified protein. Therefore, this result confirms that other potential nucleophiles in proteins were unreactive with scaffold 7 under the employed conditions. Equally, the modified derivatives obtained after the conjugation reaction, do not react with Ellmann's

reagent, meaning that all cysteine residues have been consumed (For experimental details see *Section 4.5.3*).

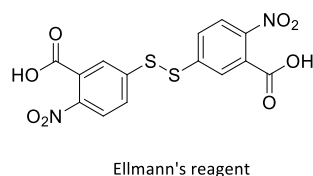


Figure 4.13: Structure of the Ellmann's reagent.

Next, before moving to the ADC synthesis, the stability of the thioether bond resulting from the bioconjugation was evaluated. C2Am-7 was used as model compound to assess the stability, and it was incubated in PBS buffer containing 20% of reconstituted human plasma at 37 °C. The degradation was monitored by ES-MS analysis and no significant degradation peaks were recorded even after 48 h incubation (**Figure 4.14**).

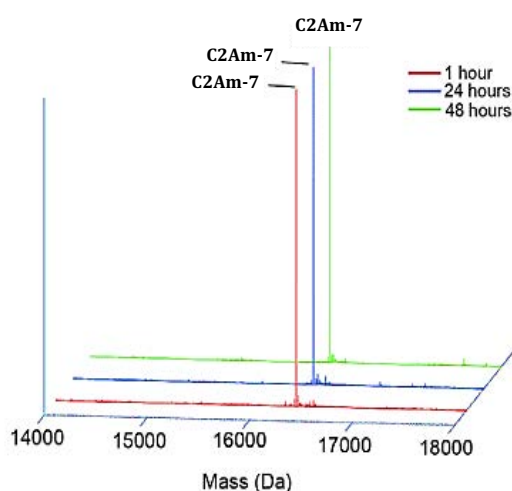


Figure 4.14: Superimposed deconvoluted MS spectra of C2Am-7 conjugate. Peak corresponding to conjugate (16431 Da) is the main peak in human plasma at 1, 24 and 48 h incubation.

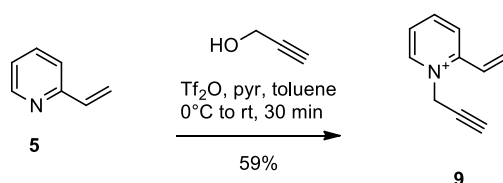
Considering those promising results, the synthesis of an ADC conjugate with this methodology represented the following step. Thus, a drug derivative bearing the vinyl pyridinium tag was synthesized.

4.3.1 Synthesis of MMAE-vinyl pyridinium derivative

To synthesize the desired compound bearing a quaternised vinyl pyridinium attached to the drug-linker system, the synthetic strategy adopted was based on a copper catalysed azido-alkyne cycloaddition. Indeed, the reagent and the product of this reaction do not compete, via Michael addition, to the activated double bond of the vinyl pyridinium. This could be the case, for instance, of the classical amide coupling, where the amine could give collateral addition to the double bond, instead of pure amide formation.

Thus, the first goal was the quaternisation of commercially available 2-vinyl pyridine in order to obtain a compound bearing an alkyne group.

Several alkylating agents were tested at this purpose, such as bromo-alkanes, iodo-alkanes, tosyl and nosyl derivatives but no satisfactory results were obtained when trying to quaternise pyridine nitrogen with these compounds. This was attributed to the competing polymerization reaction of 2-vinyl pyridine with the highly reactive vinyl pyridinium, that is much faster than nitrogen quaternisation with those alkylating agents.^[61] Fortunately, when the more reactive propargyl triflate was used, the alkylation reaction was accomplished successfully and the desired product was obtained in good yield (**Scheme 4.3**).

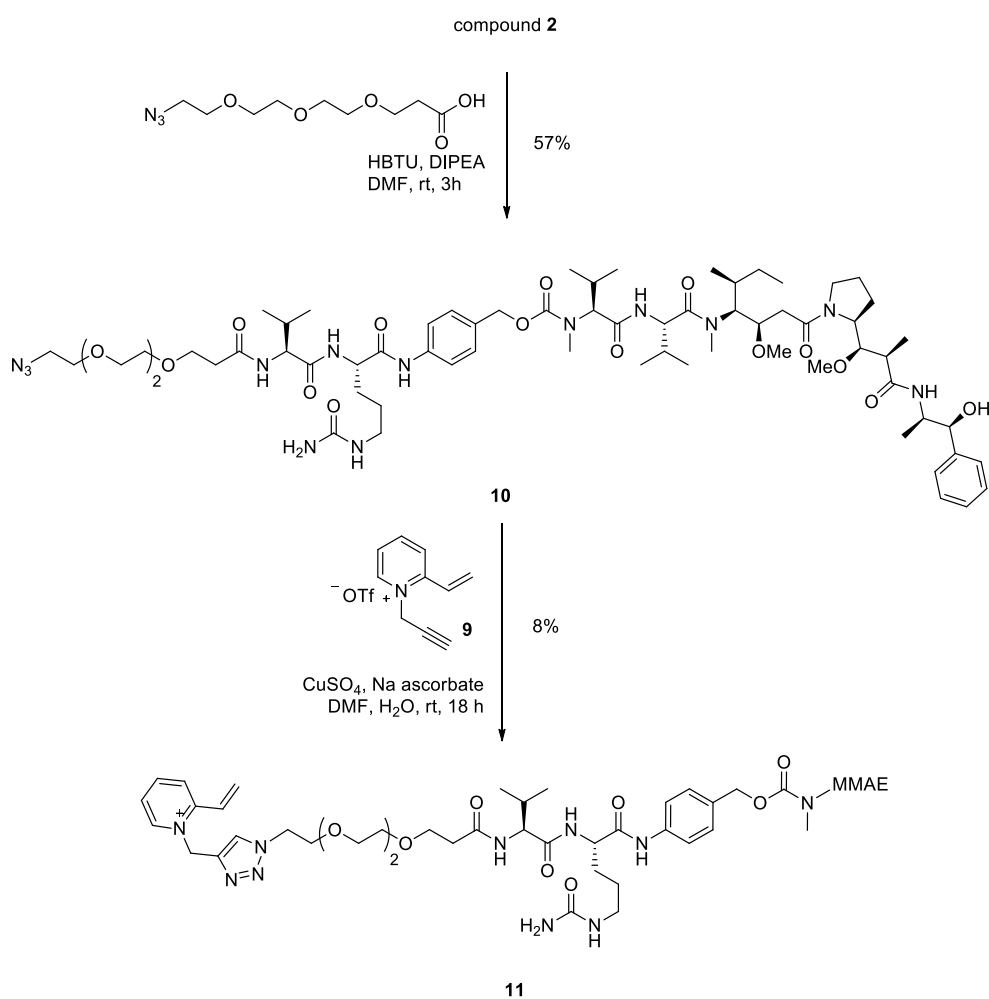


Scheme 4.3: synthesis of quaternised vinyl pyridine scaffold.

Compound **9** was obtained by treating commercially available 2-vinylpyridine with a freshly prepared solution of propargyl triflate. This one is obtained in situ by treatment of propargyl alcohol with slight excess of triflic anhydride and pyridine in toluene. The resulting solution of propargyl triflate is then separated and treated with 2-vinyl pyridine, previously dissolved in toluene. In this way, product **9** is obtained as a white

precipitate in good yield (59%) and without impurities deriving from polymerization side reactions.

Derivative **9** can be used as starting material for functionalization with azide derivatives. In our case, a MMAE derivative, bearing a spacer ending with a terminal azido group, was obtained in two steps from commercially available MMAE and ready to use for coupling reaction with alkyne **9** (**Scheme 4.4**).



Scheme 4.4: Synthesis of MMAE with the pyridinium tag **11** through copper catalysed cycloaddition.

As described for the previous synthesis (see Scheme 4.1), an enzymatically cleavable, self-immolative spacer was introduced to obtain compound **2**. Free amino group of the terminal valine was then coupled with a small PEG spacer bearing an azide as terminal group. The coupling for the corresponding amide was conducted under standard conditions with HBTU and DIPEA in DMF. Compound **10** was obtained with moderate yield (57%) after HPLC purification and it was ready to use in the copper-catalyzed azide-alkyne cycloaddition (CuAAC) with compound **9**. To this purpose, **9** was reacted with **10**, using CuSO₄ and sodium ascorbate to generate in situ the catalytically active Cu(I) species. After HPLC purification, compound **11** was obtained with high purity and ready-to-use in ADC synthesis.

4.3.2 ADC synthesis and biological assays

Finally, compound **11** and simple alkyne **9** were used for conjugation with the engineered Thiomab. Compound **11** would allow us to obtain directly an ADC containing MMAE as the warhead; in the other case, with compound **9** we could obtain easily an antibody bearing an alkyne handle. This could be interesting for further bio-orthogonal reaction with azide derivatives of biologically interesting compounds or hydrosilylation reactions, already described in protein.^[62] Again Thiomab was chosen as the targeting antibody, because of its engineered cysteine residue, that allow mono-modification of the light chain and its ability to target Her2 antigen, a common antigen expressed in mammalian cancer cell lines.

To conjugate compound **9**, a 25 μM solution of the antibody in NaPi buffer at pH 8.0 was treated with just 1 equivalent of alkyne **9**, affording complete conversion after only 1 h reaction. To obtain ADC Thiomab-**11**, an excess of compound **11** (5 equivalents for light chain) is required to have complete conversion, as detected by LC-MS analysis. However, the conjugation reaction proceeded fast and ADC Thiomab-**11**, bearing one modification per cysteine in the light chain is obtained after 1h (**Figure 4.15**). The result is a homogenous conjugate with a defined DAR of 2, bearing a new thioether bond resistant to hydrolysis in plasma (as demonstrated before for the C2Am derivative).

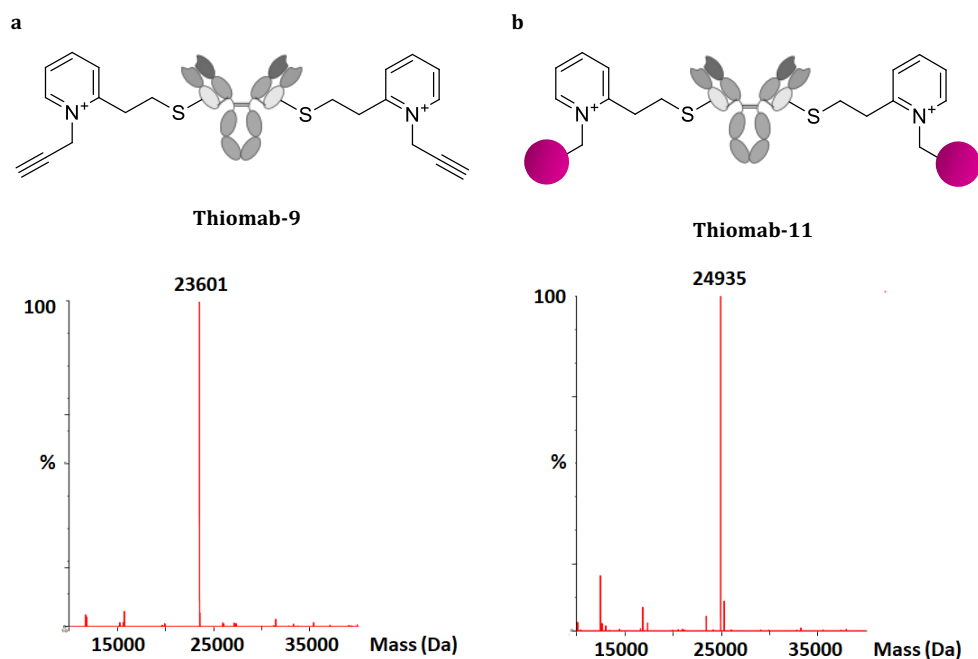


Figure 4.15: a) structures and deconvoluted mass spectrum of Thiomab-9: calcd. mass 23583; found 23601 (oxidation state); b) structures and deconvoluted mass spectrum of Thiomab-11: calcd. mass 24935; found 24935.

To determine whether the native structure of the antibody is retained, affinity assays were performed on SKBR3 cell line, and by flow cytometry analysis it was shown that the specificity towards Her2 positive cells is conserved (**Figure 4.16**).

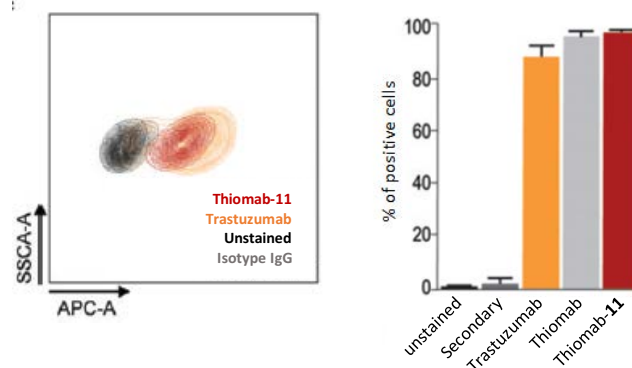


Figure 4.16: Counter plot indicates the binding affinity of Thiomab-11 to Her2 expressing SKBR3 cells at 50 nm. d) Percentage of SKBR3 cells bound to Thiomab-11 at 50 nm. Thiomab and Trastuzumab were used as positive controls and IgG Isotype was used as negative control.

4.4 Conclusions

Two different strategies for chemical modifications of proteins have been described. Firstly, driven by the excellent results obtained previously with carbonyl acrylate derivatives for selective modification of cysteine residues in proteins,^[51] we designed the synthesis of drug derivatives of carbonyl acrylamide, with the ultimate goal of obtaining a structurally defined ADC. To this purpose, two drugs were functionalised with carbonyl acrylamide handle: MMAE and Crizotinib. Both compounds were obtained in few steps and good yield, showing the synthetic accessibility of these derivatives. Two different antibodies, carrying engineered cysteines in the light chain were used for the bio-conjugation reaction. As a result, homogenous Thiomab and F16 antibody conjugates were obtained, with an exact DAR of 2, as determined by MS analysis of conjugates. In the field of ADC, the DAR value is of vital importance, since it is directly correlated with the pharmacokinetic properties of the antibody.^[63] Normally, DAR values of 2 or 4 are preferred to have a therapeutically functional conjugate, without losing the binding properties of the native structure. In our case, the

modification does not affect the structure of the antibodies, which keep their selectivity towards the antigen.

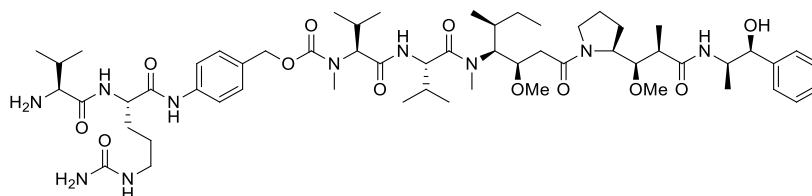
Secondly, a computational assisted study enabled the design of a new, ultrafast reagent for selective modification at cysteine residues. The selectivity of the reagents, based on pyridinium salts, was demonstrated both in small molecule models and in proteins. In fact, while cysteine alkylation is very fast (kinetic $> 10^2$), lysine residues remain unmodified. The method was optimized using commercially available 1-methyl-vinyl pyridinium **7**; then, considering the fast kinetic and mild conditions adopted for conjugation, our goal was the synthesis of a more complex structure containing MMAE as toxic warhead, as described in *Section 4.3.1*. Next, a MMAE-Trastuzumab conjugate was obtained in high yield, and it kept the structural properties necessary for antigen recognition. It will be interesting in the future evaluate the cytotoxicity of both ADCs obtained, and their selectivity both in vitro and in vivo.

Finally, it is important to note that both carbonyl acrylamide and vinyl pyridinium reagents are synthetically accessible, making this technology applicable to other demanding structures to synthesize new and homogeneous ADCs with improved properties for biological applications.

4.5 Experimental section

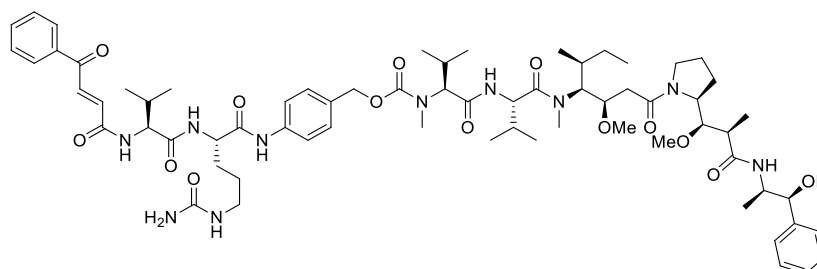
4.5.1 Synthesis

Synthesis of compound 2



This procedure is a modification of a literature protocol.^[64] Fmoc-ValCit-PAB-PNP (69 mg, 0.090 mmol) was dissolved in dry DMF (400 μ L) and to this solution HOBt (12.2 mg, 0.090 mmol) and DIPEA (31.0 μ L, 0.180 mmol) were added. The resulting mixture was added to a solution of MMAE (50 mg, 0.069 mmol) in dry DMF (100 μ L) and stirred for 16 h at room temperature. 300 μ L of DMF and 200 μ L of piperidine were then added to obtain a final piperidine concentration of 20% in DMF. After stirring for 1 h, Fmoc deprotection was confirmed by MALDI-TOF, and the crude mixture was diluted with CH₃CN and directly purified by HPLC on a Phenomenex Luna C18(2) column (10 μ , 250 mm x 21.2 mm), using the following gradient: 32.5% CH₃CN / 67.5% H₂O + 0.1% TFA to 42.5 CH₃CN / 57.5% H₂O + 0.1% TFA. Product containing fractions by mass (t_R = 13.80) were lyophilized overnight to obtain compound **2** as a white solid (42 mg, 0.034 mmol, 49% yield). HRMS (ESI+) m/z : calcd. for C₅₈H₉₅N₁₀O₁₂ [M+Na]⁺ 1123.7125, found 1123.7103. Analytical RP-HPLC: t_R = 19.2 (C18, 254 nm, gradient: from 68% H₂O with 0.1% TFA / 32% CH₃CN to 57 % H₂O + 0.1% TFA / 43% CH₃CN in 20 min).

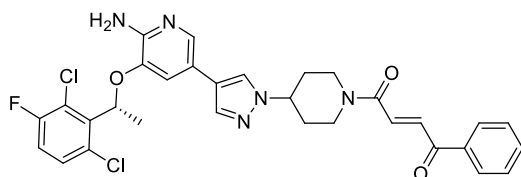
Synthesis of compound 3



Trans-3-benzoyl acrylic acid (30 mg, 0.170 mmol) was dissolved in dry DMF (1 mL) and cooled at -10 °C. Isobutyl chloroformate (26 µL, 0.204 mmol) and *N*-methylmorpholine (22 µL, 0.204 mmol) were then added under stirring. 0.5 mL of this solution was added to a solution of compound 2 (42 mg, 0.034 mmol) and NMM (4 µL, 0.036 mmol) in dry DMF (500 mL) cooled at -10 °C. After stirring for 15 min, the reaction was allowed to reach room temperature and kept stirring for an additional 1 h. Subsequently, the crude mixture was diluted with CH₃CN and purified by HPLC on a Phenomenex Luna C18(2) column (10 µ, 250 mm x 21.2 mm) using the following method: 32.5% CH₃CN / 67.5 % H₂O + 0.1% TFA to 42.5% CH₃CN over 20 min, then 42.5% solvent CH₃CN / 57.5% H₂O + 0.1% TFA to 100% CH₃CN over 10 minutes. Product containing fractions by mass (*t*_R = 26.6) were collected and lyophilized overnight to obtain compound 3 as a white solid (23.1 mg, 0.018 mmol, 53% yield). HRMS (ESI+) *m/z*: calcd. for C₆₈H₁₀₀N₁₀NaO₁₄ [M+Na]⁺ 1303.7313, found 1303.7317. ¹H-NMR (400 MHz, DMSO *d*-6) δ (ppm): 9.99 (brs, 1H amide), 8.66 (d, *J*=8.6 Hz, 1H, amide), 8.31 (d, *J*=7.5 Hz, 1H, amide), 8.05 – 7.97 (m, 2H, amide, Arom.), 7.89 (d, *J*=7.9 Hz, 0.5H), 7.76 (d, *J*=15.3, 1H, HC=CH), 7.74 – 7.69 (m, 1H, Arom.), 7.64 – 7.56 (m, 5H, Arom.), 7.32 – 7.22 (m, 7H, Ar, HC=CH), 7.20 – 7.15 (m, 1H, Arom.), 5.99 (brs, 1H), 5.39 (brs, 2H), 5.12 – 4.96 (m, 2H), 4.74 – 4.63 (m, 1H), 4.49 – 4.48 (m, 1H), 4.44 – 4.37 (m, 2H), 4.26 ('t', *J*=11.4 Hz, 1H), 4.04 – 3.92 (m, 2H), 3.78 (dd, *J*=9.4, 2.3 Hz, 0.5H), 3.59 – 3.53 (m, 2H), 3.24 – 3.23 (m, 4H), 3.20 (s, 2H), 3.18 (s, 1H), 3.12 (s, 2H), 3.06 – 3.02 (m, 2H), 2.97 (s, 2H), 2.88 – 2.78 (m, 3H), 2.41 (m, 1H), 2.27 (m, 1H), 2.18 – 1.88 (m, 4H), 1.89 – 1.67 (m, 4H), 1.48 (m, 6H), 1.0 – 0.95 (m, 7H), 0.92 – 0.71 (m, 26H); ¹³C-NMR (75 MHz, DMSO *d*-6) δ (ppm): of characteristic carbon signal: 190.5 (PhC=O), 164.0 (CH=CHCONH₂), 159.3 (C=O carbamate). Analytical RP-HPLC: *t*_R = 29.3 (C18, 254 nm, gradient: from 68% H₂O + 0.1% TFA / 32% CH₃CN to 57

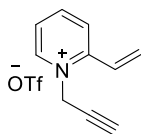
% H₂O with 0.1% TFA / 43% CH₃CN in 21 min, then from 57% to 32% H₂O with 0.1% TFA / 68% CH₃CN in 9 min).

Synthesis of compound 4

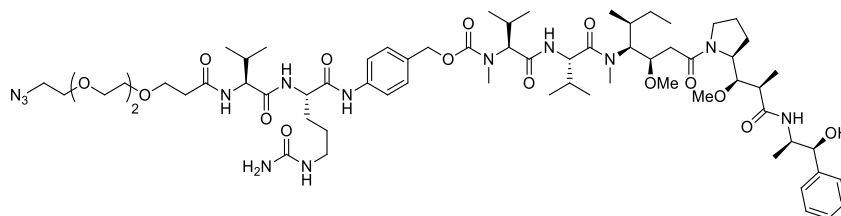


Trans-3-benzoyl acrylic acid (48 mg, 0.27 mmol), was dissolved in dry DMF (1 mL) and cooled at -10 °C. To this solution isobutyl chloroformate (IBCF, 42 μL, 0.32 mmol) and *N*-methyl

morpholine (NMM, 36 μL, 0.33 mmol) were added under stirring. 0.1 mL of the resulting mixture were then added to a solution of Crizotinib (10 mg, 0.022 mmol) and NMM (2.5 μL, 0.022 mmol) in dry DMF, cooled at -0 °C. After stirring 15 min, the reaction was allowed to reach room temperature and kept stirring for additional 1.5 h. The crude reaction mixture was concentrated and directly purified through column chromatography (eluent AcOEt:MeOH 20:1) to give compound 4 as a light yellow solid (8 mg, 60% yield). HRMS (ESI+) *m/z*: calcd. for C₃₁H₂₉Cl₂FN₅O₃ [M+H]⁺, 608.1626, found 608.1628. ¹H-NMR (400 MHz, CDCl₃) δ (ppm): 8.06 – 8.03 (m, 2H, Arom.), 7.96 (d, *J*=15.0 Hz, 1H, CH=CH), 7.74 (d, *J*=1.7 Hz, 1H, H-Arom.), 7.64 – 7.60 (m, 1H, H-Arom.), 7.57 – 7.49 (m, 5H, H-Arom.), 7.31 (dd, ⁴*J*_{C-F}=4.8 Hz, *J*_{H-H}=8.9 Hz, 1H, H-Arom.), 7.06 (dd, ³*J*_{C-F}=7.9 Hz, *J*_{H-H}=8.9 Hz, 1H, H-Arom.), 6.88 (d, *J*=1.8 Hz, 1H, H-Arom.), 6.08 (q, *J*=6.7 Hz, 1H, CHCH₃), 41.93 (brs, 2H, NH₂), 4.82 – 4.78 (m, 1H), 4.42-4.36 (m, 1H), 4.23 – 4.20 (m, 1H), 3.39 – 3.33 (m, 1H), 3.01 – 2.95 (m, 1H), 2.08 – 2.02 (m, 2H), 1.99 – 1.85 (m, 2H), 1.86 (d, *J*=6.7 Hz, 3H, CHCH₃). ¹³C-NMR (75 MHz, CDCl₃) δ (ppm): 189.4 (Cq, C=O), 164.1 (Cq, N_C=O), 157.5 (d, *J*=248.9 Hz, Cq, detected by a HMBC experiment), 148.9 (Cq), 139.9 (Cq), 136.8 (2Cq), 136.1 (CH), 134.9 (CH), 134.4 (CH), 133.8 (CH), 132.4 (CH), 129.9 (CH), 128.9, 128.9, 128.8 (5 C, Cq, 4 CH), 122.8 (CH), 122.1 (d, *J*=19.1 Hz, Cq), 120.1 (Cq), 119.0 (Cq), 116.8 (d, *J*=23.1, CH), 115.1 (CH), 72.5 (O-CHCH₃), 58.7 (CH), 44.9 (CH₂), 41.2 (CH₂), 33.0 (CH₂), 31.9 (CH₂), 18.9 (CH₃).

Synthesis of compound 9

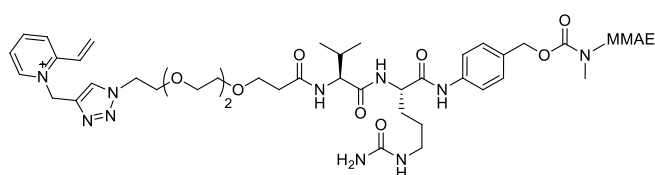
Propargyl alcohol (87 μL , 1.5 mmol) and dry pyridine (121 μL , 1.5 mmol) were dissolved in dry toluene (1 mL) under an Argon atmosphere. The resulting solution was added to a solution of Tf_2O (252 μL , 1.5 mmol) in dry toluene (1 mL) at 0 $^\circ\text{C}$ under argon. After stirring for 15 min at this temperature, a white solid is formed and allowed to precipitate. The supernatant was taken with a syringe and transferred to a schlenk. To this propargyl triflate solution, cooled at 0 $^\circ\text{C}$, a solution of 2-vinylpyridine (107 μL , 1 mmol) in 1 mL of dry toluene was added over 10 min. The reaction was stirred 10 min at room temperature, and then stopped adding 10 mL of Et_2O for complete product precipitation. The desired product was washed with Et_2O and used for the next steps without further purification (174 mg, 0.59 mmol, 59%). ^1H NMR (300 MHz, CD_3OD) δ (ppm): 9.08 (dd, $J=6.3, 1.4$ Hz, H-pyr), 8.61 (td, $J=7.7, 1.5$ Hz, H-pyr), 8.39 (dd, $J=8.2, 1.5$ Hz, H-pyr), 8.05 (ddd, $J=7.8, 6.3, 1.5$ Hz, H-pyr), 7.37 (dd, $J=17.0, 11.3$ Hz, H-vinyl), 6.54 (d, $J=17.0$ Hz, H-vinyl), 6.24 (d, $J=11.3$ Hz, H-vinyl), 5.59 (d, $J=2.6$ Hz, CH_2), 3.50 (t, $J=2.6$ Hz, CH). ^{13}C NMR (75 MHz, CD_3OD) δ (ppm): 152.8 (Cq), 146.4 (C-pyr), 144.2 (C-pyr), 129.9 (CH_2 vinyl), 126.7, 126.5 (3C, C-pyr, CH vinyl), 80.1 (C-propargyl), 73.5 (C-propargyl), 47.7 (CH_2 - N); MS (ESI+) m/z 144.08 (M+).

Synthesis of compound 10

3-(2-(2-(2-azidoethoxy)ethoxy)ethoxy) propanoic acid (10 mg, 0.039 mmol) was dissolved in dry DMF (250 μL) and reacted with DIPEA (13.6 μL , 0.078 mmol) and HBTU (14 mg, 0.035 mmol). This solution was added to compound 2 dissolved in 250 μL of DMF. The reaction mixture was stirred 3 h at room temperature, then diluted with 3 mL of CH_3CN and directly purified by HPLC on a Phenomenex Luna C18(2) column (10 μm , 250 mm x 21.2 mm), using the following gradient: 32.5% solvent B/ 67.5% solvent A to 42.5 solvent B/ 57.5% solvent A in 20 minutes, then 42.5% to 100% solvent B in 10

minutes (solvent A = deionized H₂O + 0.1% TFA, solvent B = CH₃CN). Product containing fractions by mass ($t_R = 25.3$) were lyophilized overnight to obtain compound **10** as a white solid (10 mg, 0.0074 mmol, 57% yield). HRMS (ESI+) m/z : calcd. for C₆₇H₁₀₉N₁₃NaO₁₆ [M+Na]⁺, 1374.8007; found 1374.7974. Analytical RP-HPLC: $t_R = 27.6$ (C18, 254 nm, gradient: from 68% H₂O with 0.1% TFA / 32% CH₃CN to 57% H₂O with 0.1% TFA / 43% CH₃CN in 21 min, then from 57% to 32% H₂O with 0.1% TFA / 68% CH₃CN in 9 min).

Synthesis of compound 11



To a solution of compound **10** (9.4 mg, 0.0069 mmol) and alkyne **9** (5.4 mg, 0.021 mmol) in a mixture

DMF:H₂O 1:1 (200 μ L), 22 μ L of a 0.1 M solution of CuSO₄ in H₂O and 34 μ L of a 0.1 M solution of Na ascorbate were added. The reaction was stirred for 6 hours at room temperature, then it was directly purified by HPLC on a Phenomenex Luna C18(2) column (10 μ , 250 mm x 21.2 mm), using the following gradient: 32.5% solvent B/ 67.5% solvent A to 42.5 solvent B/ 57.5% solvent A in 20 minutes, then 42.5% to 100% solvent B in 10 minutes (solvent A = deionized H₂O + 0.1% TFA, solvent B = CH₃CN). Product containing fraction ($t_R = 16.2$) were collected and lyophilized overnight to obtain compound **11** as a white solid (0.8 mg, 0.5 μ Moles, 8% yield). HRMS (ESI+) m/z : calcd. for C₇₇H₁₁₉N₁₄O₁₆ [M]⁺, 1495.8923; found 1495.8883. Analytical RP-HPLC: $t_R = 22.2$ (C18, 254 nm, gradient: from 68% H₂O with 0.1% TFA / 32% CH₃CN to 57% H₂O with 0.1% TFA / 43% CH₃CN in 21 min, then from 57% to 32% H₂O with 0.1% TFA / 68% CH₃CN in 9 min).

4.5.2 Kinetic studies

The second-order reaction constants of the reactions of electrophiles **5-8** with small-molecule models 1-propanethiol, *N*-propylamine, *N*-acetylcysteine amide and *N* α -acetyl-lysine amide were determined by ¹H NMR (400 MHz) at 298 K in deuterated NaPi buffer (100 mM, pH 7.6). Electrophile concentration was 3.0 mM in all cases. A ¹H NMR spectrum was recorded every 85 s (number of scans: 16). Around 5 min were needed

to record the first spectrum after mixing the reagents. The observed second-order rate constants k_{obs} (i.e. k_2) were derived from the slope of a linearly-fitted plot of the inverse of the electrophile concentration ($1/[E]$) versus time.

4.5.3 Antibody conjugation

Antibody drug conjugation reactions were performed by Gonçalo Bernardes group at Department of Chemistry, University of Cambridge.

General procedure for conjugation with carbonyl acrylamide derivatives

To an eppendorf tube with NaPi (50 mM, pH 8.0 or 20 mM, pH 7.0) and DMF (10% of total volume), an aliquot of a stock solution of protein (final concentration 15–25 μ M) was added. Afterwards, a solution of the carbonyl acrylamide derivative (1–10 equiv.) in DMF was added and the resulting mixture was vortexed for 10 seconds. The reaction was mixed for 2, 6 or 24 h at 37 °C. A 10 μ L aliquot at each reaction time was analysed by LC–MS and reaction progression monitored. After complete conversion, protein conjugates were purified by Zeba-Spin Desalting Column (previously equilibrated with the adequate buffer) to remove small molecules, or by dialysis. Protein concentration was determined by nano-drop or by Bradford protein assay.

Synthesis of Thiomab-1

The reaction was performed according to the general procedure, using Thiomab LC-V205C (final concentration 15 μ M), compound **1** (10 equiv.) in NaPi buffer (50 mM, pH 8.0). After 2 hours at 37 °C LC–MS indicated complete conversion to the expected product (calculated mass for the light chain, 23643 Da –1 modification– or 23846 Da – 2 modifications–; observed mass for the light chain, 23843 Da).

Synthesis of Thiomab-3

The reaction was performed according to the general procedure, using Thiomab LC-V205C (final concentration 20 μ M), compound **3** (10 equiv.) in NaPi buffer (20 mM, pH 7.0). After 6 hours at 37°C LC–MS indicated complete conversion to the expected product (calculated mass for the light chain, 24721 Da; observed mass for the light-chain, 24721 Da).

Synthesis of F16-3

The reaction was performed according to the general procedure, using F16 antibody (final concentration 5 μ M), compound **3** (10 equiv.) in NaPi buffer (20 mM, pH 7.0). After 6 hours, LC-MS showed complete conversion to the expected product (calculated mass for the light-chain, 23985 Da; observed mass for the light-chain, 23983 Da).

Synthesis of F16-4

The reaction was performed according to the general procedure, using F16 antibody (final concentration 5 μ M), compound **4** (10 equiv.) in NaPi buffer (20 mM, pH 7.0). After 6 hours, LC-MS showed complete conversion to the expected product (calculated mass for the light-chain, 23312 Da; observed mass for the light-chain, 23307 Da).

General procedure for conjugation with quaternised vinyl pyridinium reagents

To an eppendorf tube with NaPi (50 mM or 20 mM, pH 8.0) and DMF (10% of total volume), an aliquot of a stock solution of protein (final concentration 10 μ M) was added. Afterwards, a solution of the quaternised pyridine derivative (1 to 10 equiv.) in DMF was added and the resulting mixture was vortexed for 10 seconds. The reaction was mixed for 1 or 2 h at 37 °C. A 10 μ L aliquot of each reaction time was analysed by LC-MS and conversion to the expected product was observed. After complete conversion, protein conjugates were purified by Zeba-Spin Desalting Column (previously equilibrated with the adequate buffer) to remove small molecules, or by dialysis. Protein concentration was determined by nano-drop or by Bradford protein assay.

Synthesis of C2Am-7

The reaction was performed according to the general procedure, using C2Am, compound **7** (10 equiv.) in NaPi buffer (50 mM, pH 8.0). After 1 hour at 37°C, complete conversion was observed by LC-MS (calculated mass, 16340 Da; observed mass, 16339 Da).

Synthesis of Ubiquitin-7

The reaction was performed according to the general procedure, using Ubiquitin-K63C, compound **7** (1 equiv.) in NaPi buffer (50 mM, pH 8.0). After 1 hour at 37°C, complete conversion was observed by LC-MS (calculated mass, 8684 Da; observed mass, 8685 Da). The same occurred when using 10 equiv. of **2** and leaving the reaction for 2 h, which shows the selectivity for cysteine over other nucleophilic residues even when the reagent is present in excess.

Synthesis of Annexin V-7

The reaction was performed according to the general procedure, using Annexin V-Cys315, compound **7** (10 equiv.) in NaPi buffer (50 mM, pH 8.0). After 1 hour at 37°C, complete conversion was observed by LC-MS (calculated mass, 35923 Da; observed mass, 35924 Da)

Synthesis of Albumin-7

The reaction was performed according to the general procedure, using Albumin-Cys34, compound **7** (1 equiv.) in NaPi buffer (50 mM, pH 8.0). After 1 hour at 37°C, complete conversion was observed by LC-MS. A 10 µL aliquot was analysed by LC-MS and conversion to the expected product was observed (calculated mass, 66557 Da; observed mass, 66555 Da).

Synthesis of Thiomab-9

The reaction was performed according to the general procedure, using Thiomab, compound **9** (1 equiv.) in NaPi buffer (20 mM, pH 8.0). After 1 hour at 37°C, complete conversion was observed by LC-MS (calculated mass for the light-chain, 23583 Da; observed mass for the light-chain, 23601 Da –oxidation state-).

Synthesis of Thiomab-10

The reaction was performed according to the general procedure, using Thiomab, compound **10** (10 equiv.) in NaPi buffer (20 mM, pH 8.0). After 1 hour at 37°C, complete conversion was observed by LC-MS (calculated mass for the light-chain, 24935 Da;

observed mass for the light-chain, 24935 Da; calculated mass for the heavy-chain, 50595 Da; observed mass for the heavy-chain, 50590 Da).

Control Reaction of C2Am-7 with 5,5'-dithiobis(2-nitrobenzoic acid)

A 40 μL aliquot of C2Am-Cys95-7 (10 μM) was transferred to a 0.5 mL eppendorf tube. An aliquot of 0.8 μL (500 equiv.) of a stock suspension of 5,5'-dithiobis(2-nitrobenzoic acid) (0.500 mM) was added and the resulting mixture vortexed for 10 seconds. After 4 h of additional mixing at 37 $^{\circ}\text{C}$, small molecules were removed from the reaction mixture by loading the sample into a Zeba Spin Desalting Column previously equilibrated with NaPi buffer (50 mM, pH 8.0). The sample was eluted via centrifugation (2 min, 1000xg). A 10 μL aliquot was analysed by LC-MS and no conversion to a potentially doubly modified protein was observed (calculated mass for the double modification, 16537 Da; observed mass, 16341 Da).

Control Reaction of C2Am-Ellman's with 7

A 40 μL aliquot of C2Am-Ellman's (10 μM) (synthesized as described in the general procedure, using excess Ellman's reagent) was transferred to a 0.5 mL eppendorf tube. An aliquot of 1.0 μL (10 equiv.) of a stock solution of 7 (8.3 mM) was added and the resulting mixture vortexed for 10 seconds. After 1 h of additional mixing, at 37 $^{\circ}\text{C}$, a 10 μL aliquot was analysed by LC-MS and no conversion to the potentially doubly modified protein was observed (calculated mass for the double modification, 16537 Da; observed mass, 16421 Da).

General procedure for ADC stability assay

To a 20 μL aliquot of the bio-conjugate (10 μM) in NaPi buffer (50 mM, pH 8.0) 1 μL of reconstituted human plasma was added at room temperature and the resulting mixture vortexed for 10 seconds. The resulting reaction mixture was then mixed at 37 $^{\circ}\text{C}$ for 48 h, at which time a 10 μL aliquot was analysed by LC-MS.

4.5.4 Cell assays

Cell assay for ADC binding were performed by Gonçalo Bernardes group at Instituto de Medicina Molecular, Faculdade de Medicina, Universidade de Lisboa

Cell culture

SKBR3 cells (human breast adenocarcinoma cell line) were used for the in vitro studies. The cells were maintained in a humidified incubator at 37 °C under 5% CO₂ and grown using 1x DMEM (Dulbecco's modified Eagle medium) with Sodium Pyruvate and without L-Glutamine (Invitrogen, Life Technologies). Medium was supplemented with 10% heat-inactivated fetal bovine serum (FBS) (Gibco, Life Technologies), 1x MEM NEAA (Gibco, Life Technologies), 1x GlutaMAX (Gibco, Life Technologies), 200 units/mL penicillin and 200 µg/mL streptomycin (Gibco, Life Technologies) and 10 mM HEPES (Gibco, Life Technologies).

Thiomab-3 and Thiomab-11 specificity as determined by flow cytometry analysis.

The specificity of conjugates Thiomab-3 and Thiomab-11 was determined by flow cytometry analysis. For this purpose, SKRB3 cells (with high expression of HER2 receptor) were plated in 96 well round bottom plates (100.000 cells per well) and blocked for 1h with 10% FBS in 1x PBS (flow cytometry buffer). After this blocking step, the cells were incubated with 30 µL of 50 nM of Thiomab-3 and Thiomab-11 at room temperature. After 1 h of incubation cells were washed three times (100 µL flow cytometry buffer added and centrifuged for 5 min at 400 G) and incubated with 30 µL/well of Goat anti-Human IgG (H+L) Cross-Adsorbed Secondary Antibody, Alexa Fluor 647 (cat. No A21445, Life Technologies) at 10 µg/mL, for 1 h. After this incubation period, the cells were washed one time as previously described, re-suspended in 400 µL of 10% FBS in PBS and transferred to flow cytometry tubes. Acquisition was done using a BD LSR Fortessa set up with a 640 nm laser and a 670/14 nm band-pass filter (combination used for APC detection). Data analysis was done with FlowJo (version 6.3.4, FlowJo) software. Data represents mean ± s.d of 3 biological replicates and only single-cell events are shown.

4.5.5 Quantum Mechanical calculations

Quantum Mechanical Calculations were performed by Gonzalo Jiménez Osés, at Universidad de La Rioja

Full geometry optimizations were carried out with Gaussian 16^[65] using the M06-2X hybrid functional^[66] and 6-31+G(d,p) basis set in combination with ultrafine integration grids. Bulk solvent effects in water were considered implicitly through the IEF-PCM polarizable continuum model.^[67] The possibility of different conformations was taken into account. Frequency analyses were carried out at the same level used in the geometry optimizations, and the nature of the stationary points was determined in each case according to the appropriate number of negative eigenvalues of the Hessian matrix. The quasiharmonic approximation reported by Trular et al. was used to replace the harmonic oscillator approximation for the calculation of the vibrational contribution to enthalpy and entropy.^[68] Scaled frequencies were not considered. Mass-weighted intrinsic reaction coordinate (IRC) calculations were carried out by using the Gonzalez and Schlegel scheme^[69] in order to ensure that the TSs indeed connected the appropriate reactants and products. Gibbs free energies (ΔG) were used for the discussion on the relative stabilities of the considered structures. Free energies calculated using the gas phase standard state concentration (1 atm = 1/24.5 M) were converted to reproduce the standard state concentration in solution (1 M) by adding or subtracting 1.89 kcal mol⁻¹ for bimolecular additions and decompositions, respectively. The lowest energy conformer for each calculated stationary point was considered in the discussion; all the computed structures can be obtained from authors upon request. Cartesian coordinates, electronic energies, entropies, enthalpies, Gibbs free energies, and lowest frequencies of the calculated structures are available below.

4.6 References

- [1] N. Krall, F. P. da Cruz, O. Boutureira, G. J. L. Bernardes, *Nat. Chem.* **2015**, *8*, 103–113.
- [2] T. Tamura, I. Hamachi, *J. Am. Chem. Soc.* **2018**, *141*, 2782–2799.
- [3] O. Boutureira, G. J. L. Bernardes, *Chem. Rev.* **2015**, *115*, 2174–2195.
- [4] R. Fu, L. Carroll, G. Yahioğlu, E. O. Aboagye, P. W. Miller, *ChemMedChem* **2018**, *13*, 2466–2478.
- [5] K. Lang, L. Davis, J. Torres-Kolbus, C. Chou, A. Deiters, J. W. Chin, *Nat. Chem.* **2012**, *4*, 298–304.
- [6] S. Zheng, G. Zhang, J. Li, P. R. Chen, *Angew. Chemie* **2014**, *126*, 6567–6571.
- [7] M. Rashidian, E. J. Keliher, M. Dougan, P. K. Juras, M. Cavallari, G. R. Wojtkiewicz, J. T. Jacobsen, J. G. Edens, J. M. J. Tas, G. Victora, et al., *ACS Cent. Sci.* **2015**, *1*, 142–147.
- [8] M. Rashidian, L. Wang, J. G. Edens, J. T. Jacobsen, I. Hossain, Q. Wang, G. D. Victora, N. Vasdev, H. Ploegh, S. H. Liang, *Angew. Chemie* **2016**, *128*, 538–543.
- [9] Z. Zhou, N. Devoogdt, M. R. Zalutsky, G. Vaidyanathan, *Bioconjug. Chem.* **2018**, *29*, 4090–4103.
- [10] J. A. Prescher, D. H. Dube, C. R. Bertozzi, *Nature* **2004**, *430*, 873–877.
- [11] A. Beck, L. Goetsch, C. Dumontet, N. Corvaia, *Nat. Rev. Drug Discov.* **2017**, *16*, 315–337.
- [12] H. Yao, F. Jiang, A. Lu, G. Zhang, *Int. J. Mol. Sci.* **2016**, *17*, 194.
- [13] G. D. Lewis Phillips, G. Li, D. L. Dugger, L. M. Crocker, K. L. Parsons, E. Mai, W. A. Blättler, J. M. Lambert, R. V. J. Chari, R. J. Lutz, et al., *Cancer Res.* **2008**, *68*, 9280–9290.
- [14] M. T. Kim, Y. Chen, J. Marhoul, F. Jacobson, *Bioconjug. Chem.* **2014**, *25*, 1223–1232.
- [15] V. Chudasama, A. Maruani, S. Caddick, *Nat. Chem.* **2016**, *8*, 114–119.
- [16] J. M. Chalker, G. J. L. Bernardes, Y. A. Lin, B. G. Davis, *Chem. – An Asian J.* **2009**, *4*, 630–640.
- [17] P. Akkapeddi, S.-A. Azizi, A. M. Freedy, P. M. S. D. Cal, P. M. P. Gois, G. J. L. Bernardes, *Chem. Sci.* **2016**, *7*, 2954–2963.

- [18] C. D. Spicer, B. G. Davis, *Nat. Commun.* **2014**, *5*, 4740.
- [19] P. M. S. D. Cal, G. J. L. Bernardes, P. M. P. Gois, *Angew. Chemie Int. Ed.* **2014**, *53*, 10585–10587.
- [20] H. Chen, R. Huang, Z. Li, W. Zhu, J. Chen, Y. Zhan, B. Jiang, *Org. Biomol. Chem.* **2017**, *15*, 7339–7345.
- [21] M. J. Matos, B. L. Oliveira, N. Martínez-Sáez, A. Guerreiro, P. M. S. D. Cal, J. Bertoldo, M. Maneiro, E. Perkins, J. Howard, M. J. Deery, et al., *J. Am. Chem. Soc.* **2018**, *140*, 4004–4017.
- [22] M. T. Taylor, J. E. Nelson, M. G. Suero, M. J. Gaunt, *Nature* **2018**, *562*, 563–568.
- [23] S. Lin, X. Yang, S. Jia, A. M. Weeks, M. Hornsby, P. S. Lee, R. V. Nichiporuk, A. T. Iavarone, J. A. Wells, F. D. Toste, et al., *Science (80-.)*. **2017**, *355*, 597–602.
- [24] Y. Seki, T. Ishiyama, D. Sasaki, J. Abe, Y. Sohma, K. Oisaki, M. Kanai, *J. Am. Chem. Soc.* **2016**, *138*, 10798–10801.
- [25] M. Imiołek, G. Karunanithy, W.-L. Ng, A. J. Baldwin, V. Gouverneur, B. G. Davis, *J. Am. Chem. Soc.* **2018**, *140*, 1568–1571.
- [26] H. Ban, J. Gavrilyuk, C. F. Barbas, *J. Am. Chem. Soc.* **2010**, *132*, 1523–1525.
- [27] S. R. Adusumalli, D. G. Rawale, U. Singh, P. Tripathi, R. Paul, N. Kalra, R. K. Mishra, S. Shukla, V. Rai, *J. Am. Chem. Soc.* **2018**, *140*, 15114–15123.
- [28] C. B. Rosen, M. B. Francis, *Nat. Chem. Biol.* **2017**, *13*, 697–705.
- [29] S. Bloom, C. Liu, D. K. Kölmel, J. X. Qiao, Y. Zhang, M. A. Poss, W. R. Ewing, D. W. C. MacMillan, *Nat. Chem.* **2017**, *10*, 205.
- [30] N. S. Joshi, L. R. Whitaker, M. B. Francis, *J. Am. Chem. Soc.* **2004**, *126*, 15942–15943.
- [31] J. I. Macdonald, H. K. Munch, T. Moore, M. B. Francis, *Nat. Chem. Biol.* **2015**, *11*, 326–331.
- [32] N. Toda, S. Asano, C. F. Barbas III, *Angew. Chemie - Int. Ed.* **2013**, *52*, 12592–12596.
- [33] S. Kolodyhh, O. Koniev, Z. Baatarkhuu, J.-Y. Bonnefoy, F. Dabaene, S. Cianferani, A. Van Dorsselaer, A. Wagner, *Bioconjug. Chem.* **2015**, *26*, 197–200.
- [34] J. M. Chalker, L. Lercher, N. R. Rose, C. J. Schofield, B. G. Davis, *Angew. Chemie Int. Ed.* **2012**, *51*, 1835–1839.
- [35] G. J. L. Bernardes, J. M. Chalker, J. C. Errey, B. G. Davis, *J. Am. Chem. Soc.* **2008**,

- 130, 5052–5053.
- [36] J. M. Chalker, S. B. Gunnoo, O. Boutureira, S. C. Gerstberger, M. Fernández-González, G. J. L. Bernardes, L. Griffin, H. Hailu, C. J. Schofield, B. G. Davis, *Chem. Sci.* **2011**, *2*, 1666–1676.
- [37] J. Dadová, S. R. Galan, B. G. Davis, *Curr. Opin. Chem. Biol.* **2018**, *46*, 71–81.
- [38] A. M. Freedy, M. J. Matos, O. Boutureira, F. Corzana, A. Guerreiro, P. Akkapeddi, V. J. Somovilla, T. Rodrigues, K. Nicholls, B. Xie, et al., *J. Am. Chem. Soc.* **2017**, *139*, 18365–18375.
- [39] T. H. Wright, B. J. Bower, J. M. Chalker, G. J. L. Bernardes, R. Wiewiora, W.-L. Ng, R. Raj, S. Faulkner, M. R. J. Vallée, A. Phanumartwiwath, et al., *Science (80-.)*. **2016**, *354*, 597.
- [40] C. Zhang, E. V Vinogradova, A. M. Spokoyny, S. L. Buchwald, B. L. Pentelute, *Angew. Chemie Int. Ed.* **2019**, *58*, 4810–4839.
- [41] E. V Vinogradova, C. Zhang, A. M. Spokoyny, B. L. Pentelute, S. L. Buchwald, *Nature* **2015**, *526*, 687–691.
- [42] J. M. J. M. Ravasco, H. Faustino, A. Trindade, P. M. P. Gois, *Chem. – A Eur. J.* **2019**, *25*, 43–59.
- [43] C. F. Brewer, J. P. Riehm, *Anal. Biochem.* **1967**, *18*, 248–255.
- [44] J. F. Ponte, X. Sun, N. C. Yoder, N. Fishkin, R. Laleau, J. Coccia, L. Lanieri, M. Bogalhas, L. Wang, S. Wilhelm, et al., *Bioconjug. Chem.* **2016**, *27*, 1588–1598.
- [45] A. D. Baldwin, K. L. Kiick, *Bioconjug. Chem.* **2011**, *22*, 1946–1953.
- [46] N. Fishkin, E. K. Maloney, R. V. J. Chari, R. Singh, *Chem. Commun.* **2011**, *47*, 10752–10754.
- [47] D. Kalia, P. V Malekar, M. Parthasarathy, *Angew. Chemie Int. Ed.* **2016**, *55*, 1432–1435.
- [48] D. Kalia, S. P. Pawar, J. S. Thopate, *Angew. Chemie - Int. Ed.* **2017**, *56*, 1885–1889.
- [49] R. P. Lyon, J. R. Setter, T. D. Bovee, S. O. Doronina, J. H. Hunter, M. E. Anderson, C. L. Balasubramanian, S. M. Duniho, C. I. Leiske, F. Li, et al., *Nat. Biotechnol.* **2014**, *32*, 1059.
- [50] B. Shen, K. Xu, L. Liu, H. Raab, S. Bhakta, M. Kenrick, K. L. Parsons-reponte, J. Tien, S. Yu, E. Mai, et al., *Nat. Biotechnol.* **2012**, *30*, 184–189.
- [51] B. Bernardim, P. M. S. D. Cal, M. J. Matos, B. L. Oliveira, N. Martínez-Sáez, I. S.

- Albuquerque, E. Perkins, F. Corzana, A. C. B. Burtoloso, G. Jiménez-Osés, et al., *Nat. Commun.* **2016**, *7*, 13128.
- [52] B. A. Mendelsohn, S. D. Barnscher, J. T. Snyder, Z. An, J. M. Dodd, J. Dugal-Tessier, *Bioconjug. Chem.* **2017**, *28*, 371–381.
- [53] P. D. Senter, E. L. Sievers, *Nat. Biotechnol.* **2012**, *30*, 631–637.
- [54] G. M. Dubowchik, R. A. Firestone, *Bioorg. Med. Chem. Lett.* **1998**, *8*, 3341–3346.
- [55] J. J. Cui, M. Tran-Dubé, H. Shen, M. Nambu, P. Kung, M. Pairish, L. Jia, J. Meng, L. Funk, I. Botrous, et al., *J. Med. Chem.* **2011**, *54*, 6342–6363.
- [56] J. R. Junutula, H. Raab, S. Clark, S. Bhakta, D. D. Leipold, S. Weir, Y. Chen, M. Simpson, S. P. Tsai, M. S. Dennis, et al., *Nat. Biotechnol.* **2008**, *26*, 925–932.
- [57] S. S. Brack, M. Silacci, M. Birchler, D. Neri, *Clin. Cancer Res.* **2006**, *12*, 3200 LP – 3208.
- [58] D. A. Heuveling, R. de Bree, D. J. Vugts, M. C. Huisman, L. Giovannoni, O. S. Hoekstra, C. R. Leemans, D. Neri, G. A. M. S. van Dongen, *J. Nucl. Med.* **2013**, *54*, 397–401.
- [59] G. Zhang, V. Gurtu, S. R. Kain, G. Yan, *Biotechniques* **1997**, *23*, 525–531.
- [60] G. L. Ellman, *Arch. Biochem. Biophys.* **1959**, *82*, 70–77.
- [61] W. K. Fife, P. Ranganathan, M. Zeldin, *J. Org. Chem.* **1990**, *55*, 5610–5613.
- [62] T. T.-L. Kwan, O. Boutoureira, E. C. Frye, S. J. Walsh, M. K. Gupta, S. Wallace, Y. Wu, F. Zhang, H. F. Sore, W. R. J. D. Galloway, et al., *Chem. Sci.* **2017**, *8*, 3871–3878.
- [63] X. Sun, J. F. Ponte, N. C. Yoder, R. Laleau, J. Coccia, L. Lanieri, Q. Qiu, R. Wu, E. Hong, M. Bogalhas, et al., *Bioconjug. Chem.* **2017**, *28*, 1371–1381.
- [64] S. O. Doronina, B. E. Toki, M. Y. Torgov, B. A. Mendelsohn, C. G. Cerveny, D. F. Chace, R. L. DeBlanc, R. P. Gearing, T. D. Bovee, C. B. Siegall, et al., *Nat. Biotechnol.* **2003**, *21*, 778–784.
- [65] M. J. Frisch, G. W. Trucks, H. B. Schlegel, G. E. Scuseria, M. A. Robb, G. Cheeseman, J. R. Scalmani, V. Barone, G. A. Petersson, H. Nakatsuji, X. Li, et al., -, CT, Wallingford, **2016**.
- [66] Y. Zhao, D. G. Truhlar, *Theor. Chem. Acc.* **2008**, *120*, 215–241.
- [67] G. Scalmani, M. J. Frisch, *J. Chem. Phys.* **2010**, *132*, 114110.
- [68] R. F. Ribeiro, A. V Marenich, C. J. Cramer, D. G. Truhlar, *J. Phys. Chem. B* **2011**, *115*, 14556–14562.

- [69] C. Gonzalez, H. B. Schlegel, *J. Phys. Chem.* **1990**, *94*, 5523–5527.

Acetals as new acid cleavable linker for ADC and SMDC synthesis

5.1 Introduction

- 5.1.1 Acid cleavable linkers for drug release application
- 5.1.2 Use of acetals as acid cleavable linkers

5.2 Background and main goals

5.3 Coumarin based acetals

- 5.3.1 Synthesis
- 5.3.2 Coumarin derivatives stability
 - 5.3.2.1 NMR kinetic study
 - 5.3.2.2 Fluorescence release study

5.4 Duocarmycin derivatives synthesis

- 5.4.1 Stability assays

5.5 Small Molecule Drug Conjugate

- 5.5.1 SMDC synthesis and stability studies
- 5.5.2 *In vitro* assays of SMDC **33**

5.6 Antibody Drug Conjugate

- 5.6.1 Synthesis of carbonyl acrylamide derivatives
- 5.6.2 ADC synthesis and stability
- 5.6.3 *In vitro* assays
- 5.6.4 Molecular Dynamics simulations

5.7 Conclusions

5.8 Experimental section

- 5.8.1 Synthesis
- 5.8.2 Stability studies
- 5.8.3 Antibody Drug Conjugates synthesis and stability
- 5.8.4 *In vitro* assays
- 5.8.5 Molecular Dynamics simulations

5.9 References

5.1 Introduction

It is well known that the microenvironment in which cancer cells proliferate is distinguished by altered physiological conditions that allow both survival and proliferation of tumour cells. Indeed, the tumour microenvironment, which consists of extracellular matrix, stromal cells and immune cells, plays a pivotal role in tumour progression.^[1-4] Tumour acidosis, which consists in a lowered extracellular pH value (pH_e), represents one of the main features of tumour microenvironment and it is extensively recognized as a general property of tumours.^[5]

Acidosis represents a direct consequence of the increased proliferation rate of cancer cells, which need a higher amount of energy for the biosynthesis of nucleotides compared to normal differentiated adult cells. This increased metabolic demand forces the cancer cell to modify its glucose pathway: normal glycolysis is substituted by 'aerobic' glycolysis, and this is known as the Warburg effect. This effect causes that, in rapidly proliferating cells, the high amount of glucose up-taken by the cell is not completely oxidized, leading to CO_2 and H_2O , but it is converted in lactic acid. Despite the inferior ATP production and the consequent energetic disadvantage, the cell can produce higher amounts of metabolic intermediates, useful for amino acids, nucleotides and lipids biosynthesis that are necessary to maintain a fast duplication rate.^[6,7] This effect is enhanced in hypoxic solid tumours, where the reduced oxygen supply forces the cell to shift its metabolism. ^[8]

Because of the Warburg effect, the higher intracellular lactate concentration would lead to acidification of the intracellular pH that the cell needs to avoid in order to survive. This delicate equilibrium is maintained thanks to the co-operative work of several membrane transporters, ion exchange proteins and enzymes families, such as carbonic anhydrases, that keep homeostasis mainly by emission of H^+ ions outside the cell. Therefore the resulting pH is made slightly acidic, with values up to 6.0 (normal values are around 6.5), while the intracellular pH is slightly more alkaline than normal cells ($\text{pH}\sim 7.4$).^[9,10]

This reversed pH gradient, facilitates the survival of cancer, by favouring proliferation, migration and metastasis, and allows the evasion of apoptosis.^[11]

Besides the lower pH values encountered in the tumour extracellular environment, acidic pH is also a feature of several intracellular compartments. While cytosolic pH has to be slightly alkaline to allow cell survival, the organelles involved in the endocytic pathway presents lower pH values up to 4.5. Large molecules, ligands and proteins that interact with the plasma membrane are usually internalized through receptor-mediated endocytosis and encounter an increasingly acidic environment as they progress through the endocytic pathway. The first organelles formed, the early endosomes, are the least acidic (pH values from 6.5 to 5.0), while late endosome and lysosomes can reach pH values as low as 4.5–4.7 (**Figure 5.1**). Acidity is fundamental to control the activity of proteases and other enzymes, and plays an important role in the uncoupling of ligands from their receptor, which afterwards are recycled and re-exposed on cell surface. [12–14]

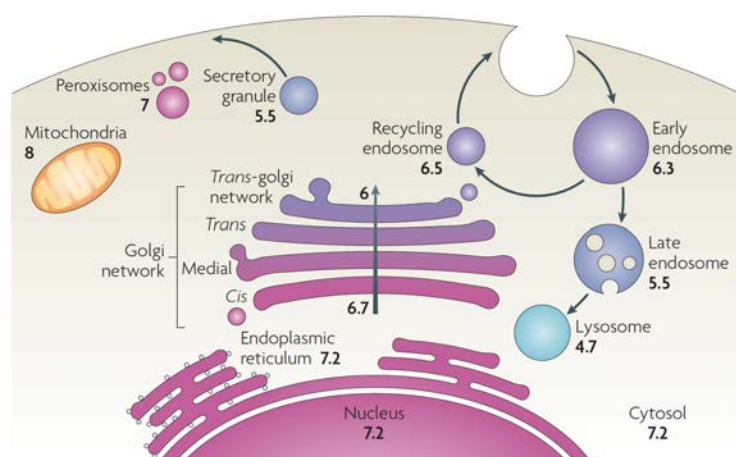


Figure 5.1: schematic representation of the endocytic pathway.^[13] Bold numbers indicate pH values for the corresponding intracellular compartment.

Therefore, the acidic conditions encountered in both intracellular compartments and extracellular environment of cancer cells offer a motivating opportunity for the selective delivery and release of cytotoxic compounds to diseased tissues.

5.1.1 Acid cleavable linkers for drug release application

Based on the above commented features, the development of new linkers and materials that are responsive to these small variations in pH and take advantage of extracellular acidity or intracellular acidic compartment for drug release has gained great interest. These linkers are based on acid sensitive functional groups, which are hydrolytically stable under slightly basic circulation conditions. In particular hydrazones,^[15,16] acetals and ketals,^[17] silyl ethers,^[18] cis-aconityl,^[19] thiomaleamic acid derivatives,^[20] imines^[21] and orthoesters^[22] are some of the most commonly used spacers for this purpose. Their structures are represented in **Figure 5.2**.

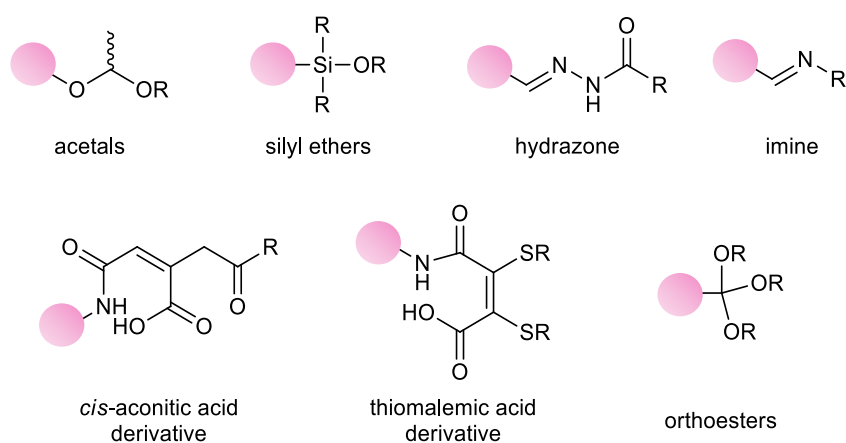


Figure 5.2: structures of acid cleavable moieties used in drug delivery.

For the purpose of this chapter, examples of the application of pH sensitive linkers in Antibody-Drug Conjugates (ADCs) are explained below; although acid cleavable linkers have found wide application in other delivery models, such as sensitive polymers and nanomaterials. ^[5,23-26]

Mylotarg[®] is the first and most relevant example among ADCs relying on acid-sensitive moieties for drug release. This ADC, used for the treatment of acute myeloid leukemia, has been approved by the FDA in 2002 and commercialized by Pfizer. The antibody in Mylotarg is the humanized P76.6 IgG4, which target CD33+ cancer cells. The antibody is heterogeneously conjugated through its lysine residues via an amide bond to the

drug, a synthetic derivative of calicheamicin γ_1 , which exerts its toxicity by irreversibly damaging the DNA. These two parts are linked through an acid cleavable hydrazone, which is hydrolysed in situ at endosome pH after ADC receptor mediated internalization.^[27] After a screening of different linkers for drug release, the structure reported in **Figure 5.3** resulted to be the best in terms of *in vitro* cytotoxicity and selectivity.^[28]

After Pfizer spontaneously withdrew the drug from the market in 2010, due to toxicity issues and not significant improvement in terms of overall survival, Mylotarg[®] has been again restored in the market after some changes in formulations and doses of the treatment.^[29]

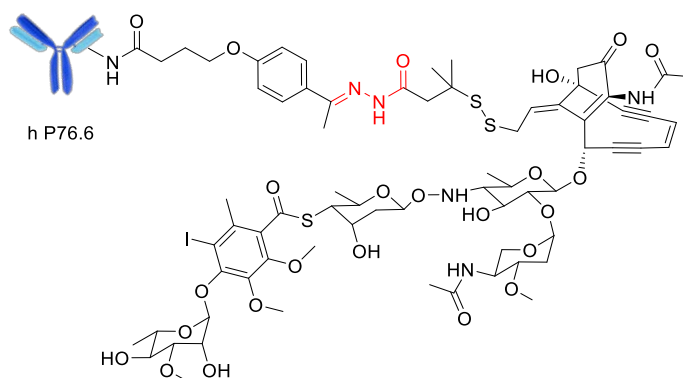


Figure 5.3: Mylotarg[®] structure; the cleavable hydrazone linker is highlighted in red.

Calicheamicin-hydrazone has also found application in the conjugation to an anti-MUC1 antibody for ovarian cancer treatment.^[30,31] More recently, Besponsa[®], an anti CD22 antibody conjugated to calicheamicin-hydrazone has been approved for the treatment of Acute Lymphoblastic Leukemia (ALL).^[32]

Despite the wide use of hydrazone in ADC design, several research groups have explored the possibility to use alternative acid cleavable linkers in this field.

As an example, doxorubicin was conjugated to the Fab region of Trastuzumab via a thiomaleamic acid linker. A plasma stable, site-selective conjugate was obtained, that completely retained the affinity of the antibody fragment for Her2 antigen. When incubated at pH 4.5, the payload was quantitatively released after acid promoted

cyclization and self-immolative para-aminobenzyl alcohol (PABA) linker degradation
(Figure 5.4).^[20]

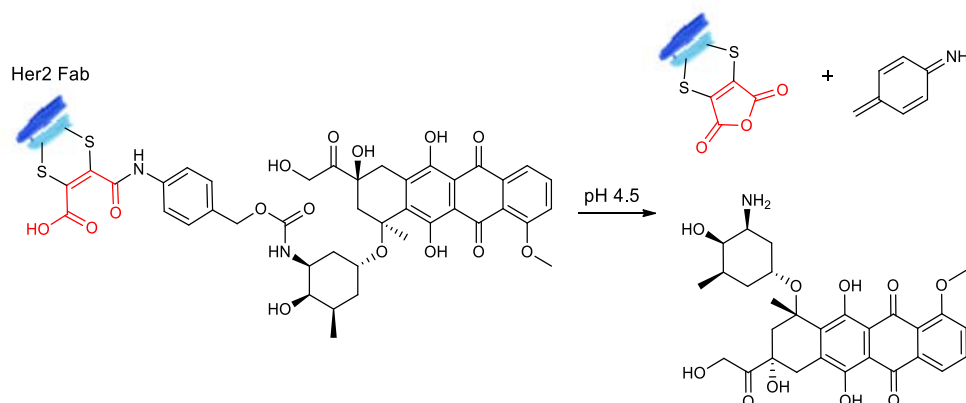


Figure 5.4: acid mediated release of DOXO from Trastuzumab Fab region.

In another example, the same antigen was targeted with a gemcitabine-Trastuzumab conjugate. A silyl-ether was used to release the drug at acidic pH, while no free gemcitabine was detected when the ADC was incubated in plasma. These results indicate that silyl-ether chemistry could serve as an alternative to hydrazones for application in ADC based drug delivery systems (Figure 5.5).^[18]

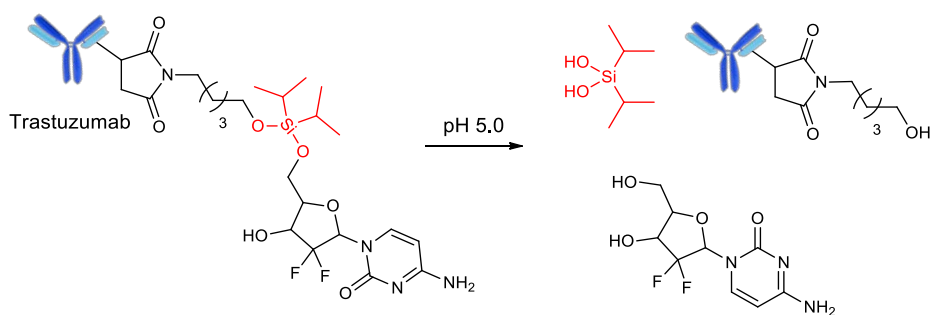
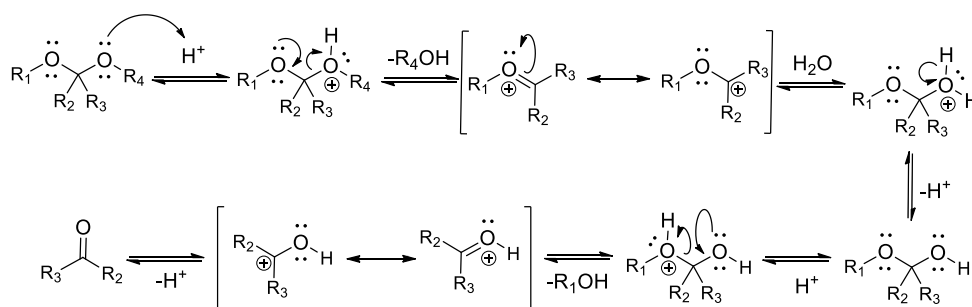


Figure 5.5: silyl ether hydrolysis for gemcitabine release in a Trastuzumab conjugate.

5.1.2 Use of acetals as acid cleavable linkers

Among acid cleavable linkers, acetals and ketals represent one of the most interesting categories. These functional groups are widely used in organic synthesis for the protection of hydroxyl function, diols and carbonyl compounds, leading to stable compounds under basic and neutral conditions that upon acid treatment recover the original functional group.^[33] Several synthetic strategies can be used to form an acetal,^[34–40] normally under mild reaction conditions that are compatible with the presence of many functional groups and very complicated structures. Furthermore, the acid hydrolysis mechanism of acetals is well established,^[41,42] allowing some degree of prediction on their kinetics and stability.



Scheme 5.1: acid-catalysed hydrolysis of acetals.

The rate-determining step of the reaction mechanism shown in **Scheme 5.1** is the formation of the resonance-stabilized carboxonium ion. As expected, the functional groups adjacent to the acetal carbon influence the intermediate stability: electron-donating substituents would likely stabilize the cationic intermediate, making the hydrolysis faster. Also, in general, R1 and R4 groups contribute to the stability of the reaction intermediate through inductive effects, whereas R2 and R3 contribute through inductive and resonance effects. In a recent work based on these statements, the effects of substituents on acetal stability are well studied, and as a result several acetal based compounds with very different stability properties were obtained.^[43]

Due to their properties, acetals and ketals are promising candidates as linkers for acid-controlled cleavage.

Ketals, for example, have been used for the controlled release of nucleic acids,^[44,45] the design of degradable polymers,^[46-48] for pro-drug formulations using nanoparticles,^[17,49-51] and for the generation of pro-drugs with higher circulation half-life and increased absorption.^[52,53]

However, the application of acetal chemistry in the field of ADC remains still quite unexplored compared to other technologies.

In an example from Yurkovetskiy^[54] and collaborators, an acetal based polymer (Fleximer) is used as a linker to synthesize a Trastuzumab conjugate with a vinka-alkaloid based drug (**Figure 5.6**). The polyacetal linker significantly reduces ADC aggregation, allowing at the same time a high Drug to Antibody Ratio (DAR) and an unaltered antibody affinity for its target. The drug is however linked via an amide bond and its release still depends in part on cell catabolism, although probably the acetal-based polymer is hydrolysed in the endosomes.

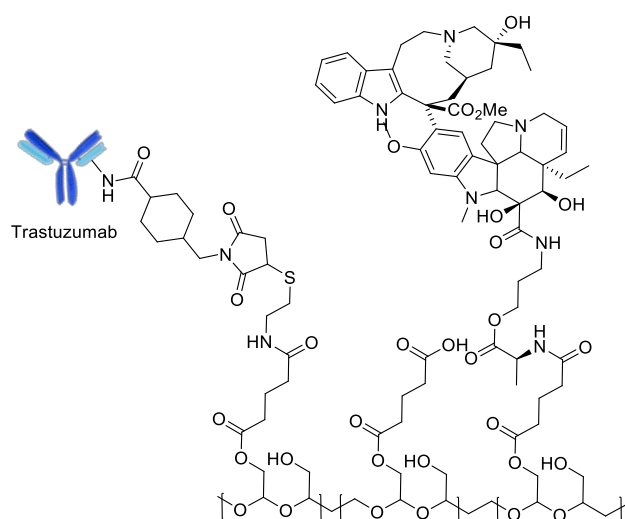


Figure 5.6: Trastuzumab-drug conjugate. The linker is an acetal-based polymer, that allows drug release upon acid hydrolysis.

In another example from Gentech, a tetrahydropyranyl acetal is used to link the hydroxyl group of a potent anthracycline to an antibody targeting LGR5 antigen, overexpressed in colon cancer cell lines (**Figure 5.7**). The final ADC shows good selectivity and toxicity, even if the release mechanism and the effects of the presence of the linker have not been studied in details.^[55]

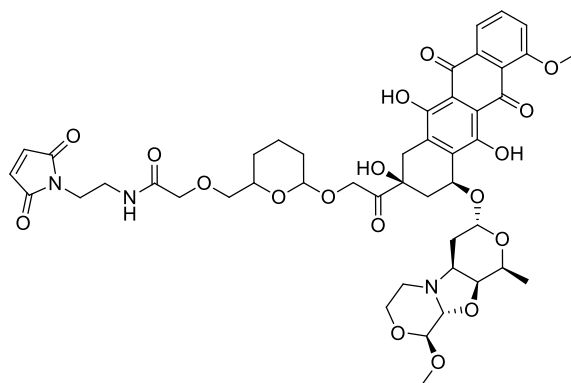


Figure 5.7: structure of linker-NMS818 drug conjugate.

In the field of Small Molecule Drug Conjugates (SMDC), the most relevant example is represented by a folate receptor ligand conjugated through a benzylidene acetal to N-hydroxyethyl vindesine (**Figure 5.8**). The SMDC showed interesting properties in terms of stability and reactivity at acid pH. However, the resulting SMDC was ineffective probably due to the low acidity of folate receptors endosomes.^[56]

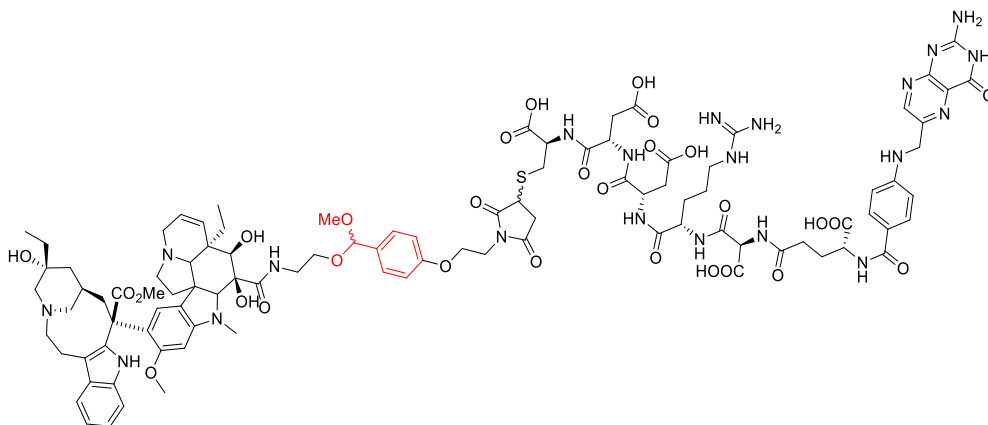


Figure 5.8: folic acid conjugate via benzylidene acetal. The acid cleavable moiety is highlighted in red.

5.2 Background and main goals

In this chapter, our study is focused on the properties of an acetal-based linker for intracellular drug release, for application in ADC and SMDC synthesis. Previous research has already demonstrated that this functional group is suitable for controlled

release applications: however, very few examples of ADC with an acetal cleavable moiety have been studied so far. Moreover, despite the presence of a great amount of drugs bearing a hydroxyl group,^[57] the acetal function is always connected to the drug through an additional spacer.

In this project, the hydroxyl function of biological interesting molecules, such as drugs and fluorophores, has been functionalized as monomethyl acetal. This linker is designed to be stable under physiological conditions, but it is able to release the drug at lower pH values. The use of this linker in combination with small molecule ligands or antibodies allows the generation of a delivery system for tumour targeting (**Figure 5.9**).

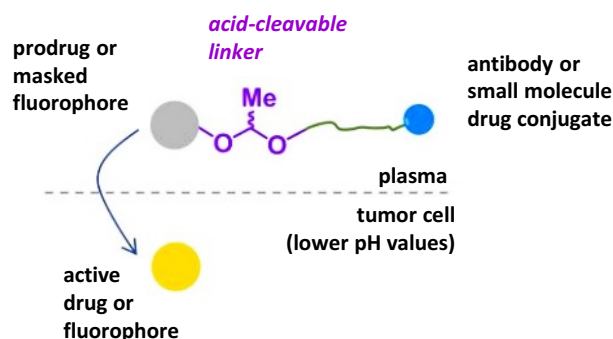


Figure 5.9: acetal-based strategy for the controlled release of drugs and fluorophores.

First, in order to optimize the linker structure, several coumarin-acetal derivatives were synthesized, and their behaviour was analysed by different techniques, namely ¹H-NMR and fluorescence spectroscopy.

Once the best linker for conjugation was chosen, it was used for the development of a duocarmycin derived pro-drug. Duocarmycins are a family of natural antibiotics that cannot be used as chemotherapeutics in an unconjugated form due to their high toxicity that would lead to severe collateral effects. Duocarmycin's toxicity is attributed to the cyclic form of the drug, which is responsible for irreversible DNA alkylation (**Figure 5.10**). The cyclopropane ring is spontaneously formed *in vivo* from the phenolic form by an intramolecular Weinstein cyclization.^[58]

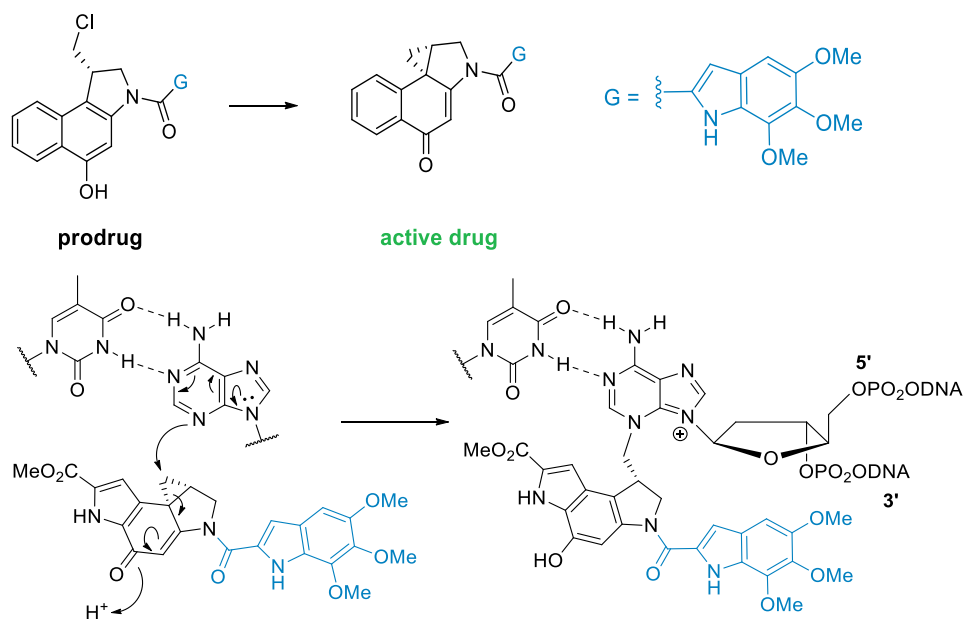


Figure 5.10: duocarmycin structure and irreversible DNA alkylation.

Therefore, controlling the cyclopropanation reaction by protecting the hydroxyl of the phenol represents an interesting strategy for the safe delivery of this potent drug, and different ways to achieve it have been reported. [59–62]

Our strategy relies on the protection of duocarmycin hydroxyl group as an acetal, which is stable in circulation but after hydrolysis in an acidic pH environment, releases the pro-drug and spontaneously forms the active drug *in situ*.

Once the acetal based pro-drug was obtained, it was conjugated to both antibodies and small molecules for cancer cells targeting.

The properties of the ADC and the SMDC were studied in order to determine their stability and the results were rationalized by molecular dynamic (MD) simulations. Finally, targeted systems were tested *in vitro* to determine affinity, cytotoxicity and selectivity towards cancer cell lines.

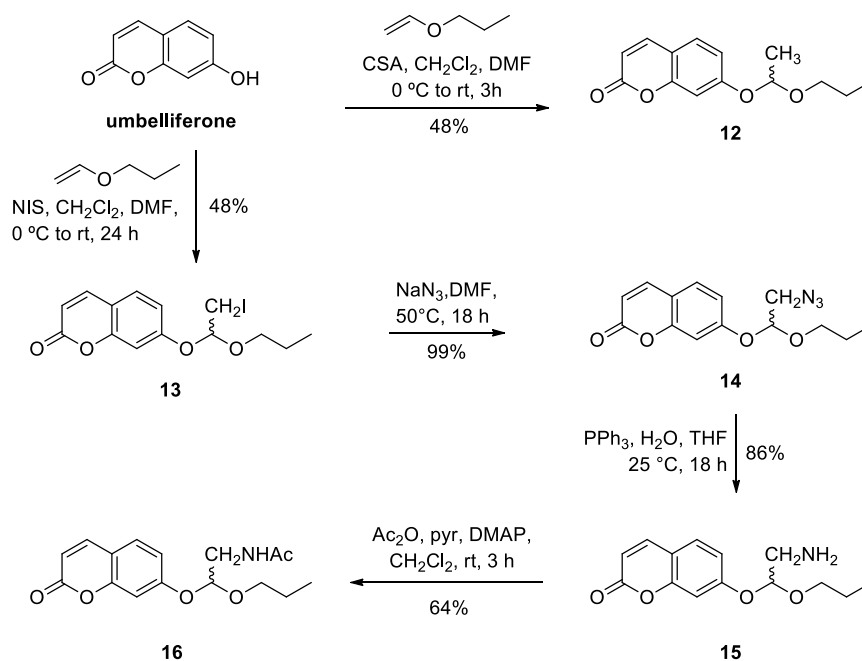
5.3 Coumarin based acetals

The study of the acetal-based linker was started choosing 7-hydroxy coumarin (umbelliferone) as a first example. Several umbelliferone-based acetals, that present differences in the linker structure, were synthesized and their kinetics under different conditions were studied by NMR or fluorescence spectroscopy. In the last case, we took advantage of the different fluorescent properties of free and protected umbelliferone. In the protected one, the fluorescence emission at around 450 nm is quenched, and it is restored after acetal cleavage, as reported in several works on this compound or similar ones.^[57,63]

5.3.1 Synthesis

Starting from commercially available 7-hydroxy coumarin, the phenolic function was protected using two different synthetic pathways, that lead to the formation of structurally different acetals (**Scheme 5.2**).

In both cases, propyl vinyl ether was chosen as starting material for the synthesis, leading to an asymmetric monomethyl acetal as reaction product. These acetaldehyde derived acetals were chosen because, according to the reaction mechanism described above (**Scheme 5.1**), they should present enough acid lability together with stability in slightly basic conditions, essential properties for the application in drug delivery systems.



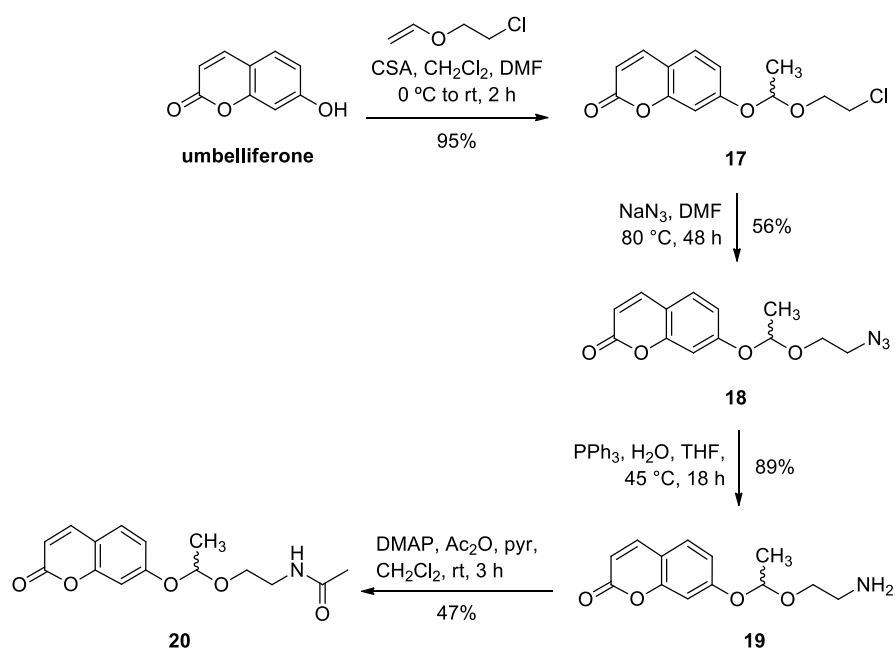
Scheme 5.2: synthetic route to obtain coumarin based acetals.

Acid catalysed activation of propyl vinyl ether, followed by the attack of commercially available **umbelliferone** lead to the formation of asymmetric acetal **12**, whose properties will be discussed below.

In parallel, a different activation of the same vinyl ether using *N*-iodosuccinimide (NIS) in CH_2Cl_2 , followed by **umbelliferone** nucleophilic attack, results in the formation of iodo-derivative **13**. In this way, a suitable handle for further structural modification is introduced. Indeed, nucleophilic displacement of iodine by NaN_3 in DMF leads to the formation of azide **14** almost quantitatively (99%) without further purification. In order to increase water solubility of the acetal for the following stability studies, the azido group of **14** was reduced to amine **15** using Staudinger conditions,^[64] which was isolated after column chromatography purification in good yield (86%). To evaluate how the presence of an amino group close to the acetal carbon influences the reactivity of the linker, amine **15** was acetylated using acetic anhydride and pyridine in CH_2Cl_2 to obtain acetylated compound **16** in 64% yield. A preliminary screening of compounds stability (See section 5.3.2.1 for the NMR study) points out that monomethyl substituted

acetal **12** presents the best properties in terms of fast acid hydrolysis. Hence, analogues of this compound bearing a chemical handle suitable for further modification and conjugation reaction to proteins or small molecules were synthesized. To afford such compounds, substituted vinyl ethers were used for the acetalization reaction.

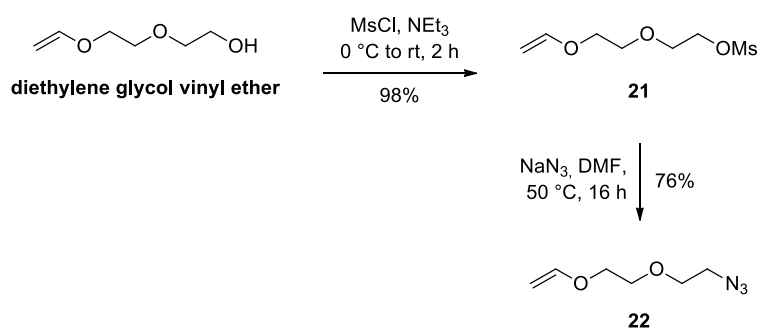
This was achieved using 2-chloroethyl vinyl ether in the first reaction step, which upon treatment with camphor-10-sulfonic acid (CSA) and umbelliferone produces in high yield (95%) acetal **17**. Chlorine substitution enables chemical modification, and in a similar way to what previously described, an azido group was introduced by reaction with NaN_3 in DMF at 80 °C. The higher temperature required for reaction completion causes a decrease in the yield (56%) due to partial acetal hydrolysis, as observed in the crude reaction mixture $^1\text{H-NMR}$. Azido-acetal **18** was reduced with PPh_3 and H_2O to obtain amine **19** that was subsequently acetylated with acetic anhydride, pyridine and catalytic amount of DMAP to obtain compound **20** in 47% yield after purification by column chromatography (**Scheme 5.3**).



Scheme 5.3: synthesis of substituted coumarin acetals.

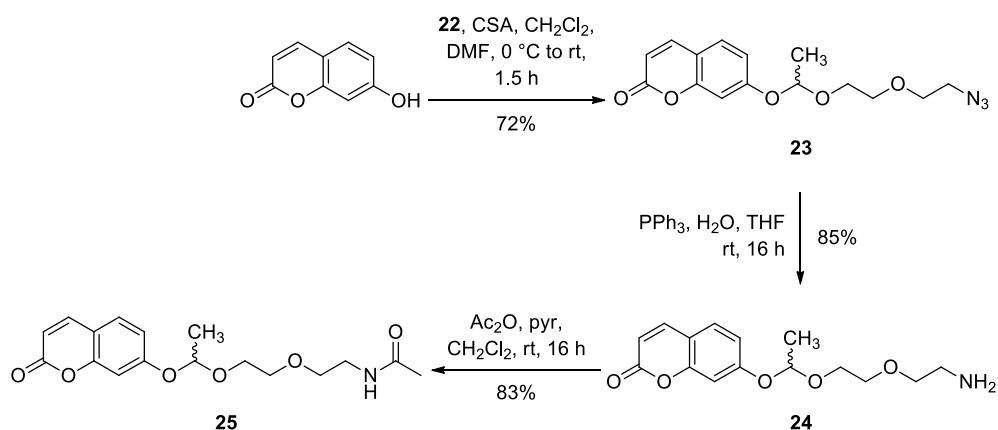
To evaluate the effect caused by the introduction of a longer spacer between the acetal group and the amino or acetamido substituent on the hydrolytic rate of the reaction, analogues bearing a small di-ethylene glycol spacer were synthesized. The ethylene glycol spacer is also expected to increase the solubility of final compounds. Moreover, since our final goal is to develop an ADC, the introduction of such hydrophilic spacer would possibly produce benefits in terms of pharmacokinetic properties and would reduce aggregation of the ADC.^[65] This represents a factor of pivotal importance when dealing with the conjugation of highly hydrophobic drugs, which is the case of most drugs used so far in targeted therapy.

For this purpose, linker **22** was synthesized as reported in the following scheme (**Scheme 5.4**).



Scheme 5.4: synthesis of diethylene glycol spacer.

From commercially available diethylene glycol vinyl ether, transformation of the alcohol into the corresponding methanesulfonate derivative **21**, followed by nucleophilic substitution gave azide **22** in good overall yield (74%). Compound **22** was used as starting material for umbelliferone derivatives synthesis shown in **Scheme 5.5**.



Scheme 5.5: synthesis of coumarin acetals with a PEG-spacer.

Monomethyl acetal **23** was obtained from **22** and **umbelliferone** using CSA as catalyst in good yield (72%). Terminal azido group was transformed to amine **24** under Staudinger conditions and it was then acetylated by treatment with acetic anhydride and pyridine to give compound **25**.

All compounds were completely characterized (*See Experimental Part, Section 5.8*) and their behaviour in acidic media was studied by NMR and fluorescence spectroscopy, as described in the next section.

5.3.2 Coumarin derivatives stability

In order to study the stability properties of coumarin derivatives previously described, both NMR kinetic experiments and UV experiments were performed.

Thus, the reactivity of the acetals in an acid buffer was monitored mainly by NMR. Equally, the UV spectra were used to determine the stability of the acetal in more complex systems, such as human serum, that was used as a model to simulate circulation conditions.

Among the compounds synthesized in the previous section, only compounds **12**, **15**, **16**, **20**, **24** and **25** were tested, due to their higher water solubility, in comparison with other synthetic intermediates.

5.3.2.1 NMR kinetic study

To study the hydrolysis kinetic at acidic pH, compounds **12**, **15**, **16**, **24** and **25** were dissolved in phosphate buffer at pH 5.7, which is the pH value that can be encountered in lysosomes or endosomes, and all compounds were incubated at 37 °C. Results obtained by NMR experiments are reported in **Table 5.1**.

Compound	k_1 (s ⁻¹)
 12	$6.4 \cdot 10^{-5}$
 25	$2.5 \cdot 10^{-5}$
 20	$2.2 \cdot 10^{-5}$
 16	$8.0 \cdot 10^{-6}$
 24	$6.2 \cdot 10^{-6}$
 15	n.d.

Table 5.1: kinetic rate constant for acetal hydrolysis at pH 5.7; n.d. = not determined.

NMR studies allowed us to understand the linker influence on acetal group hydrolysis rate. Surprisingly, compound **15** was completely stable even after 48 h incubation at 37 °C in acid media (pH 5.7). This result was rationalized considering that the primary amino group, mainly presented in the protonated form at pH 5.7, prevents the protonation of the acetal and the subsequent formation of the carboxonium

intermediate, which is the rate-determining step for acetal hydrolysis (See **Scheme 5.1**). Indeed, it would lead to the formation of a highly unstable species that presents two positive charges at close distance. That allows acetal **15** to be completely stable in acid media at 37 °C. As a proof to this hypothesis, it can be observed that the separation of the amino group from the acetal carbon, as in compound **24**, promotes the hydrolysis and the release of free coumarin. Moreover, the substitution of the amine for an acetamido group, enhances the hydrolytic rate of the monomethyl acetal (as in compounds **16** and **20**), although the hydrolysis reaction is slow at the slightly acidic pH studied. In fact, as extensively demonstrated by Liu et al.,^[43] the presence of an electron-withdrawing substituent close to the acetal moiety, as it is the case of these two compounds has a bad influence on the hydrolysis rate. This is likely the reason why compound **12**, substituted only with alkyl groups, presents the highest kinetic rate among the other acetals. For this compound, by ¹H-NMR it was observed that after 12 h incubation at pH 5.7 hydrolysis is complete. On the contrary, its analogue **16**, substituted with an acetamido group, gives only 20 % hydrolysis in the same conditions (**Figure 5.11**). Nevertheless, the absence of a suitable handle for further derivatization prevented us from using this linker in drug conjugate synthesis.

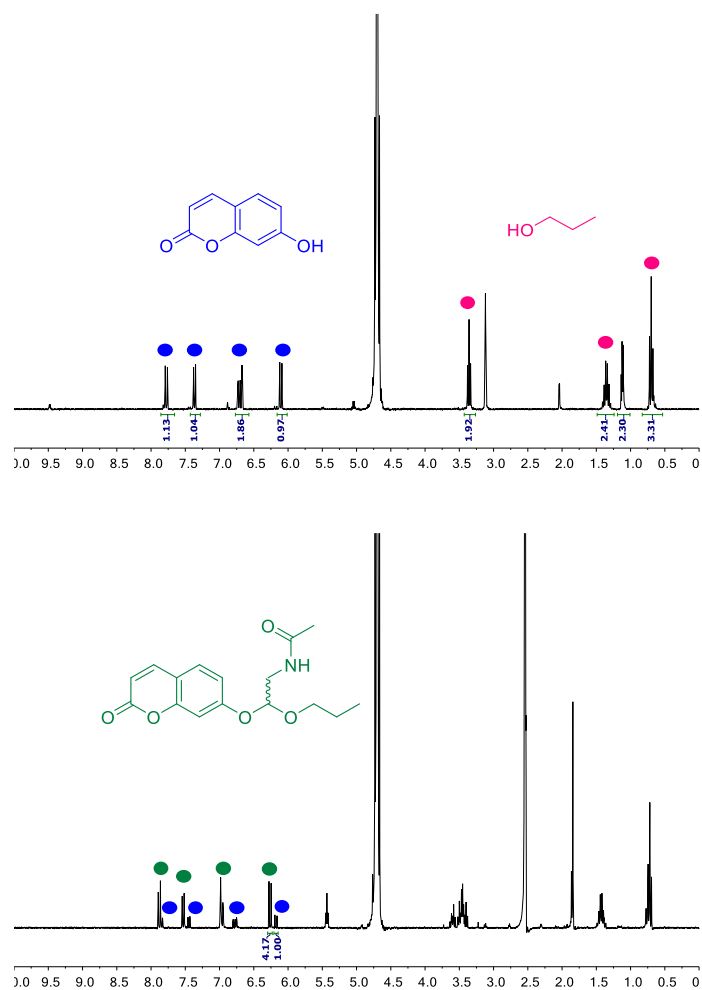


Figure 5.11: ¹H-NMR of compounds **12** (top) and **16** (bottom) after 12 h incubation in phosphate buffer (0.1 M, pH 5.7). Blue dots indicate umbelliferone signals, pink dots stand for propanol and green dots for compound **16**.

Compounds **20** and **25** present a comparable hydrolytic rate, in the order of 10^{-5} , which represents an acceptable value for de-conjugation reaction *in vivo*. As expected, the higher distance between acetamido group and acetal in compound **25** renders the hydrolysis of this compound slightly favourable, with kinetic constants of around $2.5 \cdot 10^{-5}$ in NaPi buffer at pH 5.7, compared with compound **20** that presents a kinetic constants of around 2.0×10^{-5} .

As an example, in **Figure 5.12** the monitorization by $^1\text{H-NMR}$ of the hydrolysis reaction of compound **20** is reported. The reaction proceeding is monitored by the integration of the signal corresponding to the H-3 of **20**. In the aromatic region new signals are observed, corresponding to free umbelliferone protons. According to the hydrolysis mechanism reported in **Figure 5.12 a**, acetaldehyde is also generated, and typical aldehyde's proton around 9.8-10 ppm is observed, although its intensity is very low due to the presence of an equilibrium with the hydrated form. Another signal that can be monitored to follow the reaction is the decreasing of acetal proton's intensity at around 5.6 ppm, even if its integration cannot be used for kinetic constant determination due to its proximity to water residual signal. Even if the reaction is not complete, 42% percent release of coumarin is observed after 12 hours incubation. The first order kinetic constant of the hydrolysis reaction was determined to be $k_1 (37\text{ }^\circ\text{C}) = 2.20 \cdot 10^{-5} \pm 1.60 \cdot 10^{-6} \text{ s}^{-1}$.

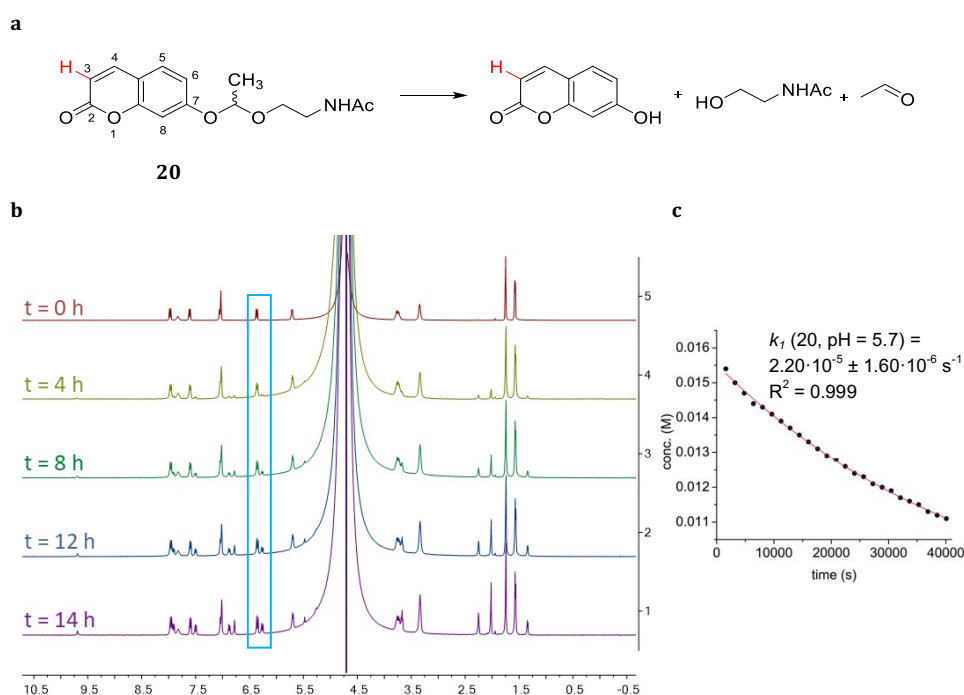


Figure 5.12: a) hydrolysis reaction of acetal **20**; b) $^1\text{H-NMR}$ of compound **20** at different times in phosphate buffer at pH 5.7; H-3 proton signal is highlighted; c) first order decay of compound **20** concentration.

5.3.2.2 Fluorescence release study

Due to the different fluorescent properties of coumarin, depending on the availability of the free phenol group, it was possible to determine the release of coumarin by fluorescence spectroscopy. This technique allows to work at lower concentration, more similar to the physiological ones. Moreover, the reaction can be monitored also in more complex systems, such as human serum.

Due to acetal protection emission fluorescence is quenched and also the emission maximum is slightly shifted towards shorter wavelengths (**Figure 5.13**).

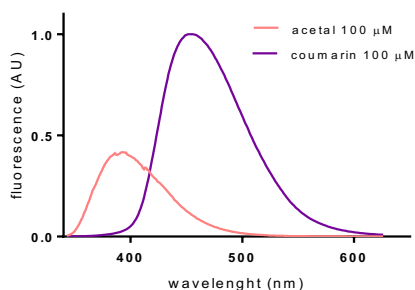


Figure 5.13: emission spectrum of free **umbelliferone** (violet) and protected derivative **20** (pink) in H₂O at 100 μ M concentration.

Acetal **20** was used for this study. This compound, according to the previous NMR study is among the ones with the fastest kinetic in acid media, together with compound **25**. The incubation of acetal **20** at acidic pH 5.0 (0.1 M acetate buffer) and pH 5.7 (0.1 M phosphate buffer) causes a fast release of free **umbelliferone** that results in the recovery of the fluorescence emission at around 450 nm. Moreover, incubation of the same compound in a 20% solution of human plasma in H₂O, produced a negligible release after 24 h, as we can see in the emission spectra in **Figure 5.14**.

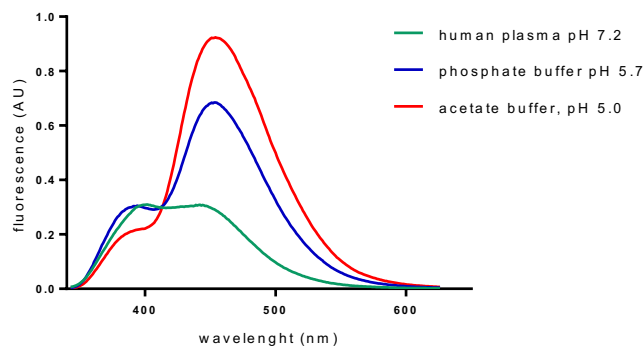


Figure 5.14: coumarin released from compound **20** after 24 hours incubation in plasma (pH 7.2, green graph), phosphate buffer (0.1 M, pH 5.7, blue graph) and acetate buffer (0.1 M, pH 5.0, red graph).

Therefore, while compound **20** is able to release **umbelliferone** in slightly acid buffer, the acetal linker is quite stable in human serum, masking the fluorophore in this media.

5.4 Duocarmycin derivatives synthesis

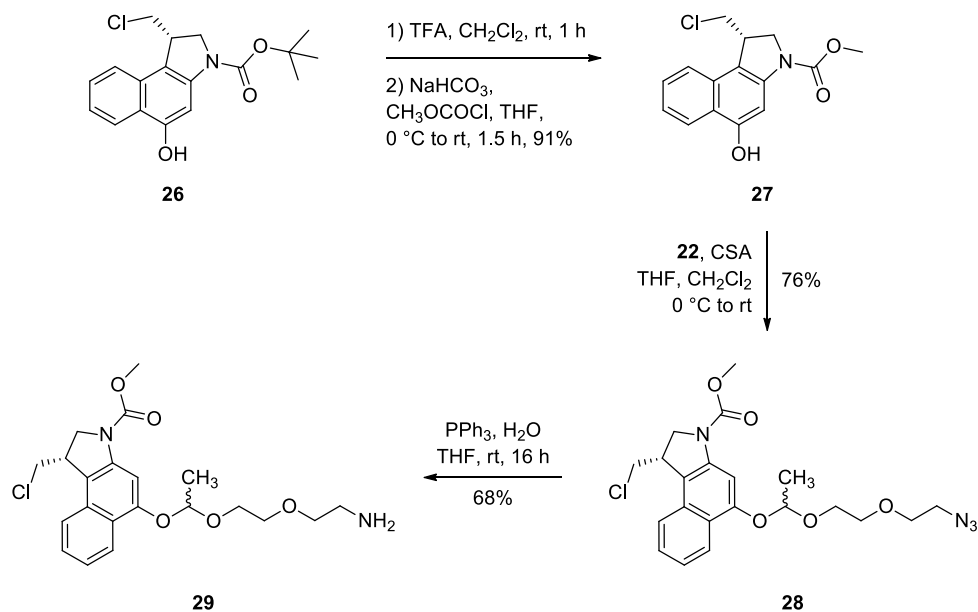
Prompted by the promising results obtained with coumarin-acetal derivatives, acetal function was then used for the generation of a pro-drug.

The alkylating unit of a duocarmycin analogue was used as a proof of concept for the experiments. The linker bearing the small PEG spacer was used in this case: such structure presents the best reactivity in acid media and its hydrophilic properties would benefit the properties of the final ADC. Additionally, the amino group allows further chemical functionalization.

With these concepts in mind, acetal **29** was prepared in few steps from commercially available *seco*-duocarmycin analogue **26**.

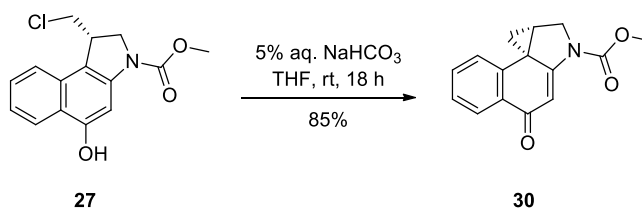
The Boc protecting group of compound **26** was removed by treatment with trifluoroacetic acid (TFA) in CH_2Cl_2 . Then, the amine group was protected as methyl carbamate by treating the crude mixture with methyl chloroformate and NaHCO_3 . This base was used to avoid undesired spiro-cyclization. The protecting group exchange is essential to avoid side reactions during acid stability experiments that can occur with the acid labile Boc group. On the contrary, methyl carbamate is known to be stable under slightly acid conditions.^[33] Afterwards, CSA catalysed acetal formation using

vinyl ether **22** and compound **27** gave acetal **28** as a diastereomeric mixture in a good yield (76%) after column purification. The azido group was reduced using Staudinger conditions to afford amine **29**, which was purified and characterised before stability assays (**Scheme 5.6**).



Scheme 5.6: Synthetic pathway to obtain compound **29**.

To get the cyclic form of the duocarmycin derivative, compound **27** was treated with aqueous NaHCO₃ in THF to obtain **30**, which was used as a control in the biological assays (**Scheme 5.7**)



Scheme 5.7: spiro-cyclization reaction to obtain duocarmycin active form.

5.4.1 Stability assays

In order to evaluate the stability of duocarmycin acetal **29**, UPLC-MS studies were performed in acid buffer and in plasma. This allowed not only the monitorization of acetal concentration decay, but also the formation of the active form of the drug **30** at the slightly acidic pH used for the assay. NMR measurements could not be used for this study, as done previously with coumarin-based acetals, due to the low concentration that needs to be used in the experiments as a consequence of the poor solubility of these compounds in buffered aqueous solutions.

As expected, the hydrolytic rate is significantly different in plasma and at endosomal pH. As we can see in **Figure 5.15**, after 48 hours, more than 60% of the drug is released in acid buffer, while more than 85% of the conjugated duocarmycin derivative is still present after the same incubation time in human serum. Interestingly, no phenolic form of the drug was detected neither in plasma nor acid buffer, suggesting that the active form of the drug is generated as soon as the acetal group is cleaved, making this approach interesting for the release of spiro-duocarmycin *in vivo*. These data also prove the wide-range applicability of the employed linker. Indeed, it can be used for the derivatization of different compounds, keeping a similar reactivity behaviour in acid buffer and plasma.

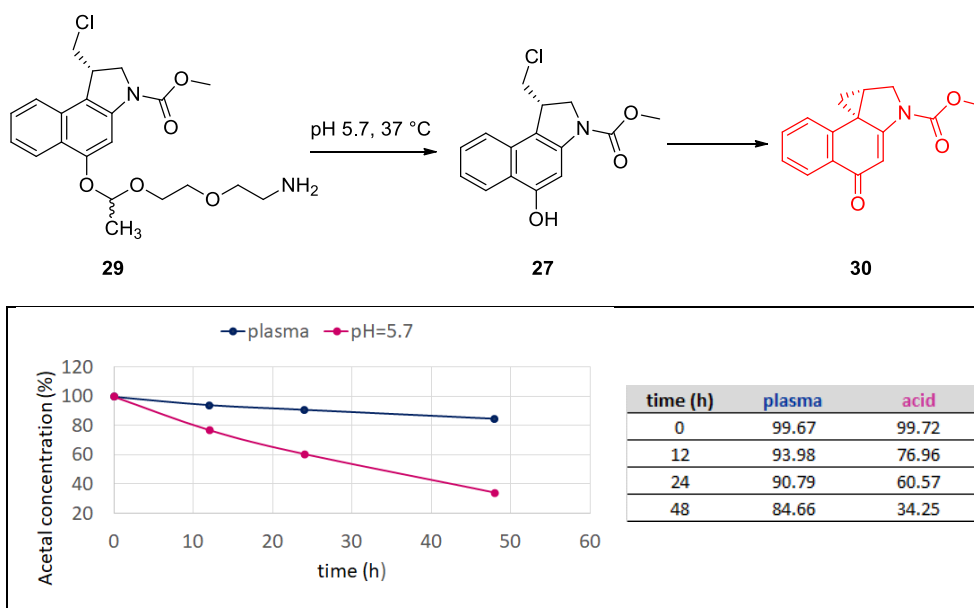


Figure 5.15: hydrolysis reaction of compound 29 (upper panel) and acetal concentration decay in acid buffer and plasma (lower panel).

To analyse the mechanism of the transformation in acid conditions, quantum mechanical (QM) calculations were performed (**Figure 5.16**).

The study indicates that the reaction may proceed through the naphthoxide derivative even at acidic pH. The alkoxide dramatically increases the nucleophilicity of the aromatic system and promotes the very fast S_N2 -type cyclopropanation reaction with concomitant departure of the chloride leaving group.

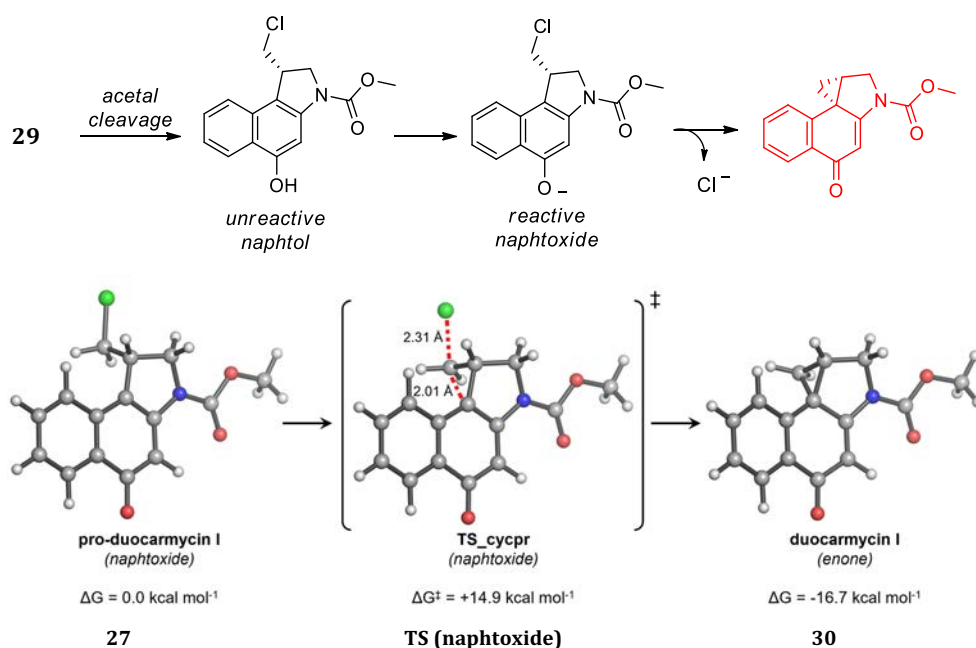


Figure 5.16: Cyclopropanation pathway calculated with PCM_{H2O}/M062X/6-31+G(d,p) for deprotonated intermediate after acetal cleavage.^[66]

Under these conditions, the reaction is exergonic, leading to a stable conjugated *enone*. On the contrary, the reaction through the protonated naphthol was calculated to be nine-fold slower and endergonic. Other potentially competing reactions, such as hydrogen-shift and ring-expansion to give 3-methylindoline and tetrahydroquinoline derivatives were calculated to be exceedingly slow compared to cyclopropanation.

Once demonstrated, both theoretically and experimentally, that acetal pro-drug **29** was able to release duocarmycin derivative **30** in a controlled way, this methodology was applied to the development of two different drug delivery systems. In fact, a small molecule drug conjugate and an antibody drug conjugate were synthesized and studied.

5.5 Small Molecule Drug Conjugate

As a first model, duocarmycin-acetal based pro-drug was applied to the development of a small molecule drug conjugate (SMDC) targeting carbonic anhydrase 9 (CAIX). This membrane enzyme is overexpressed in many solid tumours as a consequence of hypoxia and is involved in the regulation of the intracellular pH of the cancer cell.

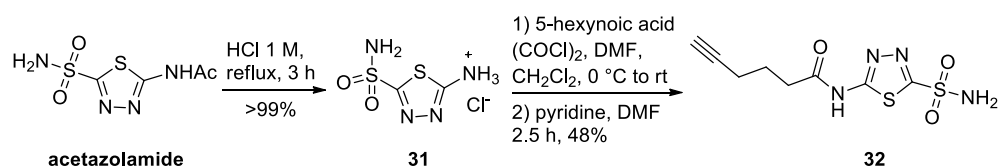
Importantly, this membrane receptor represents an interesting target for tumour-therapy due to its overexpression in cancer cells, while its expression in normal tissues is lower.^[67,68] In the field of tumour selective therapy, CAIX has been targeted both with antibodies^[69] and small molecule inhibitors^[70] that work as ligands. In this line of research, Neri and co-workers have successfully demonstrated that acetazolamide, a small sulphonamide based CAIX inhibitor with a K_d of 10 nM, can accumulate at tumour site and, when conjugated with cytotoxic payloads, it can reduce tumour progression in mice models.^[71–76]

For those reasons, acetazolamide was chosen as the targeting ligand for SMDC synthesis. Moreover, CAIX expressing tumours present low extracellular pH values, representing an interesting target to be addressed with acid sensitive delivery systems.

5.5.1 SMDC synthesis and stability studies

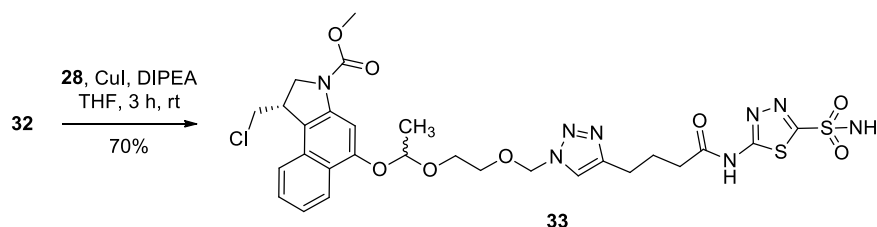
The synthesis of the acetazolamide conjugate was accomplished through a copper catalysed azide-alkyne cycloaddition between duocarmycin-azide **28**, previously described (See **Scheme 5.6**), and an acetazolamide derivative with an alkyne group.

Thus, the acetamido group of commercially available **acetazolamide** was removed by treatment with 1M HCl at reflux, which gave the hydrochloride salt **31**. This compound was reacted with pyridine and 6-hexynoyl chloride, previously generated in situ by treating the corresponding acid with oxalyl chloride and catalytic DMF in CH_2Cl_2 , to give alkyne **32** (**Scheme 5.8**).



Scheme 5.8: synthesis of acetazolamide derivative **32**, bearing an alkyne group for conjugation with duocarmycin derivative.

Once alkyne **32** was obtained, it was treated with azide **28** in presence of CuI and DIPEA in CH₂Cl₂, leading to conjugate **33** as a diastereomeric mixture in good yield (71%) (Scheme 5.9).



Scheme 5.9: Synthesis of acetazolamide-duocarmycin conjugate.

The stability of compound **33** was tested as previously done for amine derivative. Therefore, SMDC **33** was incubated in acid buffer at pH 5.7 at 37 °C and in human serum at the same temperature to simulate circulation conditions. The mixture was then analysed by UPLC-MS every 12 hours. As it is observed in **Figure 5.17**, compound **33** is highly stable in plasma, and at the same time it decomposes relatively fast at pH 5.7 and 37 °C. Under these acidic conditions, only 15% of the starting material remained unaltered after 24 h incubation (**Figure 5.17**). On the contrary, at plasma pH (~ 7.2), the hydrolysis was less than 5% after 24 h.

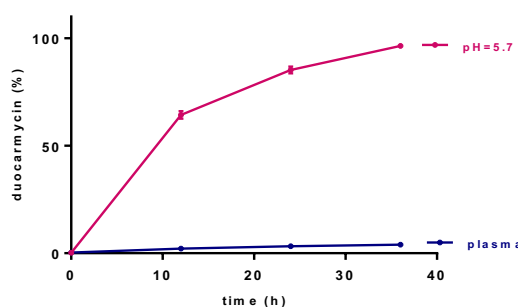


Figure 5.17: release of duocarmycin from acetal **33** at different pH values.

Relying on the good results obtained from release experiments, SMDC **33** was tested *in vitro* to define its ability to selectively kill cancer cell lines.

5.5.2 *In vitro* assays of SMDC 33

To determine its toxicity profile, targeted compound **33** was tested in the renal cancer cell line SKRC52. Toxicity assays showed that pro-drug **33** kills CAIX expressing cells in a similar way compared to free duocarmycin analogue **30** (Figure 5.18). In fact, cell viability was reduced to 16% and 12% after treatment with compound **30** (50 μ M) and **33** (50 μ M) respectively. This result suggests that the linker breaks efficiently after internalization in cancer cells, confirming what previously demonstrated by *in vitro* assays.

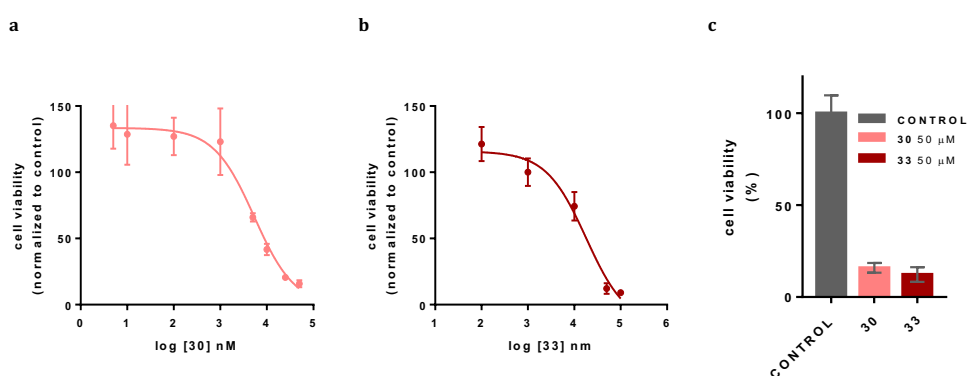


Figure 5.18: cell toxicity assay for compounds **30** and **33** in SKRC52 cell line; a) IC_{50} of duocarmycin analogue **30** ($5.4 \pm 0.1 \mu\text{M}$); b) IC_{50} of targeted compound **33** ($18.0 \pm 0.1 \mu\text{M}$); cell viability of SKRC52 cells after treatment with 50 μM of compounds **30** (pink bar) and **33** (red bar); 1% DMSO was used as control (grey bar).

To check whether the acetazolamide based delivery system was selective against CAIX⁺ cancer cell lines, compounds **30** and **33** were tested in HEK293T cell line, which does not express this enzyme. Surprisingly, the toxicity trend of free drug **30** and pro-drug **33** is the same as in SKRC52 cells. In fact, IC_{50} of free drug is $1.9 \pm 0.1 \mu\text{M}$ and of targeted system is $6.2 \pm 0.1 \mu\text{M}$. The lack of selectivity could be attributed to the small molecule system that is not enough membrane-impermeable and could be unselectively up-taken by the cell causing the observed toxicity. Also, HEK293T, like many other healthy cell lines, express other carbonic anhydrases, like carbonic anhydrase 2 (CAII), an intracellular enzyme that is unselectively bound by acetazolamide as previously described.^[72] However, this first *in vitro* toxicity experiment showed that the linker breaks efficiently inside the cell, causing the desired toxic effect. Such result reflects the

stability assays described in *Section 5.4.1*, and showed that acetal moiety can be used for the intracellular release of the drug. However, the targeting system need to be improved for efficient delivery *in vivo*.

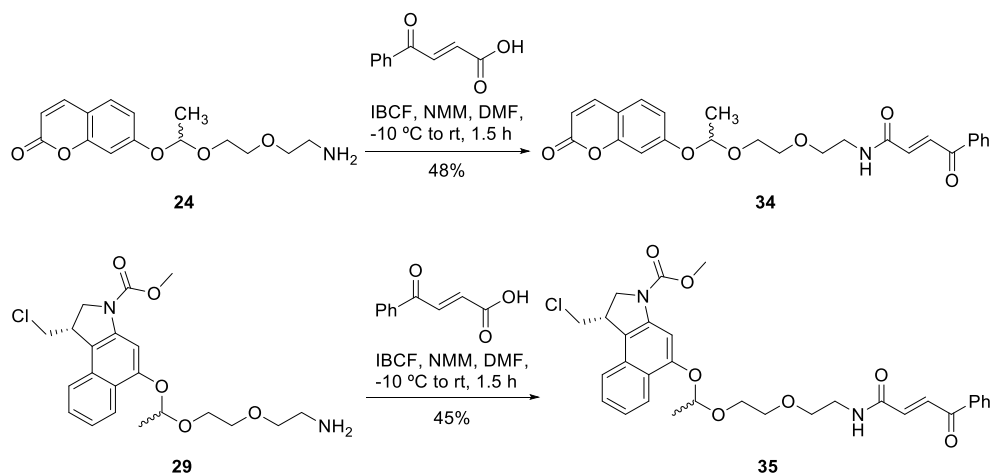
5.6 Antibody Drug Conjugate

Duocarmycin pro-drug based on acetal moiety was applied to the development of an Antibody Drug Conjugate (ADC). To this purpose, the previously described Thiomab antibody was used. This engineered antibody targets Her2 expressing cells and features a cysteine residue at position 205 of each light chain (Trastuzumab LC-V205C).^[77-80] Thus, the engineered antibody presents a single, highly reactive, exposed cysteine in the light chain that, in combination with the conjugation technology based on the *S*-Michael addition of thiols to carbonyl acrylamide handles (described in *Chapter 4*), would yield a highly homogeneous and stable ADC, with a controlled drug-to-antibody ratio (DAR).

In this way, Thiomab-coumarin and Thiomab-duocarmycin ADCs bearing an acid cleavable linker were synthesized, as will be described below.

5.6.1 Synthesis of carbonyl acrylamide derivatives

First, coumarin and duocarmycin bearing a carbonyl acrylamide handle were synthesized for their conjugation with Thiomab. Amines **24** and **29** (for their synthesis See **Scheme 5.5** and **Scheme 5.6**) were the starting material for the functionalization with carbonyl acryl amide handle.



Scheme 5.10: synthesis of carbonyl acrylamide handles for ADC synthesis.

Activation of *trans*-3-benzoylacrylic acid with isobutyl chloroformate (IBCF) and *N*-methyl morpholine (NMM) in DMF at -10 °C, followed by the addition of compound **24**, produced compound **34** in 48% yield. Equally, carbonyl acrylamide **35** was obtained from **29** in 45% yield after purification by column chromatography (**Scheme 5.10**).

5.6.2 ADC synthesis and stability

Carbonyl acrylamides **34** and **35** were then used for conjugation reaction with the antibody. The conjugation reaction proceeds smoothly in most cases, although some optimization was needed to obtain full conversion to the desired ADC with DAR 2, and avoid undesired acetal cleavage, especially when performing the conjugation with compound **35**.

The different conditions tested to optimize the conjugation reaction are resumed in **Table 5.2**.

Entry	Reaction conditions	Conversion (mass)
1	35 (1 equiv.), 2 h, NaPi (50 mM, pH 7), 25 °C	5-10% (23699)
2	35 (1 equiv.), 2 h, NaPi (50 mM, pH 8), 25 °C	5-10% (23699)
3	35 (1 equiv.), 2 h, NaPi (20 mM, pH 7), 25 °C	5-10% (24017)
4	35 (10 equiv.), 2 h, NaPi (20 mM, pH 7), 25 °C	5-10% (24018)
5	35 (10 equiv.), 6 h, NaPi (20 mM, pH 7), 25 °C	100% (24017)
6	35 (10 equiv.) 24 h, NaPi (20 mM, pH 7), 25 °C	100% (24020)
7	35 (10 equiv.), 6 h + dialysis, NaPi (20 mM, pH 7), 25 °C	100% (24021)
8	34 (20 equiv.), 3 h, NaPi (20 mM, pH 7), 25 °C	42% (23895) 58% (24347)
9	34 (6 equiv.), 3 h, NaPi (20 mM, pH 7), 25 °C	>95% (23898)
10	34 (10 equiv.), 3 h, NaPi (20 mM, pH 7), 25 °C	>95% (23898)

Table 5.2: conditions tested for Thiomab-34 and Thiomab-35 and synthesis.

As can be inferred from **Table 5.2**, full conversion of Thiomab to the duocarmycin-conjugate requires the use of 10 equivalents of carbonyl acrylamide reagent **35** for at least 6 hours reaction (entries **5** and **6**). The use of less equivalents (entry **3**) and shorter reaction times (entry **4**) gives only 5-10 % conversion to the final product. Importantly, the buffer concentration is fundamental for the good proceeding of the reaction: using 50 mM NaPi buffer causes premature hydrolysis of the acetal moiety and a compound whose mass corresponds to the conjugate with the PEG spacer is obtained (mass 23699, entry **1**). Surprisingly, this happens also when basic buffer is used (NaPi buffer 50 mM, pH 8.0, entry **2**), but the problem is overcome using 20 mM NaPi buffer at pH 7.0. Finally, full conversion is obtained when using 10 equiv. of reagent **35** in 6 hours at room temperature (entry **6**), as shown by LC-MS analysis (**Figure 5.19**). Purification by overnight dialysis does not give further problems and conjugate remains intact (entry **7**).

Conjugation with the umbelliferone derivative **34** proceeded smoothly and the cleavage of the acetal was not detected in the optimized conditions encountered. To obtain

desired conjugate, reaction was performed in NaPi buffer (20 mM, pH 7.0) at 25 °C. Notably, a doubly modified antibody (two modifications per light chain) was obtained when a high excess of compound **34** was used (entry **8**). This might be attributed to spontaneous disulfide cleavage in the antibody, which lead to a second free cysteine residue able to react with the carbonyl acrylamide reagent.^[81] However, this was easily overcome by carefully controlling the amount of reagent **34** used. Reaction of the antibody with 6 or 10 equivalents of **34** gave after 3 hours at room temperature Thiomab-**34** with >95% conversion (entry **9** and **10**), as shown by LC-MS analysis (Figure 5.19).

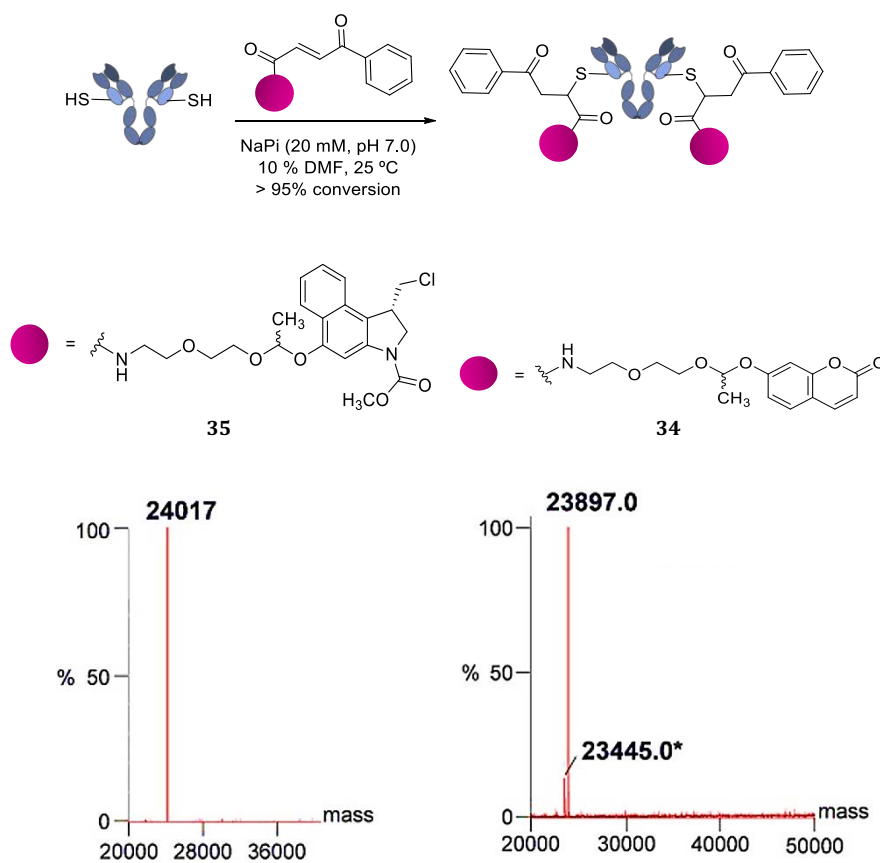


Figure 5.19: schematization of the reaction of Thiomab with derivatives **34** and **35**; deconvoluted LC-MS spectra of Thiomab-**34** (right) and Thiomab-**35** (left).

Next, the stability of Thiomab-**34** and Thiomab-**35** was evaluated in human serum.

For Thiomab-**34**, fluorescence studies were performed in order to determine the release of fluorescent **umbelliferone**. Thus, Thiomab-**34** buffer was changed to PBS, and 1% reconstituted human serum was added, followed by incubation at 37 °C. Also, to verify that 7-hydroxy coumarin was efficiently released, buffer of the antibody was exchanged to NaPi buffer at pH 5.7 and release studies were performed.

As a result, Thiomab-**34** is able to release more than 50% 7-hydroxy coumarin after 24 hours incubation in acid buffer, while more than 80% of conjugate is conserved in human serum (**Figure 5.20**). These results fit with what previously observed from experiments in small molecules (*See Section 5.3.2*).

In the case of Thiomab-**35**, a completely different behavior was observed. Thiomab-**35** is stable in human serum after 2 hours incubation (**Figure 5.20**), but after 24 hours more than 62 % release of duocarmycin is detected by LC-MS analysis.

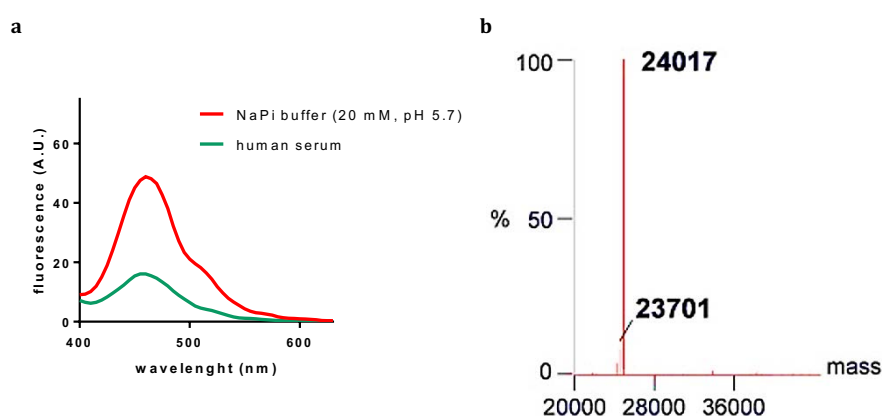


Figure 5.20: stability assays on Thiomab-**34** and Thiomab-**35**. a) fluorescence emission due to **umbelliferone** release in acid buffer (NaPi 20 mM, pH 5.7) (red) and human serum (green). Fluorescence intensities are normalized to **umbelliferone** emission at 450 nm. b) deconvoluted LC-MS analysis of Thiomab-**34** after 24 hours incubation in human serum at 37 °C.

5.6.3 *In vitro* assays

To evaluate the ability of the previously synthesized ADCs to target cancer cells and selectively delivery and release the drug in tumour cells, *in vitro* experiments on different cell lines were performed. As a model for Her2 positive tumour cells, SKBR3,

a breast cancer cell line was chosen. As negative control MDA-MB 231 cells were chosen, which represent a good model for Her2 negative breast cancer cells.

First, flow cytometry experiments were performed, to determine whether ADC structure is conserved upon conjugation reaction and it is able to selectively bind SKBR3 versus MDA-MB 231.

Thus, Thiomab-34 and Thiomab-35 conjugates binding to Her2 receptor was determined by flow cytometry analysis. As it emerges from **Figure 5.21**, while very low signal is observed for binding to MDA-MB 231 cells, Thiomab-34 and Thiomab-35 strongly bind to the surface of SKBR3 cells. Thus, the conjugation strategy and the drug or fluorophore insertion do not provoke a modification of antibody structure, as the modification does not alter binding capacity of the antibody.

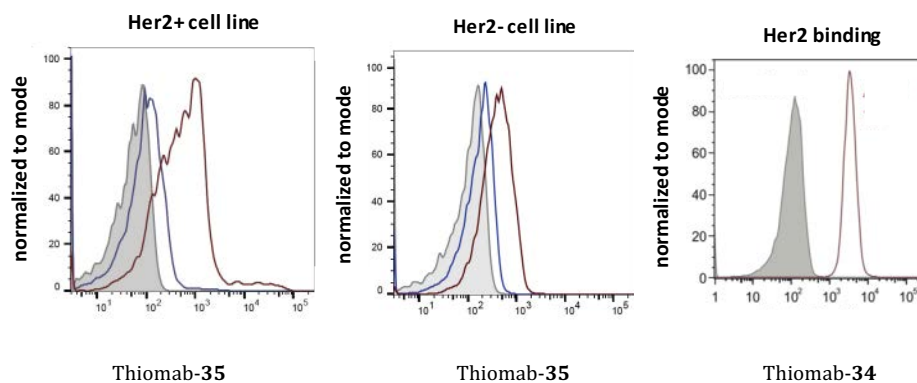


Figure 5.21: flow cytometry analysis of Thiomab conjugates. Binding of Trastuzumab-35 on SKBR3 cells (left) and MDA-MB 231 cells (middle). Grey graph represents unstained cells; blue graph represents cells treated with only secondary antibody; red graph represent cells treated with Thiomab-35 conjugate. Left panel: binding of Thiomab-34 to SKBR3 cells. Grey graph represents unstained cells; red graph represents cells treated with Thiomab-34 conjugate.

Afterwards, toxicity assays were performed on the aforementioned cell lines, to check whether the binding selectivity is reflected in selective toxicity.

Incubation of SKBR3 and MDA-MB 231 cells with increasing concentration of Thiomab-35 showed that such conjugate has a 3-fold superior toxicity in SKBR3 cells ($IC_{50} = 1.03 \pm 0.20 \mu\text{M}$) compared to the toxicity in MDA-MB 231 cells (IC_{50} of $3.04 \pm 0.37 \mu\text{M}$, **Figure 5.22**).

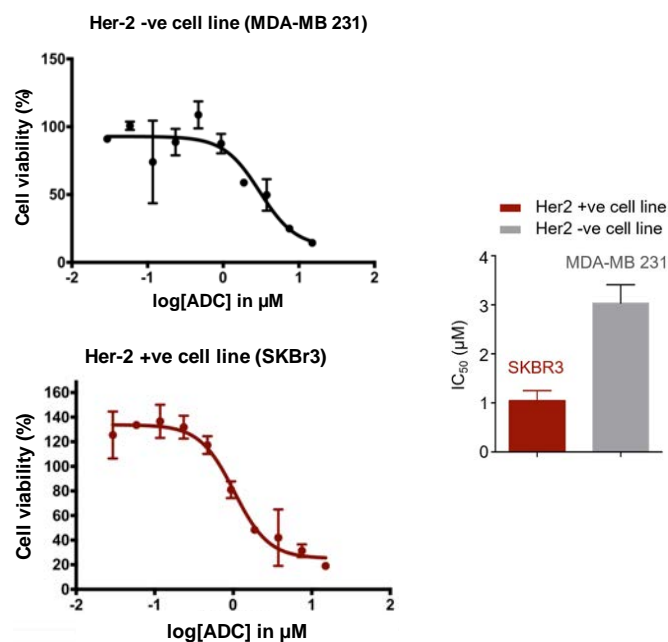


Figure 5.22: toxicity of ADC Thiomab-35 in SKBR3 and MDA-MB 231 cell lines.

Even if there is some selectivity in the toxic effect, also Her2 negative cells experience the toxic effect of free duocarmycin. This is attributable to the poor stability of the acetal bond that may cause drug release in the extracellular media. Thus, free duocarmycin may diffuse inside the cell, producing non-selective cell killing.

5.6.4 Molecular Dynamics simulations

To understand the unexpected behavior of Thiomab-35 and the different behaviors of duocarmycin and umbelliferone Thiomab conjugates, 200 ns Molecular Dynamic simulations (MD) on conjugates Thiomab-34 and Thiomab-35 were performed, considering the four possible diastereomers generated upon conjugation. These calculations were performed in explicit water and using AMBER 18 software,^[82] implemented with ff14SB^[83] and GAFF^[84] force fields to properly simulate the conformational behaviour of these conjugates.

Interestingly, this study highlighted the presence of a transient hydrogen bond between an oxygen atom of the acetal and the amino group of Lys425 in Thiomab-35 conjugate (**Figure 5.23 a**). A CH/ π interactions between the aromatic ring of the duocarmycin

derivative and the hydrogen H β of Ser133 stabilizes this conformation and keeps in close proximity Lys425 and the acetal group. Therefore, Lys425 may act as intramolecular acid catalyst for the hydrolysis reaction by protonating the acetal, which is the first step in the hydrolysis reaction. Therefore, acetal hydrolysis is accelerated and premature drug release occurs.

Such contact interaction is not appreciable in conjugate Thiomab-**34**, whose acetal group is at safe distance from Lys425 (**Figure 5.23 b**). In this case, umbelliferone payload forces a different spatial orientation and as a result the acetal conjugate presents good stability in plasma.

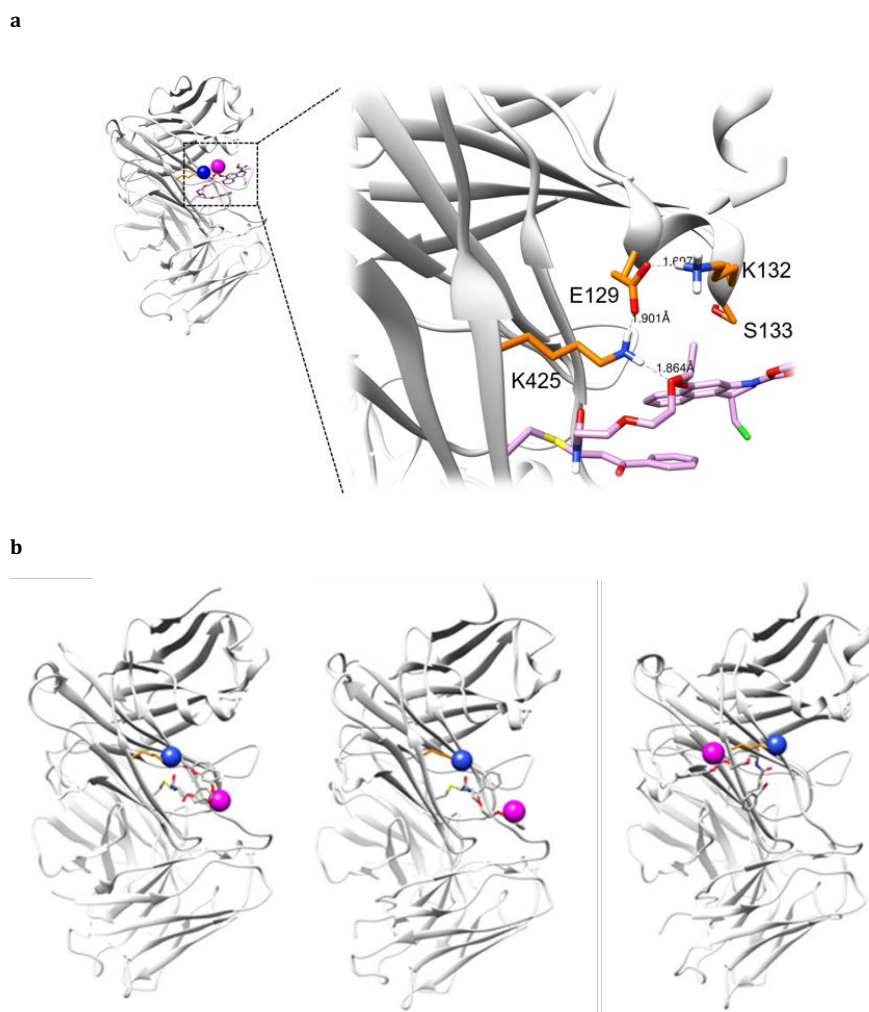


Figure 5.23: molecular dynamics simulation on Thiomab-34 and Thiomab-35 conjugates. a) zoom of the conjugation site of Thiomab-35 conjugate and its environment: Lys425 can interact through an hydrogen bond with acetal linker, increasing the rate of its hydrolysis; b) frames of the simulation of Thiomab-34 structure: Lys425 (blue dot) stays far from acetal oxygen (pink dot).

5.7 Conclusions

In this chapter, the properties of an acid cleavable linker based on the acetal group were studied.

First, small molecules bearing a coumarin and duocarmycin derivatives were synthesized, as examples of biologically interesting molecules that can be modified with

an acetal group. 7-hydroxy coumarin-acetals bearing different linkers were synthesized and their behaviour in acid media was studied. Among them, an acetal with a small PEG spacer (compound **25**) showed to be enough acid-labile to give relatively fast hydrolysis at pH 5.7, a pH value that can be encountered in lysosomes or endosomes. Thus, the corresponding duocarmycin derivative **29** was synthesized. The stability studies performed on this small molecule showed it is resistant to hydrolysis when incubated in human serum, but it readily releases active payload when incubated in slightly acid conditions. Therefore, a SMDC targeting CAIX and based on this linker-drug system was synthesized and characterized. *In vitro* assays showed that this compound has a toxicity profile similar to free duocarmycin in CAIX expressing cells, suggesting that acetal moiety cleaves efficiently inside the target cell.

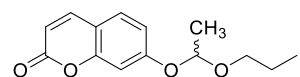
Moreover, to expand the applicability of the acetal linker, an ADC was synthesised. Engineered Thiomab, bearing a cysteine at position 205 of the light chain was conjugated using carbonyl acrylamide technology to duocarmycin derivative **35** and coumarin derivative **34** giving homogenous conjugates with DAR 2. The properties of these conjugates (Thiomab-**34** and Thiomab-**35**) were more difficult to evaluate and less predictable. In fact, a completely different stability profile from SMDC and small molecule-linkers were observed. Rationalization of this result through MD simulations showed how the conjugation site influences the stability of the linker. Also, the payload in this case has great influence on the ADC stability: in fact, changing duocarmycin with umbelliferone produces a different conformation and disposition of this compound in antibody conjugation site, that results in a higher stability, as confirmed by fluorescence assays.

Therefore, acetals can be used as linker for the controlled release of drugs from targeted delivery systems. In the case of Small molecule drug conjugates, linker stability can be easily tuned and predicted, giving conditionally stable systems. In the case of ADC, a careful control of drug, linker in combination with an adequate conjugation site are fundamental to obtain a fully stable and useful ADC. Finding right conditions, with the help of MD simulations, can allow the use of acetals for the generation of pro-drugs and their application in ADC development.

5.8 Experimental section

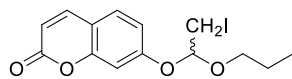
5.8.1 Synthesis

Synthesis of compound 12



Propyl vinyl ether (2.5 mmol, 213 mg) was dissolved in dry CH_2Cl_2 (1 mL) under an inert atmosphere. The mixture was cooled at 0°C and CSA (18 mg, 0.07 mmol) was added. A solution of umbelliferone (200 mg, 1.23 mmol) in dry CH_2Cl_2 (1 mL) and some drops of dry DMF were then added and the reaction mixture was stirred at room temperature for 3h. Then, the reaction mixture was diluted with Et_2O (30 mL), washed with NaHCO_3 (10 mL) and extracted with Et_2O (2 x 20 mL). The organic phase was dried over Na_2SO_4 , filtered and concentrated under reduced pressure. The crude product was purified through silica gel column chromatography (eluent AcOEt: Hexanes 1:3) to give acetal **12** with 48% yield (146 mg, 0.59 mmol). HRMS (ESI+) m/z : calcd. for $\text{C}_{14}\text{H}_{16}\text{NaO}_4$ $[\text{M}+\text{Na}]^+$: 271.0941, found 271.0941. ^1H NMR (400 MHz, CDCl_3) δ (ppm): 7.65 (d, $J=9.6$ Hz, 1H, H-4), 7.38 (d, $J=8.6$ Hz, 1H, H arom.), 6.98 – 6.93 (m, 2H, H arom.), 6.27 (d, $J=9.6$ Hz, 1H, H-3), 5.48 (q, $J=5.3$ Hz, 1H, H acetal), 3.68 – 3.62 (m, 1H, OCH_2), 3.47 – 3.42 (m, 1H, OCH_2), 1.64 – 1.58 (m, 2H, CH_2), 1.53 (d, $J=5.2$ Hz, 3H, CHCH_3), 0.91 (t, $J=7.6$ Hz, 3H, CH_3). ^{13}C NMR (101 MHz, CDCl_3) δ (ppm): 161.3 (CO), 160.2 (Cq arom.), 155.6 (Cq arom.), 143.4 (C-4), 128.7 (CH arom.), 114.5 (CH arom.), 113.5 (C-3), 113.2 (Cq arom.), 104.2 (CH arom.), 99.5 (CH acetal), 67.2 (OCH_2), 22.9 (CH_2), 19.7 (CHCH_3), 10.6 (CH_3).

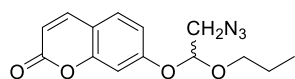
Synthesis of compound 13



A solution of *N*-iodosuccinimide (3.21 mmol, 722.2 mg) in dry CH_2Cl_2 (5 mL) under inert atmosphere was cooled at 0°C . Propyl vinyl ether (276.5 mg, 3.21 mmol) and a solution of umbelliferone (400 mg, 2.47 mmol) in dry THF (4 mL) and dry DMF (1 mL) were then added. The reaction was stirred at room temperature for 24 hours and then it was quenched with $\text{Na}_2\text{S}_2\text{O}_3$ 0.1 M (10 mL) and the compound was extracted with CH_2Cl_2 (50 mL). The organic phase was dried over Na_2SO_4 , filtered and concentrated under reduced pressure. The crude mixture was purified through column chromatography (eluent CH_2Cl_2 : Et_2O 100:1) to

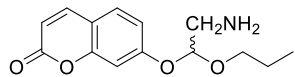
give compound **13** as an orange oil with 48% yield (386 mg, 1.03 mmol). HRMS (ESI+): m/z calcd. for $C_{14}H_{16}IO_4$ $[M+H]^+$ 375.0088, found: 375.0075. 1H NMR (400 MHz, $CDCl_3$) δ (ppm): 7.66 (d, $J=9.6$ Hz, 1H, H-4), 7.41 (d, $J=8.4$ Hz, 1H, H arom.), 6.99 – 6.95 (m, 2H, H arom.), 6.30 (d, $J=9.5$ Hz, 1H, H-3), 5.41 (t, $J=5.6$ Hz, 1H, H acetal), 3.70 – 3.67 (m, 1H, OCH_2), 3.54 – 3.48 (m, 1H, OCH_2), 3.42 (d, $J=6.0$ Hz, 2H, CH_2I), 1.63 (sx, $J=7.6$ Hz, 2H, CH_2), 0.93 (t, $J=7.6$ Hz, 3H, CH_3). ^{13}C NMR (101 MHz, $CDCl_3$) δ (ppm): 160.9 (CO), 159.5 (Cq arom.), 155.5 (Cq arom.), 143.2 (C-4), 128.9 (CH arom.), 114.4 (CH arom.), 114.1 (Cq arom.), 113.8 (Cq arom.), 104.6 (CH arom.), 101.5 (CH-acetal), 68.3 (OCH_2), 22.8 (CH_2), 10.6 (CH_3), 3.4 (CH_2I).

Synthesis of compound 14



To a solution of compound **13** (306 mg, 0.82 mmol) in DMF (3 mL), NaN_3 (266 mg, 4.08 mmol) was added. The reaction was stirred for 3 h at 50 °C. Then, AcOEt (100 mL) was added and the solid was filtered. The filtrate was washed with H_2O (3 x 50 mL). The organic phase was dried over Na_2SO_4 , filtered and concentrated. The product was purified through column chromatography (eluent CH_2Cl_2 : Et_2O 100:1) to give compound **14** as a yellow liquid with 86% yield (204 mg, 0.70 mmol). HRMS (ESI+) m/z : calcd. for $C_{14}H_{15}N_3NaO_4$ $[M+Na]^+$ 312.0955, found 312.0951; calcd. for $C_{12}H_{16}N_3O_4$ $[M+H]^+$ 290.1135, found 290.1138. 1H NMR (300 MHz, CD_3OD) δ (ppm): 7.91 (d, $J=9.6$ Hz, 1H, H-4), 7.61 – 7.59 (m, 1H, H arom.), 7.08 – 7.06 (m, 2H, H arom.), 6.32 (d, $J=9.6$ Hz, 1H, H-3), 5.60 (t, $J=5.2$ Hz, 1H, H-acetal), 3.75–3.70 (m, 1H, OCH_2), 3.62–3.58 (m, 1H, OCH_2), 3.56 (d, $J=5.4$ Hz, 2H, CH_2N_3), 1.62 (sx, $J=7.6$ Hz, 2H, CH_2), 0.94 (t, $J=7.6$ Hz, 3H, CH_3). ^{13}C NMR (75 MHz, CD_3OD) δ (ppm): 161.6 (CO), 160.1 (Cq arom.), 155.4 (Cq arom.), 144.1 (C-4), 129.3 (CH arom.), 114.2 (CH arom.), 113.9 (Cq arom.), 113.0 (CH-3), 103.8 (CH arom.), 100.7 (CH-acetal), 68.8 (OCH_2), 51.8 (CH_2N_3), 22.6 (CH_2), 9.5 (CH_3).

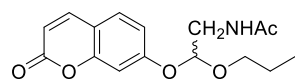
Synthesis of compound 15



To a solution of compound **14** (110 mg, 0.38 mmol) in THF (8 mL), PPh_3 was added (200 mg, 0.76 mmol) and the reaction was warmed at 45 °C. 40 minutes later, H_2O (54.7 μ L, 3.04 mmol) was added and the reaction was stirred overnight at 45 °C. The reaction was then concentrated

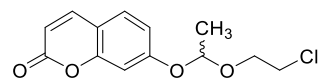
under reduced pressure and the crude product was purified by silica gel chromatography eluting with AcOEt to eliminate fosfine by-products. Amine was then eluted with CH₂Cl₂: MeOH 5:1 and concentrated under reduced pressure to give compound **15** as a yellow oil with 86% yield (86 mg, 0.33 mmol). ¹H NMR (300 MHz, CD₃OD) δ (ppm): 7.89 (d, *J*=9.5 Hz, 1H, H arom.), 7.57 (d, *J*=9.2 Hz, 1H, H arom.), 7.15 – 6.91 (m, 2H, H arom.), 6.29 (d, *J*=9.5 Hz, 1H, H arom.), 5.42 (t, *J*=5.1 Hz, 1H, H acetal), 3.72 – 3.64 (m, 1H, OCH₂), 3.57 – 3.49 (m, 1H, OCH₂), 2.97 (dd, *J*=5.1, 1.1 Hz, 2H, CH₂NH₂), 1.61 (sx, *J*=7.4 Hz, 2H, CH₂), 0.92 (t, *J*=7.4 Hz, 3H, CH₃). ¹³C NMR (75 MHz, CD₃OD) δ (ppm): 161.7 (C=O), 160.6 (Cq arom.), 155.4 (Cq arom.), 144.1 (CH arom.), 129.2 (CH arom.), 114.2 (CH arom.), 113.6 (Cq arom.), 112.8 (CH arom.), 103.6 (CH arom.), 102.4 (CH acetal), 68.3 (OCH₂), 43.3 (CH₂NH₂), 22.6 (CH₂), 9.5 (CH₃).

Synthesis of compound 16



To a solution of compound **15** (50 mg, 0.19 mmol) in CH₂Cl₂ (5 mL), pyridine (92 μL, 1.14 mmol), Ac₂O (108 μL, 1.14 mmol) and a catalytic amount of DMAP were added. After stirring for 3 h, the crude reaction mixture was washed with NH₄Cl (20 mL) and extracted with CH₂Cl₂ (50 mL). The organic phase was dried over Na₂SO₄, filtered and concentrated under reduced pressure. Crude product was purified through chromatography on silica gel (eluent AcOEt: Hexane 2:1) to give acetal **16** as a white solid with 64% yield (37.1 mg, 0.13 mmol). HRMS (ESI+) *m/z*: calcd. for C₁₆H₁₉NNaO₅ [M+Na]⁺ 328.1153, found 328.1155. ¹H NMR (400 MHz, CD₃OD) δ (ppm): 7.90 (d, *J*=9.6 Hz, 1H, H-4), 7.59 – 7.57 (m, 1H, H arom.), 7.07 – 7.05 (m, 2H, H arom.), 6.30 (d, *J*=9.6 Hz, 1H, H-3), 5.49 (t, *J*=5.2 Hz, 1H, H acetal), 3.72 – 3.66 (m, 1H, OCH₂), 3.60 – 3.48 (m, 3H, OCH₂, CH₂NH), 1.97 (s, 3H, COCH₃), 1.61 (sx, *J*=7.6 Hz, 2H, CH₂), 0.93 (t, *J*=7.6 Hz, 3H, CH₃). ¹³C NMR (101 MHz, CD₃OD) δ (ppm): 172.4 (CO-CH₃), 161.6 (CO), 160.5 (Cq arom.), 155.4 (Cq), 144.1 (CH arom.), 129.2 (CH arom.), 114.0 (CH arom.), 113.6 (Cq), 112.8 (CH arom.), 103.6 (CH arom.), 99.9 (CH acetal), 68.6 (OCH₂), 41.7 (CH₂NH), 22.5 (CH₂), 21.0 (COCH₃), 9.5 (CH₃).

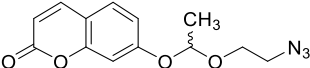
Synthesis of compound 17

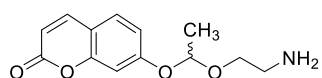


To an ice-cooled solution of CSA (17.1 mg, 0.074 mmol) in dry CH₂Cl₂ (1 mL) under argon, 2-chlorovinylether (376 μL, 3.7 mmol) and a solution of Umbelliferone (200 mg,

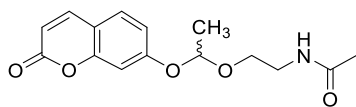
1.23 mmol) were added. The solution was allowed to warm to room temperature and stirred for 1.5 h. After this time, the reaction mixture was diluted with 20 mL of Et₂O and washed with a saturated NaHCO₃ solution (10 mL). The product was extracted with Et₂O (2 x 20 mL), organic phase was dried over Na₂SO₄, filtered and concentrated. The crude product was purified by silica gel chromatography in hexane/ethyl acetate (3:2) to give compound **17** as a yellow solid (315 mg, 95%). HRMS (ESI+): *m/z* calcd. for C₁₃H₁₃ClO₄Na [M+Na]⁺ 291.0395, found 291.0401. ¹H NMR (400 MHz, CD₃OD) δ (ppm): 7.88 (d, *J*=9.5 Hz, 1H, H-4), 7.56 – 7.54 (d, *J*=8.2 Hz, 1H, H-5), 7.04 – 7.01 (m, 2H, H-6, H-8), 6.28 (d, *J*=9.5 Hz, 1H, H-3), 5.68 (q, *J*=5.3 Hz, 1H, CH-acetal), 3.93 – 3.98 (m, 1H, OCH₂), 3.77 – 3.82 (m, 1H, OCH₂) 3.66 (t, *J*=5.5 Hz, 2H, CH₂Cl), 1.55 (d, *J*=5.3 Hz, 3H, CH₃). ¹³C NMR (101 MHz, CD₃OD) δ (ppm): 161.7 (CO), 160.1 (Cq arom.), 155.4 (Cq arom.), 144.2 (CH-4), 129.0 (CH-5), 114.3 (CH-6), 113.5 (Cq arom.), 112.7 (CH-3), 103.7 (CH-8), 99.3 (CH-acetal), 65.5 (OCH₂), 42.5 (CH₂Cl), 18.5 (CH₃).

Synthesis of compound **18**

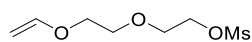
 To a solution of **17** (261 mg, 0.97 mmol) in DMF (2 mL), NaN₃ (189 mg, 2.91 mmol) was added and the reaction mixture was heated at 80 °C for 3 d. After this time, the reaction was diluted with ethyl acetate (50 mL), filtered and the resulting solution was washed with H₂O (3 x 20 mL). The organic phase was dried over Na₂SO₄, filtered and concentrated. The crude product was purified by silica gel chromatography in hexane/ethyl acetate (3:2) to give **18** (154 mg, 57%). HRMS (ESI+): *m/z* calcd. for C₁₃H₁₃N₃O₄Na [M+Na]⁺ 298.0799, found 298.0797. ¹H NMR (400 MHz, CD₃OD) δ (ppm): 7.89 (d, *J*=9.5 Hz, 1H, H-4), 7.56 (d, *J*=9.3 Hz, 1H, H-5), 7.04 – 7.02 (m, 2H, H-8, H-6), 6.28 (d, *J*=9.5 Hz, 1H, H-3), 5.70 (q, *J*=5.3 Hz, 1H, CH-acetal), 3.90 – 3.86 (m, 1H, OCH₂), 3.74 – 3.69 (m, 1H, OCH₂), 3.36 – 3.40 (m, 2H, CH₂N₃), 1.57 (d, *J*=5.3 Hz, 3H, CH₃). ¹³C NMR (101 MHz, CD₃OD) δ (ppm): 161.8 (CO), 160.1 (Cq arom.), 155.4 (Cq arom.), 144.2 (CH-4), 129.1 (CH-5), 114.2 (CH-6), 113.5 (Cq arom.), 112.6 (CH-3), 103.6 (CH-8), 99.2 (CH-acetal), 64.2 (OCH₂), 50.4 (CH₂N₃), 18.5 (CH₃).

Synthesis of compound 19

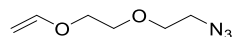
Derivative **18** (51 mg, 0.19 mmol) was dissolved in THF (3 mL) and to this solution PPh₃ (99 mg, 0.38 mmol) and H₂O (27 μ L) were added. The solution was heated at 45 °C for 16 h and then it was concentrated. The crude obtained was purified by silica gel chromatography in CH₂Cl₂/MeOH/ NEt₃ (10:1:0.1) to give **19** (25 mg, 89%). HRMS (ESI+): m/z calcd. for C₁₃H₁₄N₃O₄ [M+H]⁺ 250.1071, found 250.1074. ¹H NMR (400 MHz, CD₃OD) δ (ppm): 7.92 (d, *J*=9.5 Hz, 1H, H-4), 7.60 (d, *J*=8.6 Hz, 1H, H-5), 7.09 (d, *J*=2.4 Hz, 1H, H-8) 7.03 (dd, *J*=8.6, 2.4 Hz, 1H, H-6), 6.31 (d, *J*=9.5 Hz, 1H, H-3), 5.74 (q, *J*=5.3 Hz, 1H, H-acetal), 3.92–3.97 (m, 1H, OCH₂), 3.72–3.77 (m, 1H, OCH₂), 3.11–3.15 (m, 2H, CH₂NH₂), 1.60 (d, *J*=5.3 Hz, 3H, CH₃). ¹³C NMR (75 MHz, CD₃OD) δ (ppm): 161.7 (CO), 160.0 (Cq arom.), 155.5 (Cq arom.), 144.2 (CH-4), 129.2 (CH-5), 114.1 (CH-6), 113.6 (Cq arom.), 112.8 (CH-3), 103.4 (CH-8), 99.1 (CH-acetal), 61.6 (OCH₂), 39.4 (CH₂NH₂), 18.4 (CH₃).

Synthesis of compound 20

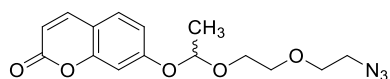
Derivative **19** (22 mg, 0.088 mmol) was dissolved in pyridine (900 μ L) and acetic anhydride (300 μ L) was added. After stirring for 1.5 h, the reaction mixture was concentrated, and the crude product was purified by silica gel chromatography in CH₂Cl₂/MeOH (20:1) to give acetal **20** (12.1 mg, 47%). HRMS (ESI+): m/z calcd. for C₁₅H₁₇NO₅Na [M+Na]⁺ 314.0999, found 314.0996. ¹H NMR (300 MHz, CD₃OD) δ (ppm): 7.92 (d, *J*=9.5 Hz, 1H, H-4), 7.57 (d, *J*=8.5 Hz, 1H, H-5), 7.06 (d, *J*=2.3 Hz, 1H, H-8), 7.02 (dd, *J*=8.5, 2.3 Hz, 1H, H-6), 6.29 (d, *J*=9.5 Hz, 1H, H-3), 5.66 (q, *J*=5.3 Hz, H-acetal), 3.78–3.71 (m, 1H, OCH₂), 3.64–3.56 (m, 1H, OCH₂), 3.36 (m, 2H, CH₂N), 1.84 (s, 3H, COCH₃), 1.55 (d, *J*=5.3 Hz, 3H, CHCH₃). ¹³C NMR (75 MHz, CD₃OD) δ (ppm): 172.0 (COCH₃), 161.7 (CO), 160.2 (Cq arom.), 155.4 (Cq arom.), 144.2 (CH-4), 129.0 (CH-5), 114.3 (CH-6), 113.3 (Cq arom.), 112.6 (CH-3), 103.5 (CH-8), 98.9 (CH-acetal), 63.0 (OCH₂), 39.0 (CH₂N), 21.0 (COCH₃), 18.4 (CHCH₃).

Synthesis of compound 21

Commercially available 2-(2-(vinylloxy)ethoxy)ethan-1-ol (1.00 g, 7.56 mmol) was dissolved in anhydrous CH_2Cl_2 (11 mL) under an Argon atmosphere. The solution was cooled at 0 °C and NEt_3 (2.11 mL, 15.12 mmol) and MsCl (0.76 mL, 9.83 mmol) were added. The mixture was allowed to warm at room temperature and stirred for 2 hours. Afterwards, the solution was diluted with AcOEt (150 mL) and washed with H_2O (3 x 30 mL). Organic phase was dried over Na_2SO_4 , filtered and concentrated to give crude compound **21** that was used in the next step without further purification (1.47 g, 7.00 mmol, 92% yield). $^1\text{H NMR}$ (300 MHz, CDCl_3) δ (ppm): 6.50 (dd, $J=14.3$, 6.8 Hz, 1H), 4.49 – 4.34 (m, 2H), 4.21 (dd, $J=14.3$, 2.2 Hz, 1H), 4.05 (dd, $J=6.8$, 2.2 Hz, 1H), 3.88 – 3.85 (m, 2H), 3.83 – 3.76 (m, 2H), 3.09 (s, 2H).

Synthesis of compound 22

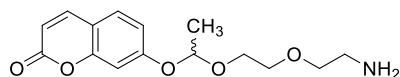
To a solution of compound **21** (200 mg, 0.95 mmol) in DMF (1.5 mL) NaN_3 (123 mg, 1.90 mmol) was added and the reaction was stirred at 50 °C for 16 hours. Afterwards, the reaction mixture was diluted with AcOEt (150 mL), the solid was filtered and the filtrate was washed with H_2O (3 x 20 mL). Organic phase was dried over Na_2SO_4 , filtered and concentrated at reduced pressure. Crude product was purified by silica gel chromatography to give compound **22** (114 mg, 0.72 mmol) with 76% yield. $^1\text{H NMR}$ (300 MHz, CDCl_3) δ (ppm): 6.53 (dd, $J=14.3$, 6.8 Hz, 1H), 4.22 (dd, $J=14.3$, 2.2 Hz, 1H), 4.05 (dd, $J=6.8$, 2.2 Hz, 1H), 3.90 – 3.87 (m, 2H), 3.82 – 3.63 (m, 4H), 3.44 (t, $J=5.1$ Hz, 2H).^[85]

Synthesis of compound 23

To an ice-cooled solution of **22** (280 mg, 1.78 mmol) in dry CH_2Cl_2 (2 mL) under nitrogen atmosphere, CSA (8 mg, 0.035 mmol) and a solution of Umbelliferone (96 mg, 0.59 mmol) were added. After 5 minutes, the solution was allowed to warm to room temperature and stirred for 1.5 h. After this time, the reaction mixture was diluted with 40 mL of CH_2Cl_2 and washed with a saturated NaHCO_3 solution (20 mL). The product was extracted with CH_2Cl_2 (2

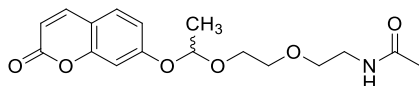
x 40 mL), the organic phase was dried over Na₂SO₄, filtered and concentrated. The crude product was purified by flash column chromatography on silica gel eluting with CH₂Cl₂:Et₂O (60:1 to 40:1). Pure compound **23** was obtained with 72% yield (135 mg, 1.28 mmol). ¹H NMR (400 MHz, CD₃OD) δ (ppm): 7.86 (d, *J*=9.5 Hz, 1H, H-4), 7.52 (d, *J*=8.5 Hz, 1H, H-5), 7.03–6.99 (m, 2H, H-6, H-8), 6.26 (d, *J*=9.5 Hz, 1H, H-3), 5.64 (q, *J*=5.3 Hz, 1H, CH-acetal), 3.87–3.82 (m, 1H, OCH₂), 3.73–3.62 (m, 5H, OCH₂, CH₂-PEG) 3.34–3.32 (m, 2H, CH₂-N₃), 1.53 (d, *J*=5.3 Hz, 3H, CH₃). ¹³C NMR (101 MHz, CD₃OD) δ (ppm): 161.7 (CO), 160.2 (Cq arom.), 155.4 (Cq arom.), 144.2 (CH-4), 129.0 (CH-5), 114.4 (CH-6), 113.4 (Cq arom.), 112.6 (CH-3), 103.8 (CH-8), 99.5 (CH-acetal), 69.9, 69.7 (2C, CH₂-PEG), 64.7 (OCH₂), 50.3 (CH₂N₃), 18.7 (CH₃).

Synthesis of compound 24



Derivative **23** (111 mg, 0.34 mmol) was dissolved in THF (10 mL) and to this solution PPh₃ (182 mg, 0.69 mmol) and H₂O (49 μL, 2.72 mmol) were added. The solution was heated at 45°C for 16 h and then it was concentrated. The crude obtained was purified by silica gel chromatography in CH₂Cl₂/MeOH/ NEt₃ (10:1:0.1) to give pure compound **24** (85 mg, 0.29 mmol, 85%). HRMS (ESI+): *m/z* calcd. for C₁₅H₂₀NO₅ [M+H]⁺ 293.1341, found 294.1331. ¹H NMR (500 MHz, CD₃OD) δ (ppm): 7.91 (d, *J*=9.4 Hz, 1H, H-4), 7.57 (d, *J*=8.6 Hz, 1H, H-5), 7.09 (d, *J*=2.3 Hz, 1H, H-8) 7.03 (dd, *J*=8.6, 2.3 Hz, 1H, H-6), 6.29 (d, *J*=9.5 Hz, 1H, H-3), 5.66 (q, *J*=5.3 Hz, 1H, H-acetal), 3.86–3.84 (m, 1H, OCH₂), 3.74–3.72 (m, 1H, OCH₂), 3.64–3.63 (m, 2H, CH₂-PEG), 3.52 (t, *J*=5.3 Hz, 2H, CH₂-PEG), 2.78 (t, *J*=5.3 Hz, 2H, CH₂NH₂), 1.55 (d, *J*=5.3 Hz, 3H, CH₃). ¹³C NMR (125 MHz, CD₃OD) δ (ppm): 161.7 (CO), 160.3 (Cq arom.), 155.4 (Cq arom.), 144.2 (CH-4), 129.0 (CH-5), 114.4 (CH-6), 113.4 (Cq arom.), 112.6 (CH-3), 103.7 (CH-8), 99.5 (CH-acetal), 71.6, 69.7 (2C, CH₂-PEG) 64.6 (OCH₂), 40.6 (CH₂NH₂), 18.6 (CH₃).

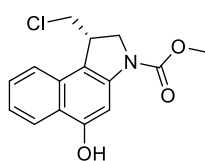
Synthesis of compound 25



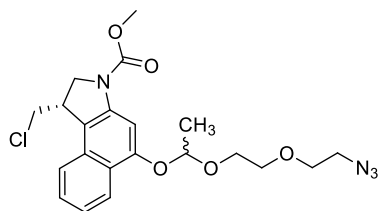
To a solution of **24** (20 mg, 0.068 mmol) in CH₂Cl₂ (1 mL) pyridine (33 μL, 0.41 mmol) and

acetic anhydride (42 μ L, 0.41 mmol) were added. After stirring for 16 h, the reaction mixture was concentrated, and the crude product was purified by flash column chromatography in AcOEt/MeOH (20:1) to give acetal **25** (19 mg, 0.056 mmol, 83%). HRMS (ESI+): m/z calcd. for $C_{17}H_{22}NO_6$ $[M+H]^+$ 336.1447, found 336.1454. 1H NMR (400 MHz, CD_3OD) δ (ppm): 7.91 (d, $J=9.5$ Hz, 1H, H-4), 7.56 (d, $J=8.6$ Hz, 1H, H-5), 7.07 – 7.02 (m, 2H, H-8, H-6), 6.29 (d, $J=9.5$ Hz, 1H, H-3), 5.66 (q, $J=5.2$ Hz, H-acetal), 3.85 – 3.83 (m, 1H, OCH₂), 3.73 – 3.70 (m, 1H, OCH₂), 3.64 – 3.61 (m, 2H, CH₂-PEG), 3.54 – 3.51 (m, 2H, CH₂-PEG), 3.34 – 3.31 (m, 2H, CH₂-NHAc), 1.94 (s, 3H, COCH₃), 1.55 (d, $J=5.2$ Hz, 3H, CHCH₃). ^{13}C NMR (101 MHz, CD_3OD) δ (ppm): 171.9 (C=O), 161.7 (CO), 160.2 (Cq arom.), 155.4 (Cq arom.), 144.2 (CH-4), 129.0 (CH-5), 114.4 (CH-6), 113.4 (Cq arom.), 112.6 (CH-3), 103.7 (CH-8), 99.6 (CH-acetal), 69.7, 69.1 (2C, CH₂-PEG), 64.7 (OCH₂), 39.0 (CH₂N), 21.1 (COCH₃), 18.7 (CHCH₃).

Synthesis of compound 27

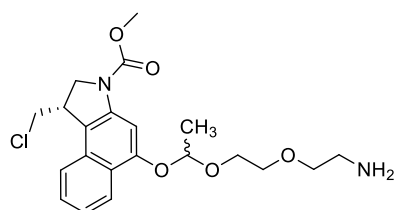


To a solution of commercially available compound **26** (80 mg, 0.24 mmol) in CH_2Cl_2 (3 mL) TFA (460 μ L) was added and the reaction was stirred at rt. After 1 h, the mixture was concentrated, and the crude product was dissolved in THF (4.2 mL), cooled at 0 $^{\circ}C$ and to this solution $NaHCO_3$ (60 mg) and CH_3OCOCl (37 μ L, 0.48 mmol) were added. After 1.5 h, the reaction was diluted with of CH_2Cl_2 (40 mL) and the organic phase washed with H_2O (20 mL), dried over Na_2SO_4 , filtered and concentrated. The solid obtained was purified by a silica gel column chromatography in hexane/ethyl acetate (1:1) to give compound **27** (64 mg, 91%) as a grey solid. HRMS (ESI+): m/z calcd. for $C_{15}H_{14}NClO_3Na$ $[M+Na]^+$ 314.0554, found 314.0550. 1H NMR (400 MHz, $CDCl_3$) δ (ppm): 8.58 (brs, 1H, OH), 8.27 (d, $J=8.4$ Hz, 1H, arom.), 7.96 (brs, 1H, arom.), 7.64 (d, $J=8.3$ Hz, 1H, arom.), 7.54 – 7.49 (m, 1H, arom.), 7.39 – 7.35 (m, 1H, arom.), 4.35 – 4.32 (m, 1H, CH₂N), 4.16 – 4.11 (m, 1H, CH₂N), 4.01 – 3.92 (m, 5H, OCH₃, 1 CH₂Cl, CH), 3.42 (‘t’, $J=10.6$ Hz, 1H, CH₂Cl). ^{13}C NMR (75 MHz, $CDCl_3$) δ (ppm): 154.8 (NCO), 154.7 (Cq arom.) 140.6 (Cq arom.), 130.3 (Cq arom.), 127.7 (CH arom.), 123.8 (CH arom.), 123.1 (CH arom.), 122.0 (Cq arom.), 121.9 (CH arom.), 114.2 (Cq arom.), 98.8 (CH arom.), 53.4 (OCH₃), 52.8 (CH₂N), 46.5 (CH₂Cl), 42.0 (CH).

Synthesis of compound 28

A solution of **27** (24 mg, 0.18 mmol) in dry CH_2Cl_2 (600 μL) was cooled at 0°C , and then **22** was added (56 mg, 0.36 mmol), followed by drops of dry THF to complete solubilisation. After that, a 5 mg/mL solution of CSA (320 μL ,

0.0072 mmol) was added and the reaction was allowed to warm to room temperature. After completion of the reaction, the mixture was diluted with CH_2Cl_2 (40 mL) and washed with H_2O (20 mL), dried over Na_2SO_4 , filtered and concentrated. The crude mixture was purified by a silica gel column chromatography in $\text{CH}_2\text{Cl}_2/\text{Et}_2\text{O}$ (70:1) to give **28** (20 mg, 56%) as a diastereomeric mixture. HRMS (ESI+): m/z calcd. for $\text{C}_{21}\text{H}_{25}\text{ClN}_4\text{O}_5\text{Na}$ $[\text{M}+\text{Na}]^+$ 471.1406, found 471.1406. ^1H NMR (400 MHz, CD_3OD) δ (ppm): 8.09 (d, $J=8.4$ Hz, 1H, arom.), 7.75 (brs, 1H, arom.), 7.63 – 7.60 (m, 1H, arom.), 7.42 – 7.38 (m, 1H, arom.), 7.26 – 7.22 (m, 1H, arom.), 5.61 (q, $J=5.2$ Hz, H-acetal), 4.17 – 4.13 (m, 1H, CH_2N), 4.06 – 4.00 (m, CH_2N), 3.97 – 3.91 (m, 1H, CH), 3.84 – 3.81 (m, CH_2Cl), 3.80–3.73 (m, 4H, OCH_3 , CH-PEG), 3.64 – 3.58 (m, 1H, CH-PEG), 3.57 – 3.47 (m, 5H, CH_2 -PEG, CH_2Cl), 3.19 – 3.15 (m, 2H, CH_2N_3), 1.52 – 1.50 (2 x d, $J=5.2$ Hz, 3H, CH_3 2 diastereomers). ^{13}C NMR (75 MHz, CD_3OD) δ (ppm): 154.0 (CO), 153.9 (Cq arom.), 140.8 (Cq arom.), 130.3 (Cq arom.), 127.3 (CH arom.), 123.2 (CH arom.), 123.1 (Cq arom.), 122.9 (CH arom.), 121.9 (CH arom.), 115.9 (Cq arom.), 100.4 (CH-acetal), 99.4 (CH arom.), 70.0, 69.7 (CH_2 -PEG), 65.5 (CH_2 -PEG, 2 diastereomers), 52.4 (CH_2N), 51.9 (OCH_3), 50.3 (CH_2N_3), 46.3 (CH_2Cl), 41.2 (CH), 19.2, 19.1 (CH_3 , 2 diastereomers)

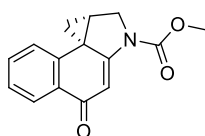
Synthesis of compound 29

To a solution of compound **28** (15 mg, 0.033 mmol) in THF (2 mL), PPh_3 (17 mg, 0.067 mmol) was added. After stirring for 20 min. at 25°C , H_2O (4.7 μL , 0.26 mmol) was added, and the mixture was stirred overnight at room temperature. The

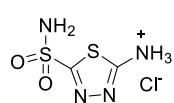
reaction was then concentrated at reduced pressure and the crude solid was purified

by silica gel column chromatography in CH₂Cl₂/MeOH (7:1) to give **29** (9 mg, 65%). HRMS (ESI⁺): *m/z* calcd. for C₂₁H₂₈ClN₂O₅ [M+H]⁺ 423.1681, found 423.1683. ¹H NMR (400 MHz, CD₃OD) δ (ppm): 8.19 (d, *J*=8.5 Hz, 1H, arom.), 7.87 (brs, 1H, arom.), 7.74 (d, *J*=8.4 Hz, 1H, arom.), 7.53 – 7.49 (m, 1H, arom.), 7.36 – 7.32 (m, 1H, arom.), 5.71 (q, *J*=5.2 Hz, H-acetal), 4.29 – 4.28 (m, 1H, CH₂N), 4.20 – 4.14 (m, 1H, CH₂N), 4.11 – 4.09 (m, 1H, CH), 3.96 – 3.95 (m, CH₂Cl), 3.93 – 3.85 (m, 4H, OCH₃, CH-PEG), 3.76 – 3.72 (m, 1H, CH-PEG), 3.65 – 3.59 (m, 3H, CH, CH₂Cl), 3.50 – 3.47 (m, 2H, CH₂-PEG), 2.77 – 2.74 (m, 2H, CH₂NH₂), 1.61 (d, *J*=5.2 Hz, 3H, CH₃). ¹³C NMR (75 MHz, CD₃OD) δ (ppm): 153.9 (2C, Cq arom., CO), 140.9 (Cq arom.), 130.3 (Cq arom.), 127.4 (CH arom.), 123.2, 132.1 (CH arom., Cq arom.), 122.9 (CH arom.), 121.9 (CH arom.), 116.1 (Cq arom.), 100.4 (CH-acetal), 99.5, 99.3 (CH arom., 2 diastereomers), 69.9 (2C, 2CH₂), 65.4 (CH₂), 52.4 (CH₂), 51.9 (OCH₃), 46.4, 46.3 (CH₂Cl, 2 diastereomers), 41.1 (CH), 40.1 (CH₂NH₂), 19.1 (CH₃, 2 diastereomers).

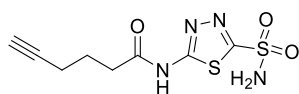
Synthesis of compound 30



Derivative **27** (8 mg, 0.027 mmol) was dissolved in THF (1 mL) and a 5% aqueous solution of NaHCO₃ was added. After stirring overnight at room temperature, the mixture was diluted with CH₂Cl₂ (10 mL) and washed with H₂O (5 mL). The organic phase was dried over Na₂SO₄, filtered, concentrated and the resulting crude product was purified by column chromatography in AcOEt/hexane (1:1) to give derivative **30** (6 mg, 87%). HRMS (ESI⁺): *m/z* calcd. for C₁₅H₁₃NO₃Na [M+Na]⁺ 278.0788, found 278.0784. ¹H NMR (300 MHz, CD₃OD) δ (ppm): 8.12 (dd, *J*=7.9, 1.4 Hz, 1H, arom.), 7.61 – 7.56 (m, 1H, arom.), 7.46 – 7.40 (m, 1H, arom.), 7.13 – 7.10 (m, 1H, arom.), 6.92 (s, 1H, arom.), 4.14 – 4.05 (m, 2H, CH₂N), 3.87 (s, 3H, OCH₃), 3.13 – 3.07 (m, CH) 1.76 (dd, *J*=7.8, 4.2 Hz, 1H, CH₂Cl), 1.55 (‘t’, *J*=4.7 Hz, 1H, CH₂Cl). ¹³C NMR (75 MHz, CD₃OD) δ (ppm): 187.1 (CO), 162.4 (Cq), 153.2 (Cq), 140.9 (Cq), 132.1 (CH arom.), 131.9 (Cq), 126.1 (CH arom.), 125.9 (CH arom.), 121.6 (CH arom.), 107.2 (CH arom.), 52.9 (CH₂N), 52.6 (OCH₃), 33.4 (Cq), 29.0 (CH₂), 24.0 (CH).

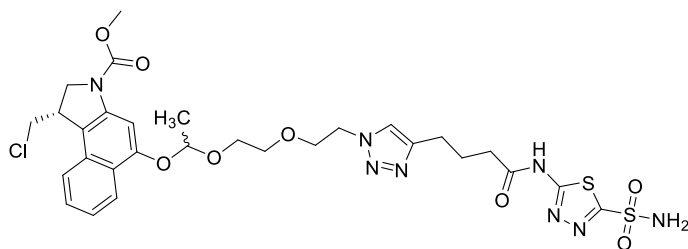
Synthesis of compound 31

N-(5-sulfamoyl-1,3,4-thiadiazol-2-yl)acetamide (1.00 g, 4.5 mmol) was suspended in 1M HCl (24 mL) and the suspension was heated at reflux for 2.5 hours. Then, solvent was evaporated and crude salt **31** was obtained as a white solid with quantitative yield (972 mg, 4.5 mmol). Product was used without further purification in the next step.

Synthesis of compound 32

A solution of 5-hexynoic acid (200 μ L, 1.84 mmol) and DMF (7 μ L) in DCM (7 mL) was cooled on ice and oxalyl chloride (141 μ L, 1.66 mmol) was added drop wise over 15 min. The reaction was allowed to warm to room temperature, stirred until evanescence ceased and then concentrated under reduced pressure. The yellow liquid was dissolve in anhydrous DMF (0.5 mL) and thi solution was added drop wise to a solution of **31** (397 mg, 1.84 mmol) and pyridine (943 μ L, 25.8 mmol) in DMF (1.5 mL) and the reaction stirred for 3 h at room temperature. The solvent was removed under reduced pressure and the residue purified by flash column chromatography (EtOAc) to give the product as an off-white solid (242 mg, 0.88 mmol, 48%).

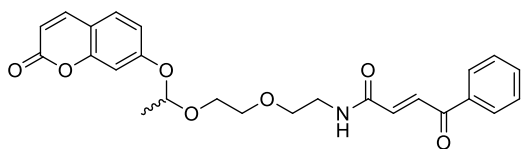
$^1\text{H-NMR}$ (300 MHz, DMSO- d_6) δ (ppm): 2.81 (t, $J=2.6$ Hz, 1H), 2.65 (t, $J=7.4$ Hz, 2H), 2.24 (td, $J=7.1, 2.6$ Hz, 2H), 1.84 – 1.77 (m, 2H).^[71]

Synthesis of compound 33

CuI (0.5 mg, 0.003 mmol) was suspended in THF (500 μ L) under an argon atmosphere and azide **28** (12 mg, 0.027 mmol), DIPEA (11 μ L, 0.064 mmol) and alkyne **32** (9 mg, 0.032 mmol) were then added. After stirring for 3 hours at room temperature, the solution was concentrated at reduced pressure. The resulting solid was suspended in MeOH and filtered over Celite, concentrated and purified by column chromatography in $\text{CH}_2\text{Cl}_2/\text{MeOH}$ (15:1) to give **33** (14 mg, 70%)

as a white solid. HRMS (ESI+): m/z calcd. for $C_{29}H_{35}ClN_8O_8S_2Na$ $[M+Na]^+$ 745.1600, found 745.1597. 1H NMR (400 MHz, CD_3OD) δ (ppm): 8.18 – 8.15 (m, 1H, arom.), 7.86 (brs, 1H, arom.), 7.73 (d, $J=8.4$ Hz, 1H, arom.), 7.68 (brs, H-triazole), 7.51 ('t', $J=7.5$ Hz, 1H, arom.), 7.36 – 7.32 (m, 1H, arom.), 5.70 (2 x q, $J=5.2$ Hz, H-acetal, 2 diastereomers), 4.47 – 4.43 (m, 2H, CH_2 -N triazole), 4.28 – 4.24 (m, 1H, CH_2N), 4.20 – 4.14 (m, 1H, CH_2N), 4.10 – 4.08 (m, 1H, CH), 3.97 – 3.81 (m, 7H, CH_2Cl , OCH_3 , CH_2 -PEG), 3.77 – 3.73 (m, 1H, H-PEG), 3.66 – 3.58 (m, 3H, CH_2 -PEG, CH_2Cl), 2.68 – 2.61 (m, 2H, CH_2), 2.52 – 2.46 (m, 2H, CH_2), 1.99 – 1.92 (m, 2H, CH_2), 1.62 – 1.60 (2 x d, $J=5.2$ Hz, 3H, CH_3 , 2 diastereomers). ^{13}C NMR (75 MHz, CD_3OD) δ (ppm): 171.8, (CO), 165.0, 161.6 (Cq acetazolamide), 153.9 (NCO, Cq arom.), 140.8 (Cq arom.), 130.3 (Cq arom.), 127.4 (CH arom.), 123.2, 123.1, 123.0, 122.9 (Cq arom., CH-triazole, CH arom.), 121.9 (CH arom.), 116.0 (Cq arom.), 100.3 (CH-acetal), 99.4 (CH arom.), 70.0 (CH_2), 68.9 (CH_2), 65.1 (CH_2), 52.4 (CH_2N), 52.0 (OCH_3), 49.9 (CH_2), 46.4 (CH_2Cl), 41.1 (CH), 34.0 (CH_2), 24.1 (2 CH_2), 19.1 (CH_3 , 2 diastereomers). Carbon peak corresponding to triazole quaternary carbon is not observed.

Synthesis of compound 34

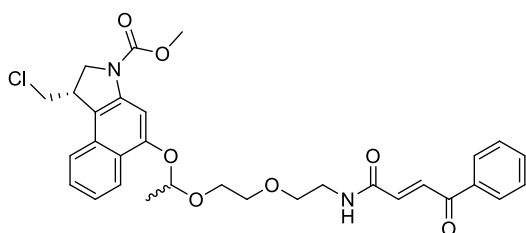


3-benzoyl acrylic acid (34mg, 0.19 mmol), was dissolved in dry DMF (1 mL) and cooled at -10 °C. To this solution IBCF (30 μ L, 0.23 mmol)

and NMM (25 μ L, 0.23 mmol) were added under stirring. Afterwards, a solution of **24** (23 mg, 0.078 mmol) in 0.5 mL of DMF was added and the reaction mixture was stirred for 15 minutes at -10 °C, then allowed to warm at room temperature. After 1.5 hours, the reaction mixture was directly concentrated under reduced pressure and purified by flash column chromatography on silica gel eluting with AcOEt:EtP (4:1) to give **34** as a light-yellow solid (17 mg, 48%). HRMS (ESI+): m/z calcd. for $C_{25}H_{26}NO_7$ $[M+H]^+$ 452.1709, found 452.1711. 1H NMR (400 MHz, CD_3OD) δ (ppm): 8.04 – 8.02 (m, 2H, H-Ph), 7.88 – 7.84 (m, 2H, H-4, $CH=CH$), 7.69 – 7.56 (m, 1H, H-Ph), 7.58 – 7.52 (m, 3H, H-5, H-Ph), 7.06 – 6.98 (m, 3H, H-8, H-6, $CH=CH$), 6.26 (d, $J=9.5$ Hz, 1H, H-3), 5.65 (q, $J=5.2$ Hz, 1H, H-acetal), 3.89 – 3.84 (m, 1H, OCH_2), 3.76 – 3.71 (m, 1H, OCH_2), 3.67 – 3.60 (m, 4H, CH_2 -PEG), 3.49 –

3.47 (m, 2H, CH₂NH), 1.53 (d, $J=5.2$ Hz, 3H, CH₃). ¹³C NMR (125 MHz, CD₃OD) δ (ppm): 190.0 (CO), 165.3 (CO amide), 161.8 (CO), 160.2 (Cq arom.), 155.4 (Cq arom.), 144.2 (C-4), 136.9 (Cq), 135.1 (CH=CH), 133.5 (CH-Ph), 132.6 (CH=CH), 129.0, 128.6, 128.4 (5C, 4 CH-Ph, C-5), 114.4 (C-6), 113.4 (Cq), 112.6 (C-3), 103.7 (C-8), 99.6 (C-acetal), 69.8, 68.8 (2C, OCH₂-PEG), 64.8 (OCH₂), 39.4 (CH₂NH), 18.7 (CH₃).

Synthesis of compound 35



3-benzoyl acrylic acid (60 mg, 0.35 mmol), was dissolved in dry DMF (1 mL) and cooled at -10 °C. To this solution IBCF (56 μ L, 0.43 mmol) and NMM (47 μ L, 0.43 mmol) were added under stirring. 0.28 mL of this solution

were added to a solution of **29** (16 mg, 0.038 mmol) in dry DMF, cooled at -10 °C. After 15 minutes, the reaction was allowed to warm at rt and kept stirring for 1.5 h. The crude reaction mixture was diluted with 20 mL of CH₂Cl₂ and washed with H₂O (20 mL). The organic phase was dried over Na₂SO₄, filtered and concentrated and the crude product was purified by column chromatography in CH₂Cl₂/acetone (20:1) to give **35** as a light-yellow solid (10 mg, 45%). HRMS (ESI+): m/z calcd. for C₃₁H₃₃ClN₂O₇Na [M+Na]⁺ 603.1869, found 603.1870. ¹H NMR (400 MHz, CD₃OD) δ (ppm): 8.20 (d, $J=8.5$ Hz, 1H, arom.), 8.02 – 7.99 (m, 2H, arom.), 7.87 – 7.81 (m, 2H, arom., CH=CH), 7.72 (t, $J=7.9$ Hz, 1H, arom.), 7.67 – 7.64 (m, 1H, arom.), 7.56 – 7.49 (m, 3H, arom.), 7.37 – 7.33 (m, 1H, CH=CH), 5.75 – 5.72 (m, H-acetal), 4.29 – 4.26 (m, 1H, CH₂N), 4.20 – 4.17 (m, CH₂N), 4.07 – 3.98 (m, 1H, CH), 3.96 – 3.90 (m, 5H, OCH₃, CH₂Cl, CH-PEG), 3.89 – 3.80 (m, 1H, CH-PEG), 3.78 – 3.67 (m, 5H, CH-PEG, CH₂Cl), 3.63 – 3.60 (m, 2H, CH₂N-amide), 1.63 (d, $J=5.2$ Hz, 3H, CH₃). ¹³C NMR (101 MHz, CD₃OD) δ (ppm): 190.0 (CO), 165.3 (Cq arom.), 153.9 (NCO, Cq arom.), 136.8 (Cq arom.), 135.1 (CH=CH, 2 diastereomers), 133.5 (CH arom.), 132.6, 132.5 (CH arom., 2 diastereomers), 130.3 (Cq arom.), 128.6, 128.4 (4 CH arom.), 127.4 (CH arom.), 123.2, 123.1 (CH arom. 2 diastereomers), 122.9 (CH arom.), 121.9 (CH arom.), 116.03 (Cq arom.), 100.5, 100.4 (CH-acetal, 2 diastereomer), 99.5, 99.4 (CH arom., 2 diastereomers), 69.9, 69.8, 68.9, 68.8 (2 CH₂, 2 diastereomers), 65.6, 65.4

(OCH₂, 2 diastereomers), 52.4 (CH₂N), 51.9 (OCH₃), 46.3 (CH₂Cl), 41.2 (CH), 39.4 (CH₂-N-amide), 19.2, 19.1 (CH₃, 2 diastereomers).

5.8.2 Stability studies

Determination of the hydrolytic rate constants by ¹H-NMR

Acetals **20**, **24** and **25** were dissolved in 540 μL NaPi buffer (0.1M, pH = 5.7) containing 60 μL of D₂O to a concentration of 16 mM. Reaction progress was monitored by ¹H NMR (400 MHz, D₂O) at 37 °C and through the integration of the signal of the methyl group at 1.55 ppm in the starting material or to the signal corresponding to the H-3 of umbelliferone.

Acetals **12**, **15** and **16** were dissolved in deuterated NaPi buffer (0.1 M, pH = 5.7) at a concentration of 14 mM. Reaction progress was monitored by ¹H NMR (400 MHz, D₂O) at 37 °C and through the integration of the signal of the methyl group at 1.55 ppm in the starting material or to the signal corresponding to the H-3 of umbelliferone. .

Coumarin release study by fluorescence emission

Acetal **20** was dissolved in CH₃CN to a final concentration of 20 mM. To evaluate the pH dependent release of fluorescent 7-hydroxy-coumarin, aliquots from the stock solution were diluted in phosphate buffer (0.1 M, pH 5.7), acetate buffer (0.1 M, pH = 5.0), or plasma (pH = 7.2, 20% human serum diluted in deionized H₂O) to a final 100 μM concentration. Then, the emission spectra were recorded every 24 h in a Jobin-Yvon Horiba Fluorolog 3-22 Tau-3 spectrofluorometer (for 7-hydroxy-coumarin: λ_{exc}=323 nm, λ_{em}=455 nm).

Stability studies of acetal **29** and SMDC **33**

Stability of the acetals **29** and **33** was assessed in human serum (pH = 7.2) and in acetate buffer (0.1 M, pH =5.7) at 37 °C. To this purpose, stock solutions (10 mM) of these acetals in DMSO were diluted in acetate buffer or in a 20% solution of human serum in water to a final concentration of 650 μM for **29** and 65 μM for acetal **33**. The solutions were incubated at 37°C and the amount of free duocarmycin **30** was determined by using Ultra Performance Liquid Chromatography-Mass Spectrometer (UPLC-MS) (Bruker micrOTOF-Q). Column:

ACQUITY UPLC BEH C18 1,7; diameter: 2.1 mm and length: 100 mm). The samples (60 μL of the acetal solution diluted with 600 μL of MeOH) were eluted following gradient: 1:99 to 60:40 $\text{CH}_3\text{CN}:\text{H}_2\text{O}$ for 6 min, then 60:40 to 100:0 $\text{CH}_3\text{CN}:\text{H}_2\text{O}$ over 0.5 minutes, with a flow of 0.45 mL/min.

5.8.3 Antibody Drug Conjugates synthesis and stability

Synthesis of ADC Thiomab-35

To an eppendorf with 23.5 μL of NaPi (20 mM, pH 7.0) and 2.78 μL of DMF, was added a 12.5 μL aliquot of a stock solution of Thiomab[®] LC-V205C (80 μM) and the resulting mixture was vortexed for 10 seconds. Afterwards, an 8.26 mM solution of compound **35** (1.2 μL , 10 equiv.) in DMF was added and the reaction mixed for 1 h at 37 °C. At each reaction time, a 10 μL aliquot was analyzed by LC-MS and conversion to the expected product was observed (calculated mass for the light chain, 24019 Da; observed mass for the light chain, 24017 Da; calculated non-modified heavy chain, 50594; observed mass for the heavy chain, 50587 and 50628 Da – oxidation states). Using 1 and 10 equiv. of the reagent the reaction was not complete after 2 h. To purify the ADC, small molecules were removed from the reaction mixture by loading the sample onto a Zeba Spin Desalting Column previously equilibrated with NaPi (20 mM, pH 7.0). The sample was eluted via centrifugation (2 min, 1500 xg). When the reaction was scaled up for in vitro studies, this procedure was followed by a dialysis to optimize the efficiency of the method. The sample was dialysed against 0.5 L of NaPi (20 mM, pH 7.0), stirring, overnight, at room temperature. The buffer solution was changed after 2 h. The following day, the buffer solution was changed once again. After 24 h, the sample was analysed by LC-MS and the concentration determined with a SpectraMax i3x.

Synthesis of ADC Thiomab-34

To an eppendorf with 32.5 μL of NaPi (20 mM, pH 7.0) and 4.4 μL of DMF, was added a 12.5 μL aliquot of a stock solution of Thiomab[®] LC-V205C (80 μM) and the resulting mixture was vortexed for 10 seconds. Afterwards, an 10 mM solution of compound **34** (0.6 μL , 6 equiv.) in DMF was added and the reaction mixed for 3 h at 37 °C, until >95% conversion to the expected product was observed by LC-MS analysis (calculated mass for the light chain, 23890 Da; observed mass for the light chain, 23898 Da). To purify

the ADC, small molecules were removed from the reaction mixture by loading the sample onto Amicon® Ultra Centrifuge filters with 10 kDa cut-off. The sample was eluted via centrifugation (2 min, 1500 xg) and the concentration was determined with a SpectraMax i3x.

Release of umbelliferone from Thiomab-34

A 20 µL aliquot of the bioconjugate Thiomab-34 (10 µM) in NaPi buffer (20 mM, pH 7.0) was thawed. 1 µL of reconstituted human plasma was added at room temperature and the resulting mixture vortexed for 10 seconds. The resulting reaction mixture was then stirred at 37 °C. Similarly, to determine the release of umbelliferone in acid condition, conjugate buffer was changed to NaPi (20 mM, pH 5.7) using Amicon® Ultra Centrifuge filters and the concentration adjusted at 10 µM. The resulting reaction mixtures were then stirred at 37 °C. After 24 hours, umbelliferone release was determined by measuring the fluorescence spectrum using a SpectraMax i3x plate reader (λ_{exc} 325 nm for free umbelliferone). To avoid interferences with fluorescence, proteic content was precipitated with 3-fold excess methanol, separated by centrifugation for 5 min at 14000 rcf and the fluorescence spectrum of free coumarin in solution was recorded.

Stability of Thiomab-35 in human serum.

A 20 µL aliquot of the bioconjugate Thiomab-35 (10 µM) in NaPi buffer (20 mM, pH 7.0) was thawed. 1 µL of reconstituted human plasma was added at room temperature and the resulting mixture vortexed for 10 seconds. The resulting reaction mixture was then mixed at 37 °C. After 2, 24 and 48 h, a 10 µL aliquot of each reaction mixture was analysed by LC-MS.

5.8.4 *In vitro* assays

Cell culture

SKRC52 (CAIX positive) and HEK293T (CAIX negative) cell line were used for the *in vitro* studies of SMDC 33, and two breast cancer cell lines were used to determine the cytotoxicity of conjugate Thiomab-35, namely SKBR3 (Her2 positive) and MDA-MB 231 cells (Her2 negative). SKBR3 and MB 231 cells were grown using 1x DMEM (Dulbecco's

modified Eagle medium) with Sodium Pyruvate and without L-Glutamine (Invitrogen, Life Technologies) supplemented with 10% heat-inactivated fetal bovine serum (FBS) (Gibco, Life Technologies), 1x MEM NEAA (Gibco, Life Technologies), 1x GlutaMAX (Gibco, Life Technologies), 200 units/mL penicillin and 200 µg/mL streptomycin (Gibco, Life Technologies) and 10 mM HEPES (Gibco, Life Technologies).

SKRC52 and HEK293T cells were routinely grown in a humidified incubator at 37 °C under 5% CO₂ and split before reaching confluence using TrypLE™ Express. Cells were grown on DMEM medium supplemented with 10% heat-inactivated FBS, 2 mM GlutaMAX™, 10 mM HEPES, 1% NEAA, 1 mM sodium pyruvate, 100 units/mL penicillin and 100 µg/mL streptomycin.

Cytotoxicity and IC₅₀ calculation

Cytotoxicity of acetal **33**, duocarmycin **30** and conjugate Thiomab-**35** was assessed using a CellTiter-Blue® Cell Viability Assay (Promega, USA), a fluorescent dye approach based on the ability of metabolically active cells to convert the dye resazurin to the fluorescent resorufin product. Briefly, cells were seeded at a concentration of 10 000 cells/well (100 µL) in flat-bottom 96 well-plates and allowed to adhere and adapt to the plates for 24 h. At this point, culture medium was exchanged to complete medium supplemented with increasing concentrations of each compound in technical triplicates. In the case of SKRC52 and HEK293T cell lines, plates were incubated for 72 hours. SKBR3 and MDA-MB 231 cells were incubated with ADC for 48 hours. After incubation, cell viability was assessed by exchanging the culture medium to medium supplemented with CellTiter-Blue Reagent (dilution 1:20 from commercial stock) and incubated for another 1 h 30 min, before analysis of fluorescence on an Infinite M200 (Tecan, USA) plate-reader ($\lambda_{exc}=560$, $\lambda_{em}=590$). Relative fluorescence units (R.L.U.) were normalized to the values obtained for the appropriate vehicle controls. Results are shown as average of 3 independent experiments. A sigmoidal curve (variable slope) was fitted to each dataset, using GraphPad Prism v6 software, and used to calculate the half-maximal inhibitory concentration (IC₅₀) for each compound.

Flow cytometry assays

Surface staining of Her-2 antigen on SKBR3 and MDA-MB231 cells.

Cells were cultured routinely as mentioned in earlier sections. On the day of experiment, cells were trypsinised and stained for the surface antigen Her-2. In brief, cells were incubated with ADCs Thiomab-**34** and Thiomab-**35** at 4 °C for 30 min. Cells were then washed with ice-cold PBS and the primary antibody was detected using a commercial Goat Alexa 647-conjugated anti-human (H+L) antibody (ThermoFischer Scientific). The samples were acquired using LSRFortessa™ flow cytometer (BD Biosciences, USA) with a 640 nm laser and a 670/41 band-pass filter (for APC detection). Data was analysed using FlowJo software and only single cell data is shown.

5.8.5 Molecular Dynamics simulations

The starting coordinates for the acetal fragments of conjugates Thiomab-**34** and Thiomab-**35** were generated and minimized with Chem3D (version 17). The crystal structure of the Fab of Thiomab LC V205C ® (PDB id: 5d6c)^[86] was used as starting coordinates for the antibody. MD simulations were performed with AMBER 18 package,^[82] implemented with ff14SB,^[83] and GAFF^[84] force fields. Parameters for the unnatural residues were generated with the antechamber module of AMBER, using GAFF force field and with partial charges set to fit the electrostatic potential generated with HF/6-31G(d) by RESP.^[87] The charges were calculated according to the Merz-Singh-Kollman scheme using Gaussian 16^[88] Each molecule was immersed in a water box with a 10 Å buffer of TIP3P water molecules.^[89] In the case of MD simulations performed on the conjugates, the system was neutralized by adding explicit counter ions (Cl⁻). A two-stage geometry optimization approach was performed. The first stage minimizes only the positions of solvent molecules and ions, and the second stage is an unrestrained minimization of all the atoms in the simulation cell. The systems were then heated by incrementing the temperature from 0 to 300 K under a constant pressure of 1 atm and periodic boundary conditions. Harmonic restraints of 10 kcal·mol⁻¹ were applied to the solute, and the Andersen temperature coupling scheme^[90] was used to control and equalize the temperature. The time step was kept at 1 fs during the heating stages, allowing potential inhomogeneities to self-adjust. Hydrogen atoms were kept fixed

through the simulations using the SHAKE algorithm.^[91] Long-range electrostatic effects were modelled using the particle-mesh-Ewald method.^[89] An 8 Å cutoff was applied to Lennard-Jones interactions. Each system was equilibrated for 2 ns with a 2-fs time step at a constant volume and temperature of 300 K. Production trajectories were then run for additional 500 ns under the same simulation conditions.

5.9 References

- [1] C. Roma-Rodrigues, R. Mendes, P. V Baptista, A. R. Fernandes, *Int. J. Mol. Sci.* **2019**, *20*, 840.
- [2] V. Salvatore, G. Teti, S. Focaroli, M. C. Mazzotti, A. Mazzotti, M. Falconi, *Oncotarget* **2016**, *8*, 9608–9616.
- [3] Y. Yuan, Y. Jiang, C. Sun, Q. Chen, *Oncol. Rep.* **2016**, *35*, 2499–2515.
- [4] H. Hamidi, J. Ivaska, *Nat. Rev. Cancer* **2018**, *18*, 533–548.
- [5] H. Tang, W. Zhao, J. Yu, Y. Li, C. Zhao, *Molecules* **2019**, *24*, 4–28.
- [6] M. G. Vander Heiden, L. C. Cantley, C. B. Thompson, *Science (80-.)*. **2009**, *324*, 1029–1033.
- [7] R. A. Gatenby, R. J. Gillies, *Nat. Rev. Cancer* **2004**, *4*, 891–899.
- [8] J. S. Burns, G. Manda, *Int. J. Mol. Sci.* **2017**, *18*, 2755–2783.
- [9] C. Corbet, O. Feron, *Nat. Rev. Cancer* **2017**, *17*, 577–593.
- [10] D. Neri, C. T. Supuran, *Nat. Rev. Drug Discov.* **2011**, *10*, 767–777.
- [11] B. A. Webb, M. Chimenti, M. P. Jacobson, D. L. Barber, *Nat. Rev. Cancer* **2011**, *11*, 671–677.
- [12] F. R. Maxfield, T. E. McGraw, *Nat. Rev. Mol. Cell Biol.* **2004**, *5*, 121–132.
- [13] J. R. Casey, S. Grinstein, J. Orłowski, *Nat. Rev. Mol. Cell Biol.* **2009**, *11*, 50–61.
- [14] I. Mellman, R. Fuchs, A. Helenius, *Annu. Rev. Biochem.* **1986**, *55*, 663–700.
- [15] K. D. Park, R. Liu, H. Kohn, *Chem. Biol.* **2009**, *16*, 763–772.
- [16] A. Dirksen, S. Yegneswaran, P. E. Dawson, *Angew. Chemie Int. Ed.* **2010**, *49*, 2023–2027.
- [17] E. R. Gillies, A. P. Goodwin, J. M. J. Fre, *Bioconjug. Chem.* **2004**, *15*, 1254–1263.
- [18] M. C. Finnis, S. Chu, Kevin, C. J. Bowerman, Z. A. Haroon, J. M. DeSimone, *Med. Chem. Commun.* **2014**, *5*, 1355–1358.
- [19] Q. Li, L. Gan, H. Tao, Q. Wang, L. Ye, A. Zhang, Z. Feng, *Carbohydr. Polym.* **2016**, *140*, 260–268.
- [20] L. Castañeda, A. Maruani, F. F. Schumacher, E. Miranda, V. Chudasama, K. A. Chester, J. R. Baker, E. B. Smith, S. Caddick, *Chem. Commun.* **2013**, *49*, 8187–8189.
- [21] Y. Tao, S. Liu, Y. Zhang, Z. Chi, J. Xu, *Polym. Chem.* **2018**, *9*, 878–884.
- [22] G. Leriche, M. Nothisen, N. Baumlin, C. D. Muller, D. Bagnard, J. Remy, S. A.

- Jacques, A. Wagner, *Bioconjug. Chem.* **2015**, *26*, 1461–1465.
- [23] I. Abdalla, J. Xu, D. Wang, H. Tong, B. Sun, B. Ding, X. Jiang, M. Zhu, *RSC Adv.* **2019**, *9*, 1814–1821.
- [24] T. Bai, D. Shao, J. Chen, Y. Li, B. Bin, J. Kong, *J. Colloid Interface Sci.* **2019**, *552*, 439–447.
- [25] G. Kocak, C. Tuncer, V. Bütün, *Polym. Chem.* **2017**, *8*, 144–176.
- [26] H. Ding, Y. Ma, *Sci. Rep.* **2013**, *3*, 2804–2810.
- [27] P. F. Bross, J. Beitz, G. Chen, X. H. Chen, E. Duffy, L. Kieffer, S. Roy, R. Sridhara, A. Rahman, G. Williams, et al., *Clin. cancer Res.* **2001**, *7*, 1490–1496.
- [28] P. R. Hamann, L. M. Hinman, I. Hollander, C. F. Beyer, D. Lindh, R. Holcomb, W. Hallett, H. Tsou, J. Upeslakis, D. Shochat, et al., *Bioconjug. Chem.* **2002**, *13*, 47–58.
- [29] E. Y. Jen, C.-W. Ko, J. E. Lee, P. L. Del Valle, A. Aydanian, C. Jewell, K. J. Norsworthy, D. Przepiorka, L. Nie, J. Liu, et al., *Clin. Cancer Res.* **2018**, *24*, 3242–3246.
- [30] P. R. Hamann, L. M. Hinman, C. F. Beyer, D. Lindh, J. Upeslakis, D. Shochat, A. Mountain, *Bioconjug. Chem.* **2005**, *16*, 354–360.
- [31] P. R. Hamann, L. M. Hinman, C. F. Beyer, L. M. Greenberger, C. Lin, D. Lindh, A. T. Menendez, R. Wallace, F. E. Durr, J. Upeslakis, *Bioconjug. Chem.* **2005**, *16*, 346–353.
- [32] Y. N. Lamb, *Drugs* **2017**, *77*, 1603–1610.
- [33] T. W. Greene, P. G. M. Wuts, *Greene's Protective Groups in Organic Synthesis*, John Wiley & Sons, Ltd, **1999**.
- [34] T. Mukai, M. Hagimori, K. Arimitsu, T. Katoh, M. Ukon, T. Kajimoto, H. Kimura, Y. Magata, E. Miyoshi, N. Taniguchi, et al., *Bioorganic Med. Chem.* **2011**, *19*, 4312–4321.
- [35] J. S. Yadav, D. Srinivas, G. S. Reddy, *Synth. Commun.* **1998**, *28*, 1399–1404.
- [36] J. M. Campelo, A. Garcia, F. Lafont, D. Luna, J. M. Marinas, *Synth. Commun.* **1994**, *24*, 1345–1350.
- [37] D. S. Brown, S. V. Ley, S. Vile, M. Thompson, *Tetrahedron* **1991**, *47*, 1329–1342.
- [38] N. M. Leonard, M. C. Oswald, D. A. Freiberg, B. A. Nattier, R. C. Smith, R. S. Mohan, *J. Org. Chem.* **2002**, *67*, 5202–5207.
- [39] Y. Zong, L. Yang, S. Tang, L. Li, W. Wang, B. Yuan, G. Yang, *Catalysts* **2018**, *8*, 48–57.

- [40] J. Grabowski, J. M. Granda, J. Jurczak, *Org. Biomol. Chem.* **2018**, *16*, 3114–3120.
- [41] E. H. Cordes, H. G. Bull, *Chem. Rev.* **1974**, *74*, 581–603.
- [42] M. M. Kreevoy, C. R. Morgan, R. W. Taft, *J. Am. Chem. Soc.* **1960**, *82*, 3064–3066.
- [43] B. Liu, S. Thayumanavan, *J. Am. Chem. Soc.* **2017**, *139*, 2306–2317.
- [44] B. J. Hong, A. J. Chipre, S. T. Nguyen, *J. Am. Chem. Soc.* **2013**, *135*, 17655–17658.
- [45] L. Cui, J. L. Cohen, C. K. Chu, P. R. Wich, P. H. Kierstead, J. M. J. Fréchet, *J. Am. Chem. Soc.* **2012**, *134*, 15840–15848.
- [46] R. A. Shenoi, J. K. Narayanannair, J. L. Hamilton, B. F. L. Lai, S. Horte, R. K. Kainthan, J. P. Varghese, K. G. Rajeev, M. Manoharan, J. N. Kizhakkedathu, *J. Am. Chem. Soc.* **2012**, *134*, 14945–14957.
- [47] M. J. Heffernan, N. Murthy, *Bioconjug. Chem.* **2005**, *16*, 1340–1342.
- [48] L. Wang, G. Liu, X. Wang, J. Hu, G. Zhang, S. Liu, *Macromolecules* **2015**, *48*, 7262–7272.
- [49] S. Guo, Y. Nakagawa, A. Barhoumi, W. Wang, C. Zhan, R. Tong, C. Santamaria, D. S. Kohane, *J. Am. Chem. Soc.* **2016**, *138*, 6127–6130.
- [50] A. J. Clark, M. E. Davis, *Proc. Natl. Acad. Sci.* **2015**, *112*, 1–6.
- [51] N. Sémiramoth, C. Di Meo, F. Zouhiri, F. Saïd-Hassane, S. Valetti, R. Gorges, V. Nicolas, J. H. Poupaert, S. Chollet-Martin, D. Desmaële, et al., *ACS Nano* **2012**, *6*, 3820–3831.
- [52] A. M. Walji, R. I. Sanchez, S. Clas, R. Nofsinger, M. D. L. Ruiz, J. Li, A. Bennet, C. John, D. J. Bennett, J. M. Sanders, et al., *ChemMedChem* **2015**, *10*, 245–252.
- [53] A. Mattarei, M. Azzolini, M. Carraro, N. Sassi, M. Zoratti, C. Paradisi, L. Biasutto, *Mol. Pharm.* **2013**, *10*, 2781–2792.
- [54] A. V Yurkovetskiy, M. Yin, N. Bodyak, C. A. Stevenson, J. D. Thomas, C. E. Hammond, L. Qin, B. Zhu, D. R. Gumerov, E. Ter-ovanesyan, et al., *Cancer Res.* **2015**, *75*, 3365–3372.
- [55] M. R. Junttila, W. Mao, X. Wang, B.-E. Wang, T. Pham, J. Flygare, S.-F. Yu, S. Yee, D. Goldenberg, C. Fields, et al., *Sci. Transl. Med.* **2015**, *7*, 314ra186.
- [56] I. R. Vlahov, C. P. Leamon, *Bioconjug. Chem.* **2012**, *23*, 1357–1369.
- [57] E. Jiménez-Moreno, Z. Guo, B. L. Oliveira, I. S. Albuquerque, A. Kitowski, A. Guerreiro, O. Boutureira, T. Rodrigues, G. Jiménez-Osés, G. J. L. Bernardes, *Angew. Chemie - Int. Ed.* **2017**, *56*, 243–247.

- [58] D. L. Boger, S. R. Brunette, R. M. Garbaccio, *J. Org. Chem.* **2001**, *66*, 5163–5173.
- [59] L. F. Tietze, K. Schmuck, H. J. Schuster, M. Müller, I. Schuberth, *Chem. – A Eur. J.* **2011**, *17*, 1922–1929.
- [60] L. F. Tietze, F. Major, I. Schuberth, *Angew. Chemie Int. Ed.* **2006**, *45*, 6574–6577.
- [61] H. J. Spijker, F. M. H. De Groot, M. M. C. Van Der Lee, R. Ubink, D. J. Van Den Dobbelen, D. F. Egging, W. H. A. Dokter, G. F. M. Verheijden, J. M. Lemmens, C. M. Timmers, et al., *Mol. Pharm.* **2015**, *12*, 1813–1835.
- [62] S. C. Jeffrey, M. Y. Torgov, J. B. Andreyka, L. Boddington, C. G. Cerveny, W. A. Denny, K. A. Gordon, D. Gustin, J. Haugen, T. Kline, et al., *J. Med. Chem.* **2005**, *48*, 1344–1358.
- [63] L. Long, L. Zhou, L. Wang, S. Meng, A. Gong, F. Du, C. Zhang, *Org. Biomol. Chem.* **2013**, *11*, 8214–8220.
- [64] F. L. Lin, H. M. Hoyt, H. van Halbeek, R. G. Bergman, C. R. Bertozzi, *J. Am. Chem. Soc.* **2005**, *127*, 2686–2695.
- [65] R. P. Lyon, T. D. Bovee, S. O. Doronina, P. J. Burke, J. H. Hunter, H. D. Neff-LaFord, M. Jonas, M. E. Anderson, J. R. Setter, P. D. Senter, *Nat. Biotechnol.* **2015**, *33*, 733–735.
- [66] Y. Zhao, D. G. Truhlar, *Theor. Chem. Acc.* **2008**, *120*, 215–241.
- [67] C. T. Supuran, *World J. Clin. Oncol.* **2012**, *3*, 98–103.
- [68] P. C. McDonald, J.-Y. Winum, C. T. Supuran, S. Dedhar, *Oncotarget* **2012**, *3*, 84–97.
- [69] H. M. Petrul, C. A. Schatz, C. C. Kopitz, L. Adnane, T. J. McCabe, P. Trail, S. Ha, Y. S. Chang, A. Voznesensky, G. Ranges, et al., *Ther. Discov.* **2012**, *11*, 340–350.
- [70] S. Cazzamalli, A. D. Corso, D. Neri, **2017**, *15*, 2926–2935.
- [71] N. Krall, F. Pretto, W. Decurtins, G. J. L. Bernardes, C. T. Supuran, D. Neri, *Angew. Chemie - Int. Ed.* **2014**, *53*, 4231–4235.
- [72] N. Krall, F. Pretto, M. Mattarella, D. Neri, *J. Nucl. Med.* **2017**, *57*, 943–950.
- [73] S. Cazzamalli, A. D. Corso, D. Neri, *J. Control. Release* **2017**, *246*, 39–45.
- [74] A. D. Corso, S. Cazzamalli, M. Mattarella, D. Neri, *Bioconjug. Chem.* **2017**, *28*, 1826–1833.
- [75] S. Cazzamalli, A. Dal Corso, D. Neri, *Mol. Cancer Ther.* **2016**, *15*, 2926–2935.
- [76] S. Cazzamalli, A. Dal Corso, F. Widmayer, D. Neri, *J. Am. Chem. Soc.* **2018**, *140*,

- 1617–1621.
- [77] F. Montemurro, *Lancet Oncol.* **2017**, *18*, 696–697.
- [78] I. Krop, E. P. Winer, *Clin. Cancer Res.* **2014**, *20*, 15–20.
- [79] J. R. Junutula, H. Raab, S. Clark, S. Bhakta, D. D. Leipold, S. Weir, Y. Chen, M. Simpson, S. P. Tsai, M. S. Dennis, et al., *Nat. Biotechnol.* **2008**, *26*, 925–932.
- [80] M. J. Matos, C. Labão-Almeida, C. Sayers, O. Dada, M. Tacke, G. J. L. Bernardes, *Chemistry* **2018**, *24*, 12250–12253.
- [81] A. M. Freedy, M. J. Matos, O. Boutureira, F. Corzana, A. Guerreiro, P. Akkapeddi, V. J. Somovilla, T. Rodrigues, K. Nicholls, B. Xie, et al., *J. Am. Chem. Soc.* **2017**, *139*, 18365–18375.
- [82] D. A. Case, S. R. Brozell, D. S. Cerutti, V. W. Cheatham, T.E. III, Cruzeiro, T. A. Darden, R. E. Duke, D. Ghoreishi, H. Gohlke, A. W. Goetz, D. Greene, et al., *AMBER 2018*, University of California, San Francisco, **2018**.
- [83] J. A. Maier, C. Martinez, K. Kasavajhala, L. Wickstrom, K. E. Hauser, C. Simmerling, *J. Chem. Theory Comput.* **2015**, *11*, 3696–3713.
- [84] J. Wang, R. M. Wolf, J. W. Caldwell, P. A. Kollman, D. A. Case, *J. Comput. Chem.* **2004**, *25*, 1157–1174.
- [85] S. Arumugam, V. V. Popik, *J. Am. Chem. Soc.* **2011**, *133*, 15730–15736.
- [86] S. M. Lehar, T. Pillow, M. Xu, L. Staben, K. K. Kajihara, R. Vandlen, L. DePalatis, H. Raab, W. L. Hazenbos, J. Hiroshi Morisaki, et al., *Nature* **2015**, *527*, 323.
- [87] C. I. Bayly, P. Cieplak, W. Cornell, P. A. Kollman, *J. Phys. Chem.* **1993**, *97*, 10269–10280.
- [88] M. J. Frisch, G. W. Trucks, H. B. Schlegel, G. E. Scuseria, M. A. Robb, G. Cheeseman, J. R. Scalmani, V. Barone, G. A. Petersson, H. Nakatsuji, X. Li, et al., -, CT, Wallingford, **2016**.
- [89] W. L. Jorgensen, J. Chandrasekhar, J. D. Madura, R. W. Impey, M. L. Klein, *J. Chem. Phys.* **1983**, *79*, 926–935.
- [90] H. C. Andersen, *J. Chem. Phys.* **1980**, *72*, 2384–2393.
- [91] S. Miyamoto, P. A. Kollman, *J. Comput. Chem.* **1992**, *13*, 952–962.

Grob fragmentation for the controlled release of drugs

6.1 Introduction

6.1.1 Fragmentations reactions: the Grob fragmentation

6.1.2 Background and main goals

6.2 Substrate screening for Grob fragmentation

6.2.1 Synthesis of Grob fragmentation substrates

6.2.2 Study of the reactions under biological conditions

6.3 Application to the controlled release of Crizotinib

6.3.1 Synthesis of Grob fragmentation scaffold with cathepsin B triggered release for conjugation with antibodies

6.4 Conclusions

6.5 Experimental section

6.5.1 Synthesis

6.5.2 NMR study of the Grob fragmentation

6.5.3 UPLC release of crizotinib derivative from **67** and **68**

6.6 References

6.1 Introduction

Self-immolative spacers are compounds able to self-degrade spontaneously and irreversibly. The process is governed by an entropy increase and by the formation of thermodynamically stable products. In order to avoid uncontrolled self-immolation process, the reactive group of such compounds (the one that 'starts' the immolation process) is 'blocked' with a protecting group. Upon specific stimulation, the active function is deprotected and the self-immolative process can occur (**Figure 6.1**).^[1-3] These compounds have experienced increasing interest in the last years, especially for applications in drug delivery and controlled release.



Figure 6.1: schematic representation of a self-immolative process. The removal of the protecting (PG, red) triggers the release of the active molecule (shown in cyano), after self-immolation of the spacer (grey).

Regarding the structures and the self-immolation mechanisms of such spacers, most of them are based on two processes: the active molecule can be formed as a result of an electronic cascade process, or disassembly can be caused by an intramolecular cyclization reaction driven by the formation of highly stable five membered or six membered rings.^[4]

Aromatic systems bearing an amino,^[5] hydroxy,^[6] or thiol^[7] substitution belong to the first class of compounds. After deprotection, that can be promoted by enzymes^[8-13] or chemical reagents,^[14-18] the free nucleophile triggers the electronic cascade and the leaving group is released. *Para*- or *ortho*-substituted benzyl alcohols present this type of reactivity (1,4-elimination process)^[19] but also cinnamyl alcohols (1,6-elimination process)^[20,21] or coumarinyl alcohols (1,8-elimination process that allows real time monitorisation of the release)^[22] follow the same self-immolative pathway (**Figure 6.2**). The nature of the leaving group influences the kinetic of the entire elimination process: for example, substitution of an ether with a carbamate or carbonate significantly increases the reaction rate. In this latter case, the formation of a stable by-product, such as CO₂ enhances the kinetic of the whole process. Also, temperature, pH

and nature of the solvent have effects on the drug release.^[1] Recently, it has been shown that quaternary amines act as leaving group when coupled to *para*-amino benzyl alcohol spacer, allowing the release of drugs bearing a tertiary amine group.^[23]

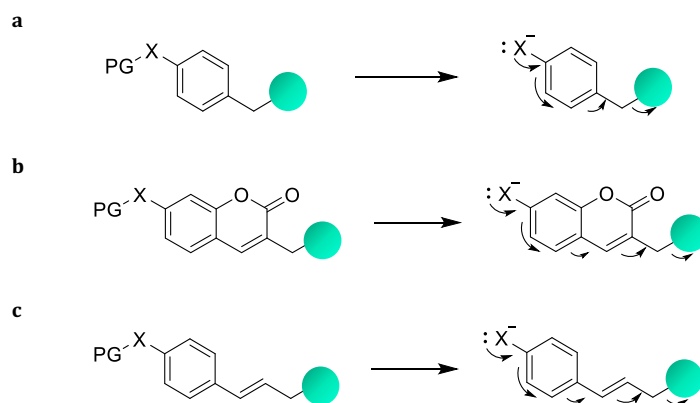


Figure 6.2: self-elimination by electronic cascade; a) benzyl alcohol-based structures; b) coumarinyl alcohol derivatives; c) cinnamyl alcohol derivatives. Leaving group is represented by coloured circles; X = NH, O, S.

Regarding the cyclization mediated release, it occurs on alkyl chains adequately substituted (i.e., a nucleophile group at suitable distance from an ester or a carbonate). Moreover, aromatic systems *ortho*-disubstituted can undergo cyclization and subsequent leaving group liberation.^[24,25] Cyclization can occur directly after activation and protecting group removal, or after a previous elimination process (**Figure 6.3**).^[26] Normally, this type of processes are slower than the elimination cascades,^[27] but they can be used to gain stability or to improve the linkage of the drug according to its functional groups.

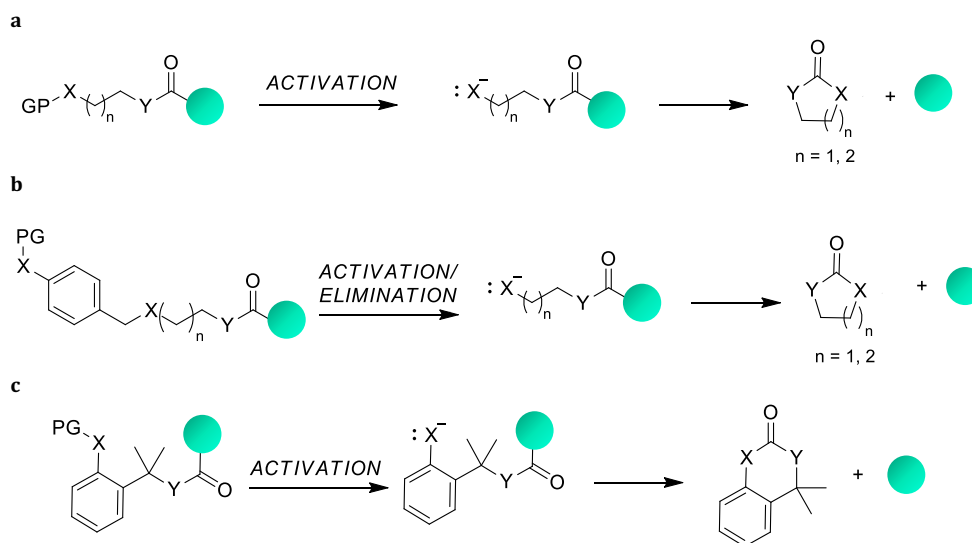


Figure 6.3: intramolecular cyclization mediated release. X = NH, O, S.

Both elimination and intramolecular cyclization processes have been widely applied in the field of drug controlled release,^[28] generation of pro-drugs^[29] and in the field of degradable polymers as new materials.^[4,30-33] In most cases, the spacer is fundamental for an efficient activation and optimal release.

As an example, most antibody drug conjugates relies on *para*-aminobenzyl alcohol spacer for intracellular liberation of the drug.^[34-37] This linker is often combined with a dipeptide (mainly, valine-citrulline) recognized by intracellular cathepsins. In this application, the spacer between the linker and the drug is necessary to allow enzymatic cleavage, that otherwise is prevented by steric hindrance. In fact, it has been shown that direct attachment of the drug doxorubicin to several enzymatically labile dipeptides does not produce drug release after treatment with Cathepsin B.^[38]

In the case of polymers, a high number of self-immolative spacer are assembled in a linear^[39] or branched way^[40] to allow multiple drug release.

Furthermore, combination of two or more self-immolative spacers has been used in the development of pro-drugs or ADCs. The improvement of the release of the drug from these structures is attributed to a better enzymatic activation, due to a facilitated recognition.^[41]

6.1.1 Fragmentations reactions: the Grob fragmentation

Fragmentations reactions are specific transformations that result in the cleavage of a C-C bond in an alkyl chain.^[42] According to Grob definition, a heterolytic fragmentation is an organic reaction occurring in substrates presenting a specific dispositions of carbon and heteroatoms (as O, N, S, P and halogens). Such structure is cleaved in three fragments following a specific mechanism.

Substrates that can undergo fragmentation are 1,3-substituted chain bearing heteroatoms at positions 1 and 3 (**Figure 6.4**)^[43,44]: X is a pushing residue, featuring a negative charge or a lone pair of electrons, and Y is a leaving group or a group that can accommodate the negative charge (pulling group).

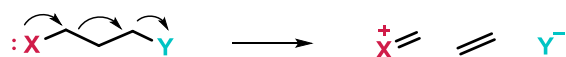
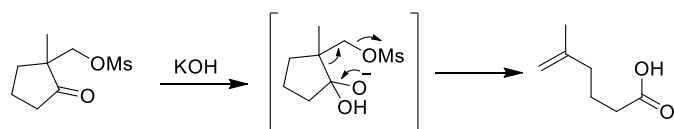


Figure 6.4: general fragmentation mechanism on 1,3-hetero-disubstituted substrates; X represents a generic atom with a negative charge or a lone pair of electrons, while Y is the leaving group or a group that can accommodate the negative charge.

Amines and alcohols are among the most typical groups that can trigger the fragmentation reaction, while halogens, sulfonates and quaternized amines are the most typical leaving groups used.

Eschenmoser described the first example of such type of reactivity in 1952. He observed the ring opening reaction of a substituted β -hydroxy ketone under basic conditions (**Scheme 6.1**).^[45]



Scheme 6.1: first example of fragmentation reported by Eschenmoser.

After his pioneer work, the investigation of Grob's group greatly contributed to the development of the reaction by understanding the fragmentation mechanism.

The reaction could occur through three different mechanisms: a two-step ion mechanism that can be cationic (**Figure 6.5 a**) or anionic (**Figure 6.5 c**), and a

synchronous mechanism (**Figure 6.5 b**), in which double bonds are formed concurrently with the cleavage of the C-C and C-X bonds.

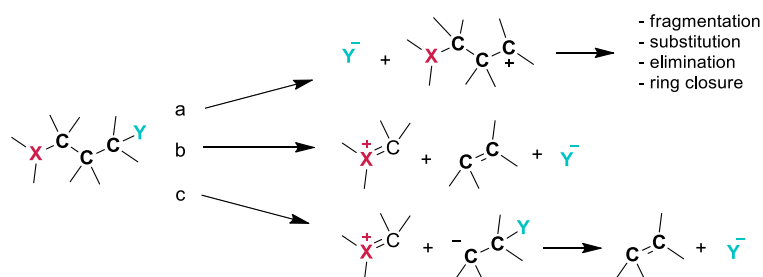
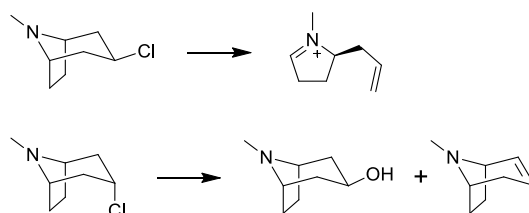


Figure 6.5: mechanisms proposed for the fragmentation.

Fragmentation may occur consequently in all these pathways; however, in the two step processes competitive reactivity may interfere with the fragmentation. Hydrolysis, ring closure reaction and elimination may occur as well. On the contrary, if the reaction goes through the synchronous mechanism the fragmentation is the only route.^[44] The concerted mechanism needs some stereo-electronic requirements to be fulfilled. More precisely, it operates only when both the orbital containing the lone pair of X and the C-Y bond are *anti* periplanar to the C-C bond that will be cleaved. As an example, Grob studied the different reactivity of 3-*exo* and 3-*endo* chlorotropanes. In the *exo* compound, the stereo-electronic requirements are met, and the reaction follows the synchronous mechanism to give quantitative fragmentation. On the contrary, in the *endo* epimer, alternative pathways led to the elimination and hydrolysis product (**Scheme 6.2**).^[46] As expected, the kinetic rate of the reaction is much lower in this case.



Scheme 6.2: reactivity of chlorotropane derivatives.

In general, Grob fragmentation have found wide application in synthetic organic chemistry. It has been applied to the synthesis of highly demanding macrocyclic structures,^[47-49] for ring opening reaction,^[50] as a key step in the total synthesis of natural compounds.^[51-54] According to the reaction mechanism, fragmentation is favoured under basic condition, but also variations in acid conditions have been developed.^[55] Synthetic modifications, including tandem reactions,^[56,57] or borane induced Grob fragmentation^[58,59] have been used and exploited for their synthetic versatility.

Interestingly, this fragmentation reaction could be useful for the development of new self-immolative spacers, which is the main goal of this chapter.

6.1.2 Background and main goals

As previously described, Grob fragmentation is an organic transformation that has proved wide utility in organic synthesis. Normally, the reactions are performed in organic solvent, at different temperatures and in presence of strong bases. Only in the first reports by Grob, fragmentation was studied in water as the main solvent, proving that the reaction proceeds also in aqueous systems. The studies on the fragmentation of 3-aminocyclohexanol derivatives showed that the *cis* isomers fragments in MeOH/H₂O at 50 °C. Under these conditions, the kinetic rate of the first order reaction was reported to be 2.94×10^{-4} , corresponding to a half-life of 39 minutes.^[60] More recently, a study on the solvolysis of 4-bromopiperidine via Grob fragmentation has been reported in water/organic solvents. The kinetic constant of the fragmentation has been determined in 30/70 MeOH/H₂O, in presence of NEt₃, and resulted to be $3.2 \cdot 10^{-4}$ (Figure 6.6).^[61]

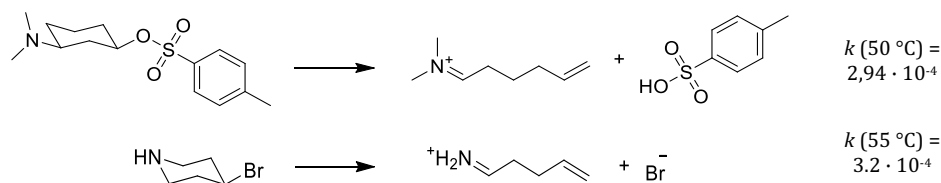


Figure 6.6: kinetic rate constants of solvolysis of 3-aminocyclohexanol derivative (top) and 4-bromo piperidine (bottom).

These previous results showed that the reaction can occur in H₂O as a solvent, but still the reaction conditions were not compatible with the typical biological ones (neutral pH and 37 °C). However, starting from these results, we envisaged in the Grob fragmentation an interesting methodology for the development of a new self-immolative spacer for drug delivery application.

The structures chosen to study the aforementioned reaction under biological conditions are reported in **Figure 6.7**. They all feature a secondary amine that acts as the pushing group, triggering the fragmentation reaction. Amines were preferred to alcohols due to the harsh conditions required in general to generate an alkoxide (such as strong bases), not compatible with biological systems. On the contrary, amines lone pair might be available at physiological pH, in a percentage that depends on its pK_a. Three-carbon chain separates the amine from the leaving group, which is a sulfonate. This is an excellent leaving group and can be found in small molecules, such as dyes, to increase their solubility. ^[62]

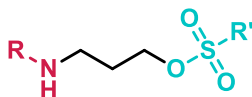


Figure 6.7: common structure of compounds studied in this chapter.

The reactivity of such compounds was studied to determine whether Grob fragmentation could be used as a new release mechanism for drug delivery application. This methodology could be an alternative to currently used self-immolative spacers, which rely on intramolecular cyclization reaction or electronic cascades for the liberation of the biologically active compound.

6.2 Substrate screening for Grob fragmentation

Several attempts were made in order to find the adequate compound that can give Grob fragmentation under physiological conditions. The minimal structure required for such fragmentation, as previously described, includes the presence of a pushing and a leaving group separated from a three-carbon atom chain. These minimal requirements are met in bicyclic nortropine derivatives, 3-aminocyclohexanol, and 3-aminopropanol structures (**Figure 6.8**).

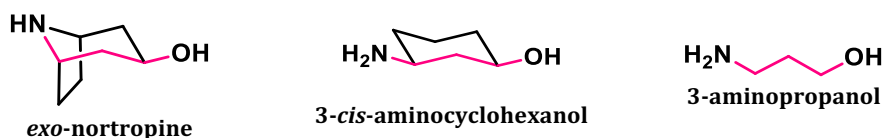


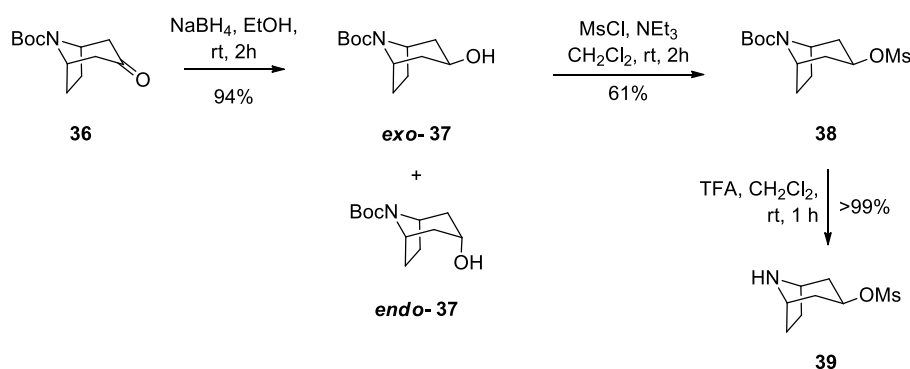
Figure 6.8: structures studied as substrate for Grob reaction.

Convenient modifications were introduced in those structures in order to transform the starting alcohol in a sulfonate, that acts as leaving group and reporter of the self-immolative fragmentation. After the synthesis, their reactivity was evaluated under biological mimicking conditions.

6.2.1 Synthesis of Grob fragmentation substrates

We started with modification of the nortropine ring to check whether Grob fragmentation is practicable under mild physiological conditions. In fact, while this structure is among the first examples reported by Grob in his work,^[46] due to its interesting reactivity in organic solvents as synthetic scaffold, no reports are focused on its reactivity in water or aqueous buffers.

Starting from commercially available *N*-Boc-nortropinone **36**, compound **39**, which presents the correct configuration of the substituents to undergo Grob fragmentation, was synthesized in three steps (**Scheme 6.3**).



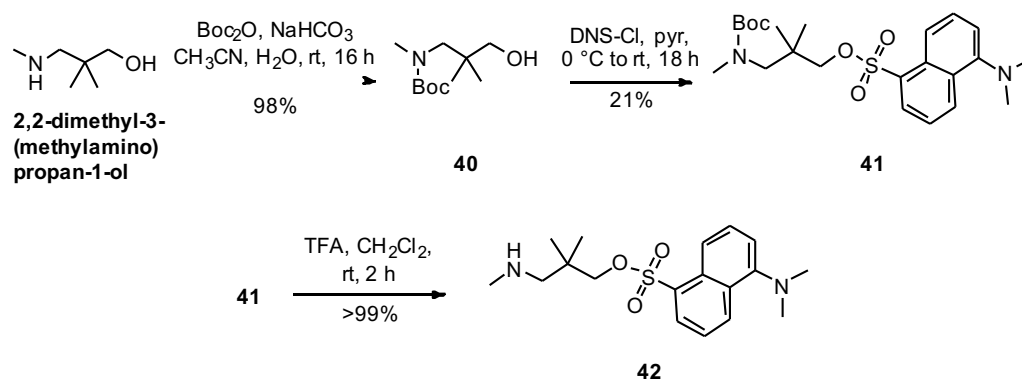
Scheme 6.3: Synthesis of nortropinone derivative **39** for Grob fragmentation; only the entire synthesis of *exo* isomer is reported, since it is the only substrate able to give the fragmentation reaction.

Compound **36** was treated with NaBH₄ in EtOH to obtain alcohol **37** as a 1:1 mixture of *endo* and *exo* isomers, which were separated by column chromatography.^[63] At this step, the assignation of the *endo* and *exo* compound was complicated by ¹H signals overlapping of H-3 and H-2 and 5, which complicates NOESY spectrum interpretation. Consequently, both compounds were transformed into their methanesulfonyl derivatives by treatment with MsCl and NEt₃, giving compound **38** in a moderate yield. At this point, NOESY studies were performed to determine which of the compounds corresponds to the *exo* isomer. Afterwards, the Boc group of compound **38** was removed by treatment with TFA in CH₂Cl₂ to obtain compound **39**.

Concerning the other structures tested (**Figure 6.8**), a similar synthetic pathway was followed. As a difference, the methanesulfonate was substituted by a dansyl sulfonate moiety as the leaving group. This modification was introduced because of the interesting features of dansyl sulfonate. Its fluorescent properties can lead to a product with potential biological application to monitor the release in cells or more complex systems. The determination for dansyl sulfonate release could be used to study Grob fragmentation reaction in cells. Moreover, to follow the reaction course by ¹H-NMR, the aromatic pattern of this group allows a more detailed study. Taking this into account, commercially available 3-amino-2,2-dimethylpropan-1-ol was conveniently modified. In this case, the presence of a primary amino group allowed the introduction of a second substituent that can modulate the pK_a of the amine, and consequently its protonation state and its reactivity, at physiological pH. Also, hydroxyl group can be easily transformed in the sulfonic ester derivative. In an attempt to increase the Grob reactivity, the 2,2 dimethyl derivative was chosen instead of the structurally easier 3-aminopropanol. In fact, considering the reaction mechanism,^[44] this compound would let to the formation of isobutylene as the resulting alkene. Such di-substituted olefin represents a more thermodynamically stable by-product than ethylene, favouring in this way the overall course of the reaction.

Taking these considerations into account, three different derivatives of 3-amino-2,2-dimethylpropan-1-ol were synthesized.

These structures were obtained in few steps, starting from commercially available 2,2-dimethyl-3-(methylamino)propan-1-ol or 2,2-dimethyl-3-aminopropan-1-ol as described in **Scheme 6.4** and **Scheme 6.5**.

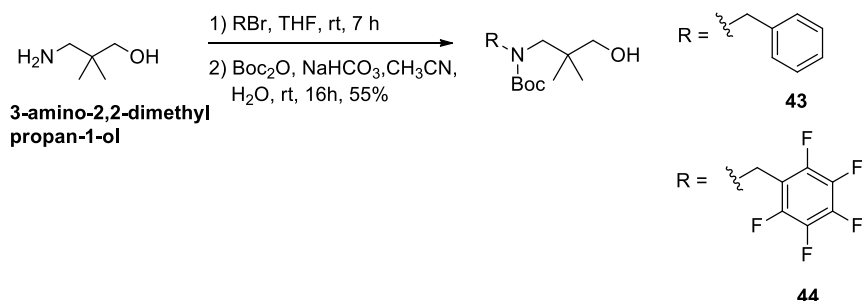


Scheme 6.4: synthesis of *N*-methylated derivative **42**.

2,2-dimethyl-3-(methylamino)propan-1-ol was conveniently protected as the corresponding Boc derivative under standard conditions, using Boc_2O and NaHCO_3 in $\text{CH}_3\text{CN}/\text{H}_2\text{O}$ solvent to obtain compound **40** quantitatively. This alcohol was readily transformed in the corresponding dansyl sulfonate using the appropriate dansyl sulfonyl chloride in pyridine in a rather low yield (21% yield). After removing the Boc group with TFA in CH_2Cl_2 , compound **42** was obtained without need for further purification.

Equally, benzylamine derivatives were obtained from the commercially available 2,2-dimethyl-3-(amino)propan-1-ol. We thought that by inserting a group able to lower the pK_a of the secondary amine, an improvement on the reaction rate would be observed. Benzylamine and pentafluorobenzyl amines were introduced at this purpose. In fact, benzylamines have one unit pK_a lower than other secondary amines (as an example: benzylamine pK_a is 9.33, while methylamine has a pK_a of 10.63 at 25°C).^[64] The presence of a fluorinated benzene ring would lower the basicity of the amine thanks to the electronegativity of fluorine atoms. Moreover, the introduction of fluorine it is well-known to be relevant in medicinal chemistry.^[65]

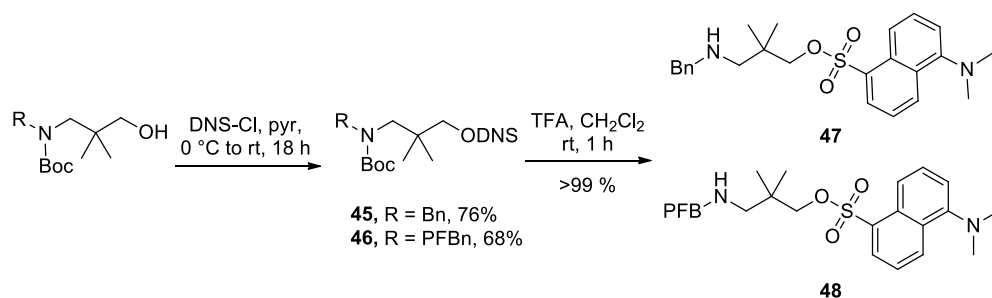
To obtain such structures, a similar synthetic pathway to what previously described was followed (**Scheme 6.5**).



Scheme 6.5: synthesis of protected secondary amines from 3-amino-2,2-dimethylpropan-1-ol.

First, secondary amines were obtained from commercially available amino-alcohols. Mono alkylation was achieved by treatment of excess amine with corresponding alkyl bromide to avoid undesired formation of tertiary amine. After 7 h at rt, the crude reaction mixture was analysed by NMR, revealing the effective formation of the desired mono alkylated product. Treatment of the crude with Boc₂O and NaHCO₃ allowed the protection of the secondary amine, as well as the quantitative recovery of 3-amino-2,2-dimethylpropan-1-ol as Boc protected carbamate (**Scheme 6.5**).

The subsequent transformation of the alcohol to the dansyl sulfonate derivative and the removal of the Boc group, following the conditions above described, afforded compounds **47** and **48** in overall good yield (76% and 68%, respectively, **Scheme 6.6**).



Scheme 6.6: synthesis of dansyl sulfonate derivatives **47** and **48**.

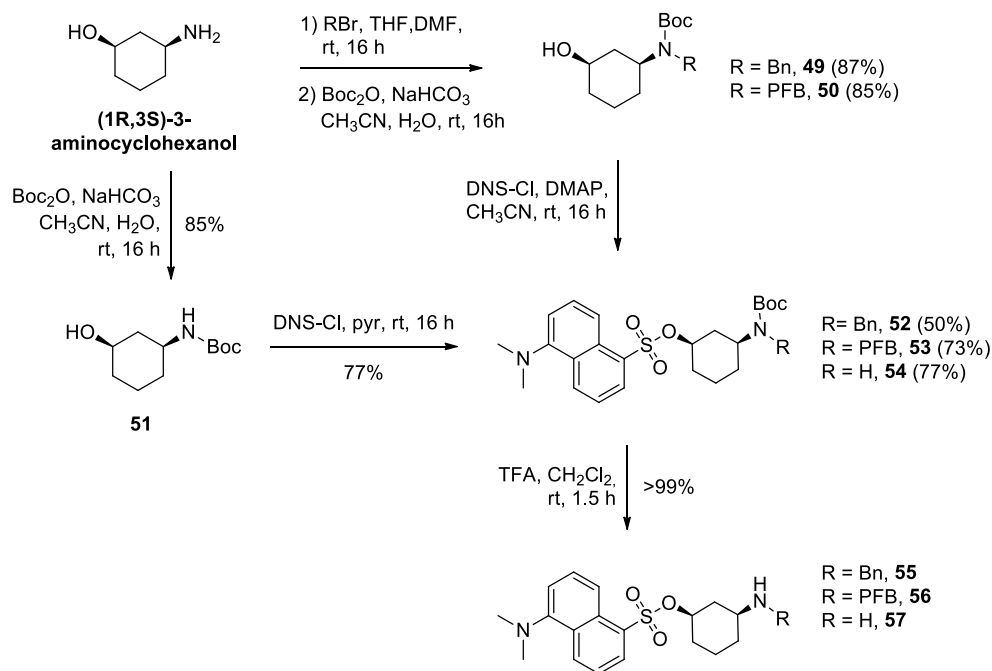
Incubation of compounds **42**, **47** and **48** in different buffers allowed the release of dansyl sulfonate, which acts as the leaving group. As will be later described, the release was induced by an intramolecular nucleophilic substitution, which is competitive with the Grob fragmentation in these structures.

To avoid this problem, a cyclic derivative, based on 3-amino-cyclohexanol scaffold, was synthesized. In this case, only the *cis* isomer displays the correct substituent disposition. In one hand, this compound allows the Grob fragmentation, in the other hand, the intramolecular nucleophilic substitution pathway is completely blocked due to the disposition of the substituents. Again, the presence of the primary amine allows modulation of the pK_a depending on the substituents previously introduced.

Because in the case of 3-amino-propanol derivatives, benzyl derivatives **47** and **48** exhibited a greater reactivity compared to methylamine **42**, we directly synthesized cyclic analogues bearing benzyl substituents, as reported in **Scheme 6.7**. Moreover, primary amine derivatives were synthesized, to check whether the absence of substituents on nitrogen eventually influences the Grob fragmentation pathway.

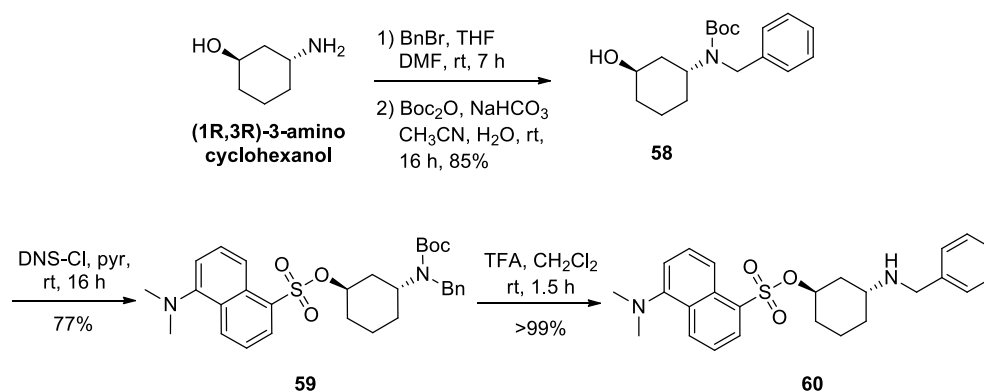
Therefore, protected secondary amines were obtained from 3-aminocyclohexanol in two steps with high yield to obtain compounds **49** and **50**. Instead, the protected primary amine was achieved directly by treating the starting material with Boc anhydride. Alcohols **49**, **50** and **51** were then converted to the dansyl sulfonate. For alcohol **51**, the conditions described above were successfully applied, giving, after treatment with dansyl chloride in pyridine, compound **54** with 77% yield. When the same conditions were applied to alcohols **49** and **50**, sulfonate esters **52** and **53** were obtained in poor yield (<10%). To obtain more amount of those compounds, sulfonate ester formation was achieved using dansyl chloride and DMAP acting both as catalyst and base, in CH_3CN as solvent. In this case, a cleaner product was obtained, with higher yield (50 % for compound **52** and 73% for compound **53** after purification by flash column chromatography) in both cases.

Removal of Boc yielded substrates **55**, **56** and **57** quantitatively (**Scheme 6.7**).



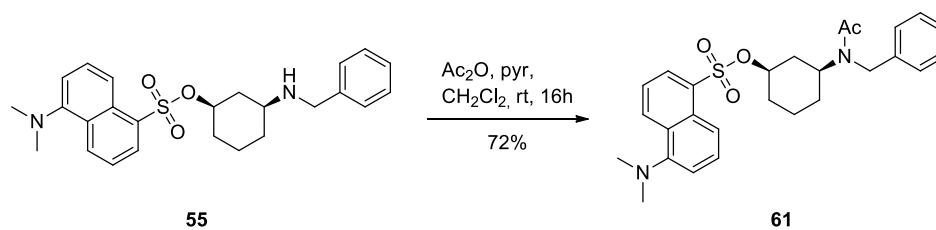
Scheme 6.7: synthesis of *cis*-3-amino cyclohexanol derivatives.

In order to confirm that the Grob fragmentation pathway is operating in the *cis* derivative, the *trans* isomer was also prepared. According to the Grob mechanism above explained, the fragmentation reaction is blocked due to an inappropriate orbital overlapping. Thus, *trans* analogue **60**, with the *N*-benzylamine, was synthesized as previously described for its analogue compound (**Scheme 6.8**).



Scheme 6.8: synthesis of *trans* cyclohexanol derivative.

The removal of the lone pair availability on the amine should block the fragmentation. To prove this hypothesis, derivative **55** was acetylated by treating it with pyridine and acetic anhydride in CH_2Cl_2 . After column purification, compound **61** was obtained in 72% yield (**Scheme 6.9**).



Scheme 6.9: synthesis of *N*-acetylated derivative **61**.

All compounds synthesized in this section were tested to determine whether they can undergo Grob fragmentation under mild conditions, mimicking typical biological ones.

6.2.2 Study of the reactions under biological conditions

In **Figure 6.9** the structures of the compounds tested in this section are shown. All of them present a three-carbon atom chain with the substituents in the appropriate disposition.

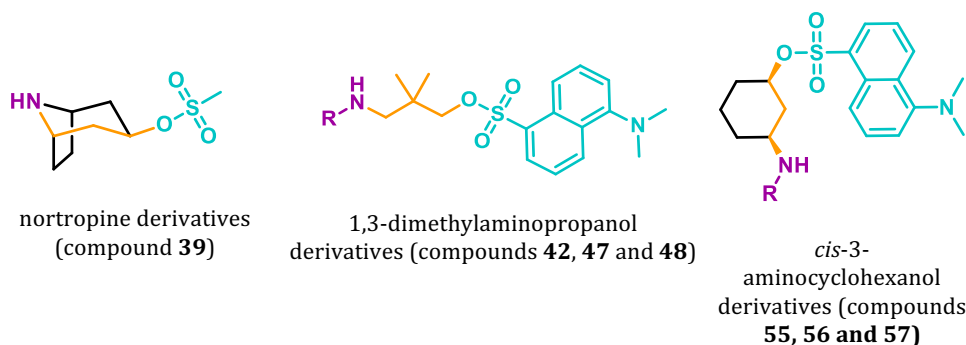


Figure 6.9: structures of the compounds tested. In yellow it is highlighted the three-carbon atom chain, in violet the nucleophile and in cyan the leaving group.

We started our study with compound **39**, which was incubated in mixtures MeOH and an aqueous buffer at different pH values. The buffers tested were PBS at pH 7.4 and NaPi buffers at pH 8.0 and pH 9.3. In those basic buffers the amine would be deprotonated in different percentages, suggesting that a different reactivity will be observed.

The reaction mixtures were incubated overnight at 37 °C. Afterwards, they were concentrated and a ^1H NMR of the crude was recorded.

While compound **39** is completely stable at pH 7.4, some fragmentation is observed at pH 8 and no starting material is observed at the highest pH 9.3, due to complete fragmentation. As an example, in **Figure 6.10** the NMRs deriving from overnight reaction in PBS and NaPi buffer at pH 8.0 are reported. While in the upper spectrum just clean starting material is observed, a more complex spectrum results from incubation at pH 8.0. While there is still starting material present (signals highlighted with blue dots), the typical terminal alkyne pattern is also observed (signals highlighted with green dots) between 5 and 6 ppm. These signals are indicative of the Grob fragmentation. Also, singlet of methanesulfonate is observable around 2.7 ppm (pink dot).

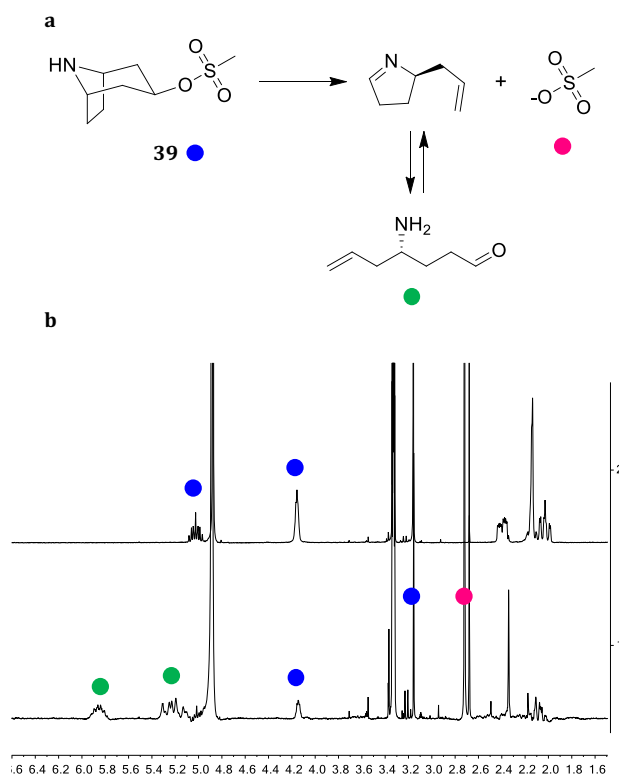


Figure 6.10: a) Grob fragmentation products obtained from compound **39**; b) $^1\text{H-NMR}$ of reaction of compound **39** in PBS buffer (upper panel) and in NaPi buffer (0.1 M, pH 8, lower panel).

Therefore, we can conclude that the reaction has a pH dependent profile and that this structure can undergo fragmentation to release, in this case, methanesulfonate. However, the reaction with structure **39** is not compatible with physiological conditions. In fact, the reaction occurs in aqueous systems at 37 °C, but only at pH > 8, which is not typically found in biological systems (if we exclude mitochondria, where pH can reach values as high as 8).^[66] Thus, the Grob substrate need to be improved by modulating the pK_a of the amine. Nortropine skeleton does not allow such structure tuning because the introduction of a substitution on nitrogen yields a tertiary amine that cannot be further functionalized as an amide or carbamate. This latter functionalization is essential to control the release *in vivo* properly.

For this reason, 3-aminopropanol derivatives were synthesized and studied. These compounds should be easy to functionalize and the free amine can be alkylated allowing modulation of its reactivity.

The reactivity of this compound was evaluated by $^1\text{H-NMR}$ spectroscopy, since it allows a better study and characterization of the products formed during the reaction.

Compounds **47**, **48** and **42** were incubated in deuterated buffer and CD_3OD to achieve complete solubility and $^1\text{H-NMR}$ spectra were recorded at different times, depending on the reaction rate. The buffers used for the study were PBS, NaPi pH 6 and NaPi pH 8. Starting from compound **42**, as expected its behaviour was similar to that of compound **39**. Dansyl sulfonate was released starting from pH 8.0, although in this case the reaction is faster to the previous compound. After 12 hours incubation in NaPi buffer at pH 8.0, > 95% of dansyl sulfonate was deconjugated. However, in PBS buffer, no reactivity was observed even after 20 hours incubation. Nevertheless, the reaction that produces the release of the living group is an intramolecular nucleophilic substitution and not the desired Grob fragmentation (**Figure 6.11 a**). Azetidine **62** by-product was observed both in $^1\text{H-NMR}$ spectra and by MS-ESI analysis of the reaction (**Figure 6.11 b** and **c**). The observed ring closing reaction could be due to the presence of a *gem*-disubstituted effect (Thorpe-Ingold effect) that forces the amino and sulfonate group to be close to each other.^[67] Notably, the intramolecular nucleophilic substitution is favoured, despite the formation of a highly tensioned 4-membered ring.

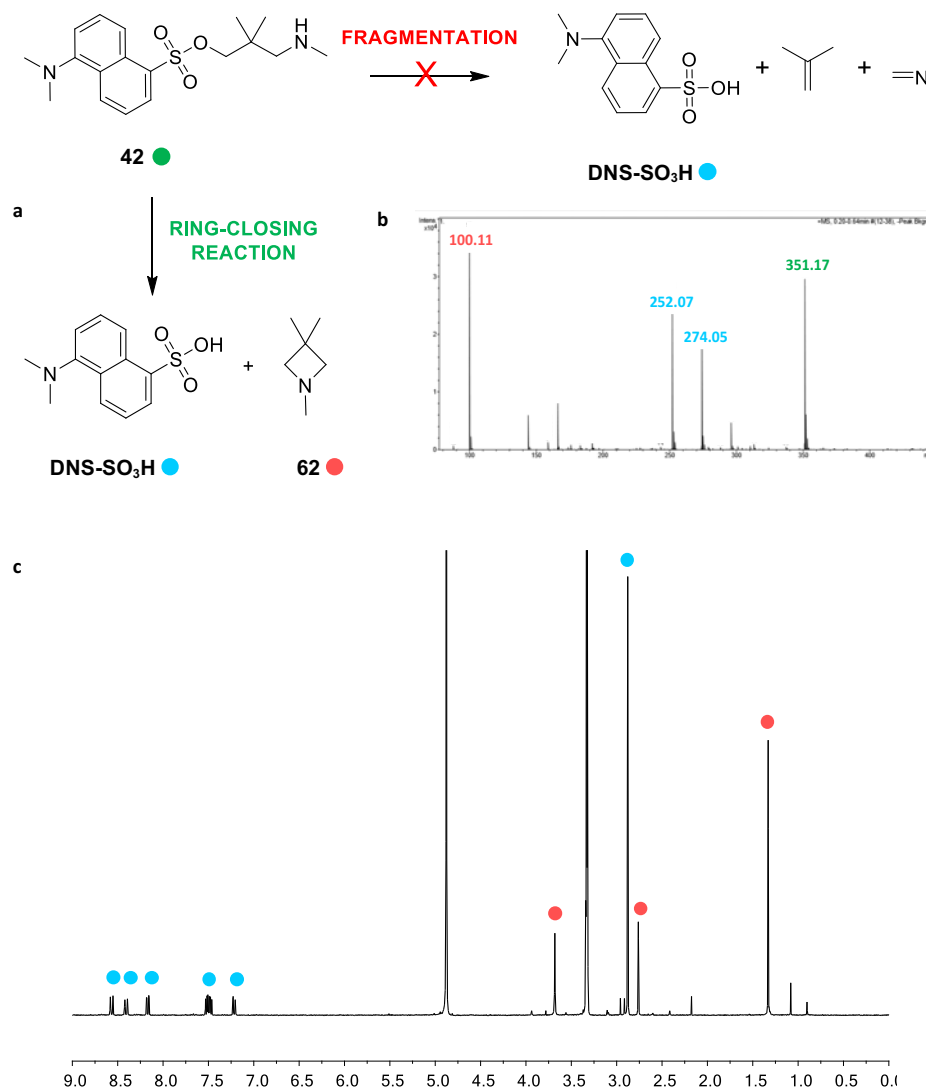


Figure 6.11: a) competitive reactions occurring on compound **42**; b) MS-ESI spectra of the reaction crude after 20 hours incubation in NaPi buffer (0.1 M, pH 8.0); c) ¹H-NMR spectrum of the reaction mixture, recorded in CD₃OD.

In an attempt to increase the reactivity of such substrates, by reducing the amount of protonated amine at neutral pH, and to prevent the intramolecular nucleophilic substitution by increasing the steric hindrance, benzyl and pentafluorobenzyl substituents were installed on the nitrogen atom (compounds **47** and **48**). The

behaviour of those compounds was studied in deuterated NaPi buffers at pH 8.0 and 6.0 and in PBS at pH 7.4. Both derivatives were able to release dansyl sulfonates in those buffers, even at pH 6.0, proving the positive effect of benzyl substituents on amino group reactivity. For example, at pH 6.0 almost complete release of the sulfonate was observed after 24 hours, as determined by $^1\text{H-NMR}$ spectroscopy for both compounds. For compound **48**, the reaction was complete in only 6 hours, even at pH 6.0, while for compound **47**, 20 hours were needed to complete the reaction. Despite the increased rate of dansyl sulfonate release, the introduced substitutions did not shift the reaction pathway towards the Grob fragmentation, and the release of the sulfonate was triggered by the intramolecular nucleophilic substitution. In fact, by $^1\text{H-NMR}$ it was clear the appearance of the signals of corresponding azetidines, together with dansyl sulfonate (**Figure 6.12**).

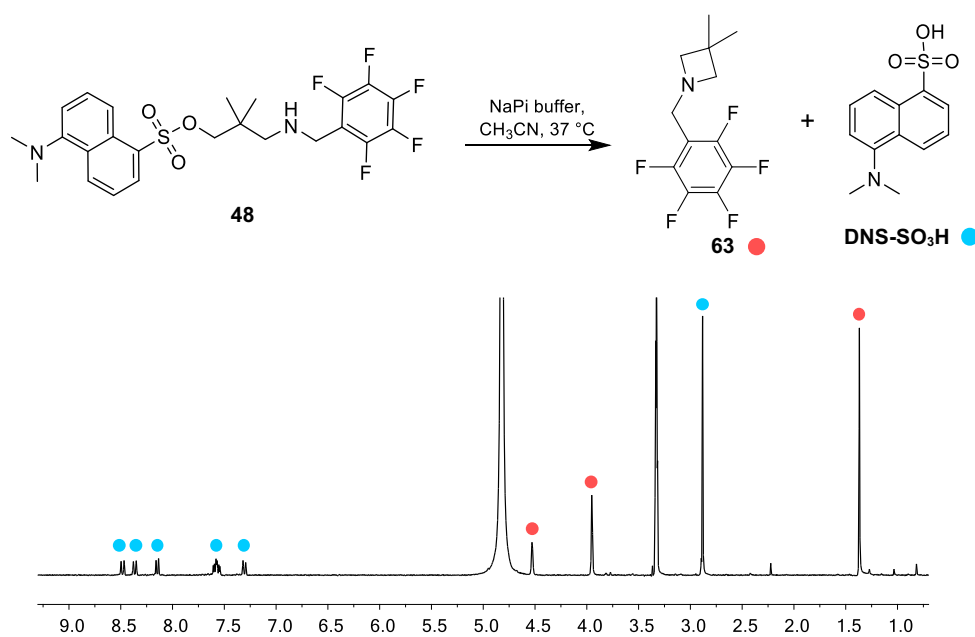


Figure 6.12: reaction pathway followed by compound **48**, incubated in CD₃OD/ deuterated NaPi buffer (0.1 M, pH 6.0) at 37 °C (top); $^1\text{H-NMR}$ of the reaction recorded at 300 MHz after 6 h incubations. Signals of azetidine **63** are observed between 1.0 and 4.5 ppm, and **DNS-SO₃H** is observed in the aromatic region. A similar behaviour is observed for analogue compound **47**.

These compounds do not represent the appropriate substrate for Grob fragmentation, but it can be interesting taking advantage of this fast cyclization reaction for the efficient

release of biologically interesting compounds. Moreover, these results showed how different reactivities could be obtained by carefully tuning the substituent. For example, the installation on the amine of groups that lower its pK_a could allow the reaction in slightly acidic conditions, as the ones encountered in tumour microenvironment and in some intracellular compartments.^[68]

To move towards the Grob fragmentation and avoid intramolecular nucleophilic substitution, cyclic analogues were synthesized, based on the structure of 3-aminocyclohexanol (**Figure 6.8**). The formation of a highly tensioned bicyclic compound, bearing both substituent in an equatorial position, would completely prevent the intramolecular nucleophilic substitution in these derivatives.

Reactivity of compounds **55**, **56** and **57** was then studied at different pH values. ^1H NMRs of these compounds were recorded at 0, 24 and 48 h of incubation, showing that compounds **55** and **56** undergo fragmentation of the cyclohexane skeleton allowing the release of the sulfonate.

^1H -NMR spectra of the reaction of compound **56** in deuterated PBS buffer (pH 7.4) is reported in **Figure 6.13**. The reaction was monitored at 0, 24 and 48 h of incubation. A zoom-in of the region between 5 and 10 ppm is reported, where the most important variation in the ^1H -NMR are observed.

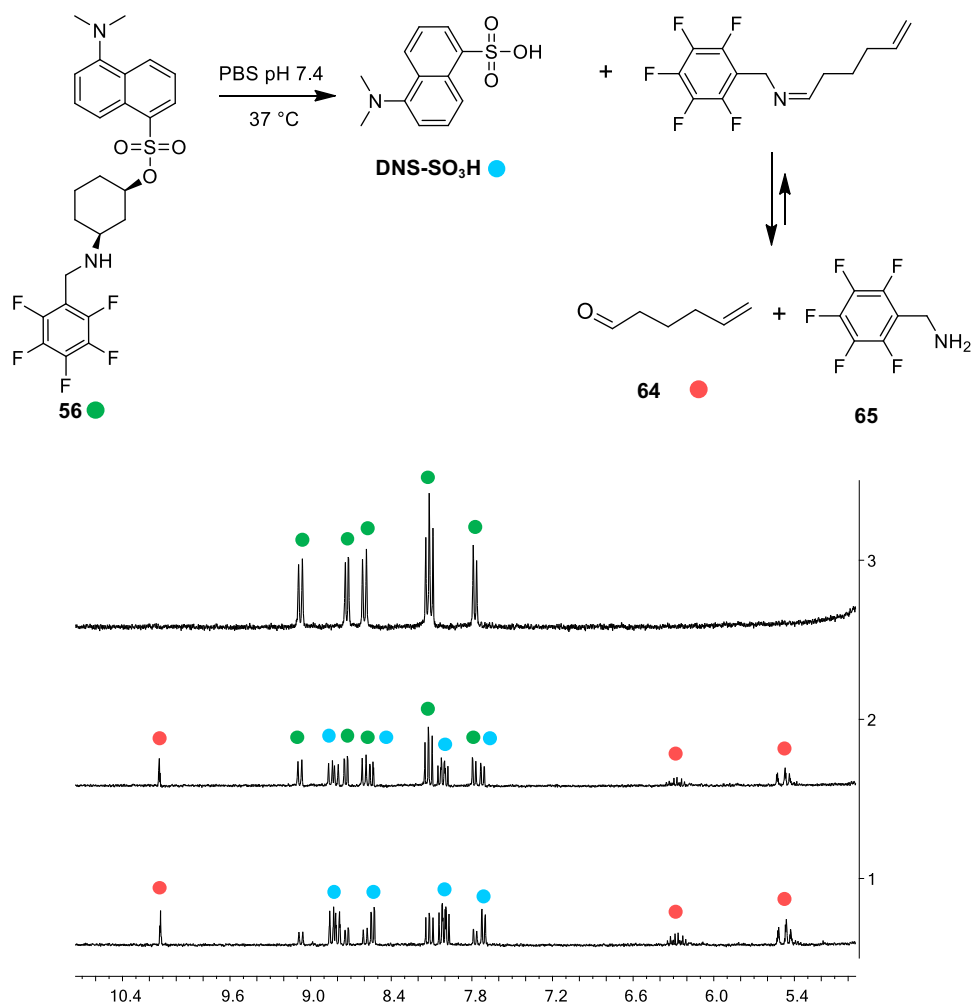


Figure 6.13: GroB fragmentation on compound **56** (top); NMRs of the reaction after 0, 24 and 48 hour-time incubation in deuterated PBS buffer (pH 7.4, bottom).

By analysing these ¹H-NMRs it is clear that the solvolysis of compound **56** is due to a fragmentation of cyclohexane ring. The peak at around 10.1 ppm can be clearly attributed to aldehyde **64**, resulting from the hydrolysis of the imine, which is the first product of the fragmentation. Also, new aromatic protons appear and correspond to dansyl sulfonic acid. In the region between 5 and 6 ppm it is observed the presence of a typical terminal alkene pattern, resulting from the cleavage of C-2 and C-1 bond.

Integration of the aromatic signals of dansyl sulfonate in the aromatic region can be used to determine the rate of the reaction. This integration is more accurate than

relying on other signals such the aldehyde proton, that might be in equilibrium with its hydrated form and the imine. In this case, 69% of dansyl sulfonate is released starting from compound **56** (-NHPFB) after 48 hours in PBS buffer. A similar reactivity is observed for compound **55** (-NHBn),

On the contrary, the compound **57** (with the primary amine, -NH₂) does not react through this route, being much more stable under the same conditions. This could be attributed to a higher pK_a of this primary amine.

Study of the reaction in buffers at different pHs displays the pH dependent profile of the reaction. If we compare the reactivity of the compounds in PBS at pH 7.4 and in NaPi buffer at pH 8.0 the amount of fragmentation products is more or less the same for the two benzylated compounds **55** and **56**. On the contrary, at pH 6.0 the amount of dansyl sulfonate released is lower for the two compounds, even if a significative release is still observed (**Figure 6.14**).

Compound **56** represents the more unstable compound under the conditions tested, due likely to its lower pK_a.

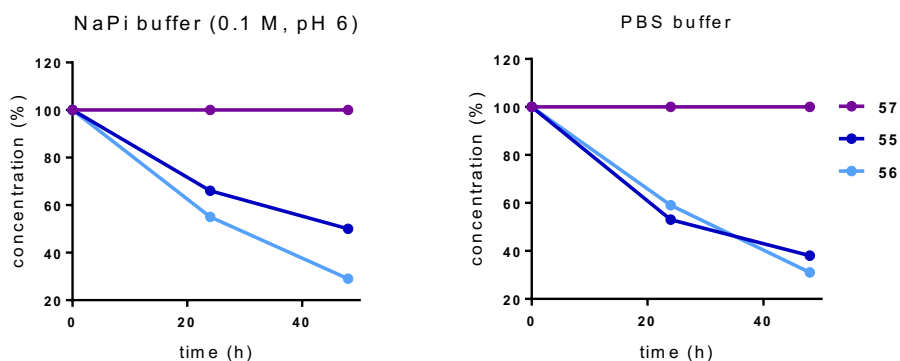


Figure 6.14: release of dansyl sulfonate from compounds **55** (NHBn), **56**(-NHPFB) and **57** (-NH₂).

As a control to determine if Grob fragmentation is the preferred reactivity pattern for this class of compound, analogue *trans*-3-aminocyclohexanol **60** was tested under the same conditions. Only the reactivity in PBS buffer (pH 7.4) was evaluated, since previous experiments showed that the isomer **55** was reactive in such reaction conditions.

The reactivity was evaluated again by NMR and as expected structure **60** was not able to give fragmentation under the same conditions. The ^1H NMR spectrum displays some changes between time 0 and time 48 hours (**Figure 6.15 a**). This can be due to some conformational equilibrium of the structure, that does not present a preferred conformation, or there might be some spontaneous hydrolysis. However, the Grob fragmentation is not observed, since peaks of the products deriving from this reaction are not observed here. This lack of reactivity of compound **60**, due to an incorrect orbital overlapping, suggests that in the other compounds Grob fragmentation was observed.

To develop a strategy that would allow the control of the Grob fragmentation *in vivo*, the stability of compound **61** (**Scheme 6.9**, -NAcBn) in PBS was evaluated. A priori, the formation of the amide bond would cause the delocalization of electron pair of the nitrogen, reducing or completely preventing the reactivity previously observed on compound **55**. Incubation of *N*-acetyl compound **61** in PBS showed that this compound is actually stable in PBS, suggesting that the formation of an amide could be a strategy to selectively block and control the Grob fragmentation. In fact, as observed in the NMR (**Figure 6.15 b**), after 48 hours incubation there is almost no modification of the aromatic region, suggesting that sulfonate is intact and this compound is stable. However, some new signals are appearing, probably due to spontaneous hydrolysis, but the release rate is significantly slower.

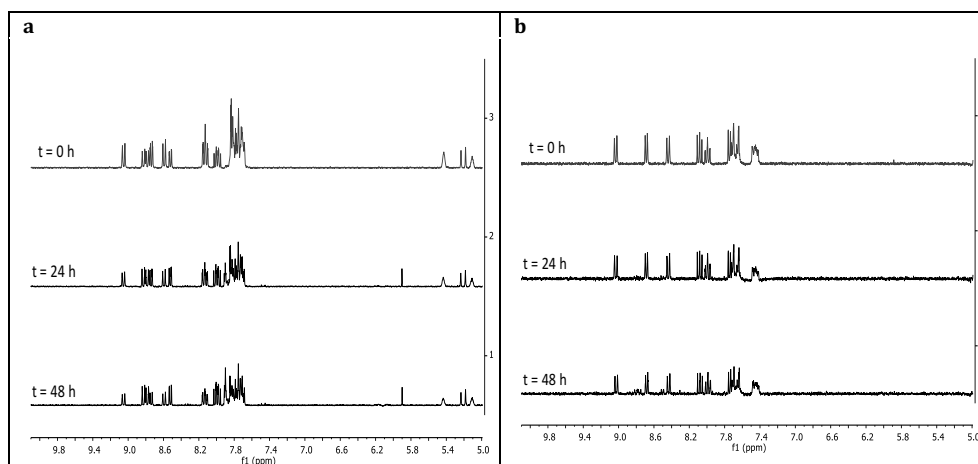


Figure 6.15: a) ^1H NMR of compound **60** incubated in CH_3CN and PBS buffer at 0, 24 and 48 h. b) stability of compound **61** in PBS buffer at 37 °C at 0, 24 and 48 h. In both cases, no peaks diagnostic of Grob fragmentation pathway, such as aldehyde and terminal double bond protons, are detected.

Therefore, it has been demonstrated that cyclohexanol structure is suitable for the controlled release of sulfonates via Grob fragmentation. Switching from the free amine to the amide or carbamate (we expect to have the same stability of the amide) decreases the rate of the reaction by completely blocking the fragmentation. In this way, a strategy to control the release was developed, and then it was applied to the release of a drug, as will be explained in the following section.

6.3 Application to the controlled release of Crizotinib

Compound **50** (for the synthesis see **Scheme 6.7**) was chosen as the starting material to synthesize the finale compound for controlled drug release via Grob fragmentation. As the drug will be released in form of the sulfonate derivative, Crizotinib was chosen as a model for this application. This drug has a nanomolar toxicity on several cancer cell lines by inhibiting phosphotyrosine kinases, such as c-MET, ALK and ROS1.^[69] It is important that the small variation that will be introduced in the structure of the drug does not affect its final toxic effect. In the case of Crizotinib, crystal structures of this compound bound to c-MET and ROS1 showed that in the recognition process 2-aminopyridine ring plays a pivotal role, while the piperidine ring stays out from the

binding pocket and exposed to the solvent (**Figure 6.16**).^[70,71] Therefore, introducing a small structural variation in this part of the molecule probably would not interfere with its properties as inhibitor and its toxicity.

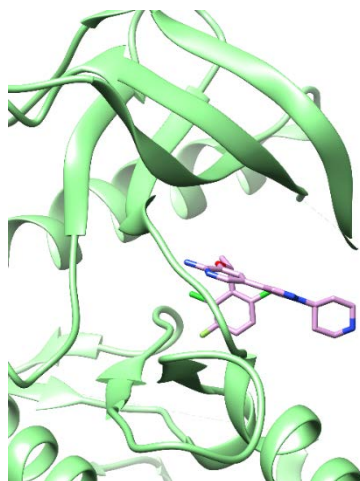
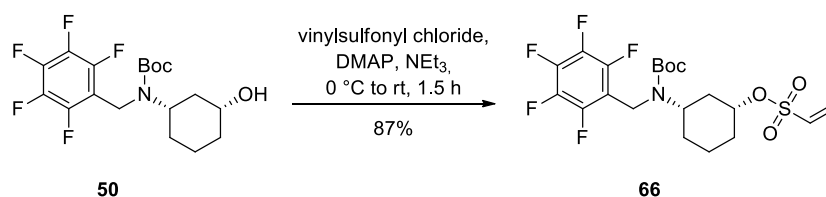


Figure 6.16: X-ray structure of Crizotinib bound to ROS1. The protein is shown as green ribbons and the ligand as sticks.

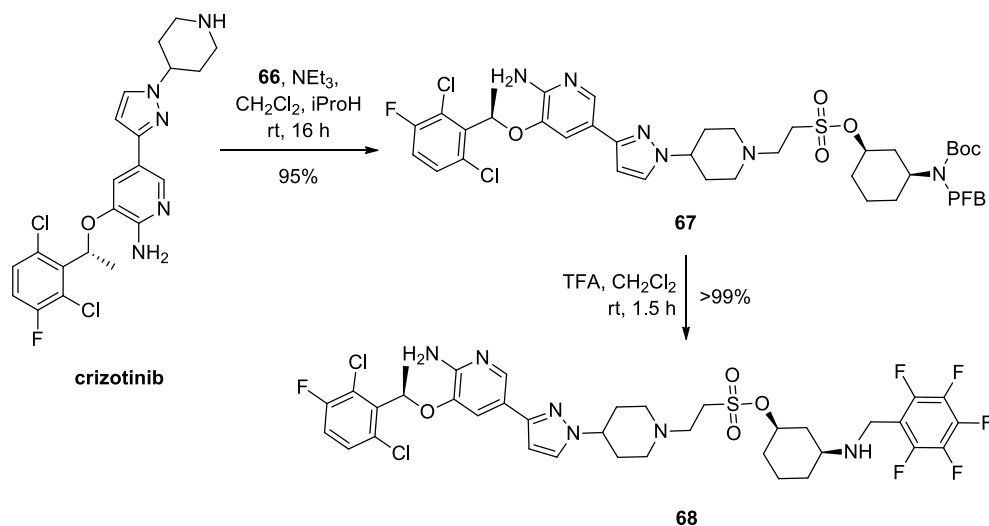
Moreover, Crizotinib is easy to functionalize, thanks to the reactivity of its piperidine ring. Our retro-synthetic strategy involved an aza-Michael addition of Crizotinib on a vinyl sulfonate, prepared in one step from precursor **50** (**Scheme 6.10**).

Alcohol **50** was transformed into the corresponding sulfonate using vinyl sulfonyl chloride, in presence of triethylamine and DMAP to catalyse the reaction. After purification, compound **66** was obtained in 87% yield. This transformation allowed the introduction in the Grob fragmentation scaffold of a highly reactive Michael acceptor.



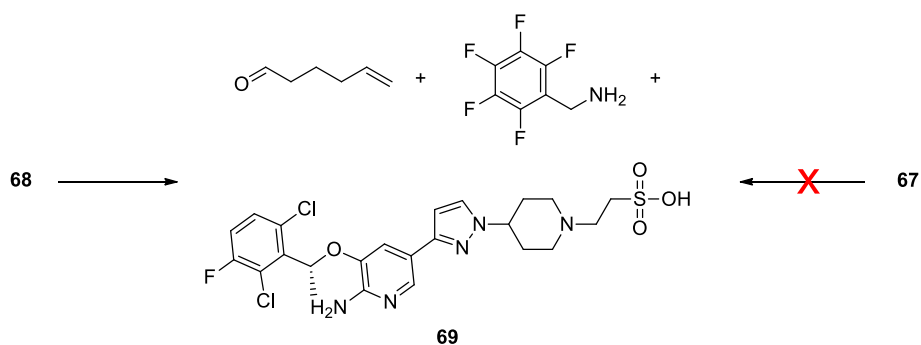
Scheme 6.10: synthesis of vinyl sulfonate **66** for Michael reaction with Crizotinib.

In fact, reaction of **66** with Crizotinib, in presence of catalytic amount of NEt_3 in a $\text{CH}_2\text{Cl}_2/\text{iPrOH}$ mixture yielded pure adduct **67** in excellent yield (95%) after purification by column chromatography. After removing the Boc protecting group, compound **68** was obtained in 99% yield and acts as the substrate for Grob fragmentation (**Scheme 6.11**).



Scheme 6.11: Synthesis of Crizotinib pro-drug releasable via Grob fragmentation.

Once obtained compound **68**, Crizotinib liberation was monitored by UPLC-MS. Both compound **67** and **68** were tested at this purpose. From this study, it is expected that derivative **68** would release sulfonate **69**, while the presence of the Boc carbamate in **67** would prevent the reaction (**Scheme 6.12**).



Scheme 6.12: release of Crizotinib analogue **69** from compound **67**.

To test this hypothesis, both compound **67** and **68** were incubated in PBS buffer at 37 °C and the solutions were analysed by UPLC to monitor liberation of dansyl sulfonate group. As expected, after 24 hours incubation, it was detected the release of sulfonate **69** from compound **68**, but not from compound **67** (**Figure 6.17**).

Regarding reactivity of compound **68**, comparing chromatograms registered directly after incubation, with the one registered after 24 hours incubation in PBS buffer at 37 °C, it is clear that peak at retention time 1.4, corresponding to compound **68** decreases. The peak increasing at retention time 1.3 corresponds to the released sulfonate **69**. Such peak is not detected in chromatograms with compound **67**, indicating that the Grob fragmentation cannot undergo as a consequence of amine protection.

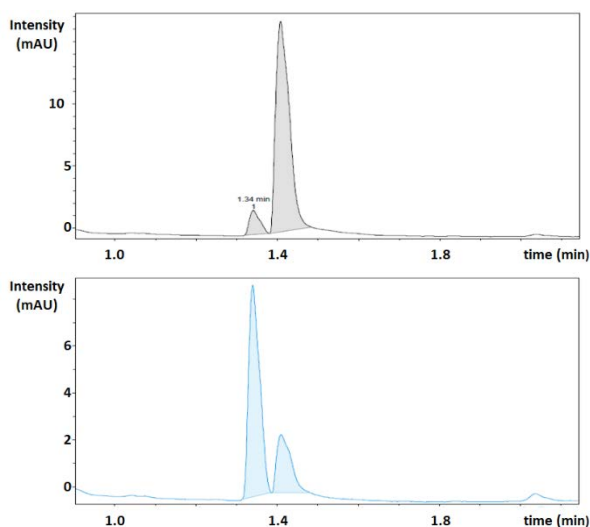


Figure 6.17: UPLC-UV chromatograms of the reaction of compound **68** in PBS buffer at 37 °C. In grey it is reported the chromatogram at time 0, in cyan it is represented the chromatogram after 24 hours incubation.

6.3.1 Synthesis of Grob fragmentation scaffold with cathepsin B triggered release for conjugation with antibodies

To apply the Grob fragmentation release strategy to the controlled liberation of drugs from antibodies, the synthesis of a suitable compound for ADC conjugation was designed. In order to obtain such structure, compound **70** was synthesized (**Figure 6.18**). This compound presents the carbonyl acrylamide tag for reaction with cysteine, Val-Cit dipeptide paired with the PABA and Grob fragmentation spacer for enzymatic triggered release and finally toxic Crizotinib as the active compound.

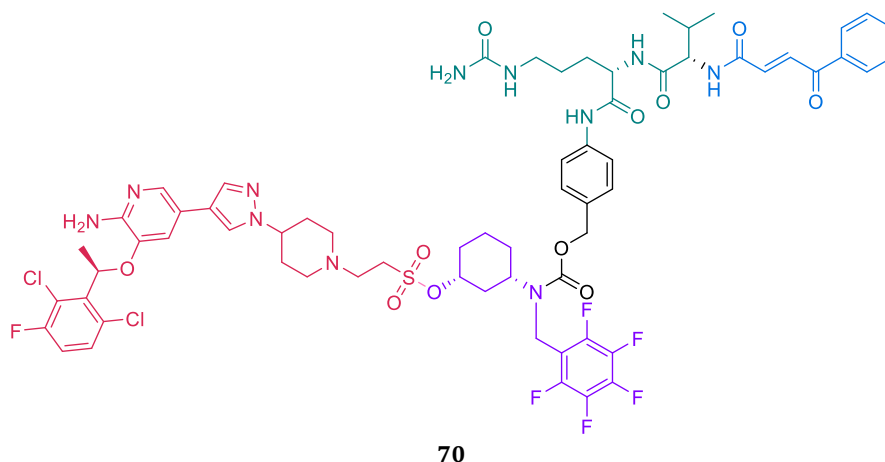
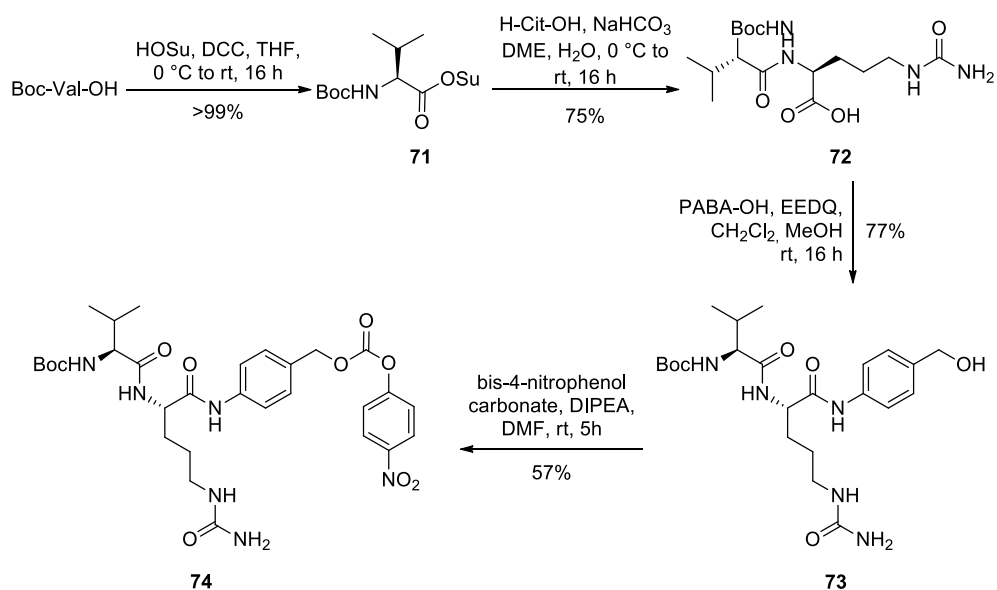


Figure 6.18: structure of the compound for ADC synthesis. Carbonyl acrylamide tag for reaction with cysteine is highlighted in blue. To trigger the release a Val-Cit linker is inserted (green) coupled with PABA (black) and Grob fragmentation (violet) self-immolative spacers. Crizotinib (red) serves as the active compound.

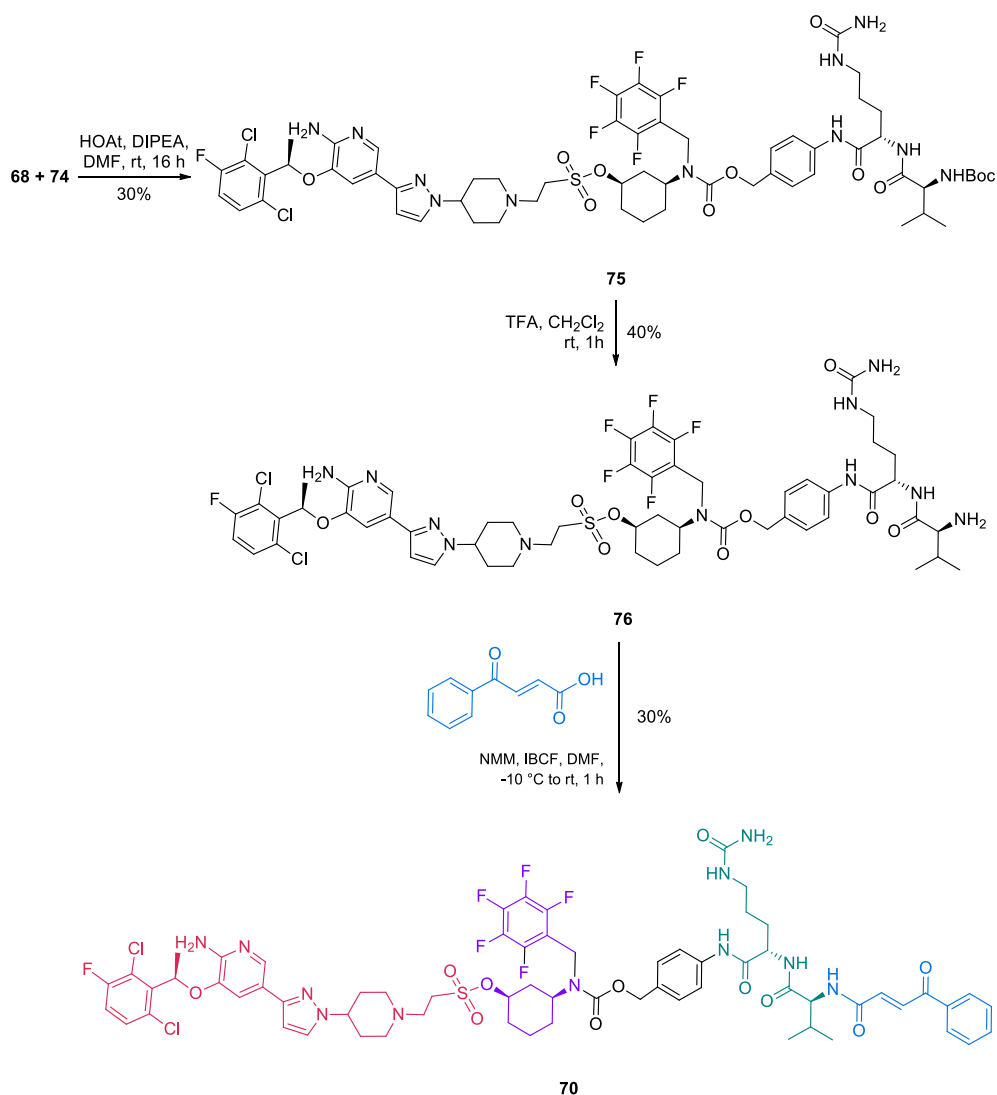
To obtain this compound, adequately activated valine-citrulline linker was synthesized. Starting from commercially available Boc protected valine, its carboxylic acid was activated as *N*-hydroxy succinimide ester using *N*-hydroxy succinimide (NHS) and *N,N'*-Dicyclohexylcarbodiimide (DCC) in tetrahydrofuran (THF) for 16 hours. Compound **71** was obtained in quantitative yield and then reacted with Citrulline using NaHCO_3 in DME and H_2O for 16 h. Thus, Boc protected dipeptide **72** was obtained in 75% yield. Free acid was then reacted with PABA-OH, using *N*-Ethoxycarbonyl-2-ethoxy-1,2-dihydroquinoline (EEDQ) as activating agent. For amide bond formation with citrulline it is important to use this coupling reagent since it avoids citrulline epimerization.^[72] As a result, compound **73** was obtained with 77% yield after purification by column chromatography. Alcohol was then activated as a 4-nitrophenol carbonate, by using bis-4-nitrophenol carbonate and DIPEA in DMF. Activated linker **74** was obtained with 57% yield after column chromatography purification (**Scheme 6.13**).



Scheme 6.13: synthesis of activated Val-Cit linker **74** for compound **70** synthesis.

Once obtained the activated carbonate, it was reacted with secondary amine **68** to give carbamate **75** in presence of DIPEA and HOAt, which is fundamental to increase the reaction yield. Afterwards, Boc protecting group was removed by treatment with TFA to afford amine **76**, which was reacted with *trans*-3-benzoyl acrylic acid, IBCF and NMM to give amide **70**. This compound features the desired carbonyl acrylate moiety for reaction with cysteine (**Scheme 6.14**).

As a next step, and out of the scope of this Thesis, this compound will be conjugated with antibodies to allow targeted delivery of Crizotinib to cancer cells.



Scheme 6.14: synthesis of compound **70** for ADC synthesis.

6.4 Conclusions

Considering the importance of self-immolative spacers in chemical biology and pro-drug synthesis, in this chapter a new degradable linker based on the Grob fragmentation was developed. After synthesizing and screening different structures (Figure 6.9), it was observed that only 3-amino cyclohexanol and nortropine

derivatives efficiently fragment under the reaction condition tested. Among them, benzylated derivatives **55** and **56** were the substrates that gives faster reaction and allows the release of fluorescent dansyl sulfonate even at pH 6.0. In particular, compound **56** was the compound with highest release rate at this slightly acidic pH. It is important to consider the pH at which the reaction is performed, especially depending on the cellular compartment or tissue that is going to be targeted. According to our results, Grob reaction can occur at pH around 6.0, typically found in endosomes and lysosomes. The results derived from the study of the reactivity by NMR suggest that a structure derived from compound **56** would be the best candidate for a self-immolative spacer to use in drug delivery.

For this reason, this structure was used to generate a pro-drug from Crizotinib, a potent phosphotyrosine kinase inhibitor used in cancer therapy. We have demonstrated that from compound **67** a potentially toxic Crizotinib analogue can be released, while no reaction was observed with the variant **68**, which presents a protected amine group. This result showed that Grob fragmentation substrates could be used as new self-immolative spacers in drug release. The reaction occurs spontaneously in physiological buffers at different pHs but can be easily controlled by protecting the free amine, which promotes the reaction.

On this basis, Grob fragmentation scaffold was equipped with a valine-citrulline linker, susceptible to cathepsin B enzyme protease activity, obtaining compound **70**. Such structure is bearing also a carbonyl acrylamide moiety for conjugation with cysteine in antibodies and proteins.

Therefore, a drug targeted delivery system that relies on Grob fragmentation for the controlled drug release has been prepared and will be conjugated to antibodies in the near future.

6.5 Experimental section

6.5.1 Synthesis

General procedure for secondary amines synthesis (General procedure A)

To a solution of primary amine (5 equiv.) in THF (0.2 M), the appropriate alkyl bromide (1 equiv.) was added at 0 °C. The reaction was allowed to reach room temperature and after complete starting material consumption, the crude mixture was directly evaporated and used for the following reaction without further purification.

General procedure for Boc protection of secondary amines (General procedure B)

The secondary amine was dissolved in a CH₃CN:H₂O 2:1 mixture (0.15 M) and to the resulting solution NaHCO₃ (2.5 equiv.) and Boc₂O (1.3 equiv.) were added. The reaction was stirred 16 hours at room temperature, and then stopped by diluting with Et₂O and washing with H₂O. Organic phase was dried with Na₂SO₄, filtered and concentrated, and the resulting crude was purified by column chromatography to give Boc-protected compound.

General procedures for Dansyl sulfonate formation

General procedure C: Alcohol (1 equiv.) was dissolved in dry pyridine (0.2 M) under inert atmosphere and cooled at 0°C. To this solution dansyl chloride (3 equiv.) was added and the reaction was stirred overnight at room temperature. Afterwards, the crude mixture was concentrated to dryness and purified by column chromatography, to give pure dansyl sulfonates.

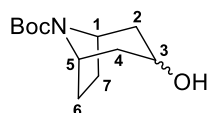
General procedure D: Alcohol (1 equiv.) and DMAP (3 equiv.) were dissolved under N₂ atmosphere in dry CH₃CN (0.1 M). Then, dansyl chloride (3 equiv.), dissolved in anhydrous CH₃CN (0.3 M), was added dropwise to the reaction mixture and stirred 16 hours at room temperature under inert atmosphere. The reaction was controlled by

TLC, and, when complete, it was concentrated to dryness and the crude solid was purified by FCC.

General procedure for Boc deprotection (General procedure E)

N-Boc protected amines were treated with a 15% solution of TFA in CH₂Cl₂ (0.05 – 0.1 M). Reaction was checked by TLC, and when complete it was evaporated to dryness by using toluene to co-evaporate TFA. The crude product was used without further purification for the following experiments.

Synthesis of compound *exo*-37



A solution of *N*-Boc-tropinone **36** (920 mg, 4.44 mmol) in EtOH (44 mL) was cooled at 0 °C and treated with NaBH₄ (335 mg, 8.88 mmol). The reaction was warmed at room temperature and after 2 hours a TLC (AcOEt:Hexanes 1:1) showed the disappearance of

starting material. The reaction was quenched by adding H₂O (40 mL) and then let stirring 10' at room temperature. After that, EtOH was evaporated and compound was extracted with AcOEt (3 x 50 mL). Organic phase was washed with brine (50 mL), dried over Na₂SO₄, filtered and concentrated. Crude compound were purified by column chromatography (AcOEt:Hexanes 1:2) giving *endo*-**37** (425 mg, 1.87 mmol, 42%) and *exo*-**37** (459 mg, 2.01 mmol, 45%). HRMS (ESI+) *m/z*: calcd. for C₁₂H₂₁NNaO₃ [M+Na]⁺ 250.1414; found 250.1420. Spectroscopic data for compound *exo*-**37**: ¹H NMR (300 MHz, CDCl₃) δ (ppm): 4.17 (brs, 2H, H-1, H-5), 4.10 – 3.96 (m, 1H, H-3) 2.70 (m, 1H, OH) 1.92 – 1.84 (m, 4H, H-2, H-4, H-6, H-7), 1.59 – 1.46 (m, 4H, H-2, H-4, H-6, H-7) 1.42 (s, 9H, Boc). ¹³C NMR (75 MHz, CDCl₃) δ (ppm): 153.3 (C=O), 79.4 (Cq, Boc), 63.6 (CH-3), 52.9 (2C, CH-1, CH-5), 40.3 (2C, CH₂-2, CH₂-4), 28.5 (3C, CH₃ Boc), 28.2 (2C, CH₂-6, CH₂-7).

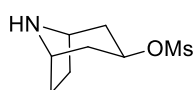
Synthesis of compound **38**



exo-**37** (109 mg, 0.48 mmol) was dissolved in anhydrous CH₂Cl₂ (2 mL) under inert atmosphere. To this solution MsCl (48 μL, 0.62 mmol) and NEt₃ (133 μL, 0.96 mmol) were added at 0 °C, and the reaction was then warmed at room temperature. After 1 hour, a TLC control showed

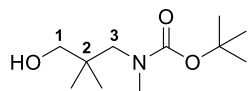
the complete consumption of starting material. The reaction was then diluted with CH_2Cl_2 (50 mL) and washed with H_2O (2x20 mL). The crude compound was purified by column chromatography (AcOEt:Hexanes 1:1) to give pure compound **3** (90 mg, 0.29 mmol, 61% yield). HRMS (ESI+) m/z : calcd. for $\text{C}_{13}\text{H}_{23}\text{NNaO}_5\text{S}$ $[\text{M}+\text{H}]^+$ 328.1189, found 328.1190. ^1H NMR (400 MHz, CDCl_3) δ (ppm): 5.02 (m, 1H, H-3), 4.23 (brs, 2H, H-1, H-5), 2.97 (s, 3H, OMs), 2.04 (brs, 2H, H-2, H-4), 1.96 (brs, H-6, H-7), 1.83 (brs, 2H H-2, H-4), 1.65 – 1.63 (m, 2H, H-6, H-7), 1.44 (brs, 9H, Boc). ^{13}C NMR (101 MHz, CDCl_3) δ (ppm): 153.1 (C=O), 79.8 (Cq, Boc), 75.1 (CH-3), 52.7 (2C, CH-1, CH-5), 39.6 (CH_3 , OMs), 37.8 (2C, CH_2 -2, CH_2 -4), 28.2 (3C, CH_3 Boc), 27.9 (2C, CH_2 -6, CH_2 -7).

Synthesis of compound 39

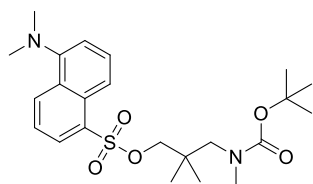


Following **General Procedure E** compound **39** was obtained from **38** (50 mg, 0.13 mmol) in quantitative yield (40 mg, 0.13 mmol). HRMS (ESI+) m/z : calcd. for $\text{C}_8\text{H}_{16}\text{NO}_3\text{S}$ $[\text{M}+\text{H}^+]$ 206.0845, found 206.0852. ^1H NMR (300 MHz, CDCl_3) δ (ppm): 5.07 – 4.96 (m, 1H, H-3), 4.17 – 4.16 (m, 2H, H-1, H-5), 3.16 (s, 3H, OMs) 2.42 – 2.34 (m, 2H, H-2, H-4), 2.18 – 2.01 (m, 6H, H-2, H-4, H-6, H-7). ^{13}C NMR (75 MHz, CDCl_3) δ (ppm): 71.7 (CH-3), 54.7 (2C, CH-1, CH-5), 36.9 (CH_3 OMs), 34.9 (2C, CH_2 -2, CH_2 -4), 25.4 (2C, CH_2 -6, CH_2 -7).

Synthesis of compound 40

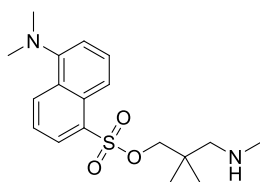


Compound **40** was obtained from 2,2-dimethyl-3-(methylamino)propan-1-ol (100 mg, 0.85 mmol) following **General Procedure B**. Purification of the crude with AcOEt:Hexanes 1:4 gave compound **40** with 78 % yield (144 mg, 0.66 mmol). ^1H NMR (300 MHz, CDCl_3) δ (ppm): 3.10 (s, 2H, H-1), 3.02 (s, 2H, H-3), 2.86, (s, 3H, NCH_3) 1.42 (s, 9H, Boc), 0.84 (s, 6H, CH_3). ^{13}C NMR (101 MHz, CDCl_3) δ (ppm): 157.8 (C=O), 80.2 (Cq, Boc), 67.8 (CH_2 -1), 56.0 (CH_2 -3), 38.0 (2C, NCH_3 , Cq-2), 28.3 (3C, CH_3 , *t*Bu), 23.3 (2 CH_3). MS (ESI+) m/z 316.18 (MNa^+).

Synthesis of compound 41

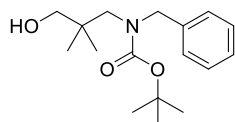
Compound **41** was obtained following **General Procedure C**, using **40** (36 mg, 0.16 mmol) as starting material. Compound **41** was obtained after purification by column chromatography (AcOEt:Hexanes 1:5) with 21% yield (15 mg, 0.03 mmol). ^1H NMR (300 MHz, CDCl_3)

δ (ppm): 8.62 (d, $J=8.5$ Hz, 1H, H-DNS), 8.34 – 8.24 (m, 2H, H-DNS), 7.67 – 7.50 (m, 2H, H-DNS), 7.22 (d, $J=7.5$ Hz, 1H, H-DNS), 3.71 (s, 2H, H-1), 3.07 (s, 2H, H-3), 2.91 (s, 6H, CH_3 -DNS), 2.79 (s, 3H, NCH_3), 1.38 (s, 9H, CH_3 Boc), 0.88 (s, 6H, CH_3). ^{13}C NMR (75 MHz, CDCl_3) (due to the presence of Boc rotamers, some carbon peak are splitted) δ (ppm): 156.6, 156.1 (C=O), 151.8 (Cq), 131.6 (CH-DNS), 131.2 (Cq), 130.5 (CH-DNS), 129.9 (Cq), 129.8 (Cq), 128.6 (CH-DNS), 123.0 (CH-DNS), 119.4 (CH-DNS), 115.6 (CH-DNS), 79.9, 79.4 (Cq, Boc), 77.2 (CH_2 -1), 56.6, 55.9 (CH_2 -3), 45.4 (2C, CH_3 -DNS), 37.7, 37.5 (2 C, NCH_3 , Cq-2), 28.3 (3C, CH_3 Boc), 22.8 (2C, CH_3). MS (ESI+) m/z 451.56 (MH^+).

Synthesis of compound 42

Compound **42** was obtained from compound **41** (57 mg, 0.13) following **General Procedure E**, with quantitative yield (44 mg, 0.13 mmol). HRMS (ESI+) m/z : calcd. for $\text{C}_{18}\text{H}_{27}\text{N}_2\text{O}_3\text{S}$ [$\text{M}+\text{H}$] $^+$ 351.1741, found 351.1734. ^1H NMR (300 MHz, CD_3OD) δ (ppm): 8.69 (dd, $J=8.6, 1.1$ Hz, 1H-DNS),

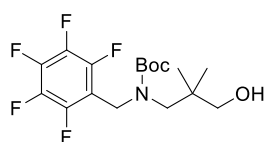
8.45 (dt, $J=8.7, 0.9$ Hz, 1H, H-DNS), 8.38 (dd, $J=7.4, 1.2$ Hz, 1H, H-DNS), 7.79 – 7.74 (m, 2H, H-DNS), 7.61 (dd, $J=7.8, 1.0$ Hz, 1H, H-DNS), 3.85 (s, 2H, H-1), 3.11 (s, 6H, CH_3 -DNS), 2.91 (s, 2H, H-3), 2.67 (s, 3H, NCH_3), 0.96 (s, 6H, CH_3). ^{13}C NMR (75 MHz, CD_3OD) δ (ppm): 148.0 (Cq), 131.2 (Cq), 131.1 (CH-DNS), 130.2 (CH-DNS), 129.5 (Cq), 128.6 (Cq), 128.5 (CH-DNS), 124.2 (CH-DNS), 121.5 (CH-DNS), 116.9 (CH-DNS), 75.7 (CH_2 -1), 55.9 (CH_2 -3), 45.0 (2C, CH_3 -DNS), 34.0 (Cq-2), 33.8 (NCH_3), 20.6 (2C, CH_3).

Synthesis of compound 43

Compound **43** was obtained following **General Procedures A and B**. First, the secondary amine was obtained by using 3-amino-2,2-dimethylpropan-1-ol (150 mg, 1.45 mmol) and

benzyl bromide (35 μ L, 0.29 mmol). Crude secondary amine was protected with Boc following **General Procedure B**. Purification of the crude by column chromatography (AcOEt:Hexanes 1:4) gave compound **43** with 98% yield over two steps (84 mg, 0.29 mmol). ^1H NMR (400 MHz, CDCl_3) δ (ppm): 7.34 – 7.31 (m, 2H arom.), 7.28 – 7.24 (m, 1H arom.), 7.16 – 7.15 (m, 2H arom.), 4.58 – 4.34 (m, 3H, CH_2Ph), 3.21 (d, $J=7.3$ Hz, 2H, H-1), 3.11 (brs, 2H, H-3, OH), 1.39 (s, 9H, Boc), 0.91 (s, 6H, CH_3). ^{13}C NMR (101 MHz, CDCl_3) δ (ppm): 157.9 (C=O), 138.3 (Cq arom.), 128.5 (2C, CH arom.), 127.1 (CH arom.), 126.7 (2C, CH arom.), 80.8 (Cq, Boc), 68.0 (CH_2 -1), 53.6, 53.4 (2 CH_2 , CH_2Ph , CH_2 -3), 38.2 (Cq-2), 28.2 (3 CH_3 , $t\text{Bu}$), 23.5 (2 CH_3). MS (ESI+) m/z 316.18 (MNa^+).

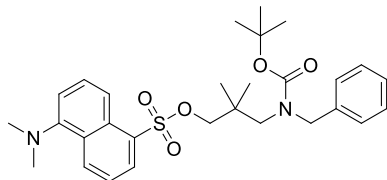
Synthesis of compound 44



Compound **44** was obtained following **General Procedures A and B**. First, the secondary amine was obtained by using 3-amino-2,2-dimethylpropan-1-ol (197 mg, 1.91 mmol) and 2,3,4,5,6-pentafluorobenzyl bromide (57 μ L, 0.38 mmol).

Crude secondary amine was protected with Boc following **General Procedure B**. Purification of the crude by column chromatography (AcOEt:Hexanes 1:4) gave compound **44** with 55% yield over two steps (80 mg, 0.21 mmol). ^1H NMR (400 MHz, CDCl_3) δ (ppm): 4.54 (brs, 2H, CH_2PFB), 3.18 – 3.13 (m, 4H, CH_2 -1, CH_2 -3), 1.41 (s, 9H, Boc), 0.93 (s, 6H, CH_3). ^{13}C NMR (101 MHz, CDCl_3) δ (ppm): 156.7 (C=O), 81.7 (Cq, Boc), 67.9 (CH_2 -1), 53.6 (CH_2 -3), 42.1 (CH_2PFB), 38.3 (Cq-2), 28.1 (3C, CH_3 Boc), 23.3 (2C, CH_3); quaternary C-F carbon are not detected. ^{19}F NMR (282 MHz, CDCl_3) δ (ppm): -141.43 (dd, $J=22.2, 8.2$ Hz, 2F), -154.55 (t, $J=20.8$ Hz, 1F), -161.91 (td, $J=22.1, 8.0$ Hz, 2F). MS (ESI+) m/z 406.13 (MNa^+).

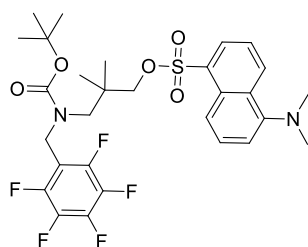
Synthesis of compound 45



Compound **45** was obtained following **General Procedure C**, using **43** (73 mg, 0.25 mmol) as starting material. Compound **45** was obtained after purification by column chromatography (AcOEt:Hexanes 1:4) with 76% yield (100 mg, 0.19 mmol). HRMS (ESI+) m/z : calcd. for $\text{C}_{29}\text{H}_{38}\text{N}_2\text{NaO}_5\text{S}$ [$\text{M}+\text{Na}$] $^+$ 549.2394; found

549.2386. ^1H NMR (400 MHz, CDCl_3) δ (ppm): 8.61 (d, $J=8.5$ Hz, 1H, H-DNS), 8.28 – 8.23 (m, 2H, H-DNS), 7.56 – 7.50 (m, 2H, H-DNS), 7.30 – 7.19 (m, 4H, H-arom., H-DNS), 7.17 – 7.08 (m, 2H, H-arom.), 4.38 (brs, 2H, CH_2Ph), 3.74 (s, 2H, CH_2-1), 3.11 (CH_2-3), 2.90 (s, 6H, CH_3 -DNS), 1.38 – 1.31 (brm, 9H, Boc), 0.88 (s, 6H, CH_3). ^{13}C NMR (75 MHz, CD_3OD) (due to the presence of Boc rotamers, some carbon peaks are splitted) δ (ppm): 156.6 ($\text{C}=\text{O}$), 151.5 (Cq), 138.6, 137.9 (1C, Cq), 131.5 (CH-DNS), 131.3 (Cq) 130.6 (CH-DNS), 129.9, 129.8 (Cq), 128.7 (CH-DNS), 128.5 (2C, CH-arom.), 127.4, 127.1, 126.8 (3C, CH arom.), 123.2 (CH-DNS), 119.6 (CH-DNS), 115.7 (CH-DNS), 80.3 – 79.9 (Cq Boc), 77.6 (CH_2-1), 53.5, 53.2, 52.8, 51.8 (2C, CH_2 -Ph, CH_2-3), 45.5 (2C, CH_3 -DNS), 37.6 (Cq-2), 28.2 (CH_3 Boc), 23.0 (2C, CH_3).

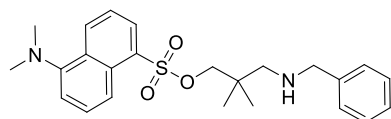
Synthesis of compound 46



Compound **46** was obtained following **General Procedure C**, using **44** (61 mg, 0.16 mmol) as starting material. Compound **46** was obtained after purification by column chromatography (AcOEt:Hexanes 1:4) with 68% yield (67 mg, 0.11 mmol). HRMS (ESI+) m/z : calcd. for $\text{C}_{29}\text{H}_{34}\text{F}_5\text{N}_2\text{O}_5\text{S}$ $[\text{M}+\text{H}]^+$ 617.2103, found 617.2100. ^1H

NMR (400 MHz, CDCl_3) δ (ppm): 8.62 (d, $J=8.5$ Hz, 1H, H-DNS), 8.33 – 8.07 (m, 2H, H-DNS), 7.67 – 7.46 (m, 2H, H-DNS), 7.16 (d, $J=7.6$ Hz, 1H, H-DNS), 4.28 (brs, 2H, CH_2PFB), 3.76 (s, 2H, H-1) 3.10 (brs, 2H, H-3) 2.91 (s, 6H, CH_3 -DNS) 1.33 (brs, 9H, Boc), 0.95 (s, 6H, CH_3). ^{13}C NMR (75 MHz, CDCl_3) δ (ppm): 155.2 ($\text{C}=\text{O}$), 151.8 (Cq), 131.7 (CH-DNS), 131.1 (Cq), 130.6 (CH-DNS), 129.8 (Cq), 128.6 (CH-DNS), 123.0 (CH-DNS), 119.1 (CH-DNS), 115.3 (CH-DNS), 80.8 (Cq, Boc), 76.8 (CH_2-1), 54.4 (CH_2-3), 45.4 (2C, CH_3 -DNS), 41.7 (CH_2PFB), 37.6 (Cq-2), 28.1 (3C, CH_3 Boc), 22.8 (2C, CH_3); quaternary C-F carbon are not detected. ^{19}F NMR (282 MHz, CDCl_3) δ (ppm): -142.27 – -124.39 (m, 2F), -155.29 – -155.59 (m, 1F), -162.23 – -162.43 (m, 2F).

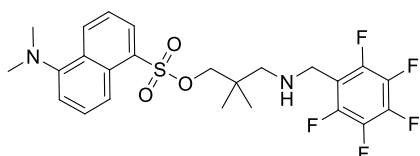
Synthesis of compound 47



Compound **47** was obtained from compound **45** (32 mg, 0.061 mmol) with quantitative yield (27 mg, 0.061 mmol) following **General Procedure E**.

HRMS (ESI+) m/z : calcd. for $C_{24}H_{31}N_2O_3S$ $[M+H]^+$ 427.2050, found 427.2045. 1H NMR (400 MHz, CD_3OD) δ (ppm): 8.67 (d, $J=8.6$ Hz, 1H, H-DNS), 8.29 (dd, $J=7.3, 1.2$ Hz, 1H, H-DNS), 8.22 (d, $J=8.6$ Hz, 1H, H-DNS), 7.68-7.63 (m, 2H, H-DNS), 7.46 – 7.42 (m, 5H, H-arom.), 7.37 (d, $J=7.6$ Hz, 1H, H-DNS), 4.16 (s, 2H, $\underline{CH_2}Ph$), 3.81 (s, 2H, CH_2-1), 2.93 (s, 6H, CH_3 -DNS), 2.90 (s, 2H, CH_2-3), 0.92 (s, 6H, CH_3). ^{13}C NMR (75 MHz, CD_3OD) δ (ppm): 148.4 (Cq), 131.2 (Cq), 130.9 (CH-DNS), 130.3 (CH-DNS), 130.2 (Cq), 129.9 (2C, CH-Arom.), 129.5 (2C, Cq, CH-Arom.), 128.9 (2C, CH-Arom.), 128.7 (Cq), 128.5 (CH-DNS), 124.1 (CH-DNS), 121.1 (CH-DNS), 116.8 (CH-DNS), 75.4 (CH_2-1), 53.3 (CH_2-3), 52.2 ($\underline{CH_2}$ -Ph), 44.9 (2C, CH_3 -DNS), 33.9 (Cq-2), 20.6 (CH_3).

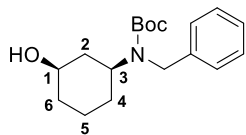
Synthesis of compound 48



Compound **48** was obtained from **46** (32 mg, 0.061 mmol) with quantitative yield (27 mg, 0.061 mmol) following **General Procedure E**. 1H NMR (400 MHz, CD_3OD) δ (ppm): 8.58 (dd,

$J=8.6, 1.2$ Hz, 1H, H-DNS), 8.19 (dd, $J=7.3, 1.2$ Hz, 1H, H-DNS), 8.13 (d, $J=8.7$ Hz, 1H, H-DNS), 7.58 – 7.54 (m, 2H, H-DNS), 7.25 (d, $J=7.5$ Hz, 1H, H-DNS), 4.31 (s, 2H, $\underline{CH_2}PFB$), 3.74 (s, 2H, H-1), 3.00 (s, 2H, H-3), 2.82 (s, 6H, CH_3 -DNS), 0.87 (s, 6H, CH_3). HRMS (ESI+) m/z : calcd. for $C_{24}H_{26}F_5N_2O_3S$ $[M+H]^+$ 517.1578, found 517.1580. ^{13}C NMR (101 MHz, CD_3OD) δ (ppm): 150.9 (Cq), 146.1 (d, $J=250.6$ Hz, C-F Arom.), 142.5 (d, $J=253.2$ Hz, C-F Arom.), 137.7 (d, $J=250.6$ Hz, C-F Arom.), 131.2 (CH-DNS), 130.8 (Cq), 130.6 (CH-DNS), 129.6 (Cq), 129.5 (Cq), 128.5 (CH-DNS), 123.3 (CH-DNS), 119.4 (CH-DNS), 115.9 (CH-DNS), 104.9 (t, $J=18.5$ Hz, Cq.), 75.0 (CH_2-1), 54.1 (CH_2-3), 44.5 (2C, CH_3 -DNS), 39.2 ($\underline{CH_2}$ PFB), 34.1 (Cq), 20.6 (2C, CH_3). ^{19}F NMR (282 MHz, CD_3OD) δ (ppm): -77.49 (s, TFA), -140.48 – -140.60 (m, 2F), -153.16 – -153.32 (m, 1F), -163.59 – -163.66 (m, 2F).

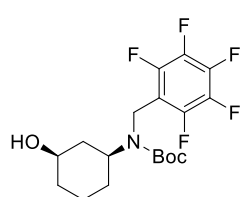
Synthesis of compound 49



Compound **49** was obtained following **General Procedures A and B**. First, the secondary amine was obtained by using (1*R*,3*S*)-3-aminocyclohexanol and benzyl bromide, with addition of 20% DMF to complete solubilisation. Crude secondary amine was protected as Boc carbamate following **General Procedure B**. Purification of the crude by column chromatography (AcOEt:Hexanes 1:2) gave

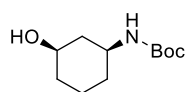
compound **49** as colourless oil with 87% yield. $^1\text{H-NMR}$ (500 MHz, CDCl_3) 7.30 – 7.21 (m, 5H, H-Ar), 4.36 (brs, 2H, CH_2Ph), 4.07 (brs, H-3), 3.63 (brs, 2H, H-4, OH), 2.04 (m, 1 H), 1.91 (d, $J=11.6$ Hz, 1 H), 1.76 – 1.73 (m, 1H), 1.76 – 1.03 (m, 14H); $^{13}\text{C-NMR}$ (125 MHz, CDCl_3) 155.7 (C=O), 140.2 (Cq arom.), 128.3, 126.7 (5C, CH arom.), 79.9 (Cq Boc), 70.0 (CH-1), 53.2 (CH-3), 46.6 (CH_2Ph), 40.4 (CH_2), 34.7 (CH_2), 29.8 (CH_2), 28.4 (3C, CH_3 *t*Bu), 22.2 (CH_2). MS (ESI+) m/z 306.21 (MH^+), 328.19 (MNa^+).

Synthesis of compound 50



Compound **50** was obtained following **General Procedures A and B**. First, the secondary amine was obtained by using (*1R,3S*)-3-aminocyclohexanol and 2,3,4,5,6-Pentafluorobenzyl bromide. Crude secondary amine was protected as Boc-carbamate following **General Procedure B**. Purification of the crude by column chromatography (AcOEt:Hexanes 1:2) gave compound **50** as colourless oil with 85% yield over two steps. $^1\text{H NMR}$ (300 MHz, CDCl_3) δ (ppm): 4.56 (brs, 2H, CH_2PFB), 3.76 – 3.60 (m, 2H, H-1, H-3), 2.06 – 1.93 (m, 2H), 1.84-1.76 (m, 1H), 1.69 – 1.62 (m 3H), 1.46 (s, 9H, CH_3 Boc), 1.42 – 1.22 (m, 2H), 1.17 – 1.04 (m, 1H). $^{13}\text{C NMR}$ (101 MHz, CDCl_3) δ (ppm): 154.9 (C=O), 146.4, 143.9, 138.7, 137.0, 136.2, 113.0, (6C, C-F arom.), 80.7 (Cq, Boc), 69.8 (CH-1), 54.8 (CH-3), 39.8 ($\text{CH}_2\text{-Ph}$), 36.9 ($\text{CH}_2\text{-2}$), 34.7 (CH_2), 29.2 (CH_2), 28.3 (3C, CH_3 Boc), 22.2 ($\text{CH}_2\text{-5}$). $^{19}\text{F NMR}$ (282MHz, CDCl_3) δ (ppm): -142.8 (brs, 2F), -155.5 – -155.6 (m, 1F), -162.1 – -162.3 (m, 2F). MS (ESI+) m/z 396.16 (MH^+), 418.14 (MNa^+).

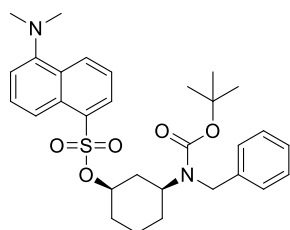
Synthesis of compound 51



Compound **51** was obtained from (*1R,3S*)-3-aminocyclohexanol following **General Procedure B**. Purification of the crude with AcOEt:Hexanes 1:1 gave compound **51** with 70 % yield. HRMS (ESI+) m/z : calcd. for $\text{C}_{11}\text{H}_{22}\text{NO}_3$ [$\text{M}+\text{H}$] $^+$ 216.1596, found 216.1594. $^1\text{H NMR}$ (400 MHz, CDCl_3) δ (ppm): 4.71 (brs, 1 H), 3.75 – 3.70 (m, 1H, H-1), 3.52 (brs, 1H, H-3), 2.19 – 2.16 (m, 1 H, H-2), 1.87 – 1.77 (m, 3H, H-4, H-5, H-6) 1.44 (s, 9H, CH_3 , Boc) 1.37 – 1.06 (m, 4H, H-2, H-4, H-5, H-6). $^{13}\text{C NMR}$ (101 MHz, CDCl_3) δ (ppm): 155.2 (C=O), 79.2 (Cq, Boc), 69.0

(CH-1), 47.8 (CH-3), 41.7 (CH₂-2), 34.5, 32.2 (2C, CH₂-4, CH₂-6), 28.4 (3C, CH₃ Boc), 20.8 (CH₂-5).

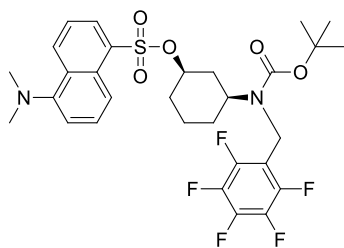
Synthesis of compound 52



Compound **52** was obtained following **General Procedure D**, using **49** (44 mg, 0.11 mmol) as starting material **52** crude was purified by column chromatography (AcOEt:Hexanes 1:4), giving pure compound **52** with 50% yield. HRMS (ESI+) *m/z*: calcd. for C₃₀H₃₉N₂O₅S [M+H]⁺ 539.2574, found 539.2575. ¹H NMR (400 MHz, CDCl₃) δ

(ppm): 8.61 (d, *J*=8.3 Hz, 1H, H-DNS), 8.26 (d, *J*=7.2 Hz, 1H, H-DNS), 8.19 (d, *J*=8.6 Hz, 1H, H-DNS), 7.56 – 7.51 (m, 2H, H-DNS), 7.26 – 7.19 (m, 4H, H-DNS, H arom.), 7.10 – 7.09 (m, 2H, H arom.), 4.34 – 4.26 (m, 3H, CH₂Ph, H-1), 3.91, 3.44 (brs, 1H, H-3), 2.90 (s, 6H, CH₃-DNS), 1.99 – 1.96 (m, 1H), 1.84 – 1.81 (m, 1H), 1.66 – 1.54 (m, 3H), 1.33 – 1.12 (m, 12H). ¹³C NMR (75 MHz, CDCl₃) δ (ppm): 155.4 (C=O), 151.6 (Cq), 139.6 (Cq), 132.6 (Cq), 131.4 (CH-DNS), 130.0 (Cq), 129.8 (CH-DNS), 128.5 (CH-DNS), 128.3 (2C, CH arom.), 126.8, 126.4 (4C, Cq, CH arom.) 123.2 (CH-DNS), 119.7 (CH-DNS), 115.5 (CH-DNS), 80.5 (Cq, Boc), 80.1 (CH-1), 52.9 (CH-3), 46.8 (CH₂-Ph), 45.5 (2C, CH₃-DNS), 37.2 (CH₂), 31.8 (CH₂), 29.4 (CH₂), 28.3 (3C, CH₃-Boc), 21.7 (CH₂).

Synthesis of compound 53

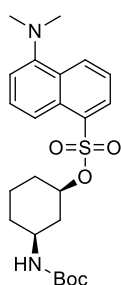


Compound **53** was obtained following **General Procedure D**, using **50** (40 mg, 0.10 mmol) as starting material. **53** was obtained after purification by column chromatography (AcOEt:Hexanes 1:4) with 73% yield (46 mg, 0.073 mmol). HRMS (ESI+) *m/z*: calcd. for C₃₀H₃₄F₅N₂O₅S [M+H]⁺ 629.2106, found 629.2103. ¹H

NMR (400 MHz, CDCl₃) δ (ppm): 8.61 (d, *J*=8.4 Hz, 1H, H-DNS), 8.26 (d, *J*=7.3 Hz, 1H, H-DNS), 8.20 (d, *J*=8.6 Hz, 1H, H-DNS), 7.56 (m, 2H, H-DNS), 7.21 (d, *J*=7.5 Hz, 1H, H-DNS), 4.43 – 4.30 (m, 3H, CH₂-PFBn, H-1), 3.52 (brs, 1H, H-3), 2.90 (s, 6H, CH₃-DNS), 1.87 (brs, 2H), 1.71 – 1.68 (m, 2H), 1.57 – 1.54 (m, 1H), 1.35 (s, 9H, Boc), 1.33 – 1.10 (m, 3H). ¹³C NMR (101 MHz, CDCl₃) δ (ppm): 154.7 (Cq, C=O), 151.7 (Cq-DNS), 145.9 (d, *J*=145.3 Hz,

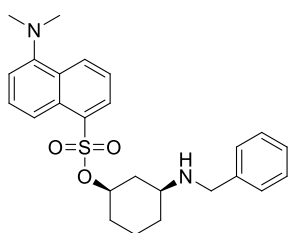
2C, C-F arom.), 140.5 (d, $J=140.5$, C-F arom.), 137.2 (m, 2C, C-F arom.), 132.7 (Cq-DNS), 131.5 (CH-DNS), 130.1 (CH-DNS), 130.0 (Cq-DNS), 129.9 (Cq-DNS), 128.5 (CH-DNS), 123.3 (CH-DNS), 119.8 (CH-DNS), 115.7 (CH-DNS), 112.8 (m, C-F arom), 81.0 (Cq Boc), 80.4 (CH-1), 54.9 (CH-3), 45.6 (2C, CH₃-DNS), 37.3 (CH₂-PFB), 36.8 (CH₂), 31.9 (CH₂), 29.8 (CH₂), 28.9 (CH₂), 28.3 (3C, CH₃ Boc), 21.9 (CH₂). ¹⁹F NMR (376 MHz, CDCl₃) δ (ppm): -146.6 (s, 2F), -159.1 (s, 1F), -165.9 (td, $J=21.6, 7.4$ Hz).

Synthesis of compound 54



Compound **54** was obtained following **General Procedure C**, using **51** (132 mg, 0.61 mmol) as starting material. Crude **54** was purified by column chromatography (AcOEt:Hexanes 1:4), to give pure compound **54** with 77% yield (210 mg, 0.47 mmol). HRMS (ESI+) m/z : calcd. for C₂₃H₃₃N₂O₅S [M+H]⁺ 449.2105, found 449.2107. ¹H NMR (300 MHz, CDCl₃) δ (ppm): 8.68 (d, $J=8.6$ Hz, 1H, H-DNS), 8.33 – 8.28 (m, 2H, H-DNS), 7.66 – 7.55 (m, 2H, H-DNS), 7.27-7.24 (m, 1H, H-DNS), 4.49 – 4.39 (m, 2H, H-1, NH), 3.43 (brs, 1H, H-3), 2.96 (s, 6H, CH₃-DNS) 2.14 – 2.07 (m, 1 H, H-2), 1.90 – 1.66 (m, 3H) 1.41 (s, 9H, CH₃, Boc) 1.39 – 1.03 (m, 4H). ¹³C NMR (75 MHz, CDCl₃) δ (ppm): 154.9 (C=O), 132.6 (Cq), 131.3 (CH-DNS), 130.9 (Cq), 130.2 (CH-DNS), 129.9 (Cq), 129.7 (Cq), 128.5 (CH-DNS), 123.4 (CH-DNS), 120.1 (CH-DNS), 115.7 (CH-DNS), 79.9 (Cq, Boc), 79.5 (CH-1), 47.4 (CH-3), 45.6 (2C, CH₃-DNS), 38.8 (CH₂-2), 31.9, 31.7 (2C, CH₂-4, CH₂-6), 28.4 (3C, CH₃ Boc), 20.6 (CH₂-5).

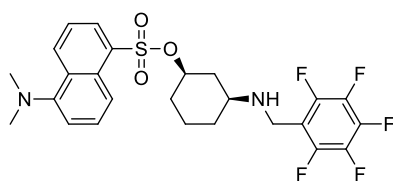
Synthesis of compound 55



Compound **55** was obtained from **52** (15 mg, 0.028 mmol) with quantitative yield (12 mg, 0.028 mmol) following **General Procedure E**. HRMS (ESI+) m/z : calcd. for C₂₅H₃₁N₂O₃S [M+H]⁺ 439.2050, found 439.2050. ¹H NMR (400 MHz, CD₃OD) δ (ppm): 8.65 (d, $J=8.6$ Hz, 1H, H-DNS), 8.32 (dd, $J=7.3, 1.0$ Hz, 1H, H-DNS), 8.28 (d, $J=8.7$ Hz, 1H, H-DNS), 7.73 – 7.55 (m, 2H, H-DNS), 7.49 – 7.28 (m, 6H, H-arom., H-DNS), 4.43 (m, 1H, H-1), 4.08 (q, $J=13.0$ Hz, 2H, CH₂Ph), 3.20 – 3.04 (m, 1H, H-3), 2.96 (m, 6H, CH₃-DNS) 2.40 – 2.31 (m, 1H, H-2), 2.05 (m, 1H, H-4), 1.85 – 1.69 (m, 2H, H-5, H-6), 1.57 (q, $J=11.7$ Hz,

1H, H-2), 1.44 – 1.15 (m, 3H, H-4, H-5, H-6). ¹³C NMR (75 MHz, CD₃OD) δ (ppm): 151.2 (Cq), 133.8 (Cq), 132.4 (Cq), 132.0 (CH-DNS), 131.6 (CH-DNS), 131.0 (Cq), 130.8 (2C, CH arom.), 130.7 (2C, CH arom.), 130.5 (Cq), 130.3 (CH-arom.), 129.7 (CH-DNS), 125.0 (CH-DNS), 121.9 (CH-DNS), 117.6 (CH-DNS), 79.9 (CH-1), 55.8 (CH-3), 48.0 (CH₂Ph), 46.1 (2C, CH₃-DNS), 36.3 (CH₂-2), 32.4 (CH₂-6), 28.4 (CH₂-4), 21.5 (CH₂-5).

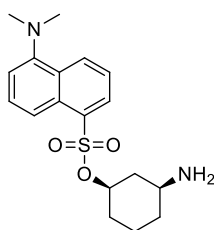
Synthesis of compound 56



Compound **56** was obtained from **53** (15 mg, 0.024 mmol) with quantitative yield (13 mg, 0.024 mmol) following **General Procedure E**. HRMS (ESI+) m/z: calcd. for C₂₅H₂₆F₅N₂O₃S [M+H]⁺ 529.1579, found 529.1573 ¹H NMR (400

MHz, CD₃OD) δ (ppm): 8.67 (d, J=8.6 Hz, 1H, H-DNS), 8.36 (t, J=8.6 Hz, 2H, H-DNS), 7.75 – 7.68 (m, 2H, H-DNS), 7.51 (d, J=7.6 Hz, 1H), 4.57 – 4.47 (m, 1H, H-1), 4.33 (q, J=13.9 Hz, 2H, CH₂PFB), 2.44 – 2.39 (m, 1H, H-2), 2.15 – 2.12 (m, 1H, H-4), 1.89 – 1.82 (m, 2H, H-5, H-6), 1.64 (q, J=11.5 Hz, 1H, H-2), 1.49 – 1.22 (m, 3H, H-6, H-4, H-5). ¹³C NMR (101 MHz, CD₃OD) δ (ppm): 151.1 (Cq), 147.2 (m, J=246.1, 2C, C-F arom.), 143.9 (d, J=256.0, C-F arom.), 139.1 (d, J=149.6 Hz, 2C, C-F arom.), 133.9 (Cq), 132.0 (CH-DNS), 131.6 (CH-DNS), 131.0 (Cq), 130.5 (Cq), 129.7 (CH-DNS), 125.1 (CH-DNS), 122.0 (CH-DNS), 117.7 (CH-DNS), 106.9 (m, Cq arom.), 79.7 (CH-1), 56.7 (CH-3), 46.1 (2C, CH₃-DNS), 36.3 (CH₂-PFB), 36.2 (CH₂-2), 32.4 (CH₂-6), 28.2 (CH₂-4), 21.4 (CH₂-5). ¹⁹F NMR (376 MHz, CD₃OD) δ (ppm): -77.45 (CF₃ TFA), -141.75 – -141.83 (m, 2F), -153.46 – -153.58 (m, 1F), -163.57 – -163.72 (m, 2F).

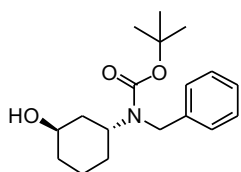
Synthesis of compound 57



Compound **57** was obtained from compound **54** (11 mg, 0.024 mmol) with quantitative yield (9 mg, 0.024 mmol) following **General Procedure E**. HRMS (ESI+) m/z: calcd. for C₁₈H₂₅N₂O₃S [M+H]⁺ 349.1580, found 349.1586. ¹H NMR (300 MHz, CD₃OD) δ (ppm): 8.68 (d, J=8.6 Hz, 1H, H-DNS), 8.34 (dd, J=7.3, 1.3 Hz, 1H, H-DNS), 8.27 (d, J=8.7 Hz, 1H, H-DNS), 7.69 – 7.66 (m, 2H, H-DNS), 7.39 (dd, J=7.7 Hz, 1H, H-DNS), 4.56 – 4.38 (m, 1H, H-1), 3.19 – 3.06 (m, 1H, H-3), 2.23

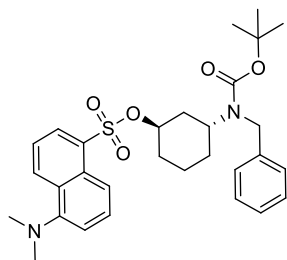
(m, 1H, H-2), 1.95 – 1.73 (m, 3H, H-4, H-5, H-6), 1.54 (q, $J=11.6$ Hz, 1H, H-2), 1.40 – 1.23 (s, 3H, H-4, H-5, H-6). ^{13}C NMR (75 MHz, CD_3OD) δ (ppm): 151.0 (Cq), 132.3 (Cq), 131.0 (CH-DNS), 130.1 (CH-DNS), 129.6 (Cq), 129.5 (Cq), 128.3 (CH-DNS), 123.3 (CH-DNS), 119.8 (CH-DNS), 115.8 (CH-DNS), 78.4 (CH-1), 47.8 (CH-3), 44.5 (2C, $(\text{CH}_3\text{-DNS})$), 36.3 ($\text{CH}_2\text{-2}$), 30.8 ($\text{CH}_2\text{-6}$), 28.70 ($\text{CH}_2\text{-4}$), 20.0 ($\text{CH}_2\text{-5}$).

Synthesis of compound 58

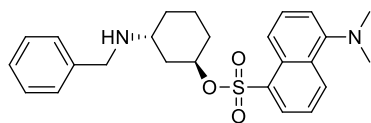


Compound **58** was obtained following **General Procedures A and B**. First, the secondary amine was obtained by using racemic *trans*-3-aminocyclohexanol and benzyl bromide, with addition of 20% DMF to complete solubilization. Crude secondary amine was protected as Boc carbamate following **General Procedure B**. Purification of the crude by column chromatography (AcOEt:Hexanes) gave compound **58** with 60% yield. ^1H NMR (400 MHz, CDCl_3) δ (ppm): 7.31 – 7.22 (m, 5H, arom.), 4.37 (brs, 3H, CH_2Ph , H-3), 4.18 (brs, 1H, H-1), 1.74 – 1.65 (m, 5H), 1.56 (m, 12H). ^{13}C NMR (75 MHz, CDCl_3) = 155.7 (C=O), 140.2 (Cq arom.), 128.2, 126.6 (5C, CH- arom.), 79.7 (Cq, Boc), 67.2 (CH-1), 50.7 (CH-3), 47.4 (CH_2Ph), 37.7 (CH_2), 31.6 (CH_2), 30.8 (CH_2), 28.4 (3C, CH_3 Boc), 19.8 (CH_2). MS (ESI+) m/z 306.21 (MH^+), 328.19 (MNa^+).

Synthesis of compound 59

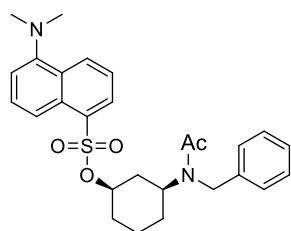


Compound **59** was obtained following **General Procedure C**, using **58** (12mg, 0.039 mmol) as starting material. **59** was purified by column chromatography (AcOEt:Hexanes 1:4), giving pure compound **59** with 77% yield. This compound could not be completely characterized due to its instability. Therefore, only ^1H NMR description will be reported. ^1H NMR (300 MHz, CDCl_3) δ (ppm): 8.63 (d, $J=8.6$ Hz, 1H), 8.32 (d, $J=8.6$ Hz, 1H), 8.26 (dd, $J=7.3, 1.3$ Hz, 1H), 7.63 (dd, $J=8.6, 7.1$ Hz, 1H), 7.55 (dd, $J=8.6, 7.3$ Hz, 1H), 7.39 – 6.84 (m, 4H), 7.11 – 7.08 (m, 2H), 4.89 (brs, 1H), 4.39 (brs, 1H), 4.14 – 3.82 (m, 2H), 2.93 (s, 6H), 1.85 – 1.32 (m, 17H).

Synthesis of compound 60

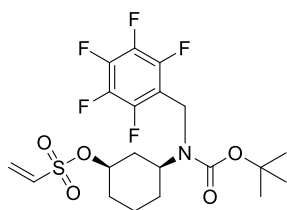
Compound **60** was obtained from **59** (8 mg, 0.15 mmol) with quantitative yield following **General Procedure E**. HRMS (ESI+) m/z : calcd. for $C_{25}H_{31}N_2O_3S$ $[M+H]^+$ 439.2050, found 439.2043. 1H

NMR (300 MHz, CD_3OD) δ (ppm): 8.69 (d, $J=8.6$ Hz, 1H, H-DNS), 8.34 (dd, $J=7.3, 1.3$ Hz, 1H, H-DNS), 8.27 (d, $J=8.7$ Hz, 1H, H-DNS), 7.77 – 7.65 (m, 3H), 7.48 – 7.33 (m, 5H), 5.01 – 4.98 (m, 1H, H-1), 3.89 – 3.82 (m, 2H, $\underline{CH_2}Ph$), 3.40 – 3.35 (m, 1H, H-3), 2.88 (s, 6H, CH_3 -DNS), 2.22 – 2.13 (m, 2H), 1.78 – 1.39 (m, 6H). ^{13}C NMR (75 MHz, CD_3OD) δ (ppm): 152.1 (Cq), 132.2 (Cq), 131.5 (Cq), 131.0 (CH-DNS), 130.1 (CH-DNS), 129.8 (Cq), 129.5 (CH), 129.4 (CH), 129.0 (CH), 128.9 (Cq), 128.6 (CH-DNS), 123.2 (CH-DNS), 118.9 (CH-DNS), 115.5 (CH-DNS), 78.3 (CH-1), 52.8 (CH-3), 48.0 ($\underline{CH_2}Ph$), 44.3 (2C, CH_3 DNS), 32.7 (CH_2), 28.9 (CH_2), 27.8 (CH_2), 18.3 (CH_2).

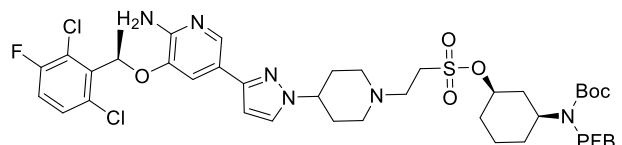
Synthesis of compound 61

Compound **55** (9 mg, 0.017 mmol) was dissolved in CH_2Cl_2 (0.2 mL), and to this solution Ac_2O (9 μL) and pyridine (8.1 μL) were added. After 3 hours, the reaction was concentrated and crude product was purified by column chromatography to give compound **61** (7 mg, 0.014 mmol, 86% yield). HRMS (ESI+) m/z : calcd. for $C_{27}H_{33}N_2O_4S$

$[M+H]^+$ 481.2155, found 481.2161. 1H NMR (400 MHz, $CDCl_3$) δ (ppm): 8.60 (d, $J=8.4$ Hz, 1H, H-DNS), 8.21 (d, $J=7.3$ Hz, 1H, H-DNS), 8.13 (d, $J=8.7$ Hz, 1H, H-DNS), 7.54 – 7.42 (m, 2H, H-DNS), 7.23 – 7.19 (m, 4H, H-DNS, H arom.), 7.02 – 7.01 (m, 2H arom.), 4.39 – 4.29 (m, 4H, $\underline{CH_2}Ph$, H-1, H-3), 2.88 (s, 6H, CH_3 -DNS), 1.91 (s, 3H, $COCH_3$), 1.90 – 1.45 (m, 5H), 1.16 – 1.04 (m, 3H). ^{13}C NMR (101 MHz, $CDCl_3$) δ (ppm): 171.4 (C=O), 137.7 (Cq), 132.6 (Cq), 131.3 (CH-DNS), 130.2 (CH-DNS), 129.8 (Cq), 129.5 (Cq), 128.8 (2C, CH arom.), 128.4 (Cq), 128.3 (CH-DNS), 127.4 (CH arom.), 126.8 (Cq), 125.7 (2C, CH arom.) 123.5 (CH-DNS), 120.3 (CH-DNS), 115.7 (CH-DNS), 80.4 (CH-1), 51.1 (CH-3), 47.8 ($\underline{CH_2}Ph$), 45.6 (2C, CH_3 -DNS), 36.6 (CH_2 -2), 31.8 (CH_2), 29.7 (CH_2), 22.4 ($COCH_3$), 21.6 (CH_2 -5).

Synthesis of compound 66

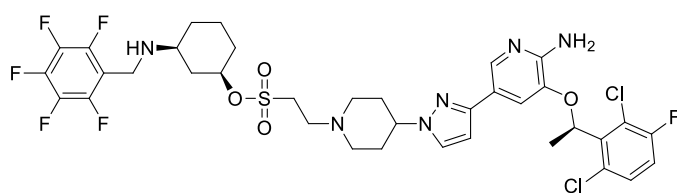
Compound **50** (80 mg, 0.2 mmol) was dissolved in dry CH_2Cl_2 (1 mL) and the solution was cooled at 0 °C. Then, DMAP (1.2 mg 0.01 mmol), NEt_3 (42 μL , 0.3 mmol) and vinyl sulfonylchloride (28 μL , 0.22 mmol) were added. The reaction was let to warm at room temperature, and stirred for 1 hour, until a TLC (AcOEt:Hexanes 1:2) showed the completion of the reaction. Then, the reaction was diluted with CH_2Cl_2 (30 mL) and washed with H_2O (15 mL). The organic phase was dried over Na_2SO_4 , filtered and concentrated. The crude was purified through column chromatography, eluting with AcOEt:hexanes 1:4, giving compound **66** as a colourless oil (85 mg, 0.17 mmol, 87% yield). HRMS (ESI+) m/z : calcd. for $\text{C}_{20}\text{H}_{25}\text{F}_5\text{NO}_5\text{S}$ $[\text{M}+\text{H}]^+$ 486.1368, found 486.1366. ^1H NMR (300 MHz, CDCl_3) δ (ppm): 6.60 – 6.35 (m, 2H, H-vinyl), 6.12 (d, $J=9.6$ Hz, 1H, H-vinyl), 4.53 (brs, 2H, CH_2PFB), 4.48 – 4.39 (m, 1H, H-1), 3.75 (m, 1H, H-3), 2.21 – 2.07 (m, 2H), 1.90 – 1.77 (m, 2H), 1.69 – 1.66 (m, 1H), 1.46 – 1.27 (m, 12H). ^{13}C NMR (75 MHz, CDCl_3) δ (ppm): 154.7 (C=O), 133.5 (CH-vinyl), 129.5 (CH₂-vinyl), 81.1 (Cq, *t*Bu), 80.3 (CH-1), 54.9 (CH-3), 37.4 (CH_2Ph), 36.9 (CH₂), 32.0 (CH₂), 28.8 (CH₂), 28.3 (3C, CH₃ *t*Bu), 21.9 (CH₂). ^{19}F NMR (282 MHz, CDCl_3) δ (ppm): -142.60 (brs, 2F), -154.95 (t, $J=20.8$ Hz, 1F), -161.24 – -162.57 (m, 2F).

Synthesis of compound 67

Compound **66** (11 mg, 0.022 mmol) and **Crizotinib** (5 mg, 0.011 mmol) were dissolved together in a mixture CH_2Cl_2 /iPrOH 5/1 (600 μL). To the solution NEt_3 (1 μL , 0.011 mmol) was added, and the reaction was stirred overnight at room temperature. Afterwards, the solution was concentrated to dryness and the crude was directly purified by column chromatography (CH_2Cl_2 :MeOH 9:1) to give pure compound **67** (9.5 mg, 0.01 mmol, 92%). HRMS (ESI+) m/z : calcd. for $\text{C}_{41}\text{H}_{47}\text{Cl}_2\text{F}_6\text{N}_6\text{O}_6\text{S}$ $[\text{M}+\text{H}]^+$ 935.2524, found 935.2553. ^1H NMR (300 MHz, CDCl_3) δ (ppm): 7.77 (d, $J=1.8$ Hz, 1H), 7.57 – 7.50 (m, 2H), 7.33 (dd, $J=8.9$, 4.8 Hz, 1H), 7.07 (dd, $J=8.9$, 7.9 Hz, 1H), 6.89 (d, $J=1.7$ Hz, 1H), 6.10 (q, $J=6.6$ Hz,

1H), 4.82 (brs, 2H), 4.68 – 4.48 (m, 3H), 4.16 – 4.08 (m, 1H), 3.67 (s, 1H), 3.32 (m, 2H), 3.05 – 3.01 (m, 2H), 2.96 – 2.91 (m, 2H), 2.34 – 2.26 (m, 7H), 1.91 – 1.87 (m, 4H), 1.71 – 1.67 (m, 4H), 1.46 – 1.33 (m, 12H). ¹⁹F NMR (282 MHz, CDCl₃) δ (ppm): - 112.0 (1F), - 42.5 (2F), -154.9 (1F), -161.75, -161.78 -161.93 (2F). Analytical RP-HPLC: t_R = 12.9 (C18, 254 nm, gradient: from 75% solvent H₂O + 0.1% TFA / 25% CH₃CN to 100% CH₃CN over 20 min).

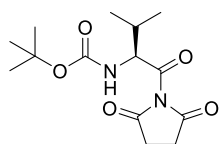
Synthesis of compound 68



Compound **67** (3 mg, 0.003 mmol) was dissolved in CH₂Cl₂ (600 μL) and to this solution TFA (100 μL) was added.

After 1 hour stirring at room temperature, the reaction was concentrated in vacuo to give compound **68** (2.2 mg, 0.0027 mmol, 88% yield). HRMS (ESI+) m/z: calcd. for C₃₆H₃₉Cl₂F₆N₆O₄S [M+H]⁺ 835.2029, found 835.2000. ¹H NMR (300 MHz, CD₃OD) δ (ppm): 8.02 – 7.95 (m, 1H), 7.70 (brs, 1H), 7.63 (d, J=1.6 Hz, 1H), 7.52 (dd, J=9.0, 4.8 Hz, 1H), 7.31 (dd, J=9.0, 8.2 Hz, 1H), 7.17 (d, J=1.6 Hz, 1H), 6.38 (q, J=6.6 Hz, 1H), 4.8 – 4.80 (m, 2H), 4.68 – 4.53 (m, 1H), 4.49 (brs, 2H), 3.97 – 3.92 (m, 2H), 3.82 – 3.77 (m, 2H), 3.71 – 3.66 (m, 2H), 3.54 – 3.43 (m, 1H), 2.4 – 2.35 (m, 4H), 2.33 – 2.21 (m, 2H), 2.09 – 2.06 (m, 1H), 1.97 (d, J=6.6 Hz, 3H), 1.77 (q, J=11.6 Hz, 1H), 1.67 – 1.45 (m, 5H). ¹⁹F NMR (282 MHz, CD₃OD) δ (ppm): -77.12 (s, TFA), -113.95 (s, 1F), -140.13 – -145.14 (m, 2F), -153.43 (t, J=20.2 Hz, 1F), -161.63 – -166.88 (m, 2F). Analytical RP-HPLC: t_R = 8.1 (C18, 254 nm, gradient: from gradient 75% solvent H₂O + 0.1% TFA / 25% CH₃CN to 100% CH₃CN over 20 min).

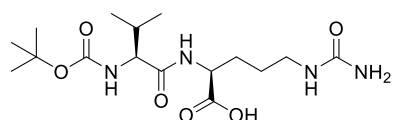
Synthesis of compound 71



To an ice-cooled solution of BocValOH (490 mg, 2.2 mmol) in THF (6 mL), DCC (463 mg, 2.24 mmol) and N-hydroxy succinimide (285 mg, 2.48 mmol) were added. After 10 minutes, the reaction was allowed to reach room temperature, and it was stirred 16 hours. Afterwards, solid was filtered and the solution was concentrated at

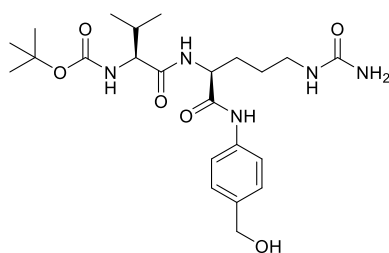
reduced pressure. Crude solid was dissolved in CH_2Cl_2 (100 mL) and organic phase was washed with saturated NaHCO_3 solution (2 x 30 mL). Organic phase was dried over Na_2SO_4 , filtered and concentrated to give compound **71** as a white solid (687 mg, 2.18 mmol, 99%). ^1H NMR (300 MHz, CDCl_3) δ (ppm): 5.05 – 5.02 (m, 1H, NH) 4.60 (dd, $J=9.2$, 4.9 Hz, H- α), 2.85 (s, 4H), 2.35 – 2.26 (m, 1H, H- β), 1.08 (d, $J=6.9$ Hz, 3H, CH_3), 1.05 (d, $J=6.8$ Hz, 3H, CH_3). [73]

Synthesis of compound 72



To an ice-cooled solution of (687 mg, 2.18 mmol) in DME (5 mL), a solution of Citrulline (573 mg, 3.27 mmol) and NaHCO_3 (274 mg, 3.27 mmol) in H_2O (5 mL) was added. The reaction was kept at 0 °C for 30 minutes, then it was warmed at room temperature and stirred 16 hours. Afterwards, it was stopped by adding H_2O (10 mL) and a saturated NaHCO_3 solution (1 mL). Resulting mixture was washed with AcOEt (30 mL) and the aqueous phase was acidified with HCl at pH 3. Product was extracted using 25% of $i\text{PrOH}$ in CHCl_3 (3 x 60 mL). Organic phase was dried over Na_2SO_4 , filtered and concentrated to give compound **72** (609 mg, 1.63 mmol, 75% yield). Crude product was used for the next step without further purification. ^1H NMR (300 MHz, CDCl_3) δ (ppm): 7.58 (brs, 1H), 6.07 (brs, 1H), 5.69 (m, 1H), 4.49 (brs, 1H), 4.01 (m, 1H), 3.13 (brs, 2H), 2.06 (m, 1H), 1.90 (m, 1H), 1.75 (m, 1H), 1.55 (m, 2H), 1.42 (s, 9H), 0.92 (m, 6H). MS (ESI+) m/z 397.22 (MNa^+).

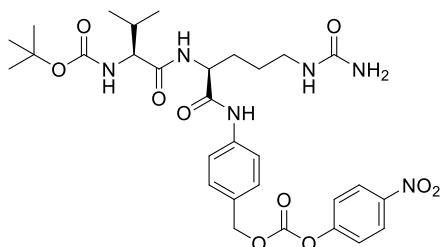
Synthesis of compound 73



Compound **72** (200 mg, 0.40 mmol) was dissolved in CH_2Cl_2 (2 mL) and MeOH (1 mL) and to the resulting solution PABA-OH (79 mg, 0.64 mmol) and EEDQ (195 mg, 0.80 mmol) were added. The reaction was stirred at room temperature and in darkness for 16 hours, and then it was concentrated at reduced pressure. The crude solid was purified by column chromatography (CH_2Cl_2 : MeOH 7:1) to give pure compound **73** (146 mg, 0.30 mmol) with 77% yield. ^1H NMR (300 MHz, CD_3OD) δ (ppm): 7.57 (d, $J=8.5$ Hz, 2H, H-Arom.),

7.31 (d, $J=8.5$ Hz, 2H, H-arom.), 4.57 (s, 3H, H- α , CH_2Ph), 3.95 (m, 1H, H- α), 3.26 – 2.98 (m, 2H, H- β Cit), 2.25 – 2.00 (m, 1H), 1.95 – 1.83 (m, 1H), 1.86 – 1.71 (m, 1H), 1.67 – 1.53 (m, 2H), 0.99 (d, $J=6.8$ Hz, 3H, $\text{CH}_3\text{-Val}$), 0.95 (d, $J=6.8$ Hz, 3H, $\text{CH}_3\text{-Val}$). MS (ESI+) m/z 480.28 (MH+).^[74]

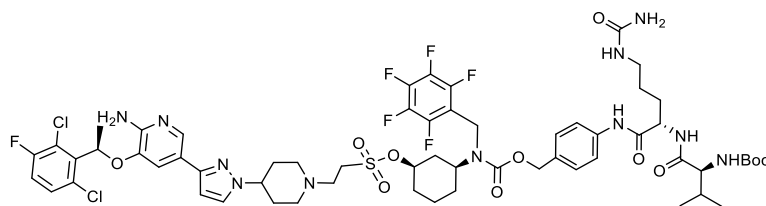
Synthesis of compound 74



To a solution of compound **73** (146 mg, 0.30 mmol) in DMF (3 mL) bis-4-nitrophenyl carbonate (463 mg, 1.52 mmol) and DIPEA (270 μL , 1.52 mmol) were added. After 5 hours at room temperature, a TLC showed no more starting material and the solution

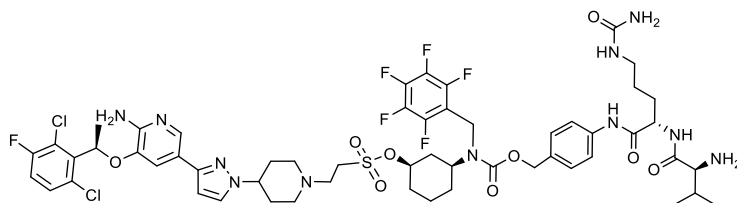
was concentrated at reduced pressure. Crude product was purified by column chromatography ($\text{CH}_2\text{Cl}_2\text{:MeOH}$ 8:1) to give pure compound **74** (109 mg, 0.17 mmol) with 57% yield. HRMS (ESI+) m/z : calcd. for $\text{C}_{30}\text{H}_{40}\text{N}_6\text{NaO}_{10}$ $[\text{M}+\text{Na}]^+$ 667.2698, found 667.2695. ^1H NMR (400 MHz, CD_3OD) δ (ppm): 8.36 – 8.27 (m, 2H, Arom.), 7.74 – 7.62 (m, 2H, Arom.), 7.51 – 7.39 (m, 4H, Arom.), 5.27 (s, 2H, OCH_2Ph), 4.62 – 4.51 (m, 1H, H- α), 3.93 (d, $J=6.7$ Hz, 1H, H- α), 3.27 – 3.20 (m, 1H, H- δ Cit), 3.16 – 3.09 (m, 1H, H- γ Cit), 2.10 – 2.02 (m, 1H, H- β Val), 2.00 – 1.86 (m, 1H, H- β Cit), 1.78 (m, 1H, H- β Cit), 1.71 – 1.53 (m, 2H, H- γ Cit), 1.46 (s, 9H, Boc), 0.99 (d, $J=6.8$ Hz, 3H, CH_3 Val), 0.96 (d, $J=6.8$ Hz, 3H, CH_3 Val). ^{13}C NMR (75 MHz, CD_3OD) δ (ppm): 173.3 (C=O amide), 171.0 (C=O amide), 160.9 (C=O), 156.8 (C=O), 155.8 (C=O), 152.6 (Cq), 145.5 (Cq), 138.8 (Cq), 130.6 (Cq), 129.1 (2C, CH-arom.), 124.9 (2C, CH-arom.), 121.9 (2C, CH-arom.), 119.8 (2C, CH-arom.), 79.3 (Cq Boc), 70.2 (OCH_2Ph), 60.4 (CH- α Val), 53.5 (CH- α Cit), 38.9 ($\text{CH}_2\text{-}\delta$ Cit), 30.5 (CH- β Val), 29.1 ($\text{CH}_2\text{-}\beta$ Cit), 27.3 (3C, CH_3 Boc), 26.4 ($\text{CH}_2\text{-}\gamma$ Cit), 18.3 (CH_3 Val), 17.2 (CH_3 Val).

Synthesis of compound 75



Compound **74** (9 mg, 0.02 mmol) was dissolved in CH₃CN (200 uL) and DMF (60 uL). To this solution HOAt (4 mg, 0.029 mmol), DIPEA (5 uL, 0.058 mmol) and a solution of compound **68** (10 mg, 0.011 mmol) in CH₃CN (200 uL) were added. The reaction mixture was stirred 16 hours at room temperature and then concentrated. Compound **75** (8 mg, 0.006 mmol, 30% yield) was purified by flash column chromatography on silica gel, eluting with CH₂Cl₂:MeOH 10:1. HRMS (ESI+) *m/z*: calcd. for C₆₀H₇₄Cl₂F₆N₁₁O₁₁ [M+H]⁺ 1340.4566, found 1340.4571. Analytical RP-HPLC: *t_R* = 11.9 (C18, 254 nm, gradient: from gradient 75% solvent H₂O + 0.1% TFA / 25% CH₃CN to 100% CH₃CN over 20 min).

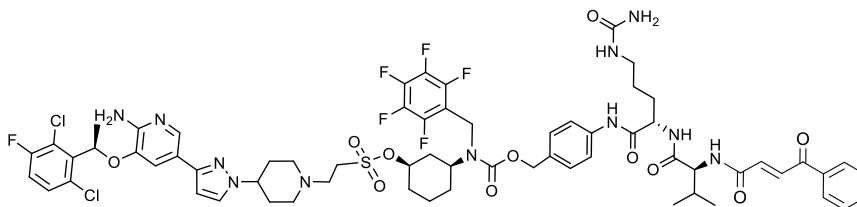
Synthesis of compound 76



Compound **75** (8 mg, 0.006 mmol) was dissolved in CH₂Cl₂ (400 uL) and TFA (50 uL) was added to the solution. After 1 hour at room temperature, analytical HPLC showed completion of the reaction, which was concentrated at reduced pressure. Resulting crude was purified by preparative HPLC on a Phenomenex Luna C18(2) column (10 μ, 250 mm x 21.2 mm) using the following gradient: from 75% H₂O + 0.1% TFA / 25% CH₃CN to 35% H₂O + 0.1% TFA / 65% CH₃CN. Fractions containing product by mass (*t_R*=21.5) were lyophilized to give compound **76** (3 mg, 0.0024 mmol, 40% yield). HRMS (ESI+) *m/z*: calcd. for C₅₅H₆₆Cl₂F₆N₁₁O₉S [M+H]⁺ 1240.4041, found 1240.3990.

Analytical RP-HPLC: $t_R = 11.2$ (C18, 254 nm, gradient: from gradient 65% solvent H₂O + 0.1% TFA / 35% CH₃CN to 35% solvent H₂O + 0.1% TFA / 65% CH₃CN over 30 min).

Synthesis of compound 70



trans-3-benzoyl acrylic acid (17 mg, 0.094 mmol) was dissolved in dry DMF (0.33 mL) and cooled at -10 °C. Isobutyl chloroformate (15 μ L, 0.11 mmol) and *N*-methylmorpholine (12 μ L, 0.11 mmol) were then added under stirring. 23 μ L of this solution was added to a solution of compound **76** (3 mg, 0.0024 mmol) in dry DMF (0.2 mL) cooled at -10 °C. After stirring for 15 min at -10 °C, the reaction was allowed to reach room temperature and kept stirring for an additional 1 h. Subsequently, the crude mixture was diluted with CH₃CN and purified by HPLC on a Phenomenex Luna C18(2) column (10 μ , 250 mm x 21.2 mm) using the following method: 65% H₂O / 35% CH₃CN to 35% H₂O / 65% CH₃CN over 30 min. Product containing fractions by mass ($t_R = 20.5$) were collected and lyophilized overnight to obtain compound **70** as a white solid (0.6 mg, 0.4 μ mol, 21% yield). HRMS (ESI+) m/z : calcd. for C₆₅H₇₂Cl₂F₆N₁₁O₁₁S [M+Na]⁺ 1398.4409, found 1398.4425. Analytical RP-HPLC: $t_R = 19.1$ (C18, 254 nm, gradient: from gradient 65% solvent H₂O + 0.1% TFA / 35% CH₃CN to 35% solvent H₂O + 0.1% TFA / 65% CH₃CN over 30 min).

6.5.2 NMR study of the Grob fragmentation

Compound **39** was dissolved in a mixture 1:1 of MeOH/ buffer (PBS, NaPi 0.1M pH 8.0, NaPi 0.1 M pH 9.3) or MeOH/H₂O at a final 20 Mm concentration. After 12 hours the solution was concentrated ad reduced pressure and an NMR in CD₃OD was recorded. Compounds **42**, **47**, **48**, **55**, **57**, **60** and **61** were dissolved in a mixture 1:1 of CD₃CN/ deuterated buffer (PBS, NaPi 0.1 M pH 6.0, NaPi 0.1 M pH 8.0; for compound **60** and **61** only PBS buffer was used) at a final 5 mM concentration. When compound was not

completely soluble, more amount of organic solvent was added. NMR tubes were incubated at 37°C and spectra were recorded at different times, depending on the reaction kinetics.

6.5.3 UPLC release of crizotinib derivative from 67 and 68

To monitor Crizotinib-derivative **69** release in different conditions by UPLC, compound **67** and **68** were dissolved at 0.5 mM concentration in MeOH/PBS buffer and incubated at 37 °C. At 0, 4, 8, 12 and 24 hours incubation, a 100 µL aliquot was taken, and kept at -20 °C until the time of the analysis. To analyse the proceeding of the reaction, aliquots taken were diluted 1:10 with MeOH, and 5 µL of the diluted solution were analysed by using Ultra Performance Liquid Chromatography-Mass Spectrometer (UPLC-MS) (Bruker micrOTOF-Q). Column: ACQUITY UPLC BEH C18 1,7; diameter: 2.1 mm and length: 100 mm. Samples were eluted following gradient: 1:99 to 60:40 CH₃CN:H₂O for 6 min, then 60:40 to 100:0 CH₃CN:H₂O over 0.5 minutes, with a flow of 0.45 mL/min.

6.6 References

- [1] A. Alouane, R. Labruère, T. Le Saux, F. Schmidt, L. Jullien, *Angew. Chemie - Int. Ed.* **2015**, *54*, 7492–7509.
- [2] C. D. Spicer, B. G. Davis, *Nat. Commun.* **2014**, *5*, 4740.
- [3] J. Yan, S. Lee, A. Zhang, J. Yoon, *Chem. Soc. Rev.* **2018**, *47*, 6900–6916.
- [4] C. A. Blencowe, A. T. Russell, F. Greco, W. Hayes, D. W. Thornthwaite, *Polym. Chem.* **2011**, *2*, 773–790.
- [5] F. M. H. De Groot, C. Albrecht, R. Koekkoek, P. H. Beusker, H. W. Scheeren, *Angew. Chemie - Int. Ed.* **2003**, *42*, 4490–4494.
- [6] S. C. Jeffrey, J. B. Andreyka, S. X. Bernhardt, K. M. Kissler, T. Kline, J. S. Lenox, R. F. Moser, M. T. Nguyen, N. M. Okeley, I. J. Stone, et al., *Bioconjug. Chem.* **2006**, *17*, 831–840.
- [7] P. D. Senter, W. E. Pearce, R. S. Greenfield, *J. Org. Chem.* **1990**, *55*, 2975–2978.
- [8] R. Walther, J. Rautio, A. N. Zelikin, *Adv. Drug Deliv. Rev.* **2017**, *118*, 65–77.
- [9] X. Li, Y. Hou, X. Meng, C. Ge, H. Ma, J. Li, J. Fang, *Angew. Chemie Int. Ed.* **2018**, *57*, 6141–6145.
- [10] T. Legigan, J. Clarhaut, I. Tranoy-Opalinski, A. Monvoisin, B. Renoux, M. Thomas, A. Le Pape, S. Lerondel, S. Papot, *Angew. Chemie Int. Ed.* **2012**, *51*, 11606–11610.
- [11] A. D. Corso, S. Cazzamalli, M. Mattarella, D. Neri, *Bioconjug. Chem.* **2017**, *28*, 1826–1833.
- [12] K. Haba, M. Popkov, M. Shamis, R. A. Lerner, C. F. Barbas III, D. Shabat, *Angew. Chemie Int. Ed.* **2005**, *44*, 716–720.
- [13] M. P. Hay, B. M. Sykes, A. Denny, C. J. O. Connor, *J. Chem. Soc. Perkin Trans. 1* **1999**, 2759–2770.
- [14] D. R. Kim, T. S. Kim, E. Kim, S. J. Min, D. Shin, D. R. Ahn, *Bioorganic Med. Chem. Lett.* **2014**, *24*, 209–213.
- [15] A. Ortiz, C. S. Shanahan, D. T. Sisk, S. C. Perera, P. Rao, D. V McGrath, *J. Org. Chem.* **2010**, *75*, 6154–6162.
- [16] R. A. Mosey, P. E. Floreancig, *Org. Biomol. Chem.* **2012**, *10*, 7980–7985.
- [17] Z. Deng, S. Yuan, R. X. Xu, H. Liang, S. Liu, *Angew. Chemie - Int. Ed.* **2018**, *57*, 8896–8900.
- [18] M. Shamis, H. N. Lode, D. Shabat, *J. Am. Chem. Soc.* **2004**, *126*, 1726–1731.

- [19] R. Erez, D. Shabat, *Org. Biomol. Chem.* **2008**, *6*, 2669–2672.
- [20] H. Y. Lee, X. Jiang, D. Lee, *Org. Lett.* **2009**, *11*, 2065–2068.
- [21] S. S. Matikonda, J. M. Fairhall, J. D. A. Tyndall, S. Hook, A. B. Gamble, *Org. Lett.* **2017**, *19*, 528–531.
- [22] R. Weinstain, E. Segal, R. Satchi-Fainaro, D. Shabat, *Chem. Commun.* **2010**, *46*, 553–555.
- [23] L. R. Staben, S. G. Koenig, S. M. Lehar, R. Vandlen, D. Zhang, J. Chuh, S.-F. Yu, C. Ng, J. Guo, Y. Liu, et al., *Nat. Chem.* **2016**, *8*, 1112–1119.
- [24] S. Huvelle, A. Alouane, T. Le Saux, L. Jullien, F. Schmidt, *Org. Biomol. Chem.* **2017**, *15*, 3435–3443.
- [25] O. A. Okoh, P. Klahn, *ChemBioChem* **2018**, *19*, 1668–1694.
- [26] M. A. Dewit, E. R. Gillies, *J. Am. Chem. Soc.* **2009**, *131*, 18327–18334.
- [27] C. de Gracia Lux, C. L. McFearin, S. Joshi-Barr, J. Sankaranarayanan, N. Fomina, A. Almutairi, *ACS Macro Lett.* **2012**, *1*, 922–926.
- [28] S. Chen, X. Zhao, J. Chen, J. Chen, L. Kuznetsova, S. S. Wong, I. Ojima, *Bioconjug. Chem.* **2010**, *21*, 979–987.
- [29] L. Hu, T. Quach, S. Han, S. F. Lim, P. Yadav, D. Senyschyn, N. L. Trevaskis, J. S. Simpson, C. J. H. Porter, *Angew. Chemie Int. Ed.* **2016**, *55*, 13700–13705.
- [30] H. Wang, Q. Huang, H. Chang, J. Xiao, Y. Cheng, *Biomater. Sci.* **2016**, *4*, 375–390.
- [31] R. Amir, N. Pessah, M. Shamis, D. Shabat, *Angew. Chemie - Int. Ed.* **2003**, *42*, 4494–4499.
- [32] M. Shamis, D. Shabat, *Chem. – A Eur. J.* **2007**, *13*, 4523–4528.
- [33] A. Sagi, R. Weinstain, N. Karton, D. Shabat, *J. Am. Chem. Soc.* **2008**, *130*, 5434–5435.
- [34] T. H. Pillow, M. Schutten, S.-F. Yu, R. Ohri, J. Sadowsky, K. A. Poon, W. Solis, F. Zhong, G. Del Rosario, M. A. T. Go, et al., *Mol. Cancer Ther.* **2017**, *16*, 871–878.
- [35] P. D. Senter, E. L. Sievers, *Nat. Biotechnol.* **2012**, *30*, 631–637.
- [36] M. J. Matos, C. D. Navo, T. Hakala, X. Ferhati, A. Guerreiro, D. Hartmann, B. Bernardim, K. L. Saar, I. Compañón, F. Corzana, et al., *Angew. Chemie Int. Ed.* **2019**, *58*, 6640–6644.
- [37] B. Bernardim, M. J. Matos, X. Ferhati, I. Compañón, A. Guerreiro, P. Akkapeddi, A. C. B. Burtoloso, G. Jiménez-Osés, F. Corzana, G. J. L. Bernardes, *Nat. Protoc.* **2019**,

- 14, 86–99.
- [38] G. M. Dubowchik, R. A. Firestone, L. Padilla, D. Willner, S. J. Hofstead, K. Mosure, J. O. Knipe, S. J. Lasch, P. A. Trail, *Bioconjug. Chem.* **2002**, *13*, 855–869.
- [39] R. A. McBride, E. R. Gillies, *Macromolecules* **2013**, *46*, 5157–5166.
- [40] G. Liu, G. Zhang, J. Hu, X. Wang, M. Zhu, S. Liu, *J. Am. Chem. Soc.* **2015**, *137*, 11645–11655.
- [41] F. M. H. De Groot, W. J. Loos, R. Koekkoek, L. W. A. Van Berkom, G. F. Busscher, A. E. Seelen, C. Albrecht, P. De Bruijn, H. W. Scheeren, *J. Org. Chem.* **2001**, *66*, 8815–8830.
- [42] M. A. Drahl, M. Manpadi, L. J. Williams, *Angew. Chemie Int. Ed.* **2013**, *52*, 11222–11251.
- [43] K. Prantz, J. Mulzer, *Chem. Rev.* **2010**, *110*, 3741–3766.
- [44] C. A. Grob, *Angew. Chemie - Int. Ed.* **1969**, *8*, 535–546.
- [45] A. Eschenmoser, A. Frey, *Helv. Chim. Acta* **1952**, *35*, 1660–1666.
- [46] A. T. Bottini, C. A. Grob, E. Schumacher, J. Zergenyi, *Helv. Chim. Acta* **1966**, *49*, 2516–2524.
- [47] C. M. Amann, P. V. Fisher, M. L. Pugh, F. G. West, *J. Org. Chem.* **1998**, *63*, 2806–2807.
- [48] W. Zhang, P. Dowd, *Tetrahedron Lett.* **1996**, *37*, 957–960.
- [49] G. Mehta, R. S. Kumaran, *Tetrahedron Lett.* **2005**, *46*, 8831–8835.
- [50] G. Barbe, M. St-Onge, A. B. Charette, *Org. Lett.* **2008**, *10*, 5497–5499.
- [51] X.-S. Peng, H. N. C. Wong, *Chem. – An Asian J.* **2006**, *1*, 111–120.
- [52] R. Villagómez-Ibarra, C. Alvarez-Cisneros, P. Joseph-Nathan, *Tetrahedron* **1995**, *51*, 9285–9300.
- [53] D. Renneberg, H. Pfander, C. J. Leumann, *J. Org. Chem.* **2000**, *65*, 9069–9079.
- [54] O. V. Larionov, E. J. Corey, *J. Am. Chem. Soc.* **2008**, *130*, 2954–2955.
- [55] J. Barluenga, M. Álvarez-Pérez, K. Wuerth, F. Rodríguez, F. J. Fañanás, *Org. Lett.* **2003**, *5*, 905–908.
- [56] A. S. Kende, I. Káldor, *Tetrahedron Lett.* **1989**, *30*, 7329–7332.
- [57] G. W. Kabalka, N.-S. Li, D. Tejedor, R. R. Malladi, S. Trotman, *J. Org. Chem.* **1999**, *64*, 3157–3161.
- [58] J. A. Marshall, G. L. Bundy, *J. Am. Chem. Soc.* **1966**, *88*, 4291–4292.

- [59] S. V Ley, A. Antonello, E. P. Balskus, D. T. Booth, S. B. Christensen, E. Cleator, H. Gold, K. Högenauer, U. Hüniger, R. M. Myers, et al., *Proc. Natl. Acad. Sci. U. S. A.* **2004**, *101*, 12073–12078.
- [60] U. Burckhardt, C. A. Grob, H. R. Kiefer, *Helv. Chim. Acta* **1967**, *50*, 231–244.
- [61] D. N. Kevill, Z. H. Ryu, M. J. D'Souza, *Eur. J. Chem.* **2017**, *8*, 162–167.
- [62] A. Choi, S. C. Miller, *Org. Biomol. Chem.* **2017**, *15*, 1346–1349.
- [63] T. Nagase, T. Takahashi, T. Sasaki, H. Kitazawa, M. Kanosaka, R. Yoshimoto, *J. Med. Chem. Lett.* **2009**, *52*, 4111–4114.
- [64] “Dissociation constants of organic acids and bases,” can be found under https://labs.chem.ucsb.edu/zhang/liming/pdf/pKas_of_Organic_Acids_and_Bases.pdf, **n.d.**
- [65] E. P. Gillis, K. J. Eastman, M. D. Hill, D. J. Donnelly, N. A. Meanwell, *J. Med. Chem.* **2015**, *58*, 8315–8359.
- [66] J. R. Casey, S. Grinstein, J. Orłowski, *Nat. Rev. Mol. Cell Biol.* **2009**, *11*, 50–61.
- [67] M. E. Jung, G. Piizzi, *Chem. Rev.* **2005**, *105*, 1735–1766.
- [68] J. R. Casey, S. Grinstein, J. Orłowski, *Nat. Rev. Mol. Cell Biol.* **2009**, *11*, 50–61.
- [69] A. Sgambato, F. Casaluce, P. Maione, C. Gridelli, *Expert Rev. Anticancer Ther.* **2018**, *18*, 71–80.
- [70] J. J. Cui, M. Tran-Dubé, H. Shen, M. Nambu, P. Kung, M. Pairish, L. Jia, J. Meng, L. Funk, I. Botrous, et al., *J. Med. Chem.* **2011**, *54*, 6342–6363.
- [71] M. M. Awad, R. Katayama, M. McTigue, W. Liu, Y.-L. Deng, A. Brooun, L. Friboulet, D. Huang, M. D. Falk, S. Timofeevski, et al., *N. Engl. J. Med.* **2013**, *368*, 2395–2401.
- [72] B. Wei, J. Gunzner-Toste, H. Yao, T. Wang, J. Wang, Z. Xu, J. Chen, J. Wai, J. Nonomiya, S. P. Tsai, et al., *J. Med. Chem.* **2018**, *61*, 989–1000.
- [73] R. J. Cregge, S. L. Durham, R. A. Farr, S. L. Gallion, C. M. Hare, R. V. Hoffman, M. J. Janusz, H. O. Kim, J. R. Koehl, S. Mehdi, et al., *J. Med. Chem.* **1998**, *41*, 2461–2480.
- [74] S. Boyd, L. Chen, S. Gangwar, V. Guerlavais, K. Horgan, L. Zhi-Hong, S. Bilal, *Chemical Linkers and Conjugates Thereof*, **2005**, WO2005112919 A2.

Conclusions

- 7.1 Conclusions
- 7.2 Conclusiones
- 7.3 Scientific publications derived from this dissertation
- 7.4 Other scientific publications
- 7.5 Contribution to congresses

7.1 Conclusions

The following conclusions can be drawn from the results obtained along this PhD dissertation:

- Carbonyl acrylamide technology was applied to the synthesis of homogeneous ADCs. This methodology is cysteine selective, presents fast kinetic and allows modification of proteins and antibodies with high conversion.
Derivatives of highly cytotoxic drugs, such as MMAE and Crizotinib, equipped with a carbonyl acrylamide scaffold were synthesised, proving the synthetic accessibility of the reagents even when dealing with very complex structures. These compounds were then conjugated to an engineered Trastuzumab antibody (Thiomab), giving as a result a homogeneous ADC with DAR = 2. Importantly, the modification yields a stable conjugate, improving results obtained with other accepted methodologies, and does not induce significant modification in the antibody structure, as demonstrated by binding assays.
- In a similar way, quaternised vinyl pyridinium reagents were used for modification of proteins and antibodies. Studies performed on small molecules showed that quaternised vinyl pyridinium scaffolds were extremely reactive and selective towards cysteine. This property makes them ideal candidates for site-selective protein and antibody modification, as corroborated by reactions with various protein scaffolds. Also, final conjugates present high stability in plasma. As a proof of concept, a MMAE derivative bearing the vinyl pyridinium tag was synthesized. This compound was used for the conjugation with antibodies to generate a homogenous and fully functional ADC with DAR = 2. Notably, the ADC conserves the binding properties of the original antibody, resulting interesting for *in vitro* and *in vivo* biological applications.
- The synthesis and the kinetics studies of several linkers based on the acetal group were also performed. The acetal group was used to generate a prodrug and a pre-fluorophore starting from duocarmycin and coumarin, respectively. Markedly,

these small molecules are fully stable in plasma but readily hydrolysed in acid conditions allowing conditional release. Therefore, the acetal-based linker was applied to the synthesis of a SMDC and an ADC. Regarding the SMDC study, acetal based pro-drug showed comparable toxicity with the parental drug, suggesting that the acetal group is cleaved, and the active form of the drug is released inside the cell. Concerning the ADC, very few examples of acetal-based linkers have been described to date for application in ADC synthesis, despite the well-known acid labile behaviour of this moiety. In this work, we have conjugated the acetal linker bearing duocarmycin and coumarin to Thiomab, obtaining homogenous conjugates with DAR = 2. With these conjugates in hand, we have demonstrated that their properties are closely related not only to the microenvironment of the conjugation site, but also to the nature of the payload. In fact, our results showed that two ADC featuring the same acetal linker but varying exclusively on the payload present completely different stability in plasma. Extensive MD simulations performed on the ADCs were essential to explain how the different 3D orientation of the linker-payload could be responsible for this difference in stability. This unexpected finding enhances the importance of payload choice in ADC synthesis.

- The Grob fragmentation was studied under physiological mimicking conditions. For this purpose, several Grob fragmentation substrates were synthesized and their reactivity was evaluated under different conditions and at different pH values, producing the release of a fluorophore or a drug. We went one step further and changed the free amine for an amide or carbamate, allowing the total control of release of the payload. The combination of the Grob fragmentation substrate with an enzymatically cleavable linker would allow controlled intracellular drug release. These outcomes point out that Grob fragmentation substrates can act as novel self-immolative spacers in controlled drug release.

7.2 Conclusiones

Del trabajo desarrollado en esta tesis doctoral se pueden extraer las siguientes conclusiones:

- Se ha aplicado con éxito la utilización de carbonil acrilamidas para la síntesis de conjugados fármaco-anticuerpo (ADC). Estos derivados de acrilamida reaccionan rápidamente y de forma selectiva con los residuos de cisteína del anticuerpo, permitiendo así la modificación de proteínas y anticuerpos con alta conversión. Dichas carbonil acrilamidas se han acoplado satisfactoriamente a fármacos muy tóxicos, como el MMAE o el Crizotinib, lo que demuestra la accesibilidad sintética de los reactivos, incluso cuando se trata de estructuras muy complejas. Además, estos compuestos se han conjugado con una versión modificada del Trastuzumab, generando un ADC homogéneo, con una relación fármaco/anticuerpo = 2. Es importante destacar que la modificación produce un conjugado estable, mejorando los resultados obtenidos con otras metodologías muy utilizadas, y no afecta de forma significativa a la estructura y actividad del anticuerpo.
- Se han utilizado reactivos de vinil piridinio cuaternizados para la modificación selectiva de proteínas y anticuerpos. Los estudios realizados en moléculas pequeñas han mostrado que los compuestos de vinil piridinio cuaternizados son también extremadamente reactivos y selectivos para cisteína. Además, los conjugados finales presentan alta estabilidad en plasma. Como ejemplo, se sintetizó un derivado de MMAE acoplado a un de vinilo piridinio. Este compuesto se usó para la conjugación con anticuerpos para generar un ADC homogéneo y completamente funcional con DAR = 2. El ADC conserva las propiedades de unión del anticuerpo original, resultando interesante para aplicaciones biológicas.
- Se han realizado estudios de síntesis y cinética de varios *linkers* basados en acetales. Estos acetales se han utilizado para generar un pre-fármaco de duocarmicina y un fluoróforo de derivado de cumarina. Estas pequeñas moléculas son completamente estables en plasma, pero se hidrolizan fácilmente en condiciones ácidas permitiendo así la liberación controlada del fármaco o del fluoróforo. El *linker* con el derivado de duocarmicina se ha unido a una pequeña molécula (acetazolamida) y a un anticuerpo, dando lugar a un SMDC o a un ADC, respectivamente. En el caso del conjugado SMDC, el pre-fármaco mostró una toxicidad *in vitro* comparable a la

duocarmicina libre, lo que sugiere que el grupo acetal se rompe y la forma activa del fármaco se libera dentro de la célula. Con respecto al ADC, se ha conjugado los acetales que contienen duocarmicina y cumarina con Thiomab, obteniendo así ADC homogéneos con relación fármaco-anticuerpo = 2. Una vez obtenidos estos conjugados, se ha demostrado que su estabilidad están relacionadas no solo con el del sitio de conjugación, sino también con el tipo de compuesto que se ha conjugado. De hecho, nuestros resultados han mostrado que dos ADC con el mismo *linker* pero que varían exclusivamente en la presencia del fármaco o del fluoróforo presentan una estabilidad completamente diferente en el plasma. Simulaciones MD realizadas sobre los ADC fueron esenciales para explicar cómo las diferentes disposiciones de los *linkers* podrían ser responsables de esta diferencia en la estabilidad. Este resultado puede ser relevante a la hora de seleccionar el fármaco/fluoróforo en la síntesis de ADC.

- La fragmentación de Grob se ha estudiado en condiciones similares a las fisiológicas. Para ello, se han sintetizado varios sustratos de fragmentación de Grob y se ha evaluado su reactividad en diferentes condiciones y a diferentes valores de pH, produciendo la liberación de un fluoróforo o de un fármaco. La sustitución de la amina libre por una amida o carbamato ha permitido el control total de la liberación del fármaco. La combinación del sustrato de fragmentación de Grob con un *linker* labil a la acción de enzimas presentes en células tumorales permitirá la liberación controlada del fármaco una vez alcanzado el tumor. Estos resultados demuestran que los sustratos que dan la fragmentación de Grob pueden actuar como nuevos *linkers* autoinmolativos en la liberación controlada de fármacos.

7.3 Scientific publications derived from this dissertation

- ❖ Derived from [Chapter 4](#): Efficient and irreversible antibody–cysteine bioconjugation using carbonylacrylic reagents.
B. Bernardim, M.J. Matos, [X. Ferhati](#), I. Compañón, A. Guerreiro, P. Akkapeddi, A. C. B. Burtoloso, G. Jiménez-Osés, F. Corzana, G. J. L. Bernardes.
Nature Protocols, **2019**, *14*, 86-99.

- ❖ Derived from Chapter 4: Quaternization of Vinyl/Alkynyl Pyridine Enables Ultrafast Cysteine-Selective Protein Modification and Charge Modulation.
M. Matos, C. D. Navo, T. Hakala, X. Ferhati, A. Guerreiro, D. Hartmann, B. Bernardim, K. L. Saar, I. Compañón, F. Corzana, T. P. J. Knowles, G. Jiménez-Osés, G. J. L. Bernardes.
Angewandte Chemie – International Edition, **2019**, *58*, 6640-6644.

- ❖ Derived from Chapter 5: Acetals as Efficient Acid-Sensitive Cleavable Linkers for Targeted Drug-Delivery.
X. Ferhati, P. Akkapeddi, E. Jiménez Moreno, M. J. Matos, N. Salaverri, G. Jiménez-Osés, G. J. L. Bernardes, F. Corzana.
Submitted

7.4 Other scientific publications

- ❖ Dual targeting of PTP1B and glucosidases with new bifunctional iminosugar inhibitors to address type 2 diabetes.
X. Ferhati, C. Matassini, M. G. Fabbrini, A. Goti, A. Morrone, F. Cardona, A. J. Moreno-Vargas, P. Paoli.
Bioorganic Chemistry, **2019**, *87*, 534-549.

- ❖ Probing the influence of linker length and flexibility in the design and synthesis of new trehalase inhibitors.
G. D'Adamio, M. Forcella, P. Fusi, P. Parenti, C. Matassini, X. Ferhati, C. Vanni, F. Cardona.
Molecules, **2018**, *23*, 436.

- ❖ Antigenic GM3 Lactone Mimetic Molecule Integrated Mannosylated Glycopeptide Nanofibers for the Activation and Maturation of Dendritic Cells.
G. Gunay, M. Sardan Ekiz, X. Ferhati, B. Richichi, C. Nativi, A. B. Tekinay, M. O. Guler.

ACS Applied Materials and Interfaces, **2017**, *9*, 16035-16042.

- ❖ Polyhydroxyamino-piperidine-type iminosugars and pipercolic acid analogues from a D -mannose-derived aldehyde.
C. Matassini, S. Mirabella, X. Ferhati, C. Faggi, I. Robina, A. Goti,
European Journal of Organic Chemistry, **2014**, *25*, 5419-5432.

- ❖ A Structurally Simple Therapeutic Vaccine Against Triple Negative Breast Cancer Reduces Tumor-Size and Lung Metastasis in Mice: One Step Towards a Human Vaccine.
A. Amedei, F. Asadzadeh, F. Papi, M. Vannucchi, M. Fragai, I. Bermejo, V. Ferrucci, C. Vieira De Almeida, L. Cerofolini, S. Giuntini, M. Bombaci, E. Pesce, E. Niccolai, F. Natali, E. Guarini Grisaldi Del Taja, F. Gabel, X. Ferhati, C. Traini, S. Catarinichia, F. Corzana, F. Berti, M. Zollo, R. Grifantini, C. Nativi.
Submitted

7.5 Contribution to congresses

- ❖ Poster presentation: *The use of Grob fragmentation in controlled drug release*.
X. Ferhati, G. Bernardes, F. Corzana. 2nd PSL Chemical Biology Symposium.
Paris, 17-18th of 2019.

- ❖ Poster Presentation: *A new antibody drug conjugate using cysteine selective carbonylacrylic reagent*. X. Ferhati, I. Compañón, M. J. Matos, G. Bernardes, F. Corzana. 16th Iberian Peptide Meeting (16EPI) / 4th Chemical Biology Group Meeting (4GEQB). Barcelona, 5-7th of 2018.

- ❖ Poster presentation: *Design of acid cleavable linkers ready to use in Drug Delivery*. X. Ferhati, G. Bernardes, F. Corzana. Reunión Bienal de la Real Sociedad Española de Química. Sitges (Spain). June 25-29th of 2017.

- ❖ Poster presentation: *Antibody-drug conjugation through an acid cleavable linker*. X. Ferhati, F. Corzana, J. Castro-López, R. Hurtado-Guerrero. XIII Simposio de Investigadores Jóvenes RSEQ – Sigma Aldrich. Logroño (Spain). November 8-11th of 2016.

Supplementary informations

- 8.1 Reagents and general synthetic procedures**
- 8.2 General protein conjugation methods**
- 8.3 Supplementary information of *Chapter 4***
- 8.4 Supplementary information of *Chapter 5***
- 8.5 Supplementary information of *Chapter 6***

8.1 Reagents and general synthetic procedures

Commercial reagents were used without further purification. Analytical thin layer chromatography (TLC) was performed on Macherey-Nagel precoated aluminium sheets with a 0.20 mm thickness of silica gel 60 with fluorescent indicator UV254. TLC plates were visualized with UV light and by staining with phosphomolybdic acid (PMA) solution (5 g of PMA in 100 mL of absolute ethanol), KMnO_4 solution or sulfuric acid-ethanol solution (1:20). Column chromatography was performed on silica gel (230–400 mesh). ^1H , ^{13}C NMR and ^{19}F NMR spectra were measured with a 500 MHz, 400 MHz or 300 MHz spectrometers with TMS as the internal standard. Multiplicities are quoted as singlet (s), broad singlet (br s), doublet (d), doublet of doublets (dd), triplet (t), sextet (sx) or multiplet (m). C_q stands for quaternary carbon atom. Spectra were assigned using COSY and HSQC experiments. All NMR chemical shifts (δ) were recorded in ppm and coupling constants (J) were reported in Hz. High resolution electrospray mass (ESI) spectra were recorded on a microTOF spectrometer; accurate mass measurements were achieved by using sodium formate as an external reference.

8.2 General protein conjugation methods

LC-MS method for analysis of protein conjugation

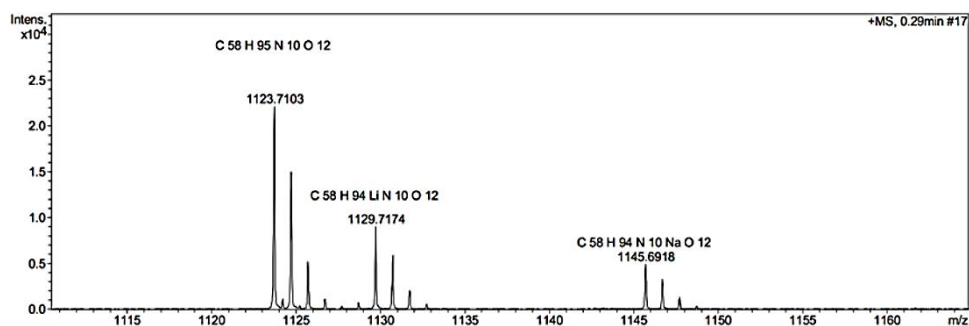
LC-MS was performed on a Water Acquity UPLC system equipped with a single quadrupole mass detector using an Acquity UPLC protein BEH C4 column, 300 Å, (1.7 mm, 2.1 × 50 mm). Solvents A, water with 0.01% formic acid and B, 71% acetonitrile, 29% water and 0.075% formic acid were used as the mobile phase at a flow rate of 0.2 mL/min from 0-20 min, and 0.05 mL/min from 20–30 min. The electrospray source was operated with a capillary voltage of 3.0 kV and a cone voltage of 20 V. Nitrogen was used as the desolvation gas at a total flow of 8 L/h. Total mass spectra were reconstructed from the ion series using the MaxEnt algorithm preinstalled on MassLynx software (v. 4.1 from Waters) according to the manufacturer's instructions. To obtain the ion series described, the major peak(s) of the chromatogram were selected for integration and further analysis.

Analysis of protein conjugation by LC-MS

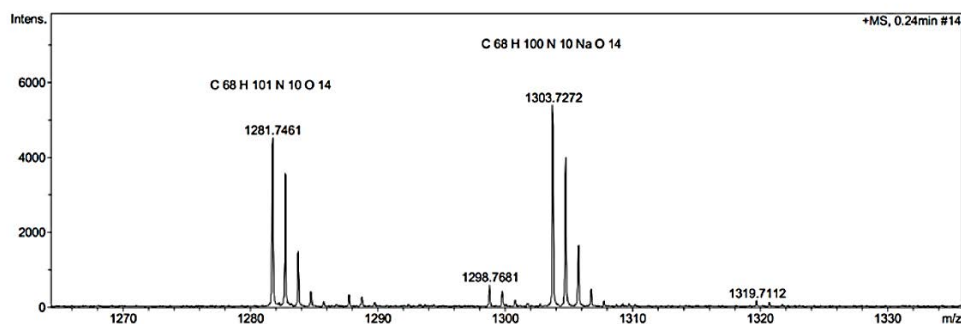
Briefly, the total ion chromatogram, combined ion series and deconvoluted spectra are measured for the starting material and the product of the bioconjugation reaction. This allows to monitor progress of the conversion of the non-modified antibody to the conjugated antibody. After size exclusion purification, SpectraMax i3x protein analysis is used to determine the yield of the reaction.

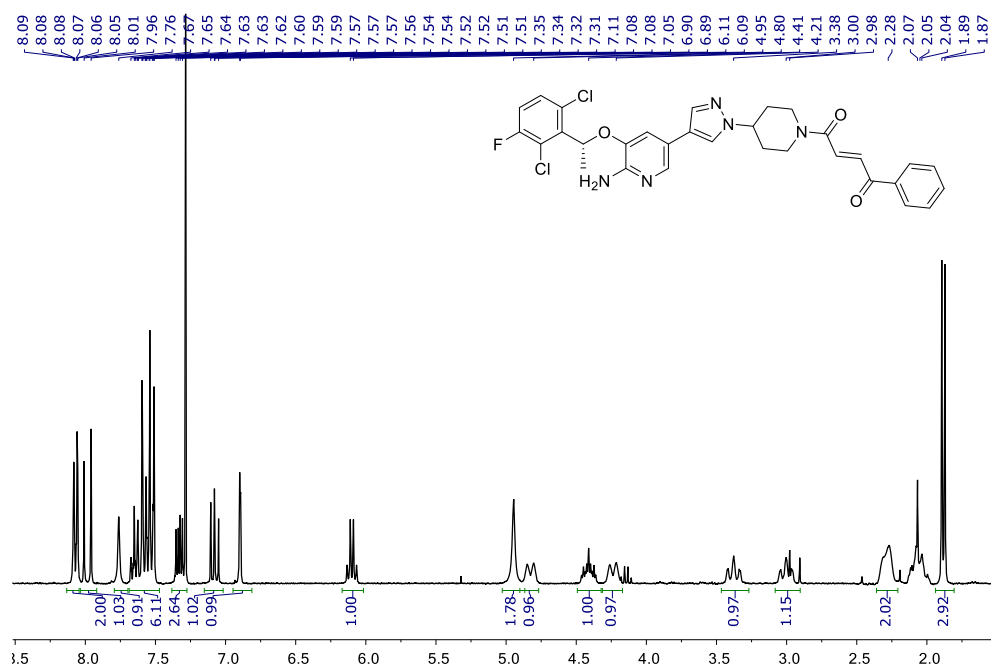
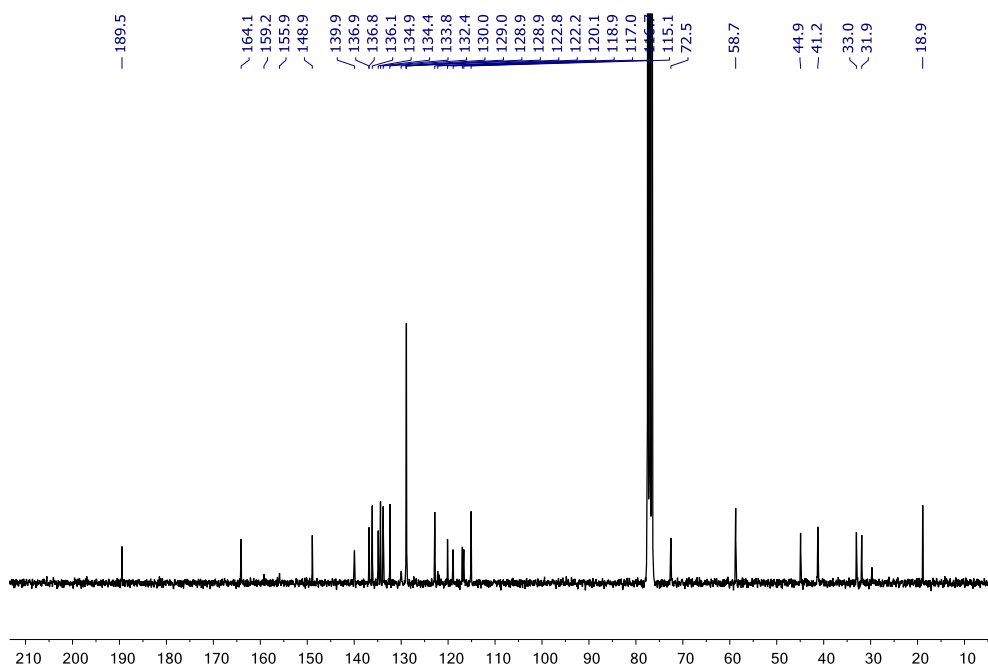
8.3 Supplementary information of Chapter 4

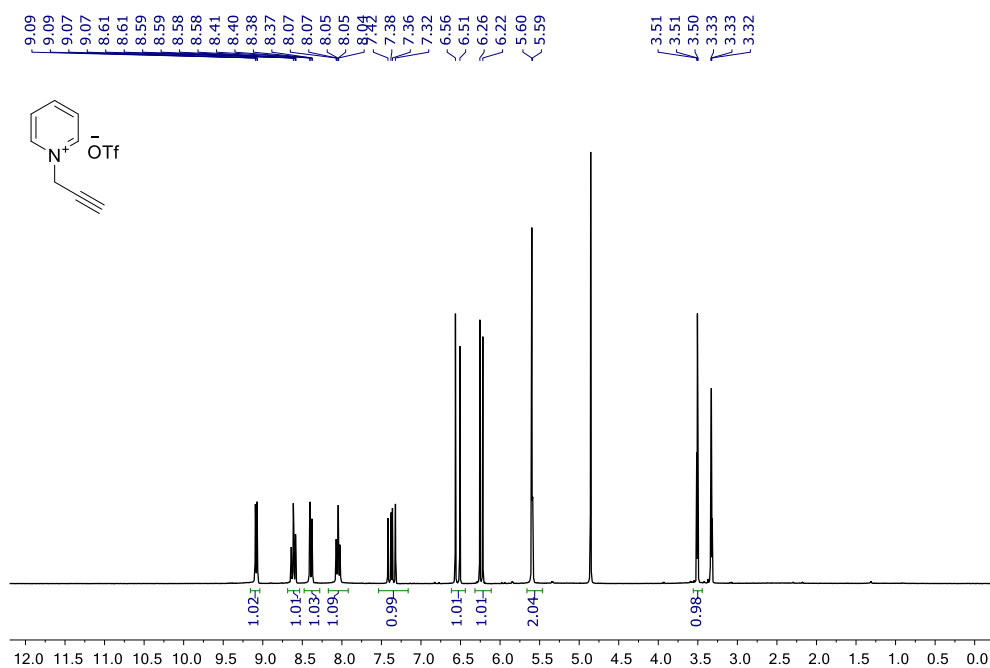
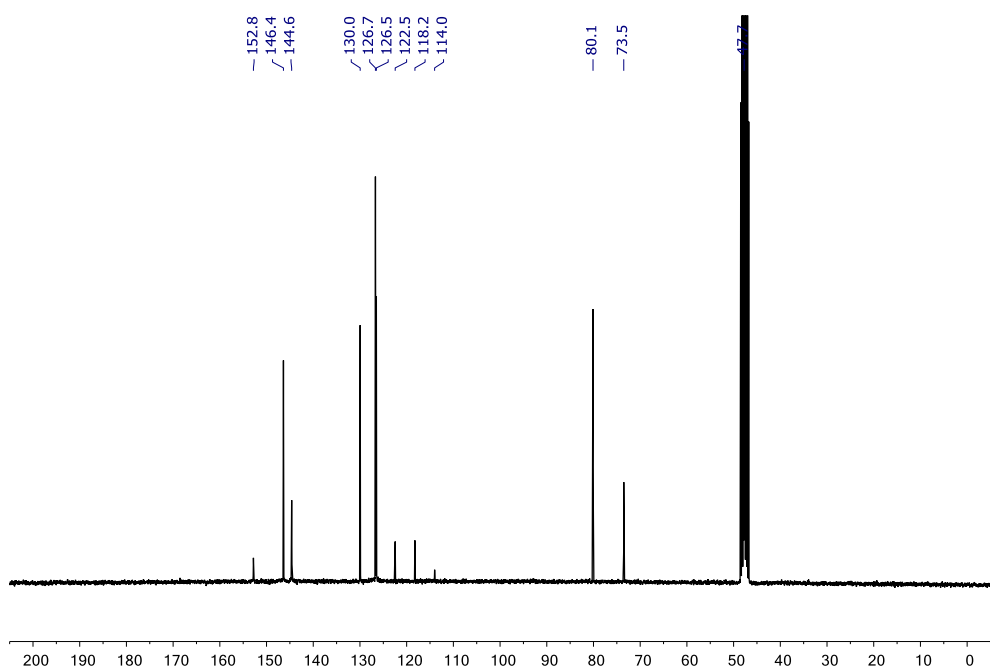
HRMS-ESI spectrum of compound 2

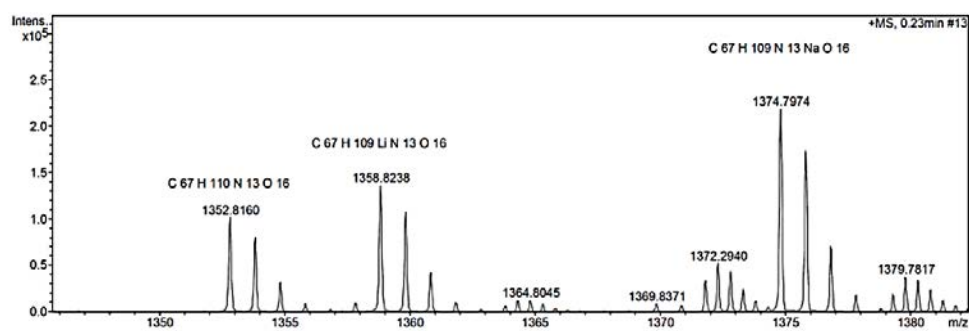
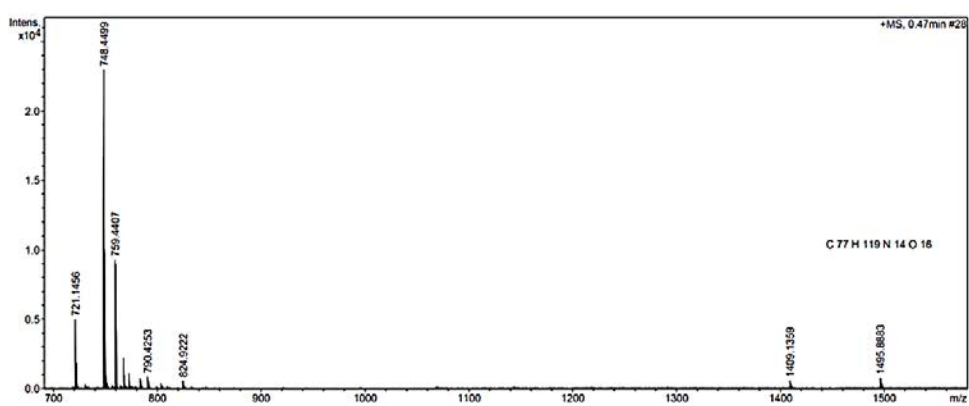


HRMS-ESI spectrum of compound 3



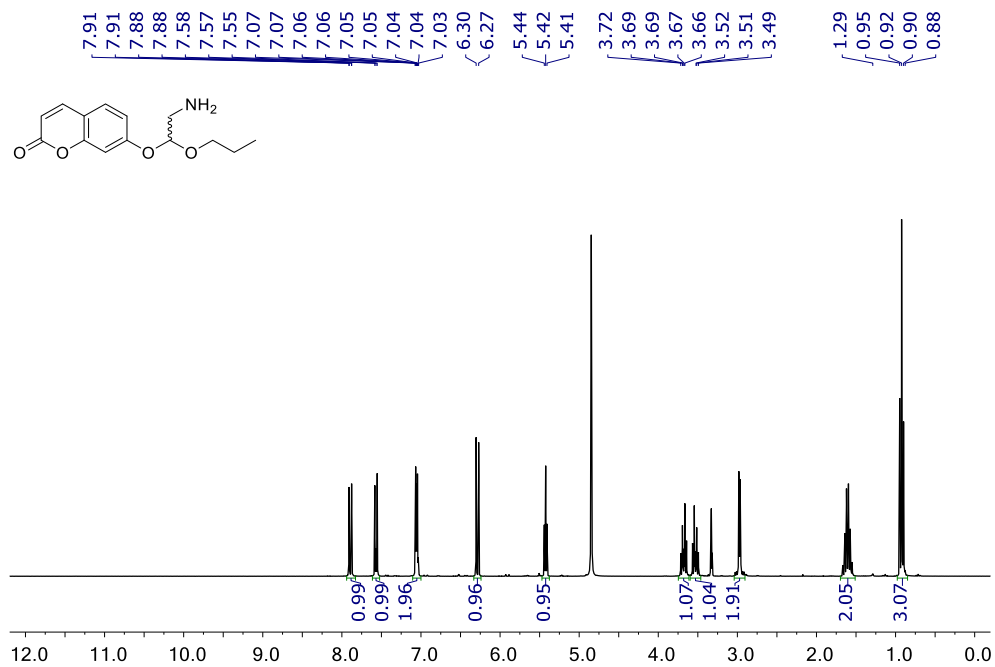
^1H NMR of compound **4** (400 MHz, CDCl_3) ^{13}C NMR of compound **4** (101 MHz, CDCl_3)

^1H NMR of compound **9** (300 MHz, CD_3OD) ^{13}C NMR of compound **9** (75 MHz, CD_3OD)

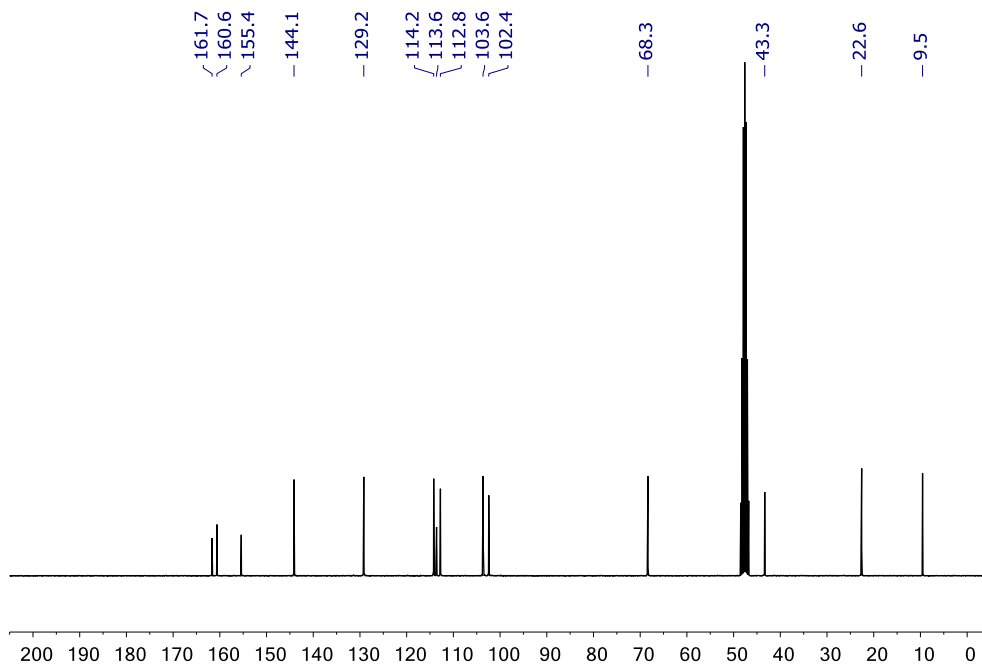
HRMS-ESI of compound **10**HRMS-ESI of compound **11**

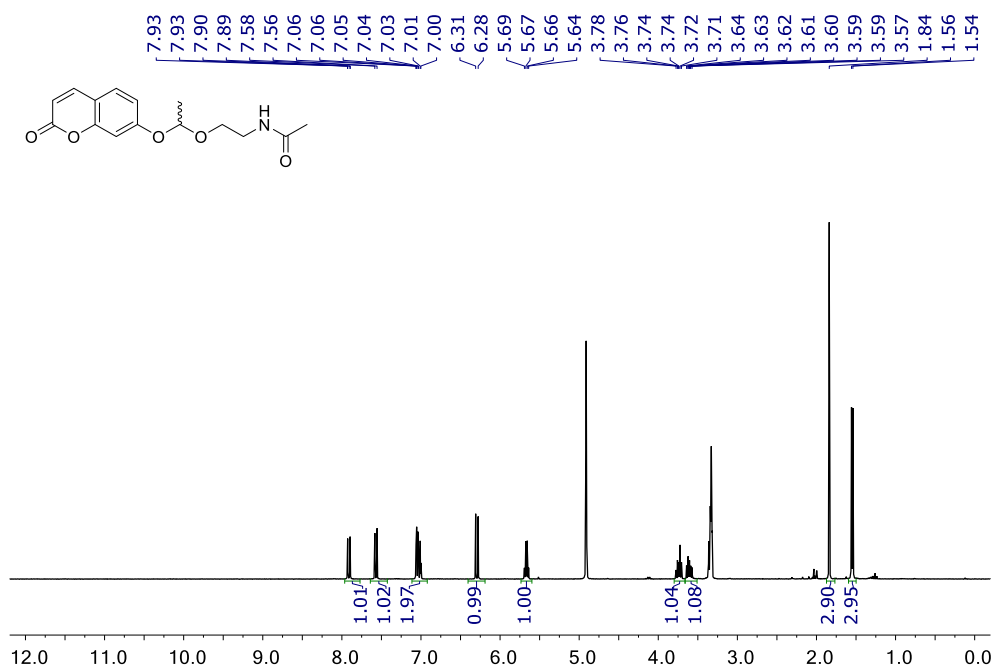
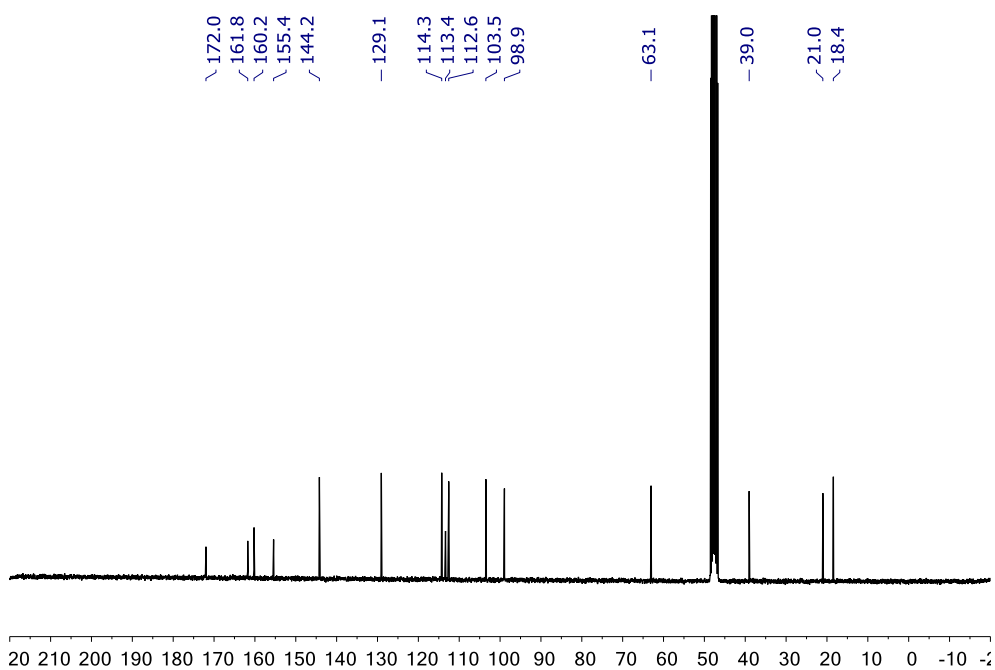
8.4 Supplementary information of Chapter 5

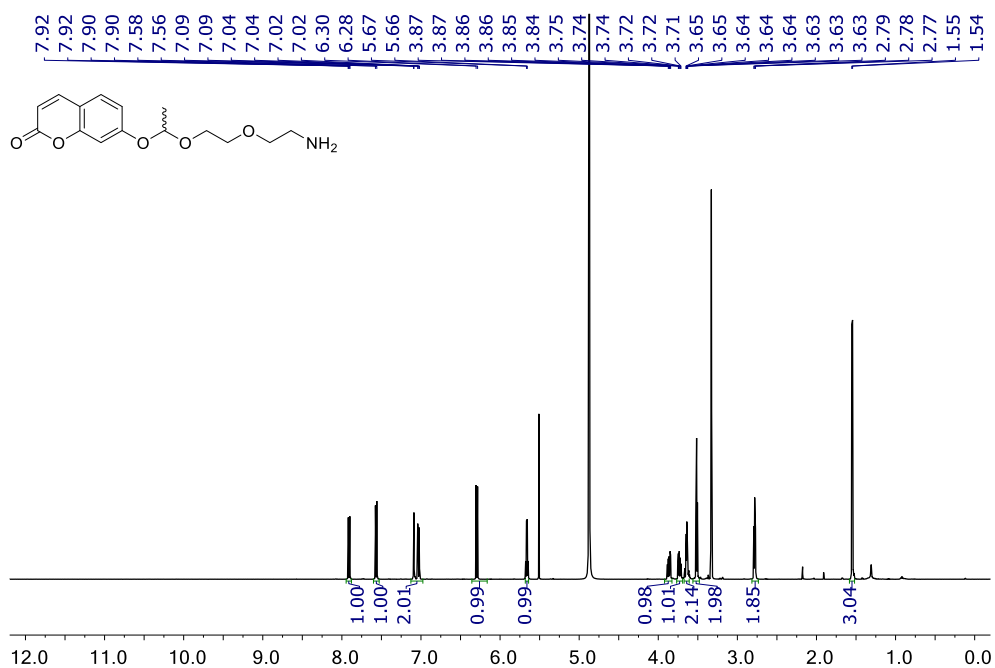
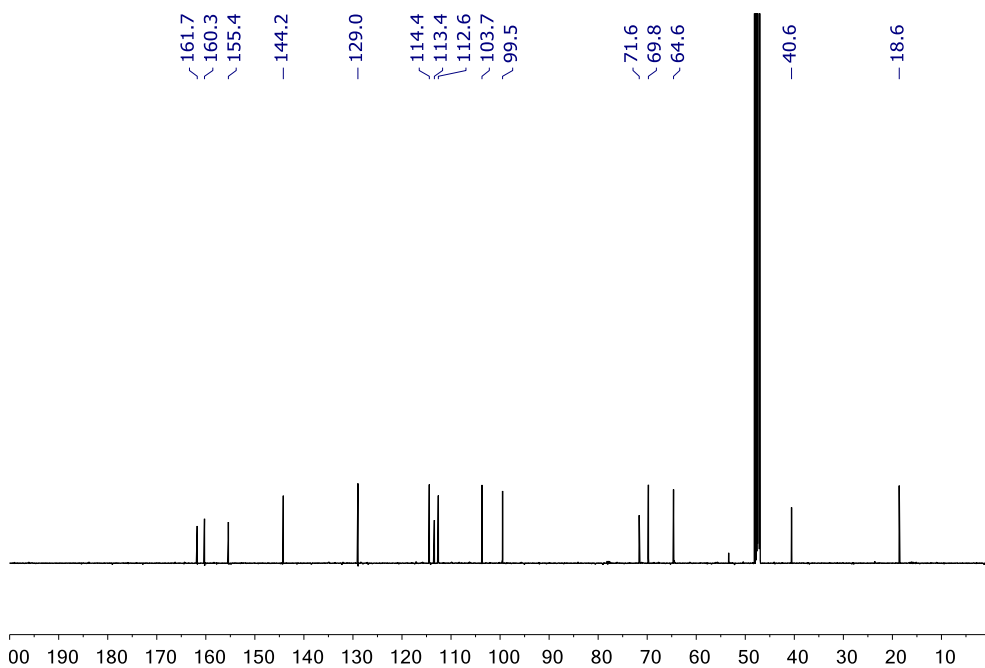
^1H NMR of compound **15** (300 MHz, CD_3OD)

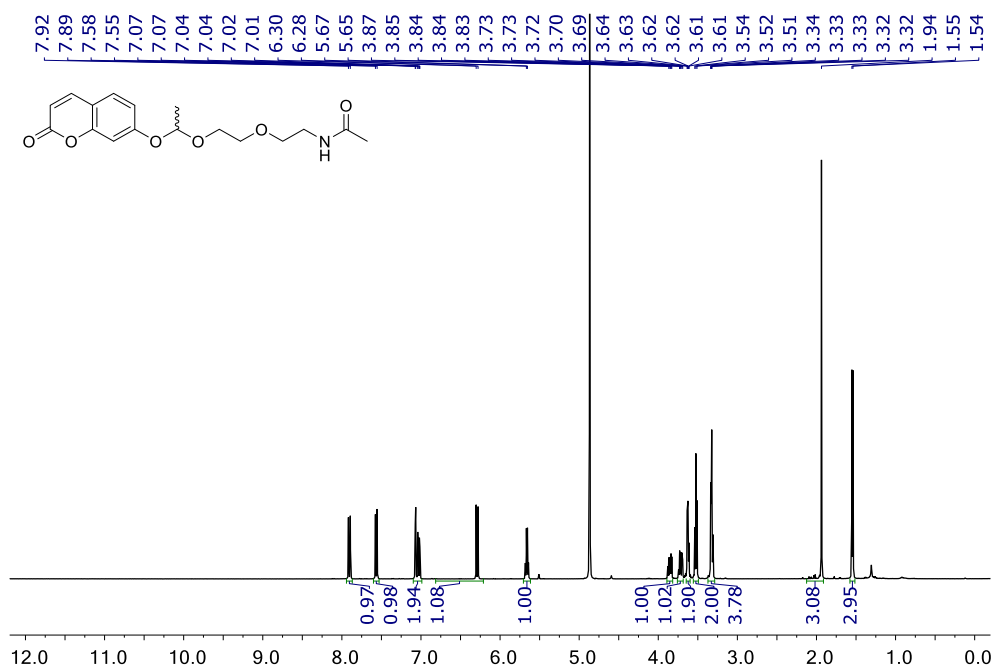
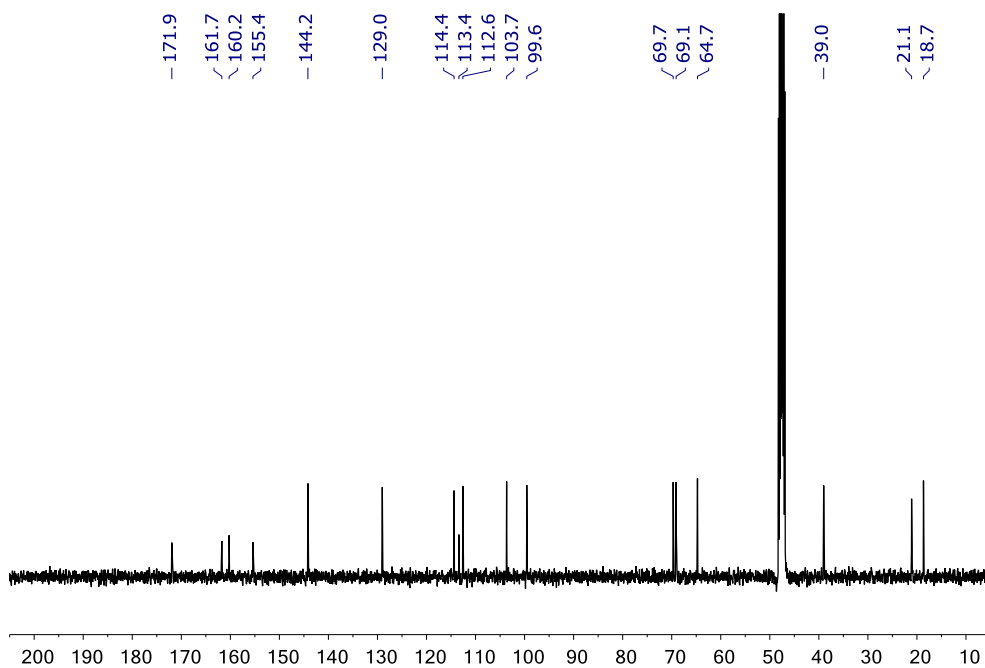


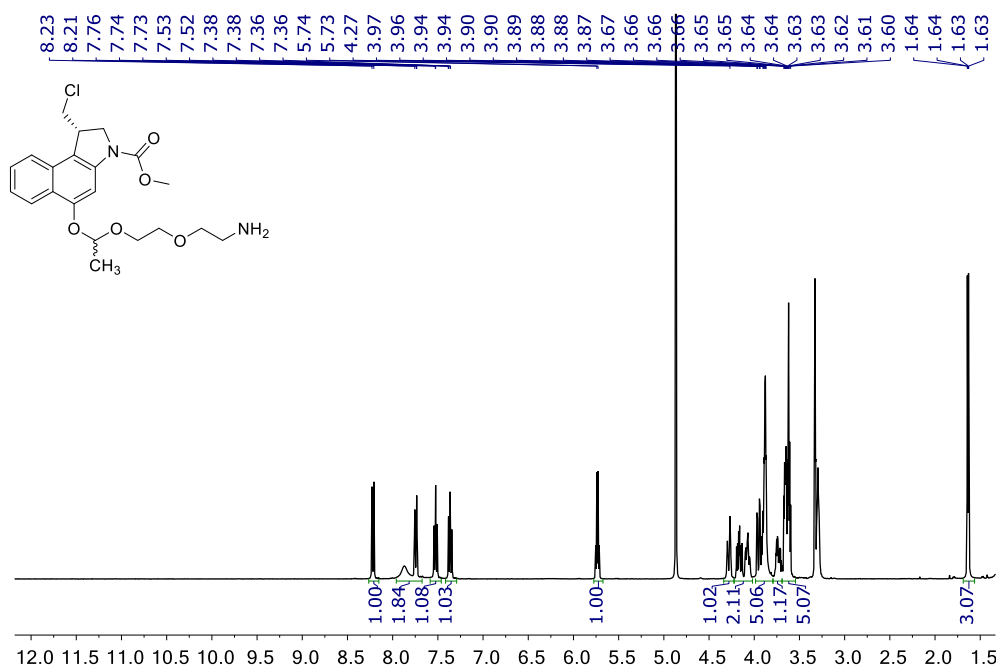
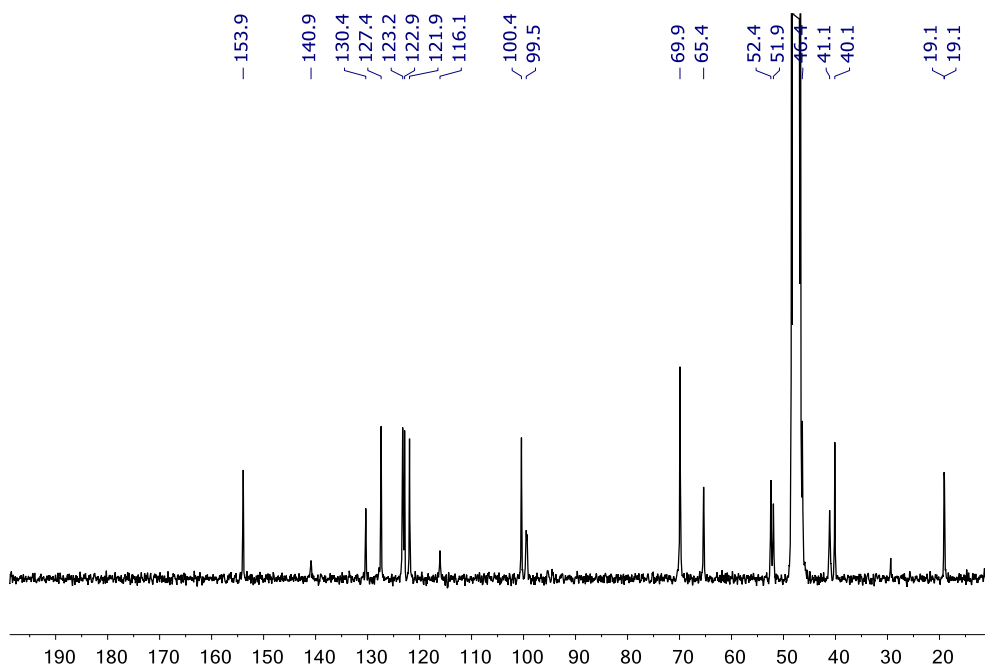
^{13}C NMR of compound **15** (75 MHz, CD_3OD)

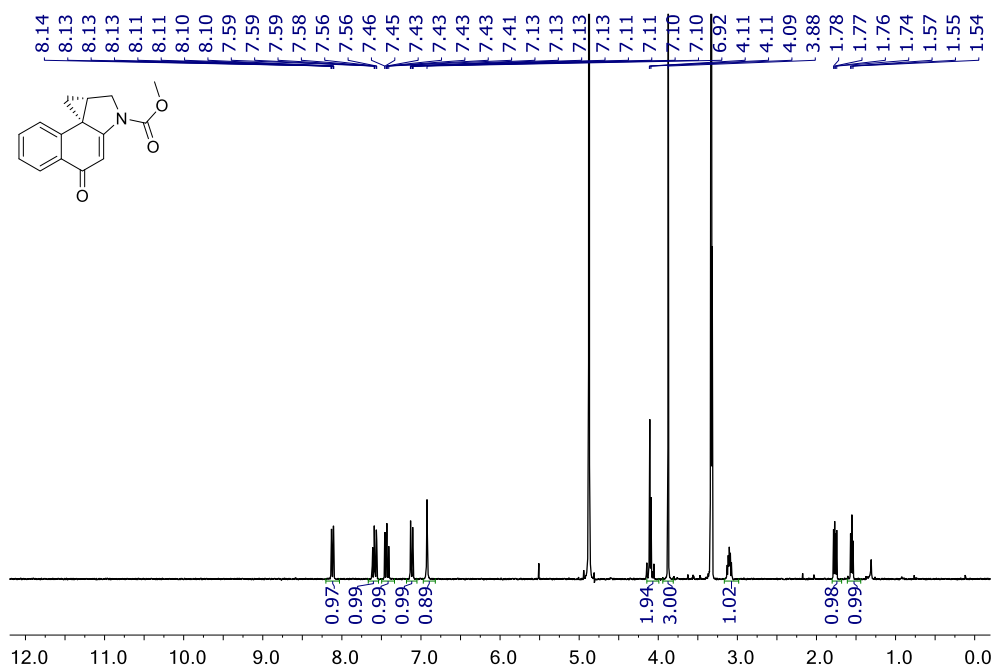
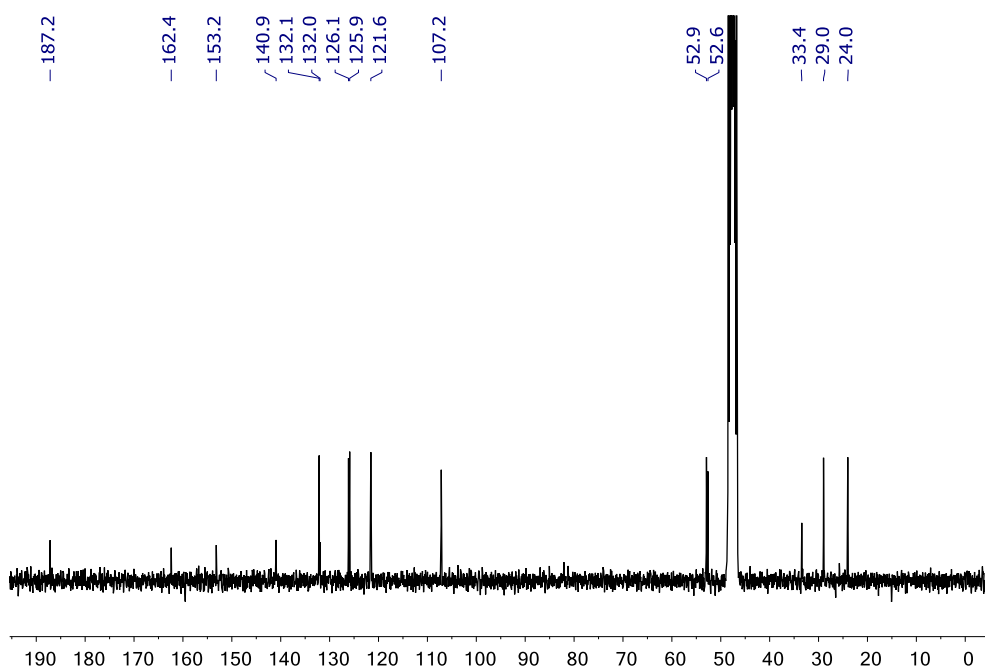


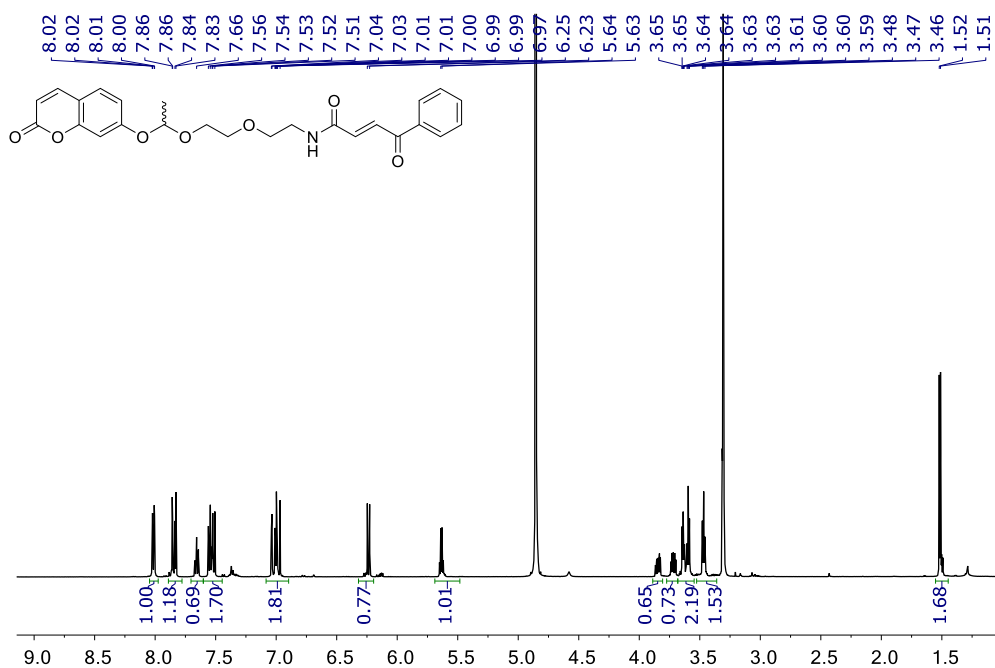
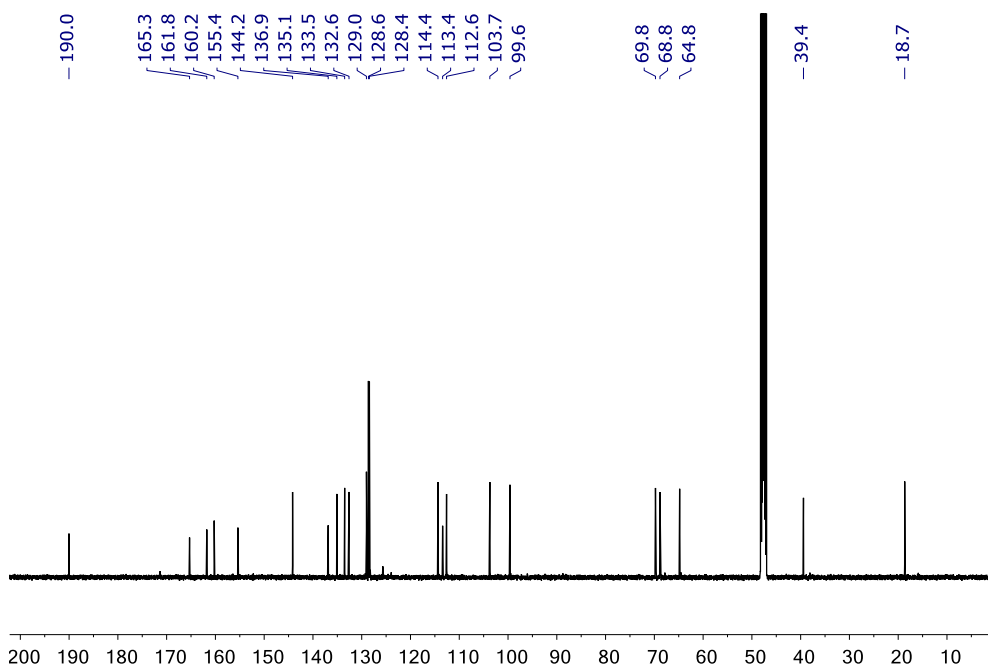
^1H NMR of compound **20** (300 MHz, CD_3OD) ^{13}C NMR of compound **20** (75 MHz, CD_3OD)

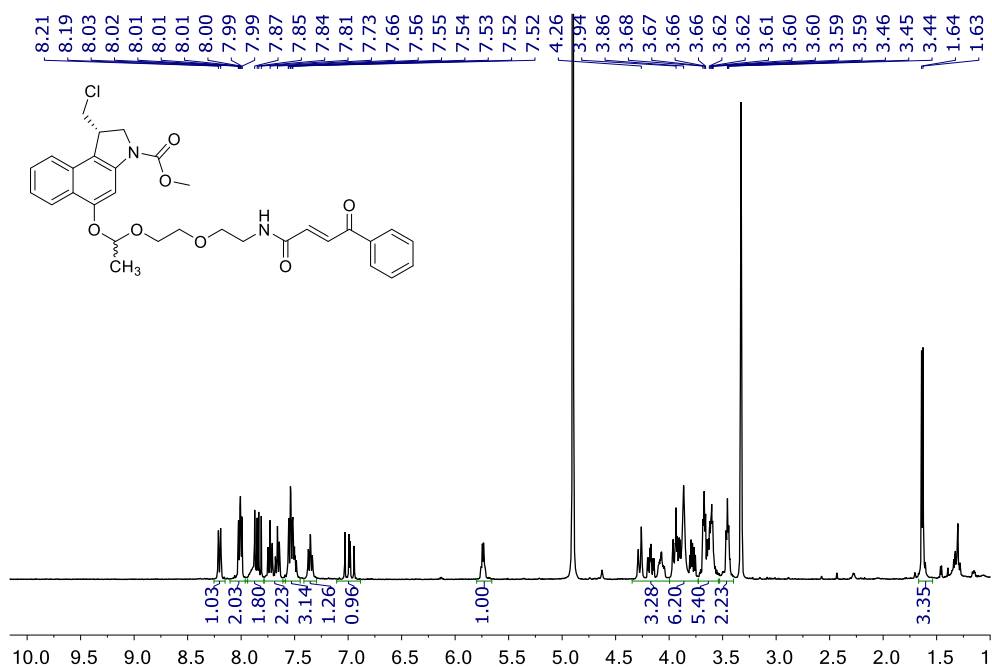
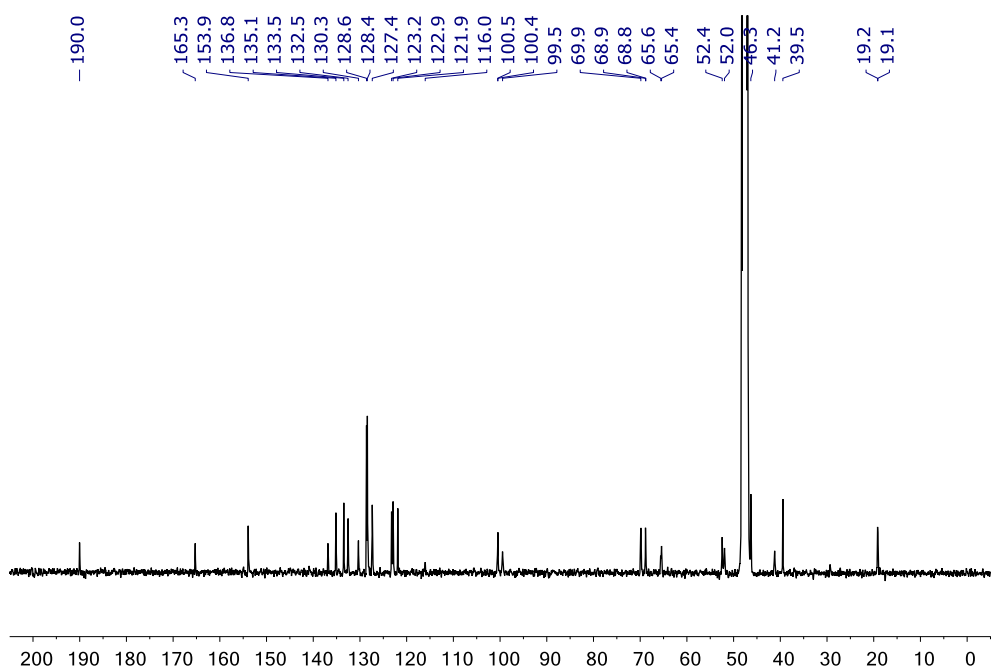
^1H NMR of compound **24** (500 MHz, CD_3OD) ^{13}C NMR of compound **24** (125 MHz, CD_3OD)

^1H NMR of compound **25** (400 MHz, CD_3OD) ^{13}C NMR of compound **25** (101 MHz, CD_3OD)

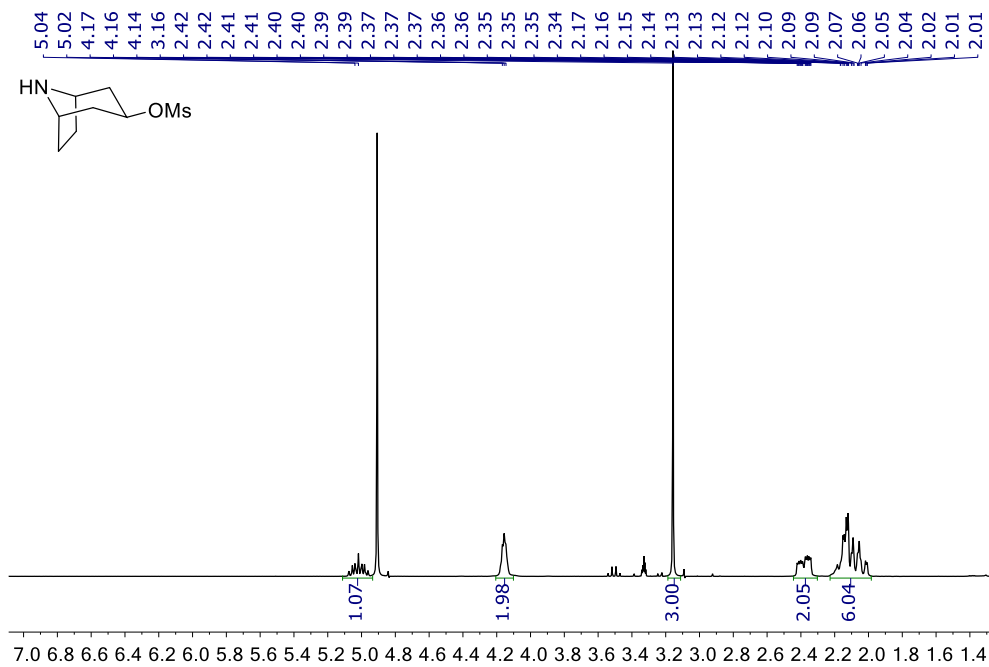
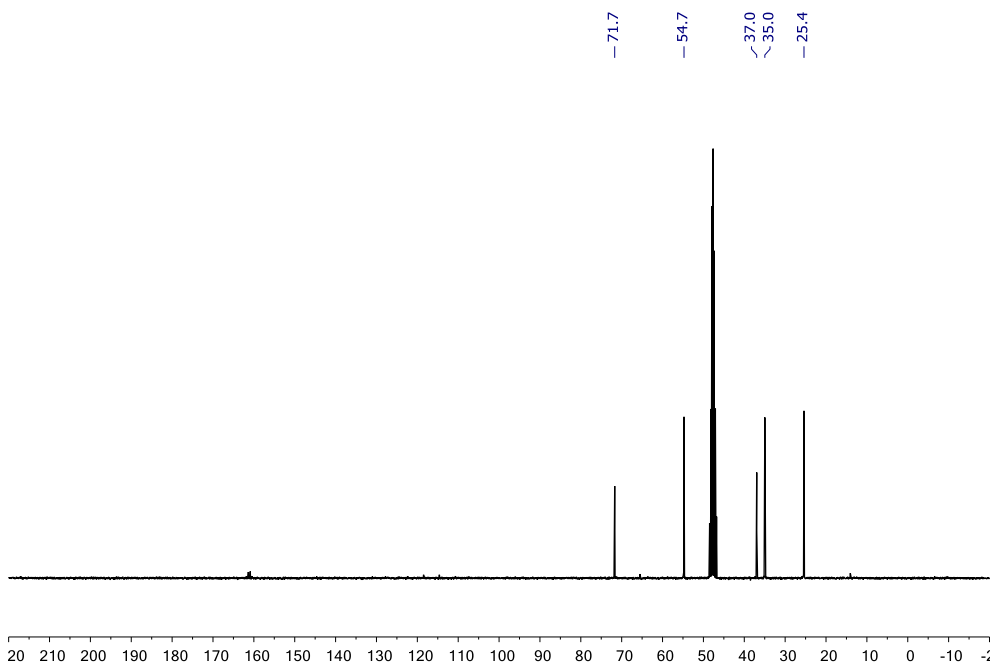
^{13}C NMR of compound **29** (400 MHz, CD_3OD) ^{13}C NMR of compound **29** (75 MHz, CD_3OD)

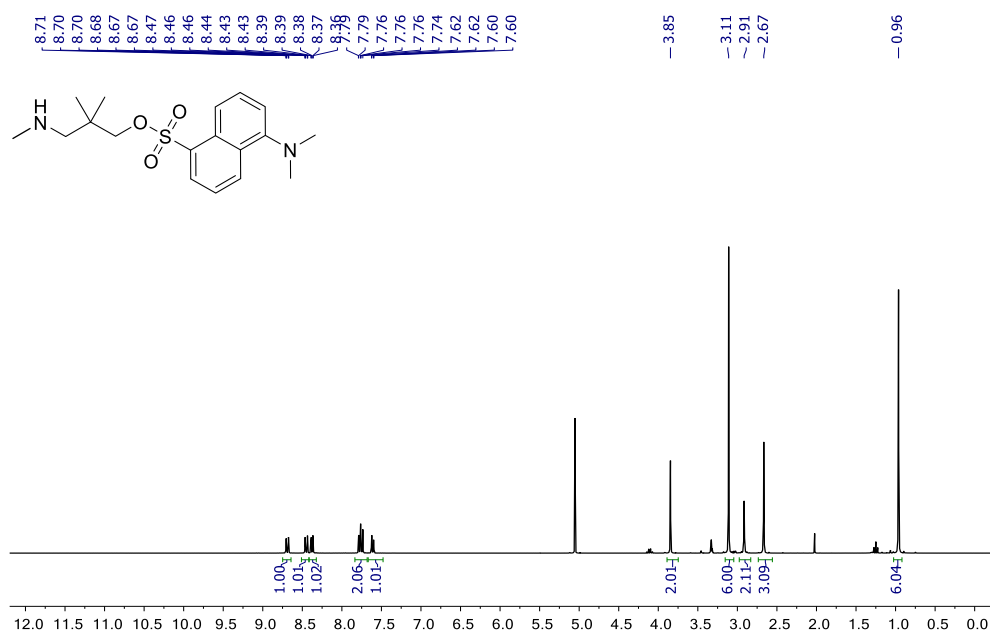
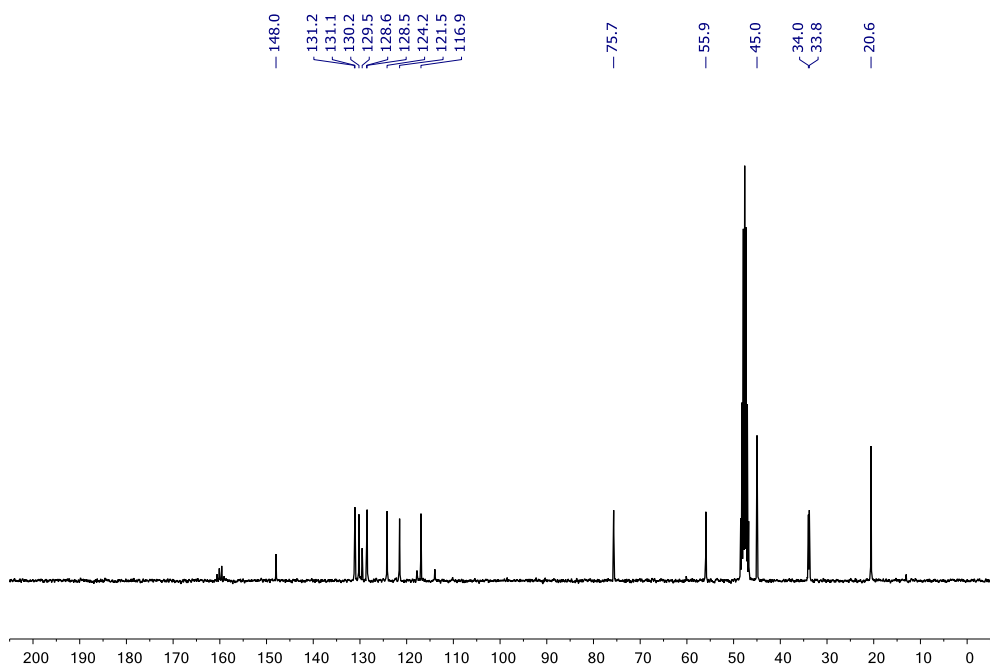
^1H NMR of compound **30** (300 MHz, CD_3OD) ^{13}C NMR of compound **30** (75 MHz, CD_3OD)

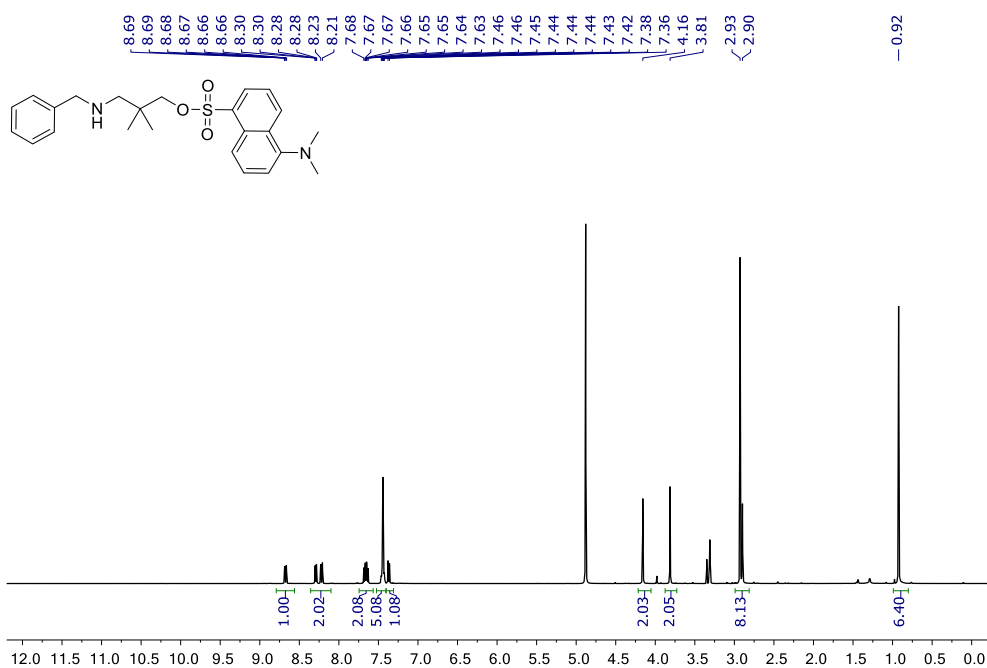
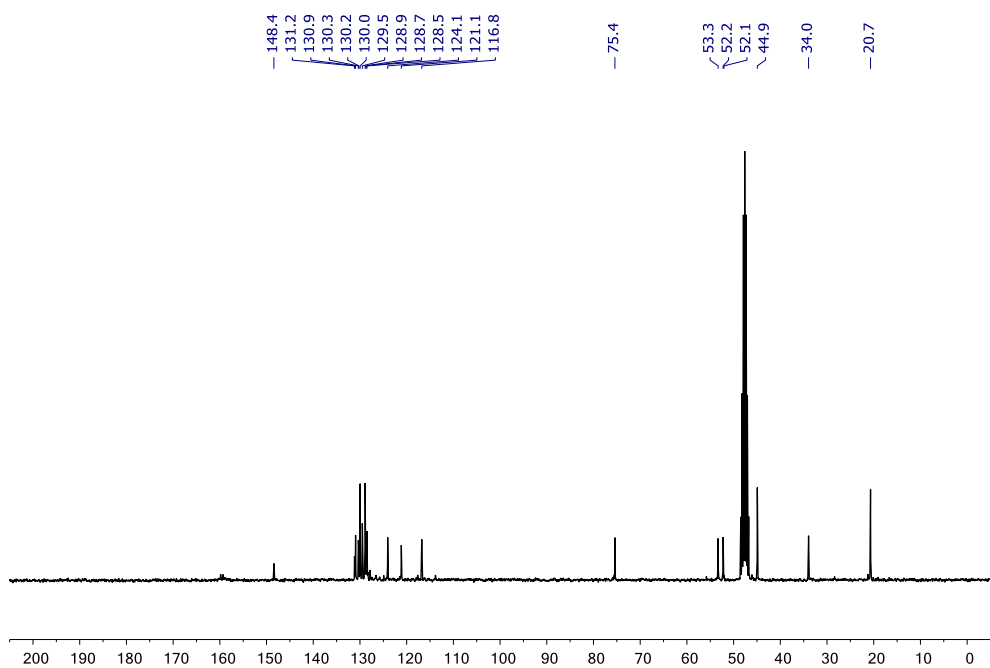
^1H NMR of compound **34** (400 MHz, CD_3OD) ^{13}C NMR of compound **34** (125 MHz, CD_3OD)

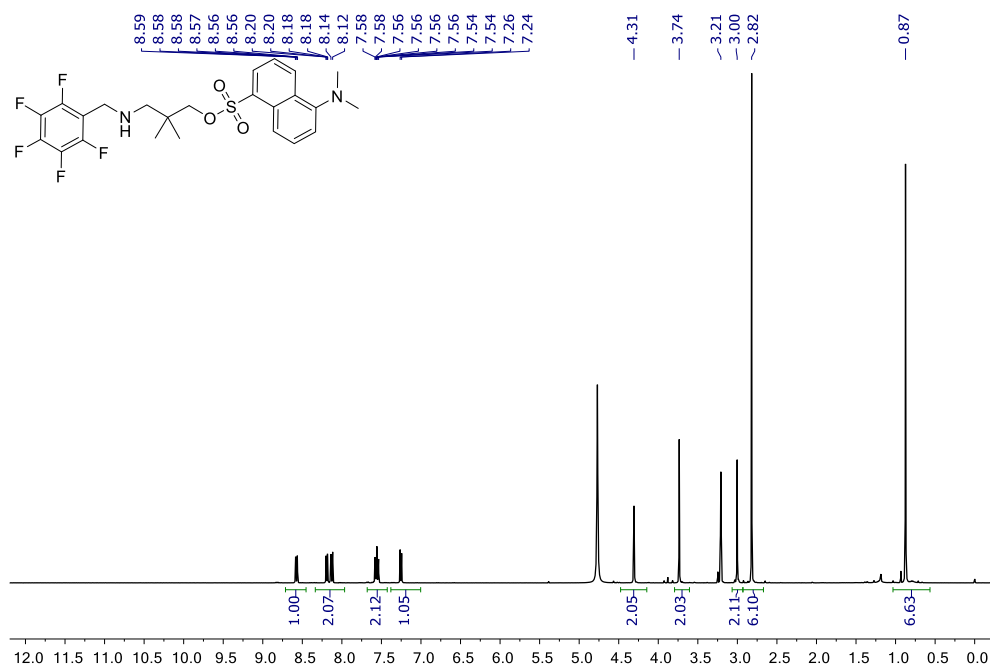
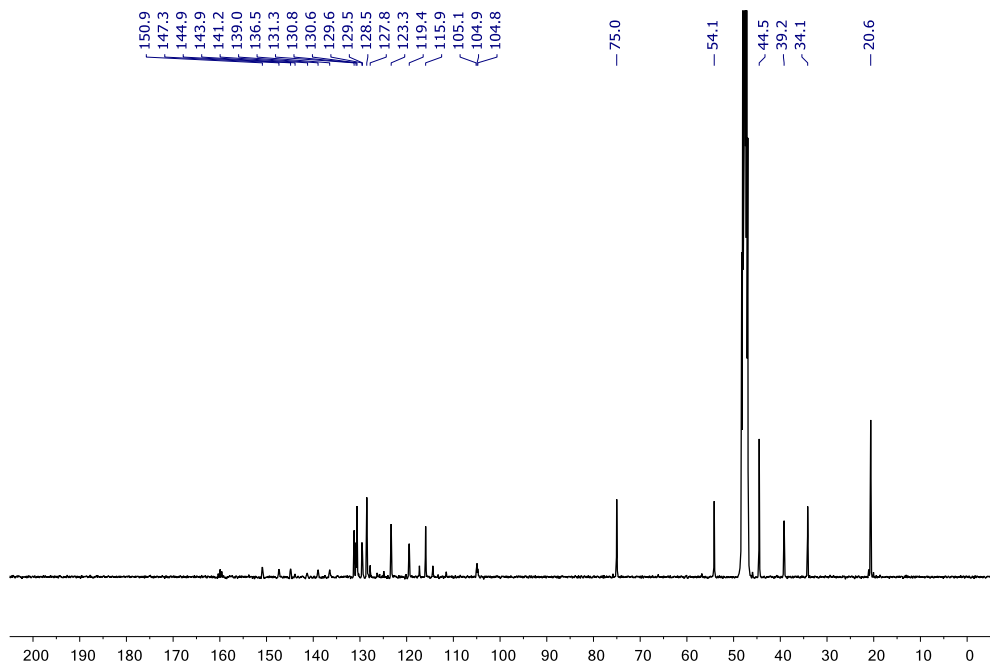
^1H NMR of compound **35** (400 MHz, CD_3OD) ^{13}C NMR of compound **35** (101 MHz, CD_3OD)

8.5 Supplementary information of Chapter 6

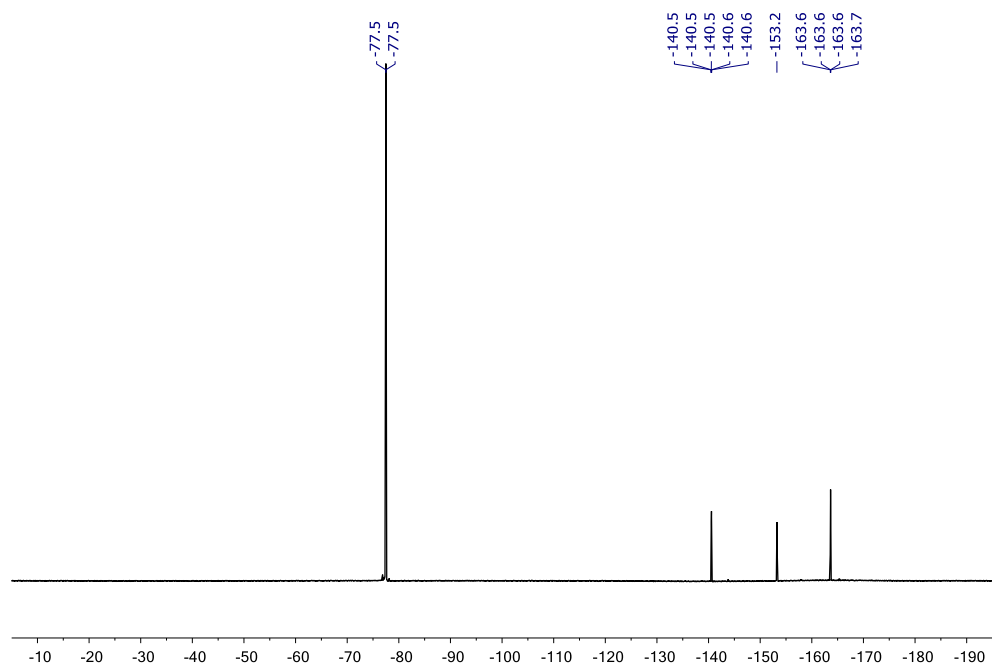
 ^1H NMR (300 MHz, CD_3OD) of compound **39** ^{13}C NMR (75 MHz, CD_3OD) of compound **39**

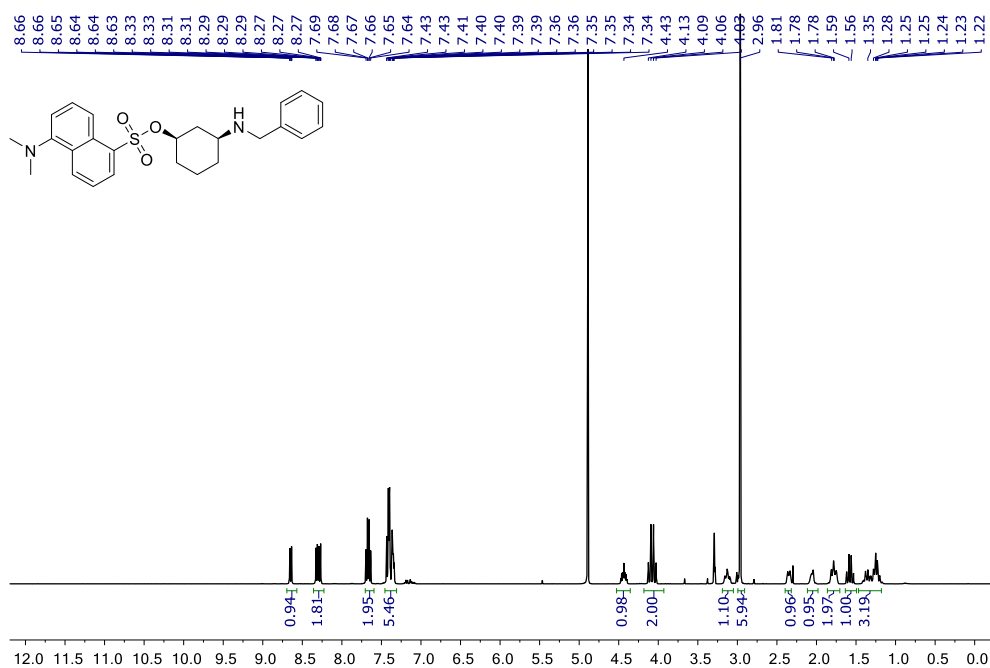
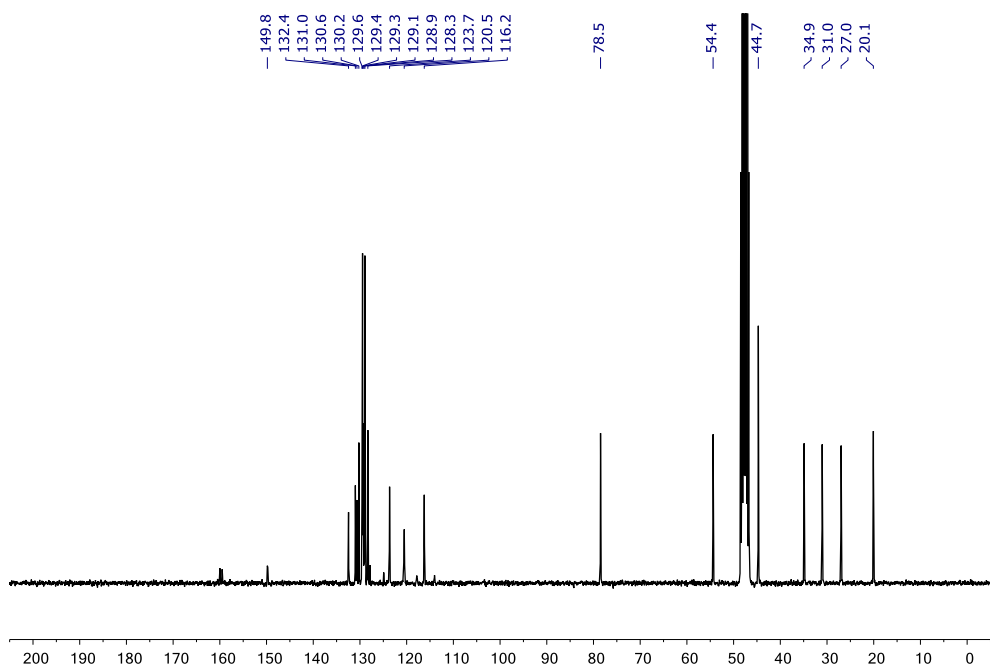
^1H NMR (300 MHz, CD_3OD) of compound **42** ^{13}C NMR (75 MHz, CD_3OD) of compound **42**

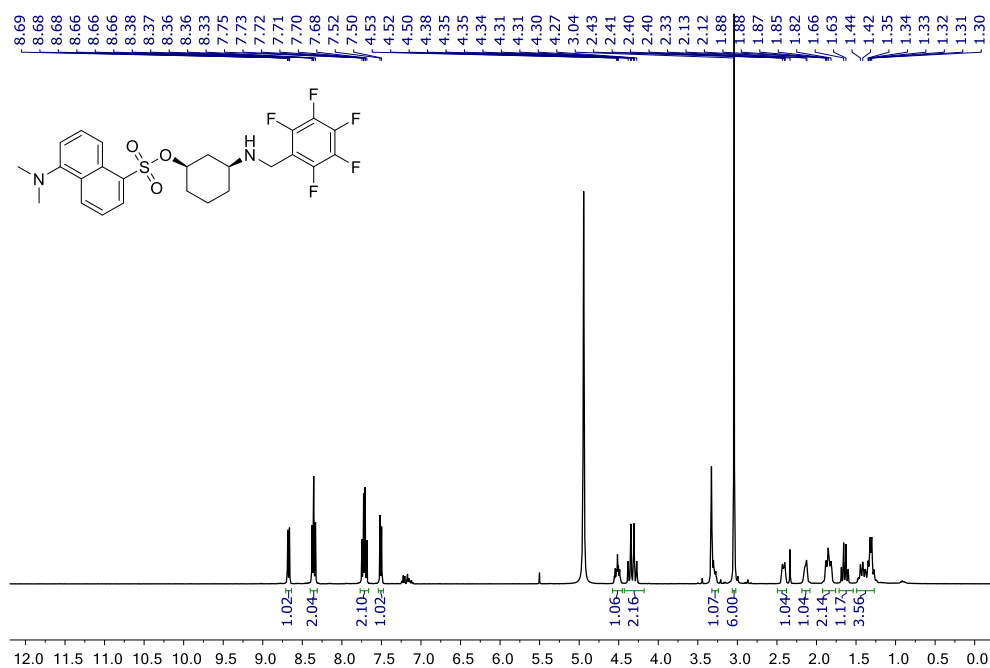
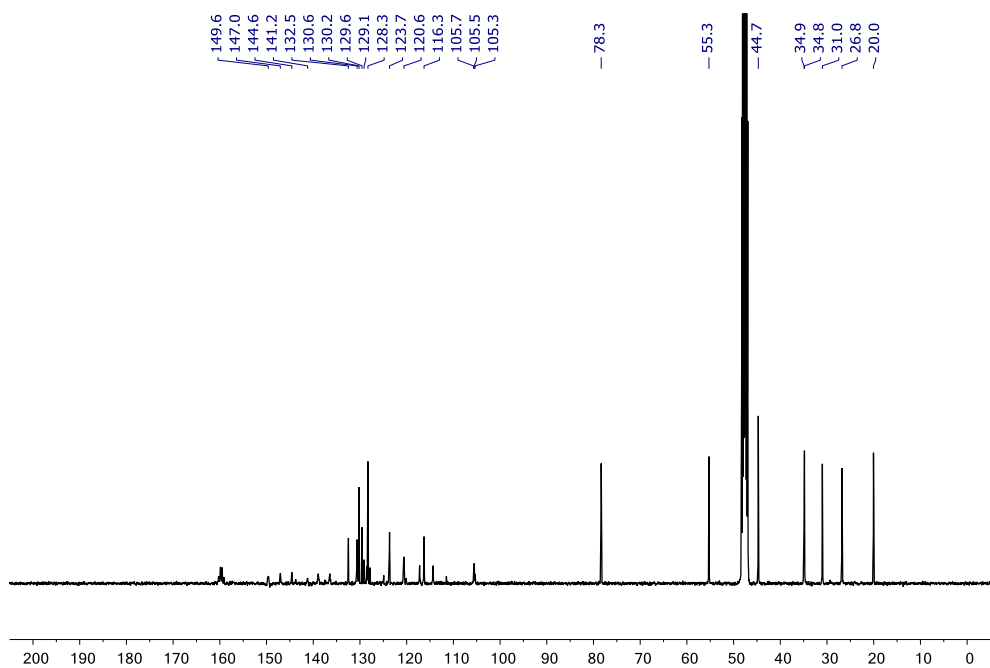
^1H NMR (400 MHz, CD_3OD) of compound **47** ^{13}C NMR (101 MHz, CD_3OD) of compound **47**

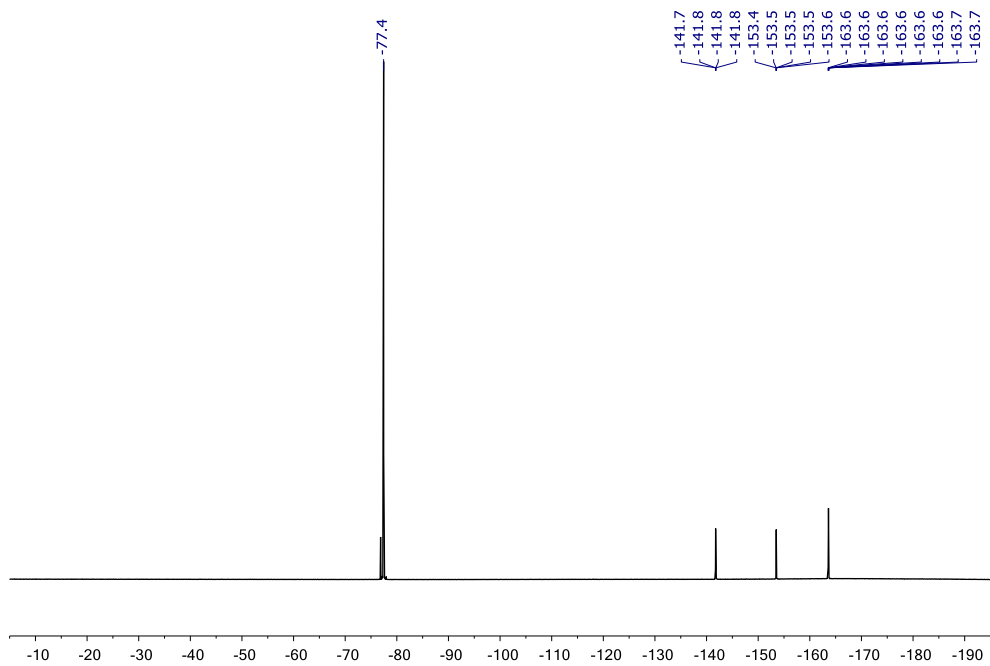
^1H NMR (400 MHz, CD_3OD) of compound **48** ^{13}C NMR (101 MHz, CD_3OD) of compound **48**

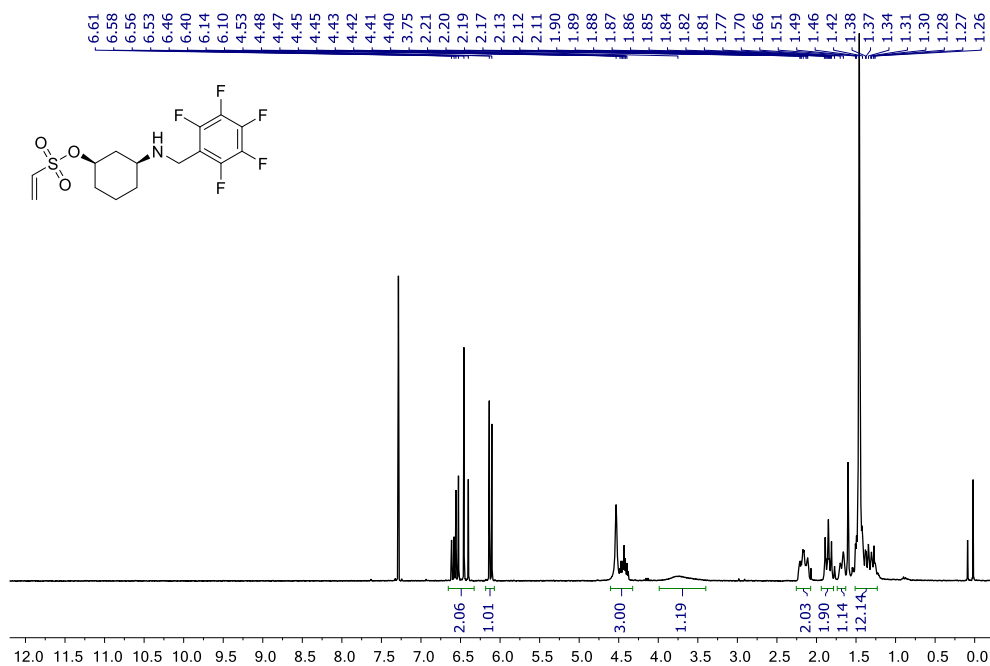
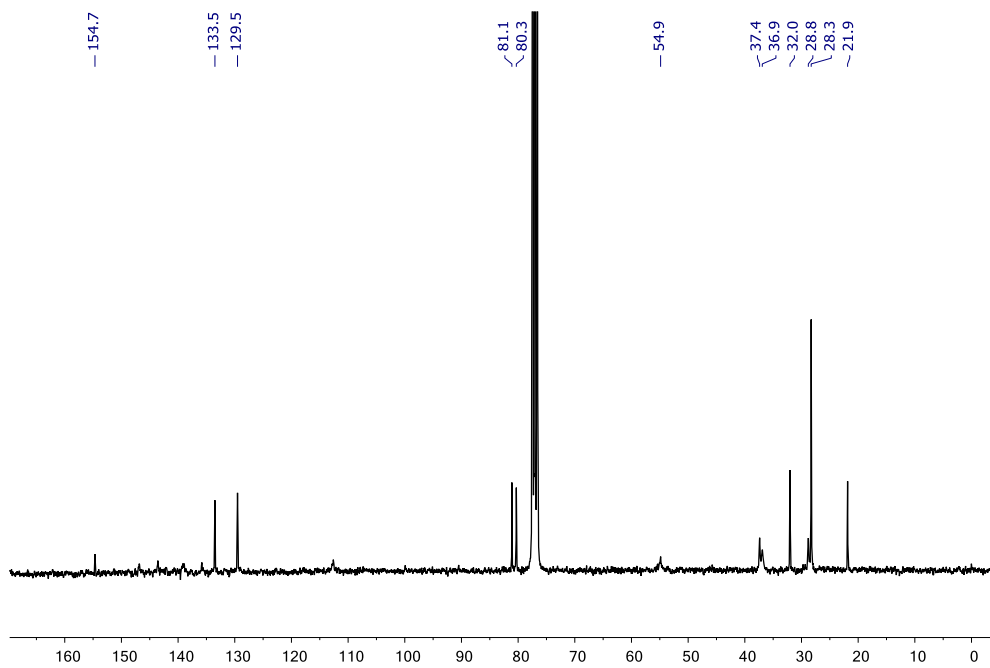
^{19}F NMR (282 MHz, CD_3OD) of compound **48**



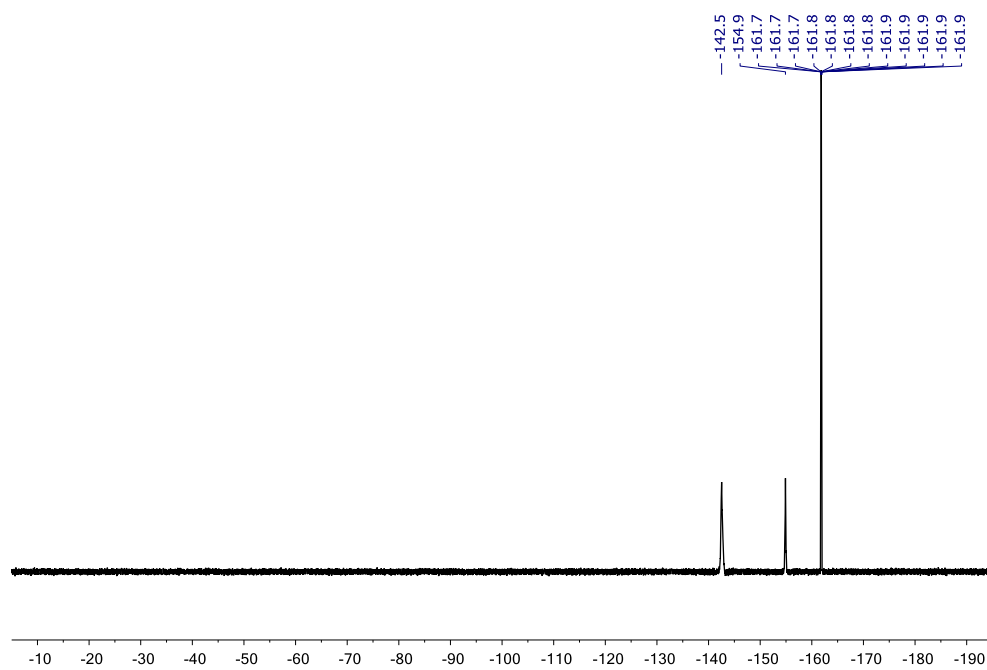
^1H NMR (400 MHz, CD_3OD) of compound **55** ^{13}C NMR (101 MHz, CD_3OD) of compound **55**

^1H NMR (400 MHz, CD_3OD) of compound **56** ^{13}C NMR (101 MHz, CD_3OD) of compound **56**

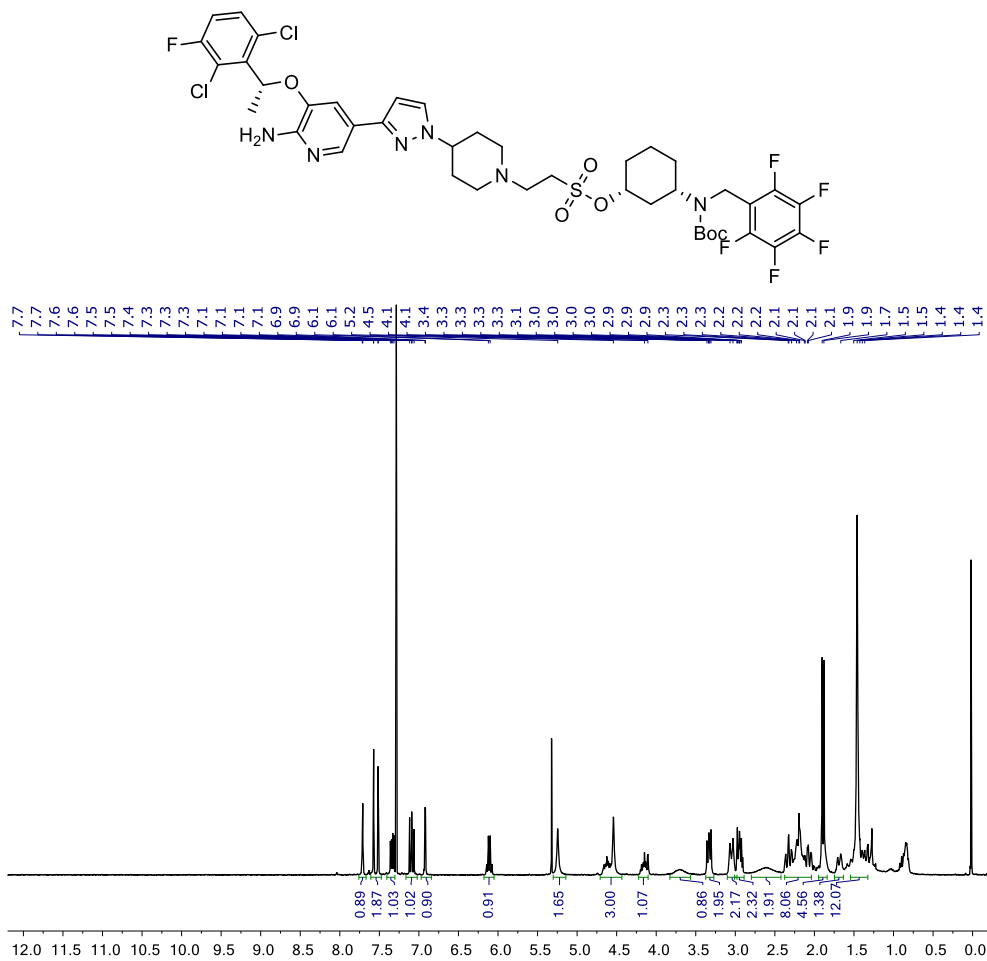
^{19}F NMR (376 MHz, CD_3OD) of compound **56**

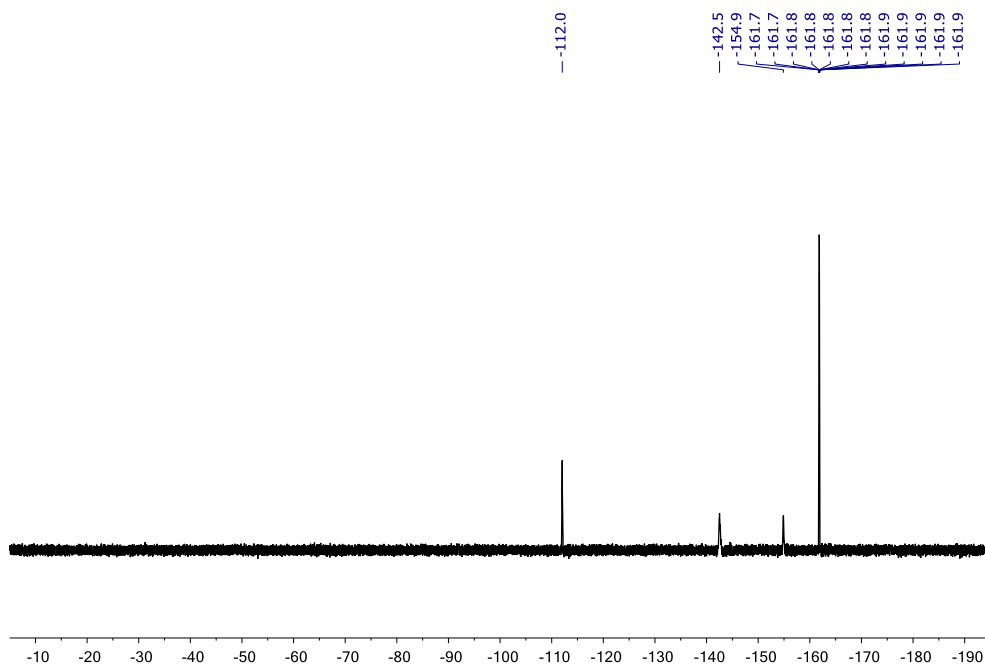
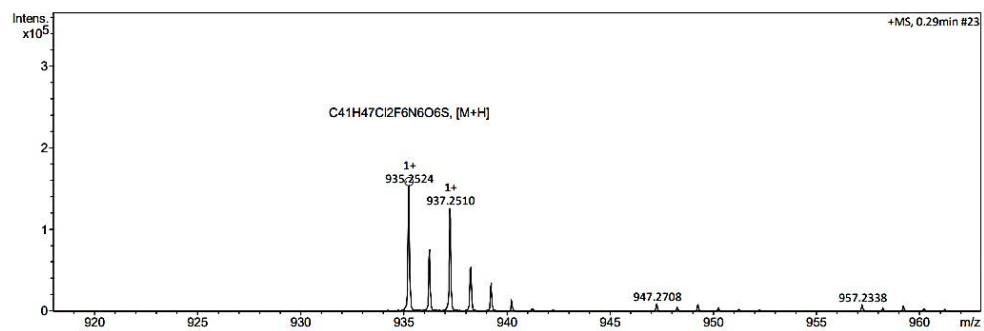
^1H NMR (300 MHz, CDCl_3) of compound **66** ^{13}C NMR (75 MHz, CDCl_3) of compound **66**

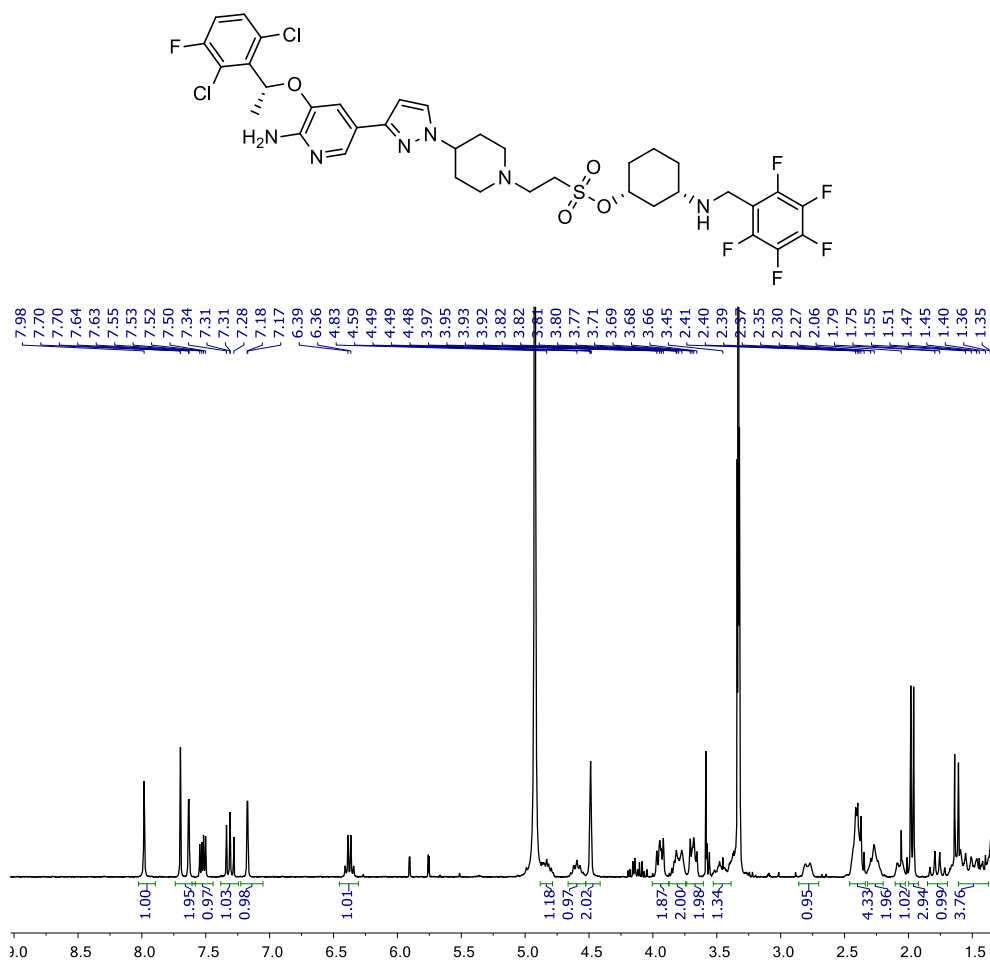
^{19}F NMR (282 MHz, CDCl_3) of compound **66**

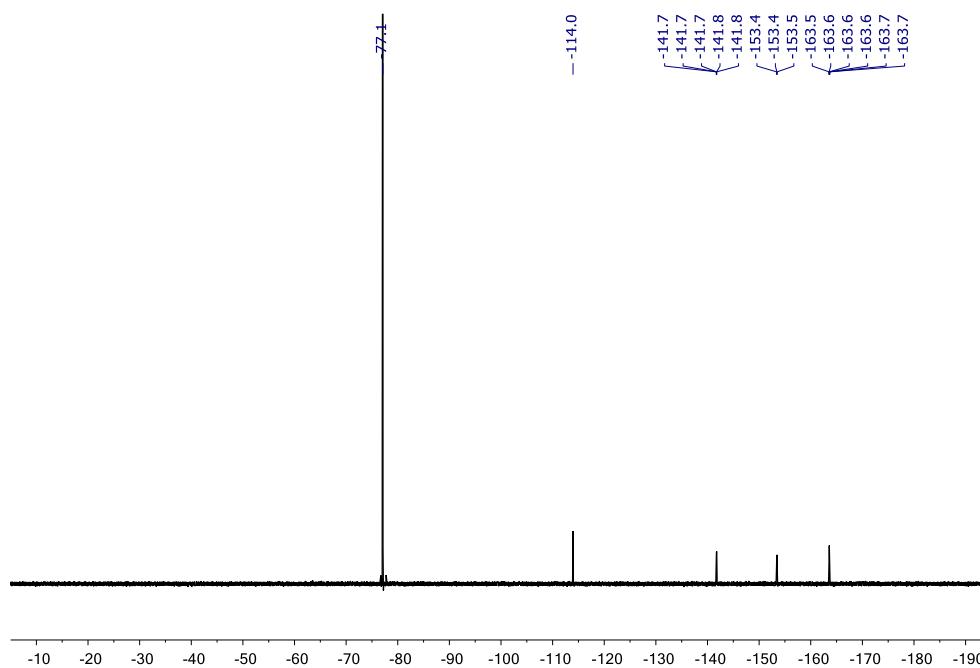
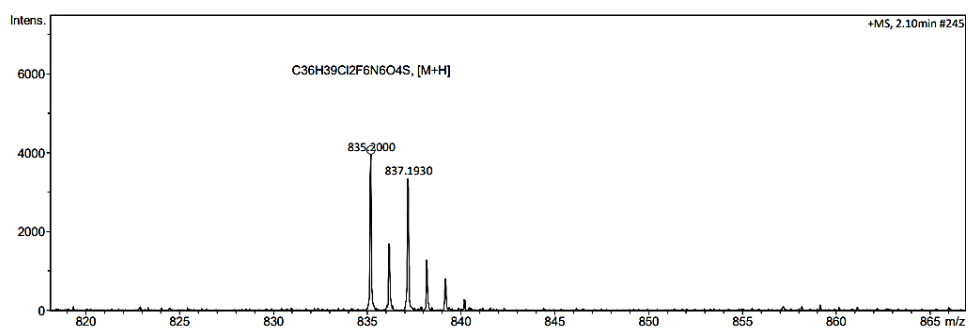


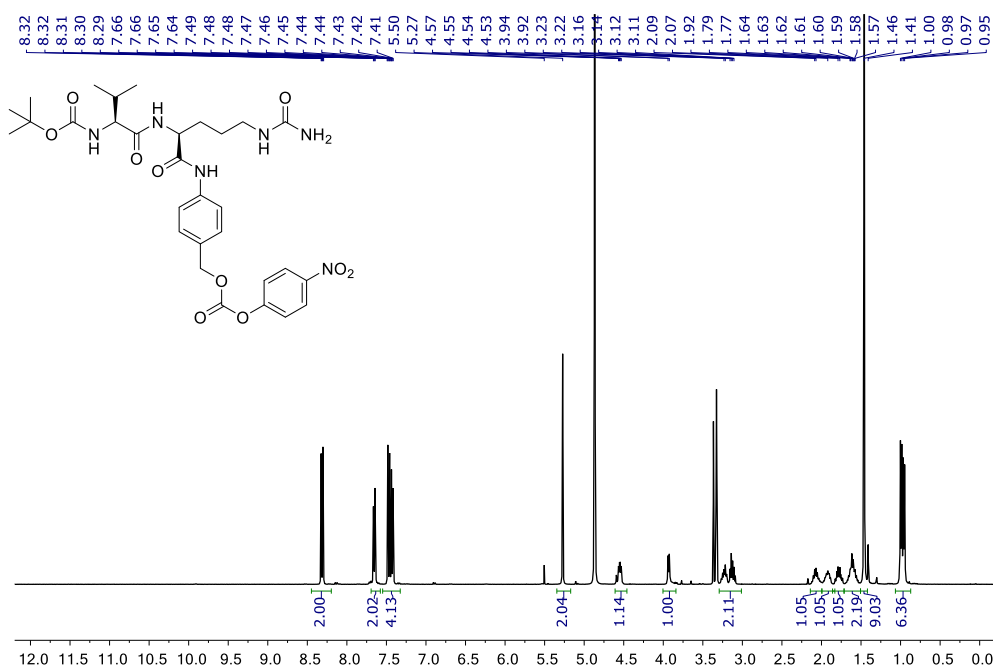
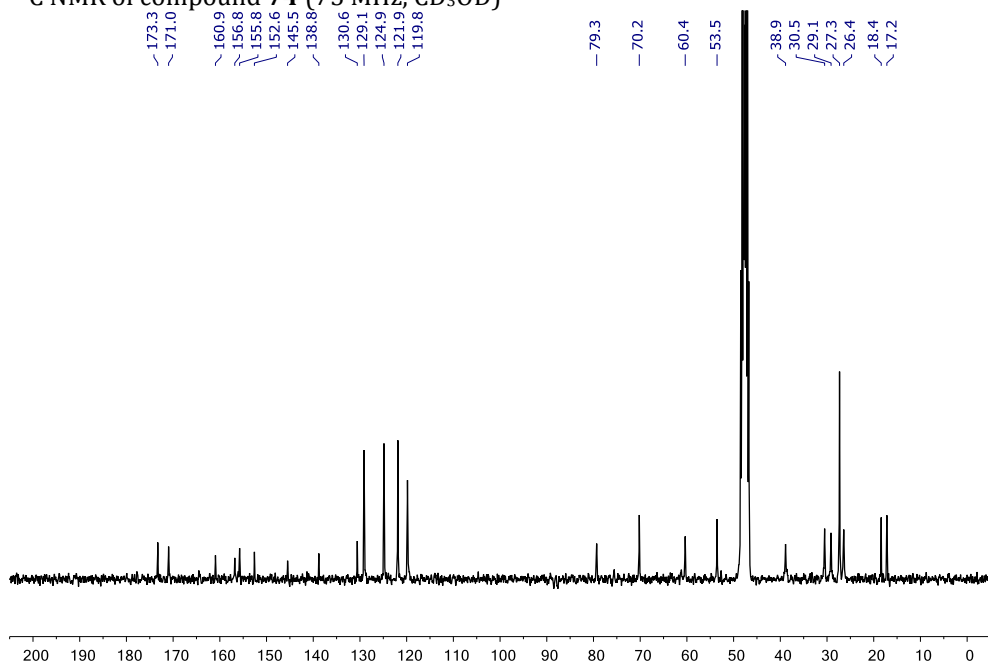
^1H NMR of compound **67** (300 MHz, CDCl_3)



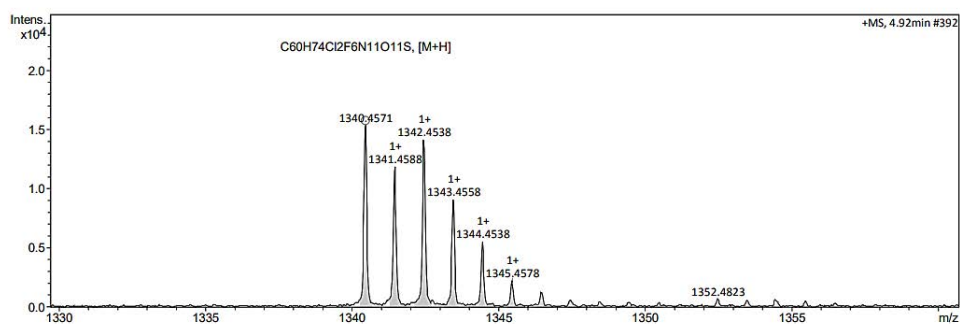
^{19}F NMR of compound **67** (282 MHz, CDCl_3)HRMS-ESI of compound **67**

^1H NMR of compound **68** (300 MHz, CD_3OD)

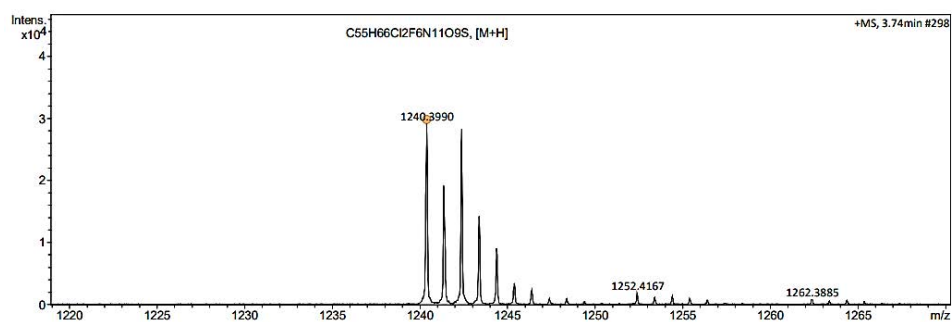
^{19}F NMR of compound **68** (282 MHz, CD_3OD)HRMS-ESI of compound **68**

^1H NMR of compound **74** (300 MHz, CD_3OD) ^{13}C NMR of compound **74** (75 MHz, CD_3OD)

HRMS-ESI of compound 75



HRMS-ESI of compound 76



HRMS-ESI of compound 70

